Pharmacological therapies for monogenic obesity caused by MC4R dysfunction

Gooljar, Sakina B

Pharmacological therapies for monogenic obesity caused by MC4R dysfunction

Sakina B. Gooljar

This thesis is submitted for the degree of Doctor of Philosophy (Ph.D) at Queen Mary and Westfield University of London

May 2010

Centre for Endocrinology, William Harvey Research Institute, Barts and the London, Queen Mary, University of London

Abstract

Mutations in the melanocortin-4 receptor (MC4R) are the most common cause of monogenic obesity. The majority of MC4R mutations are predicted to cause the receptor to aberrantly fold. Misfolded MC4R fails to traffic to the plasma membrane (PM) and is retained in the endoplasmic reticulum (ER). Recent studies with other G-protein coupled receptors have shown that stabilisation of misfolded receptor, by pharmacological chaperones, promotes trafficking to the cell surface where the receptor may be functional. The objective of this thesis was to develop a rapid throughput cell culture based assay to monitor MC4R trafficking to the PM and to screen chemical chaperones and inducers and inhibitors of endogenous molecular chaperones, for the ability to promote folding and cell surface expression of mutant MC4R.

The work presented here confirmed that clinically occurring MC4R mutants S58C, N62S, P78L, D90N, L106P, C271Y and P299H are intracellularly retained in HEK 293 cells. The cell culture assay was used to screen a number of compounds, which have been previously reported to act as chemical chaperones by stabilising protein folding. Treatment with 4-phenyl butyric acid (4-PBA) and trehalose increased total cellular levels of wild-type and mutant MC4R. The benzoquinone ansamycin, geldanamycin, has been identified as a potent inhibitor of Hsp90 activity and an inducer of the heat shock response. Geldanamycin treatment altered the cell surface expression of wild-type and mutant MC4R. Furthermore, over expression of Hsp90 co-chaperone Aha1, also effected MC4R processing. Over-expression of Hsp70 has been shown to promote the trafficking of other aberrantly folded proteins. Over-expression of Hsc70 increased trafficking levels of wild-type and mutant MC4R and promoted mutant MC4R functional expression.

In conclusion this data suggests using compounds that stabilise protein folding and/or targeting endogenous molecular chaperone machineries may have efficacy for altering cell surface expression of mutant MC4R.

Statement of Originality

I confirm that the work presented in this thesis is my own. Where information has been derived from other sources I confirm that they are fully acknowledged in accordance with the standard referencing practises of the discipline.

Sakina B. Gooljar

Acknowledgements

I would like to start by thanking my supervisor Dr Paul Chapple for providing me with the opportunity to embark on this PhD project. I am also grateful for all his guidance, support and enduring patience, which was essential for the completion of this thesis. I would also like to thank Professor Adrian Clark for his guidance on this thesis and for creating an enjoyable working environment at the Centre for Endocrinology. I am very thankful to all the PhD students and postdoctoral research fellows within the Centre for Endocrinology for making my PhD years so fun and memorable. My thanks goes out to the incredible PC team including, David Parfitt, Dr Natasha Prodromou, Dr Esmeralda Vermeulen and in particular Dr Eirini Meimaridou who I worked with in conjunction on experiments involving Hsc70. Thank you for being such as wonderful supportive team and for being great friends.

I am also grateful to Professor Mike Cheetham at the Institute of Ophthalmology for his guidance on this project. I am especially grateful to Professor Alison Hardcastle who inspired me to pursue a scientific career and for her support throughout this PhD. I owe a special thanks to Simon, Jane, Suba, Neil, Louise, Marghe and Naheed for their support and friendship.

Thank you to Dr Shazeen Hasan for her endless encouragement and for allowing me the time to complete this thesis. Thanks boss!

Finally, I would like to express my gratitude to my parents for their unwavering support throughout this project. This is dedicated to you!

This PhD studentship was supported jointly by the Barts and the London Charity Research Advisory Board and a Barts and the London's School for Medicine and Dentistry MRC studentship.

Contents

List of figures

List of tables

Abbreviations

ACTH	Adrenocorticotropic hormone
ANOVA	Analysis of variance
ARPE-19	Human retinal epithelial cell line
ATP	Adenosine triphosphate
bp	base pair
BSA	Bovine serum albumin
cDNA	Complementary deoxyribonucleic acid
cAMP	Cyclic adenosine monophosphate
CFTR	Cystic fibrosis transmembane conductance regulator
CHO	Chinese hamster ovary cells
Co-IP	Co-immunoprecipitation
COP II	Coat protein vesicles
C-terminal	Carboxyl-terminal
DAPI	4',6-diamidino-2-phenylindole
dATP	2'-deoxyadenosine 5'-triphosphate
dCTP	2'-deoxycytidine 5'-triphosphate
DEPC	Diethyl pyrocarbonate
dGTP	2'-deoxyguanosine 5'-triphosphate
DMEM	Dulbecco's Modified Eagle Medium
DMSO	Dimethyl sulphoxide
DNA	Deoxyribonucleic acid
DNase	Deoxyribonuclease
dNTP	Deoxyribonucleotide triphosphate
dTTP	2'-deoxythymidine 5'-triphosphate
E.*coli*	*Escherichia coli*
EDTA	Ethylenediaminetetraacetic acid
ELISA	Enzyme-linked immunosorbent assay
ENDOH	Endoglycosidase H
ER	Endoplasmic reticulum

ERAD	Endoplasmic reticulum associated degradation
FCS	Foetal calf serum
FGD	Familial Glucocorticoid Deficiency
FLAG	DYKDDDDK epitope tag
GAPDH	Glyceraldehyde-3-phosphate dehydrogenase
GFP	Green fluorescent protein
GPCR	G protein-coupled receptor
HA	Hemagglutinin epitope tag YPYDVPDYA
HD	Huntington's disease
HEK293T	Human Embryonic Kidney 293T cells
HRP	Horse radish peroxidase
IBMX	3-isobutyl-1-methylxanthine
Kb	Kilobase pairs
kDa	Kilodaltons
KO	knock-out
LB	Luria Bertoni
M	Molar
MC2R	Melanocortin-2-receptor
MCRs	Melanocortin receptors
M-MLV RT	Moloney Murine Leukaemia Virus Reverse Transcriptase
MRAP	Melanocortin 2 receptor accessory protein
MRAP2	Melanocortin 2 receptor accessory protein 2
mRNA	Messenger ribonucleic acid
ND	Not determined
NDP-MSH	(Nle^{4},D-Phe^{7})-α-MSH
MSH	Melanocyte stimulating hormone
mTOR	mammalian target of rapamycin
ORF	Open reading Frame
PBS	Phosphate buffered saline
PCR	Polymerase chain reaction
PM	Plasma membrane

PNGaseF	N-Glycosidase F
POMC	Proopiomelanocortin
PVDF	Polyvinylidene Difluoride
RNase	Ribonuclease
RNA	Ribonucleic acid
rpm	Rotations per minute
RT-PCR	Reverse Transcription-polymerase chain reaction
SDS-PAGE	Sodium dodecyl sulphate polyacrylamide gel electrophoresis
SK-N-SH	Human neuroblastoma derived cell line
SOC	Super optimal culture
TAE	Tris-acetate-ethylenediaminetetraacetic acid
TMAO	Trimethylamine N-oxide
TBS	Tris buffered saline
TM	Transmembrane domain
Tris	Tris(hydroxymethyl)aminomethane
WT	Wild-type

CHAPTER 1

Introduction

1.1 Obesity

The World Health Organisation projections for 2005 indicate that globally over 1.6 billion adults are overweight (body mass index ≥ 25kg/m^2); with 400 million individuals considered clinically obese (body mass index ≥ 30 kg/m^2) (http://www.who.int, factsheet 311 September 2006). Obesity is a metabolic disorder that occurs when there is an excess in energy intake over energy expenditure, leading to an accumulation of excess fat (Ben-Sefer et al., 2009). Obesity is linked to a number of diseases including, cancer, osteoarthritis and an increased predisposition to diabetes mellitus and heart disease (Oswal & Yeo., 2007). Worryingly, the number of obese children has risen considerably over the last ten years largely due to an increase in food availability and a change in lifestyle, with an estimated 20 million children overweight in 2005 (http://www.who.int, factsheet 311 September 2006). Although environmental factors are involved in obesity it has been consistently reported that genetic factors also play a role. Quantitative genetic analyses, comprising of family based studies and twin studies, have produced high heritability for obesity with estimates of typically above 70% (Walley et al., 2006).

1.1.1 Genetics of Obesity

Obesity is a complex metabolic disease, and in recent years the genetic, biological and biochemical factors underlying this disease have begun to unravel. Obesity can be split into three different genetic types: polygenic obesity, syndromic obesity and monogenic obesity.

1.1.2 Polygenic Obesity

Polygenic obesity refers to the involvement of a number of different genes in the disease. Two different approaches have been adopted to find the genes responsible for polygenic obesity, linkage studies and association studies (Ichihara & Yamada, 2008). Both approaches have yielded results, with linkage studies

identifying a number of different gene variants in different ethnic groups. For example in West African families three quantitative trait loci (QTL) affecting body fat mass have been linked to chromosomes 2p16-p13.3 (D2S2739-D2S441), 4q24 (D4S1647-D4S2623), and 5q14.3 (D5S1725), whilst in a separate study QTLs influencing BMI in European-American families were linked to 2p24.2 and 4q28.3 and over a broad region of chromosome 13q21.1-q32.2 (Rankinen et al., 2006). Genome-wide association studies (GWAS) have identified single-nucleotide polymorphisms (SNPs), in a number of other obesity linked genes (Table 1.1). The human gene most strongly associated with obesity, identified by GWAS, is 'Fat Mass and Obesity Associated gene' (*FTO*) located on chromosome 16. SNPs within a 47-kb region, containing parts of the first two introns as well as exon 2 of *FTO* were identified to have an association with obesity in children from the age of 7 years into old age (Frayling et al., 2007). Furthermore, the transcriptional start of *RPGRIP1L* (the human ortholog of mouse *Ftm,* referred as FTM) has been reported to be ~3.4kb upstream of *FTO* in humans (Stratigopoulos et al., 2008). Therefore, due to their close proximity, it has been proposed that either *FTO* or *FTM* or both may account for the differences in adiposity in humans (Stratigopoulos et al., 2008). However it has been subsequently shown that in FTO knockout mice, where FTM expression is unaltered, a significant reduction in body weight, adipose tissue and adipocyte size was reported (Fischer et al., 2009).

1.1.3 Syndromic Obesity

Syndromic obesity describes clinically obese patients that also suffer from additional symptoms such as mental retardation and developmental abnormalities arising from discrete genetic defects or chromosomal abnormalities (Mutch & Clément, 2006). Multiple forms of syndromic obesity have been reported with the most common disorders being Prader-Willi syndrome (PWS) and Bardet-Biedl syndrome (BBS).

PWS arises from the loss of expression of the paternally transmitted genes in the imprinted region of 15q11-13. The genes expressed within this region include, *SNRPN* encoding the small nuclear ribonucleoprotein polypeptide N thought to be involved in alternative splicing of neuronal genes (Schmauss et al., 1992), *NDN* gene encoding the protein necdin a cell cycle regulatory protein (Baker & Salehi, 2002) and a cluster of small nucleolar RNAs required for RNA post-transcriptional modification (Hamma & Ferré-D'Amaré, 2010). Many of the PWS deleted genes are normally expressed in the hypothalamus, the area of the brain known to regulate energy homeostasis. Their lack of expression could indicate a central mechanism for obesity. However to date no gene within this region has been shown to be in linkage or in association with obesity. Recent studies have shown that PWS individuals have increased circulating levels of ghrelin, a hormone that stimulates food intake and acts as an endogenous ligand for the growth hormone secretagogue receptor (GHS-R) in the hypothalamus (Cummings et al., 2002). Further elucidating these mechanisms might prove useful in identifying the genes linking PWS with obesity.

Mutations in at least 12 genes have been identified as causative for BBS (Harville et al., 2009). Localisation studies have shown BBS gene products to be associated with primary cilia (Bell et al., 2005). Recent studies have shown that disruption of cilia function, by utilising conditional null alleles of ciliogenic genes *Tg737* and *Kif3a*, in adult mice caused the mice to become obese, with elevated levels of serum insulin, glucose and leptin (Davenport et al., 2007). Furthermore, by specifically disrupting cilia on pro-opiomelanocortin expressing cells, mice became obese, suggesting the involvement of neuronal cilia function in pathways regulating satiety responses (Davenport et al., 2007). Moreover BBS genes have also been shown to be required for leptin receptor signalling (LepR) in the hypothalamus and mediate LepR trafficking (Seo et al., 2009). It was reported that Bbs2(-/-), Bbs4(-/-) and Bbs6(-/-) mice, compared to wild-type (WT) littermates, did not show decreased weight loss or appetite when leptin injections were administered. The leptin resistance in these mice was attributed to attenuated leptin signalling in pro-

opiomelanocortin (POMC) neurons, as decreased levels of phosphorylated signal transducer and activator of transcription 3 (STAT3) and *Pomc* transcripts was observed (Mok et al., 2010). Interestingly, BBS1 protein has been shown to physically interact with the LepR in HEK293 cells and in ARPE-19 cells (human retinal pigment epithelial cell line) was shown to mediate the trafficking of LepR between the golgi and cell surface (Mok et al., 2010). The BBSome is a complex composed of seven of the BBS proteins and is thought to mediate vesicle trafficking to the ciliary membrane (Seo et al., 2010). In addition BBS proteins, BBS6, BBS10, and BBS12, have chaperonin-like function and form a complex with CCT/TRiC chaperonins to mediate BBSome assembly (Seo et al., 2010).

1.1.4 Monogenic Obesity

Monogenic obesity results from mutations within a single gene. Homologues for many of these genes have been identified in mice, and which, when mutated cause obesity, providing useful disease models (Oswal & Yeo, 2007). The majority of the products of these genes function in the leptin/melanocortin pathway, which is critical in the regulation of energy homeostasis (Rankinen et al., 2006). Friedman et al (1994) discovered that a mutation in the obese gene (ob) in mice resulted in no production of leptin and caused severe obesity in mice (Zhang et al., 1994). Human congenital leptin deficiency was first described in 1997 in two severely obese cousins of Pakistani origin (Montague et al., 1997). Since 1997 an additional five other affected individuals, from four different Pakistani families, homozygous for the same mutation in leptin have been identified along with three related Turkish individuals carrying a homozygous missense mutation (Arg105Trp) in the *LEP* gene (Farooqi & O'Rahilly, 2009). Leptin's involvement in regulating energy homeostasis is largely mediated by the hypothalamic melanocortin pathway. Leptin acts on two distinct sets of neurons in the arcuate nucleus (ARC); one class co-expressing POMC and Cocaine and Amphetamine Related Transcript (CART), which act to reduce food intake and a second class co-expressing neuropeptide Y (NPY) and agouti-related protein (AGRP), which increases food intake. Proteolytic

processing of the large POMC precursor by prohormone convertase 1 and 2 occurs in a tissue specific manner and results in an array of smaller biologically active products including the melanocortin peptides adrenocorticotrophic hormone (ACTH) and α, β and γ melanocyte stimulating hormone (MSH). The melanocortin peptides bind to and act as agonists for a family of five G-protein coupled receptors known as the melanocortins receptors (MCRs) with melanocortin 4-receptor (MC4R) involved in the leptin pathway. A single mutation in any one of the genes encoding leptin, the leptin receptor or another member of the leptin/melanocortin pathway results in monogenic obesity. Interestingly, mutations within MC4R are the most common cause of monogenic obesity (Fig.1.1) (Farooqi & O'Rahilly, 2009).

1.1.5 MC4R's association with Obesity

Multiple studies have reported that the genes encoding the melanocortin receptors are involved in obesity in different ethnic populations (Table 1.1). In a Québec family study both MC4R and MC5R were found to be linked to obesity phenotypes (such as adiposity, energy metabolism, and insulin and glucose homeostasis) (Chagnon et al., 1997). In a separate study in North Americans, MC4R but not MC3R mutations were found to be associated with severely obese adults (Calton et al., 2009). More recently genome-wide association studies from individuals of European descent, Indian Asians and Danes have identified variants near MC4R that are associated with increased fat mass, increased weight (Loos et al., 2008), increased waist circumference, increased insulin resistance (Chambers et al., 2008), and increased BMI (Zobel et al., 2009). These newly identified SNPs are possibly involved in regulation of the MC4R gene. Interestingly, studies investigating some specific MC4R polymorphisms have reported negative association with obesity. For example, in children and adult populations of European origin, MC4R polymorphism I251L was found to be in negative association with BMI (Stutzmann et al., 2007) and in a large meta-analysis including individuals of East Asian ancestry MC4R polymorphism V103I was also found to be negatively associated with obesity (Wang et al., 2010). Functional

studies reported that I251L increased the receptor's basal activity and V103I had decreased orexigenic antagonist affinity (Xiang et al., 2006).

Overall these studies implicate MC4R as a key modulator of body weight (Table 1.1). The importance of MC4R in the regulation of human body weight became apparent in 1998, when mutations in the human MC4R were first described as a cause for human obesity. Two separate studies reported heterozygous frameshift mutations in the human MC4R that co-segregated in a dominant fashion with severe early-onset obesity (Yeo et al., 1998; Vaisse et al., 1998). Subsequently, multiple missense and nonsense mutations in MC4R have been reported, largely in patients with severe obesity commencing in childhood. MC4R mutations now represent the commonest known monogenic cause of non-syndromic human obesity. To date over 130 human obesity causing mutations have been identified in MC4R, with approximately 2-6% of morbidly obese patients harboring mutations within MC4R (Hinney et al., 2009).

Table 1.1: Genes identified in genome wide association studies associated with obesity

Gene or SNPs	Population	Reference
SOX 6 (rs297325 & rs4756846)	Caucasians	(Liu et al., 2009)
Near MC4R (rs12970134)	Indian Asians	(Chambers et al., 2008)
Near MC4R (rs17782313)	European Ancestry	(Loos et al., 2008)
FTO (rs9939609)	U.K population	(Frayling et al., 2007)
FTO, MC4R, BDNF & SH2B1	Icelanders, Dutch, African Americans & European Americans	(Thorleifsson et al., 2009)
FTO, MC4R, TMEM18, KCTD15, GNPDA2, SH2B1, MTCH2 &NEGR	European Ancestry	(Willer et al., 2009)
NCP1, near MAF (rs1424233), Near PTER (rs10508503)	European population	(Meyre et al., 2009)
FTO, MC4R, GNPDA2, SH2B1 & NEGR	Swedish population	(Renström et al., 2009)
FTO, MC4R, NRXN3	Caucasians	(Heard-Costa et al., 2009)

1.2 Melanocortin 4-receptor: A key regulator of energy homeostasis

There are five members of the melanocortin receptor family, MC1R-MC5R, all of which have potency for MSH ligands except for MC2R which specifically binds to ACTH (Tatro JB, 1996) (Table 1.2). The MC1R is expressed in the skin and controls pigmentation. MC2R is the ACTH receptor and is expressed in the adrenal gland regulating adrenal steroidogenesis and growth. MC3R and MC4R are expressed primarily in the brain and regulate different aspects of energy homeostasis (Butler, 2006). MC5R is expressed in exocrine glands and regulates secretion from these glands. All endogenous agonists of melanocortin receptors are encoded by a single gene that generates a large precursor, POMC. This undergoes post-translational processing by prohormone convertase PC1 and PC2

to generate α-MSH, ACTH, β-MSH, γ-MSH and β-endorphin in a tissue specific manner (Table 1.2) (Nargund et al., 2006).

In 1993, the fourth melanocortin receptor was first cloned (Gantz et al., 1993). It was localised to chromosome 18 (q21.3) and found to encode a 333 amino acid protein (Gantz et al., 1993). Direct evidence that MC4R is a key regulator of appetite and body weight was provided by Huszar et al (1997), who demonstrated that mice with a targeted disruption of the MC4R gene have increased food intake, obesity and hyperinsulinaemia (Huszar et al., 1997). Animals heterozygous for the null allele showed an intermediate obesity phenotype when compared with their wildtype counterparts and homozygous WT littermates (Huszar et al., 1997).

Table 1.2: Members of the Melanocortin receptor family

Receptor	Ligand Specificity	Main site of Expression	Physiological function	Disease
MC1R	α-MSH=β-MSH= ACTH>γ-MSH	Melanocytes	Pigmentation, inflammation	Increase risk of skin cancers
MC2R	ACTH	Adrenal cortex	Adrenal steroidogenesis	FGD
MC3R	γ-MSH=ACTH= α-MSH=β-MSH	CNS, GI tract, kidney	Energy homeostasis	Obesity
MC4R	α-MSH=β-MSH= ACTH >γ-MSH	CNS	Energy homeostasis, appetite	Obesity
MC5R	α-MSH>β-MSH= ACTH>γ-MSH	Exocrine cells	Exocrine function, regulation of sebaceous glands	Decreased production of sebaceous lipids in mice

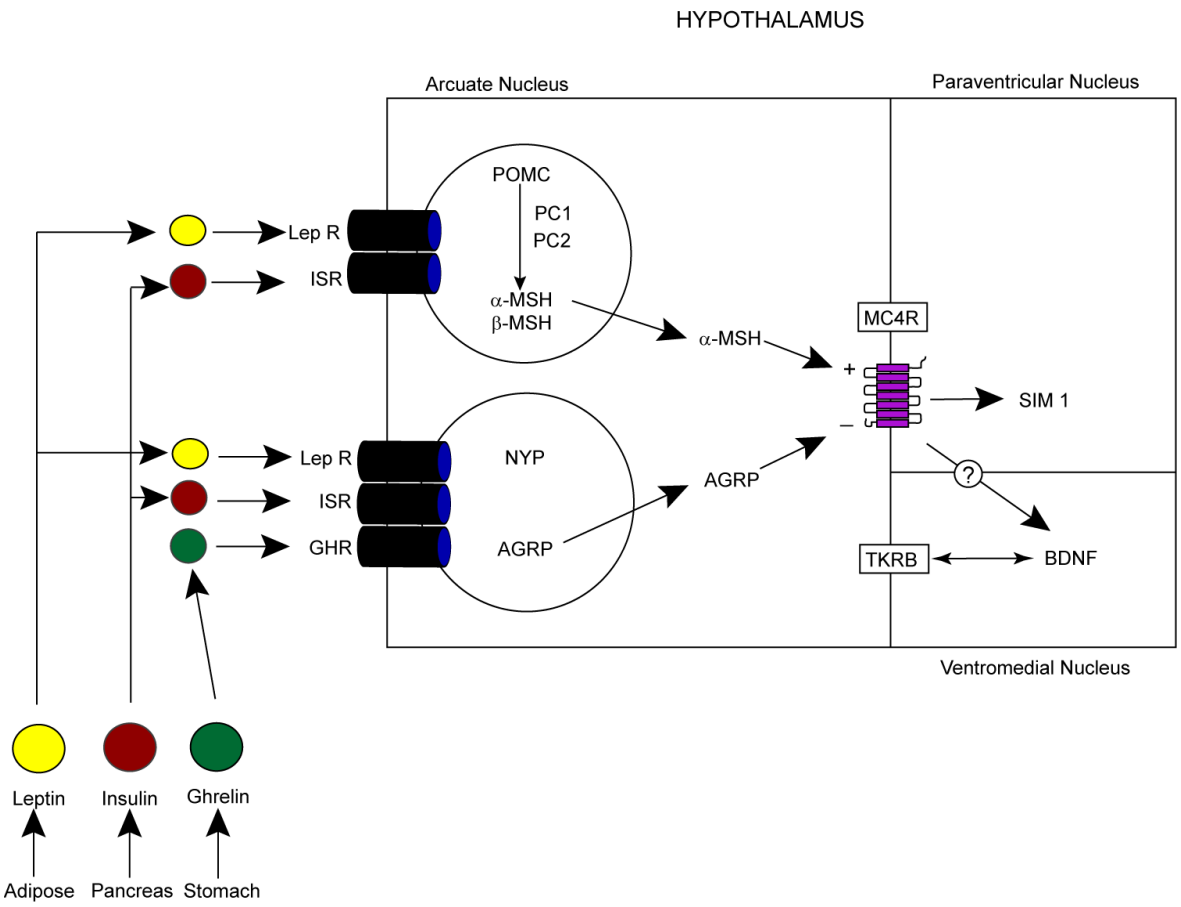

Figure 1.1: The melanocortin pathway

Distinct neuronal populations control and regulate food intake and satiety. POMC neurons in the arcuate nucleus are activated by leptin and insulin and produce α-MSH, which leads to the activation of MC4R in the paraventricular nucleus, resulting in a satiety signal. A separate population of neurons expressing NYP and AGRP produce molecules that inhibit MC4R signalling. The downstream roles of SIM1, BDNF, and TKRB in energy homeostasis remains to be fully elucidated. POMC, proopiomelanocortin; α-MSH, alpha melanocyte stimulating hormone; NYP, neropeptide Y; PC1 and 2, proconvertase 1 and 2; GHR, ghrelin receptor; ISR, insulin receptor; LepR, leptin receptor; SIM1, single-minded homologue 1 (*Drosophila*); TRKB, tyrosine kinase receptor; BDNF, brain-derived neurotrophic factor. Adapted from Balthasar et al (2005).

1.3 MC4R: A G-protein coupled receptor

MC4R is a member of the G-protein coupled receptor family (GPCRs). GPCRs are the largest class of transmembrane proteins in the human genome. The crystal structures of two GPCRs, Rhodopsin and human β2 adrenergic receptor, have been solved leading to a better understanding of GPCRs active and non-active conformations (Palczewski et al., 2000; Rasmussen et al., 2007). The structural features of GPCRs include (Rosenbaum et al., 2009; Hofmann et al., 2009):

- Seven transmembrane (TM) spanning helices with a cytoplasmic 8^{th} helix running parallel to the membrane surface
- For rhodopsin the extracellular domain and the ligand binding site is very compact to shield the hydrophobic ligand but for other GPCRs the extracellular domain has been reported to have a more open conformation to allow for the entrance of diffusible water soluble ligands
- The conserved DRY motif forms part of a hydrogen bonding network linking TM3 and TM6 in an 'ionic lock' stabilising the inactive state of rhodopsin
- The NPXXY motif localised to the cytoplasmic end of TM7 causes a conformational change in the inactive GPCR allowing for the formation of hydrogen bonds which presumably stabilises the inactive GPCR, but the bonds formed are thought to be weak allowing for the rapid toggling to the active state upon agonist binding

All GPCRs have the basic structural elements (listed above) but are divided into six different classes based on sequence similarity between the seven transmembrane (TM) regions and function (Gao & Wang, 2006):

- Class A- Rhodopsin-like
- Class B- Secretin receptor family
- Class C- Metabotropic glutamate/pheromone
- Class D- Fungal mating pheromone receptors
- Class E- Cyclic AMP receptors
- Class F- Frizzled/Smoothened

The Class A (Rhodopsin-like) GPCRs, of which MC4R is a member, comprises over a 1000 receptors and can be further divided into sub-classes with the amine and olfactory receptors including ~165 and ~551 proteins respectively (Gao & Wang, 2006).

1.3.1 Trafficking of GPCRs

Before GPCRs can carry out their functions they need to acquire the correct native conformation. Different organelles within the cell, such as the endoplasmic reticulum (ER) and mitochondria, possess different folding conditions for proteins of different functions (Riemer et al., 2009). The cellular conditions within the ER favour folding of ER, transmembrane and secreted proteins including GPCRs. The ER possesses a highly oxidising environment to promote the formation of disulfide bonds required for protein folding/stabilisation and the homeostatic balance of the redox environment of the ER is maintained by numerous redox proteins including, thiol-disulfide oxidoreductases, protein disulfide isomerase (PDI) and associated flavoprotein Ero1p (Sevier et al., 2007). Synthesis of transmembrane polypeptides occurs on membrane bound ribosomes. Nascent polypeptides are co-translationally translocated into the ER through the Sec61 translocon complex (Naidoo, 2009). To preserve cellular homeostasis a number of molecular chaperones reside within the ER and are involved with the assembly, folding and

the quality control of nascent polypeptides. There are three main groups of ER chaperones (Ni & Lee, 2007):

(a) chaperones of the heat shock family e.g. BiP, GRP79
(b) chaperone lectins e.g. calnexin, calreticulin, EDEM
(c) substrate specific chaperones e.g. Hsp47

Calnexin an ER membrane protein and calrecticulin an ER luminal protein recognise nascent polypeptides with monoglycosylated N-linked glycans and target them for subsequent folding and assembly steps. If correct folding of the protein is not achieved another ER protein UDP-glucose glycoprotein-glucosyltransferase (UGGT) is thought to recognise the exposed hydrophobic regions on the unfolded/misfolded polypeptide (Ni & Lee, 2007). UGGT catalyses the transfer of a glucose unit to a specific mannose residue within the N-linked glycan, resulting in the regeneration of a polypeptide with monoglycosylated N-linked glycans, and provides a new binding site for calnexin/calrecticulin for refolding of the peptide (Ni & Lee, 2007). BiP, an ER member of the Hsp70 protein family possesses an ATPase binding domain and a peptide domain. BiP also recognises exposed hydrophobic regions on misfolded polypeptides and within a large multi-complex protein unit, including GRP94 (Hsp90 ER homologue), misfolded protein substrates are processed for assembly and folding (Ni & Lee, 2007).

Once the native conformation of the receptor is achieved GPCRs are able to exit the ER in COP II (coat protein) vesicles mediated by ER export signal in the C-termini of the GPCR binding to components of the COP II vesicles (Dong et al., 2007). There are several motifs that have been identified in the C-terminus for different GPCRs that play a critical role for ER export. These include the $FN(X)_2LL(X)_3L$ motif found within the vasopressin receptors, the $E(X)_3LL$ (dileucine) motif for GPCRs including the vasopressin V2 receptor, and the melanocortin receptors; $F(X)_3F(X)_3F$ (triple phenylalanine) motif found in the dopamine D1 receptor, and the $F(X)_6LL$ motif found within the $\alpha_{2\beta}$-adrenergic receptor ($\alpha_{2\beta}R$) and the angiotensin II type 1 receptor (Dong et al., 2007). N-terminal export signals

have not been fully elucidated and although necessary for some GPCRs to be exported from the ER (e.g.endothelin B receptor and $\alpha_{2\beta}$R) they are not necessary for the export of other GPCRs (α_{1D}R) (Dong et al., 2007).

Packaged in COP II transport vesicles, GPCRs exit the ER via the ER-Golgi intermediate complex (ERGIC), through the Golgi and then the trans-Golgi network (TGN). As the receptor progresses through the secretory pathway it undergoes post translational modifications until finally the mature GPCR reaches its functional destination at the cell surface (Dong et al., 2007). RabGTPases have been found to be involved in almost every step of GPCR anterograde trafficking in particular with targeting, tethering and fusion of receptor transport vesicles with the appropriate cell surface membrane (Dong et al., 2007).

1.3.2 Post-translational modifications of GPCRs

1.3.2.1 Glycosylation of GPCRs

The majority (~ 95%) of GPCRs undergo the addition of saccharides to nascent polypeptides in the biosynthetic events of glycosylation (Yurugi-Kobayashi et al., 2009). N-linked glycosylation involves the addition of, three glucose, nine mannose and two *N*-acetylglucosamine molecules, to the nascent polypeptide chain as it is translocated into the ER lumen and this occurs at the consensus sequence Asn-Xaa-Ser/Thr (Duvernay et al., 2005). N-linked glycoslation has been shown to be essential for GPCRs to achieve the correct conformation to be exported from the ER. For example, shifting the N-linked glycoslation site of the human angiotensin II receptor subtype 1 caused it to have reduced cell surface expression and binding affinity due to an abnormal conformation of the polypeptide (Lanctot et al., 2005). A similar result was also observed for the neurokinin 1 receptor (NK1R) where glycosylation mutants possessed half the signalling capabilities of the (WT) receptor and double mutants internalised more rapidly indicating that N-linked glycoslation may be required for the stabilisation of NK1R in the plasma membrane

(Tansky et al., 2007). Further processing of the glucose and mannose chains occurs after export of the folded and immaturely glycoslated protein from the ER to the Golgi. The Golgi is thought to be the site of *O*-linked glycosylation. *O*-linked glycosylation involves the addition of N-acetyl-galactosamine to serine or threonine residues followed by the addition of other carbohydrates such as glucose or sialic acids to form a mature glycoprotein (Ruddock & Molinari 2006). However unlike N-linked glycosylation, *O*-linked glycosylation lacks a known consensus motif and therefore has been more difficult to study (Duvernay et al., 2005).

1.3.2.2 Palmitoylation of GPCRs

Other post-translational modifications of GPCRs occur. This includes the addition of lipids, most commonly in the form of the 16 carbon saturated fatty acid, palmitic acid to cysteine residues proximal to the cytosolic end of the seventh transmembrane (in the case of rhodopsin and the β_2-adrenergic receptor) (Qanbar & Bouvier, 2003). The extent of GPCR palmitoylation has been shown to depend on agonist activation in that agonist binding increases the proportion of receptors being palmitoylated or agonist binding increases the turnover rate of receptor-linked palmitate (Chini & Parenti, 2009). Palmitoylation has a number of functional consequences for GPCRs. Lack of palmitoylation has been shown to cause a decrease in the cell surface expression of some GPCRs including the dopamine, vasopressin, chemokine and δ-opioid receptors, indicating palmitoylation occurs at the ER (Chini & Parenti, 2009). Palmitoylation of the β_2-adrenergic receptor has been shown to be necessary for the efficient coupling of the receptor to Gs protein and also affects its desensitisation and internalisation upon agonist stimulation (Chini & Parenti, 2009).

1.3.2.3 Phosphorylation of GPCRs

It is thought that the primary function of receptor phosphorylation is to cause the attenuation of GPCR signalling by promoting the recruitment of arrestin (Tobin et al., 2008). Phosphorylation sites for the majority of GPCRs are located at the C-terminus or within the third intracellular loop. Phosphorylation is regulated by members of the G-protein-coupled-receptor kinase (GRK) family (Tobin et al., 2008). For MC4R it has been shown that both protein kinase A (PKA) and GRKs, in particular GRK2, are involved in MC4R phosphorylation and that Thr312 and Ser329/330 in the C-terminal tail are potential sites for PKA and GRK phosphorylation (Shinyama et al., 2003).

Phosphorylation of non-visual GPCRs results in a ~2-3 fold increase in affinity binding sites for β-arrestins, resulting in the uncoupling of the G proteins from the receptor and receptor desensitisation (Tobin, 2008). It is thought that β-arrestin-1 and -4 are expressed solely in rod and cone photoreceptors and regulate the phototransduction of visual GPCR rhodopsin, with arrestin-2 and -3 regulating the signalling of non-visual GPCRs (Tobin, 2008). For MC4R, (a non visual GPCR), overexpression of dominant-negative mutants of β-arrestin1-V53D was found to prevent desensitisation and subsequent internalisation of MC4R in HEK293 cells (Shinyama et al., 2003). Recently, it has been shown that β-arrestins act as scaffolding proteins and are involved in numerous developmental signalling pathways including Hedgehog, Wnt, Notch, and TGFbeta pathways (Kovacs et al., 2009). Interestingly, β-arrestin has been implicated in the regulation of inflammatory signalling cascades involving mitogen activated protein kinases (MAPK) (Kovacs et al., 2009) and MC4R activation *in vitro* has also been shown to increase the phosphorylation of MAPK in hypothalamic neurons indicating MC4Rs involvement in inflammatory pathways (Lasaga et al., 2008).

β-arrestin binding to the GPCR also mediates the formation of clathrin-coated-vesicles that causes endocytosis of the GPCR. At this point the GPCR can become

degraded by lysosomes, causing a down-regulation of GPCR at the cell surface, or may recycle back to the cell surface for re-signalling (Gao et al., 2003). Exposure to α-MSH causes rapid internalisation of MC4R in HEK293 cells (Gao et al., 2003; Shinyama et al., 2003). Furthermore, inefficient recycling back to the cell surface was observed for MC4R and MC4R ligand in HEK293 cells (Gao et al., 2003). In addition, another study has reported that MC4R inverse agonist AGRP also induces β-arrestin mediated endocytosis of MC4R in a cell line derived from murine hypothalamic neurons endogenously expressing MC4R (Breit et al., 2006).

1.3.2.4 GPCR dimerisation

Numerous GPCRs have been shown to oligomerise with varying stability. In some cases they form permanent covalent bonds existing as dimers, or contrastingly, have fleeting unstable interactions (Gurevich & Gurevich, 2008). The majority of GPCR dimers are believed to be homodimers. However, there is increasing evidence of GPCR heterodimerisation (Milligan et al., 2008).

Extensive studies on Class C GPCRs provide an insight into what domains are involved in the formation of GPCRs dimers. For Class C GPCRs cystine rich domains (CRDs) have been shown to have a high propensity to dimerise (Gurevich & Gurevich, 2008). In addition, Class C GPCRs (e.g. glutamate receptors) have an N-terminal Venus flytrap module (VFT), and when expressed with an unrelated receptor (e.g natriuretic peptide receptor) are able to dimerise with its transmembrane domain, with or without ligands (Gurevich & Gurevich, 2008). For MC4R it has been shown that the receptor dimerises independently of unpaired extracellular cysteine residues indicating that the transmembrane region may be involved in receptor dimerisation (Elsner et al., 2006).

Dimerisation of GPCRs is thought to occur at the ER. This has been shown for the class A, β_2-adrenoceptor and chemokine receptors and the class C, metabotropic glutamate receptor-like $GABA_B$ receptor (Milligan, 2010). For MC4R a disulphide bond forms between C271-C277 and if disrupted cell surface expression of the

receptor is greatly reduced. However, MC4R mutants that lacked this disulphide bond showed a dimerisation pattern comparable to the WT receptor indicating that MC4R dimerisation occurs early in GPCR life cycle possibly at the ER (Elsner et al., 2006).

It has been shown for rhodopsin, the β_2-adrenoceptor (β_2AR) and the neurotensin NTS1 receptor, three receptors that couple to three different G proteins, that one monomer in its active conformation is required to couple to a G protein and that dimeric forms of the receptor reduces or do not augment signalling (Gurevich & Gurevich, 2008). However receptor dimerisation, if not required for signalling, may be required for receptor desensitisation and intracellular trafficking (Gurevich & Gurevich, 2008).

1.3.2.5 GPCR signalling and conformational states

After agonist binding to the transmembrane and/or extracellular regions, GPCRs undergo a conformational change from their inactive state to their active state (Ritter & Hall, 2009). Acting as guanine nucleotide exchange factor, GPCRs interact with heterotrimeric G proteins catalysing the exchange of GDP (guanosine diphosphate) for GTP (Guanosine-5'-triphosphate) on the Gα subunit, initiating the dissociation of Gα and Gβγ from each other and from the GPCR (Ritter & Hall, 2009). Subsequently, the activated GTP Gα subunit can regulate the activity of downstream effectors such as adenylyl cyclase, that then go on to modulate further downstream effectors such as PKA through the generation of second messengers (e.g. cyclic AMP) (Fig. 1.2) (Ritter & Hall, 2009). Attenuation of GPCR signalling can be mediated through phosphorylation of the receptor resulting in receptor internalisation. However, it has been shown that some GPCRs can remain associated with their cognate G protein subunit after internalisation and continue to stimulate cAMP production within endosomal compartments (Jalink & Moolenaar, 2010). Furthermore, some GPCRs are capable of signalling independent of G protein activation (Sun et al., 2007). For example, the β_2AR has been shown to

switch from G protein-coupled to G protein-independent ERK (extracellular signal-regulated kinase) activation in an agonist dosage-dependent manner (Sun et al., 2007). It is thought that MC4R couples exclusively to G proteins (G_S coupling specificity) with α-MSH binding sites on the first extracellular loop and the N-terminus (Srinivasan et al., 2003).

The exact way in which conformational change of the receptor occurs after ligand binding has not yet been elucidated for MCRs, but the structural changes observed for rhodopsin and human β_2 adrenergic receptor have lead to a number of kinetic models to describe the conformational changes for GPCRs in general. The simplest of these models proposes that the receptor exists primarily in two states, an active state (R*) and an inactive state (R). If this model where applied to MC4R then in the absence of its ligand, α-MSH, the basal level of MC4R would be determined by the equilibrium between R* and R. Full agonists such as α-MSH would fully bind to MC4R and stabilise R*, while inverse agonists, AGRP, bind to and stabilise R. Partial agonists would have some affinity for both R and R* and therefore would be less effective in shifting the equilibrium towards R* (Kobilka, 2007).

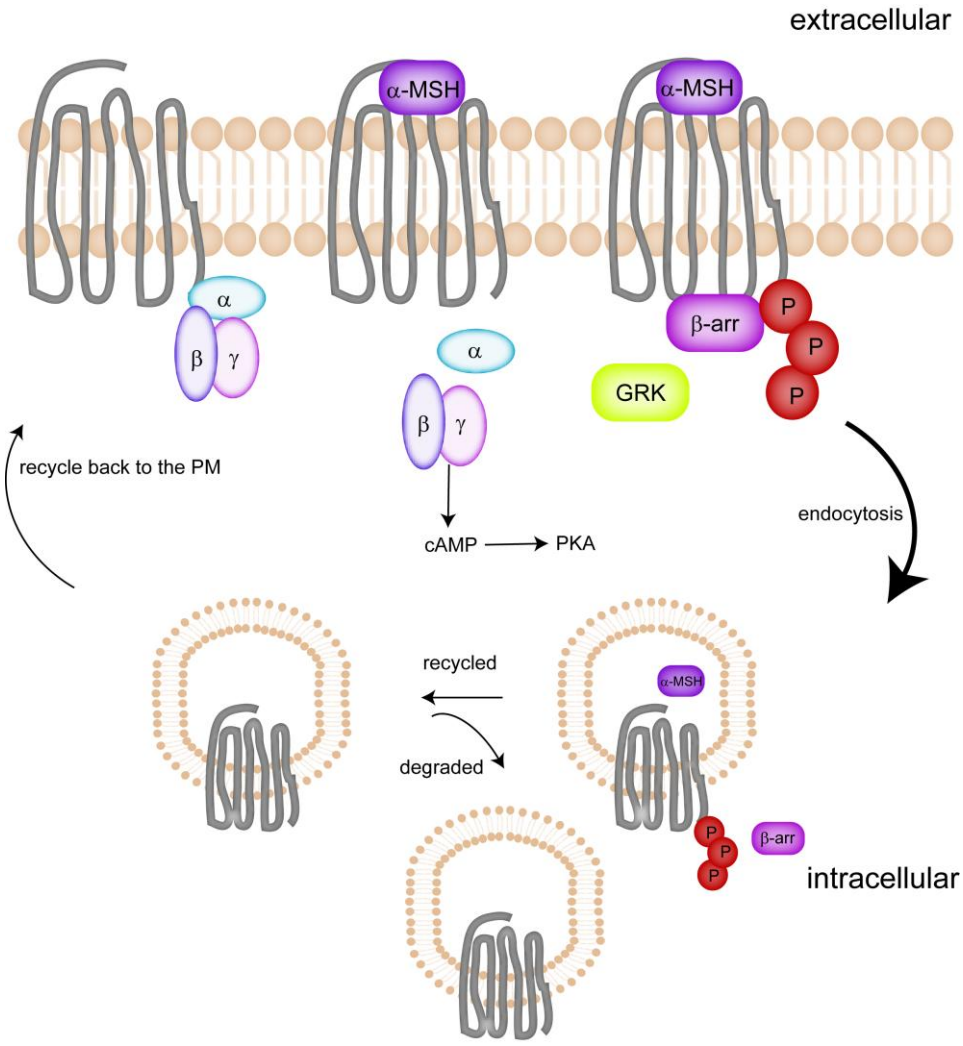

Figure 1.2 Schematic of MC4R signalling and phosphorylation

The GPCR is activated by agonist leading to activated G protein leading to an increase in cAMP production which in turn activates PKA. The agonist-occupied GPCR is subsequently phosphorylated by GRK and arrestin binds to the phosphorylated GPCR, leading to receptor desensitisation, internalisation, dephosphorylation and recycling of the GPCR. Particularly with longer agonist treatments, internalised GPCR may also be targeted for degradation.

α, β, γ, G-protein subunits; α-MSH, alpha melanocyte stimulating hormone; cAMP, cyclic adenosine monophosphate; PKA, protein kinase A; GRK, G protein-coupled receptor kinase; β-arr, β-Arrestins; P, phosphate group. Adapted from Ritter & Hall (2009).

1.4 MC4R mutations

Over 70 missense, nonsense and frame shift mutations in MC4R have been identified; these are found across several different ethnic groups. Based on the life cycle of GPCRs a general classification scheme has been established to categorise GPCR mutations; Class I: defective receptor biosynthesis, class II: defective trafficking to the cell surface, class III: defective ligand binding, Class IV: defective receptor activation and Class V: mutant with no known defects (Tao, 2005). An increasing number of MC4R mutations have been functionally characterised with many showing decreased cell surface expression resulting in reduced receptor function (Table 1.3). These mutations have been categorised as class II MC4R mutations. The defective trafficking to the cell surface of these mutants is believed to be due to misfolding of the protein leading to its detection by ER quality control systems, retention in the ER and subsequent degradation by ER associated protein degradation (ERAD) (discussed in Chapter 1, Section 1.9.3). For this study seven point mutations were selected all of which have been previously reported to have reduced cell surface expression and have been characterised as Class II mutations. These were, Ser58Cys, Asn62Ser, Pro78Leu, Asp90Asn, Leu106Pro, Cys271Tyr and Pro299His (Fig.1.3).

The missense mutation Ser58Cys (S58C) was identified as dominantly inherited in 4 of 63 severely obese children in a Turkish population (Dubern et al., 2001). In a separate French study mutant MC4R (S58C) was shown to have impaired response to α-MSH (Lubrano-Berthelier et al., 2003).

Ans62Ser (N62S) was the first homozygous mutation to be described in obese individuals and inherited with as a recessive allele. MC4R (N62S) was found in five children with severe obesity from a consanguineous pedigree of Pakistani origin. Heterologously expressed MC4R (N62S) in HEK293 cells showed a limited response to α-MSH (Farooqi et al., 2000).

Screening the coding region of MC4R in 306 extremely obese children and adolescents (mean body mass index: BMI 34.4 ± 6.6 kg/m^2) by single strand conformation polymorphism analysis identified the missense mutation Pro78Leu (P78L) (Hinney et al., 1999). The mutation was identified in only extremely obese patient whose BMIs were all above the 99th percentile, suggesting that MC4R (P78L) is a severe mutation. Furthermore, functional studies show P78L had poor cell surface expression and reduced activation upon agonist stimulation possibly due to intracellular retention (Nijenhuis et al., 2003).

Asp90Asn (D90N) was the first MC4R mutation reported to have a dominant negative effect on the WT receptor, through the formation of receptor heterodimers. The D90N loss of function mutation was found to have some cell surface expression, but loss of Gs/adenylyl cyclase activation (Biebermann et al., 2003).

The mutation Leu106Pro (L106P), located in the first extracellular loop of the receptor was found to be associated with severe familial early onset obesity and to have a limited response to α-MSH (Yeo et al., 2003).

Cys271Tyr (C271Y) was identified in a U.K based study, where it was shown to be inherited in an autosomal dominant manner in an early onset severely obese cohort (Farooqi et al., 2003). C271Y was shown to have a lack of cell surface expression and reduced signalling compared to WT receptor (Tao & Segaloff, 2003).

A French cohort of 172 patients presenting with severe childhood obesity and a family history of obesity, identified Pro299His (P229H) in 3 individuals. Functional studies indicated that P299H had a reduced cell surface expression compared to the WT receptor and no activation upon agonist (α-MSH) stimulation (Lubrano-Berthelier et al., 2003).

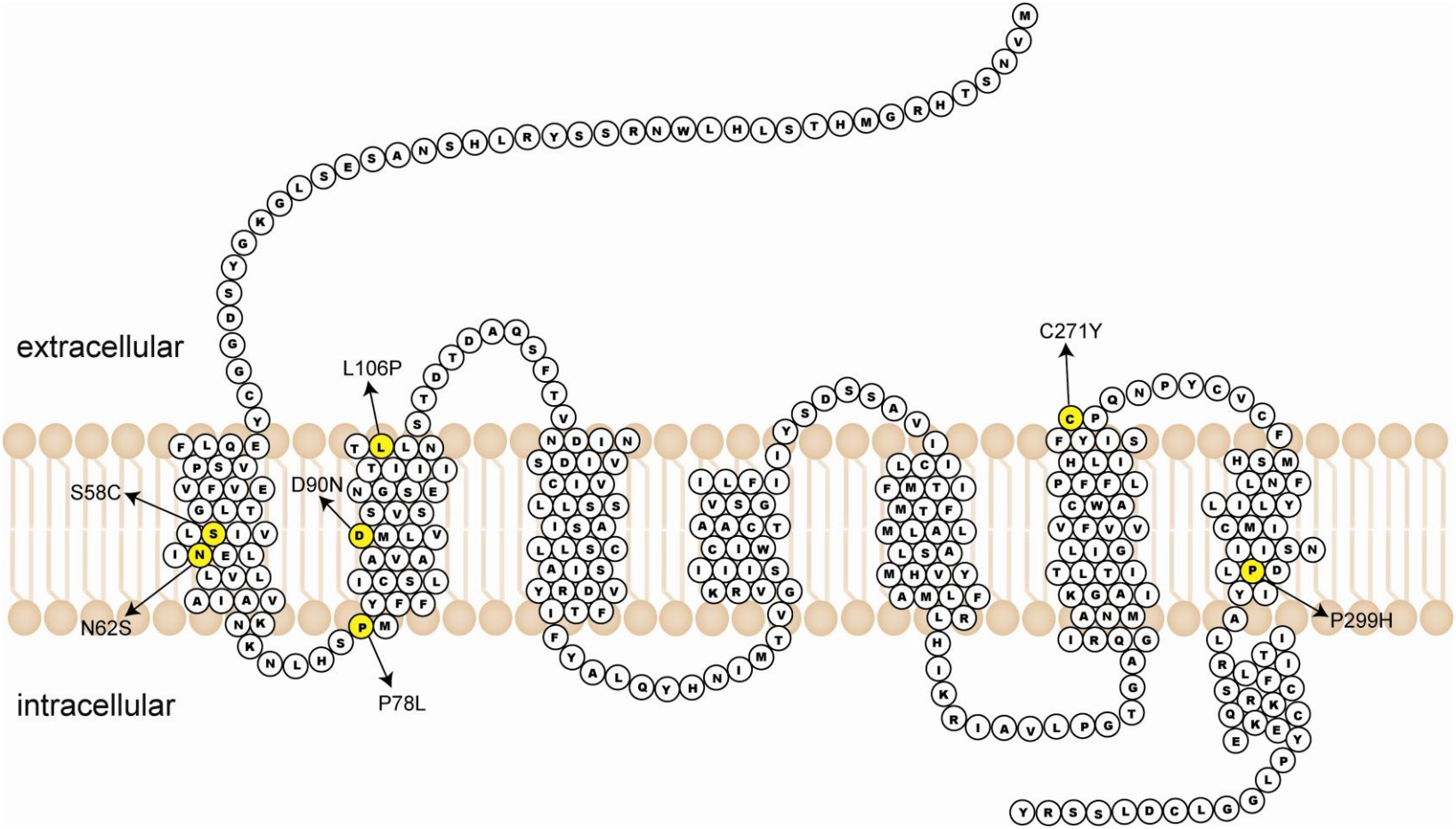

Figure 1.3: Clinically occurring MC4R mutations used in this study

Table 1.3: MC4R mutations response upon agonist stimulation and reported cell surface expression

Mutation	Response to NDP-MSH stimulation	Reported cell surface expression	Reference
Frameshift CTCT (@ codon 211)	no response	ND	(Lubrano-Berthelier et al., 2003)
Insertion TGAT (@ codon 244)	ND	ND	(Tao & Segaloff, 2003)
750-751GA	ND	ND	
S58C	partial	decreased	(Lubrano-Berthelier et al., 2003)
N62S	partial	decreased	(Farooqi et al., 2000)
P78L	no response	decreased	(Nijenhuis et al., 2003)
G98R	no response	ND	(Kobayashi et al., 2002)
I102S	partial	0-10% expression	(Xiang et al., 2006)
L106P	no response	11-50% expression	(Yeo et al., 2003)
I125K	no response	0-10% expression	(Xiang et al., 2006)
R165Q	partial	11-50% expression	(Xiang et al., 2006)
R165W	ND	11-50% expression	(Xiang et al., 2006)
N240S	partial	YES	(Tao & Segaloff, 2003)
L250Q	ND	decreased	(Xiang et al., 2006)
Y287X	no response	11-50% expression	(Xiang et al., 2006)
C271R	ND	decreased	(Tarnow et al., 2003)
C271Y	partial	11-50% expression	(Tao et al., 2003)
P299H	no response	11-50% expression	(Lubrano-Berthelier et al., 2003)
I316S	partial	decreased	(Xiang et al., 2006)
I317T	partial	decreased	(Xiang et al., 2006)
D90N	partial	YES	(Biebermann et al., 2003)
I125K	partial	11-50% expression	(Xiang et al., 2006)
V103I	YES	YES	(Xiang et al., 2006)

Mutation	Response to NDP-MSH stimulation	Reported cell surface expression	Reference
I170V	ND	decreased	(Xiang et al., 2006)
S30F	partial	decreased	(Xiang et al., 2006)
G252S	partial	decreased	(Xiang et al., 2006)
R165Q	ND	ND	(Xiang et al., 2006)
Y157S	partial	decreased	(Lee et al., 2008)
Y35stop	NO	0-10% expression	(Xiang et al., 2006)
V95I	NO	0-10% expression	(Xiang et al., 2006)
N97D	ND	11-50% expression	(Xiang et al., 2006)
I130T	ND	11-50% expression	(Xiang et al., 2006)
TM5del	NO	0-10% expression	(Xiang et al., 2006)
TM6Ins	NO	0-10% expression	(Xiang et al., 2006)
L54P	partial	decreased	(Tan et al., 2009)
E61K	partial	decreased	(Tan et al., 2009)
I69T	partial	decreased	(Tan et al., 2009)
S136P	partial	decreased	(Tan et al., 2009)
M161T	partial	decreased	(Tan et al., 2009)
T162I	partial	decreased	(Tan et al., 2009)
I269N	partial	decreased	(Tan et al., 2009)
G55V	partial	YES	(Tan et al., 2009)
G55D	partial	YES	(Tan et al., 2009)
S136F	partial	YES	(Tan et al., 2009)
A303T	partial	YES	(Tan et al., 2009)
S127L	partial	YES	(Xiang at el., 2006)
A244E	partial	YES	(Xiang at el., 2006)
V253I	partial	YES	(Xiang at el., 2006)
L250Q	ND	decreased	(Lubrano-Berthelier et al., 2003)

1.5 The fate of misfolded proteins

For MC4R mutations, the most common functional defect is intracellular retention; this is believed to be a result of aberrant folding of the protein (Lubrano-Berthelier et al., 2003). Generally, misfolded proteins can compromise the viability of a cell by either loss of function, gain of function or both. For example, Huntington's disease (HD) is caused by trinucleotide CAG repeats in the coding sequence of the HD gene. This translates into the expansion of polyglutamine tracts in the cytosolic huntingtin protein, which is thought to cause a toxic gain of function with the mutant huntingtin protein interfering with the functions of other proteins (Zoghbi & Orr, 2000; Rubinsztein, 2003). Whereas, for spinobulbar muscular atrophy, the expansion of the CAG repeats in the coding region of the androgen receptor gene is thought to cause partial loss of function of the androgen receptor, resulting in androgen insensitivity in affected males (Zoghbi & Orr, 2000). Therefore a sophisticated quality control mechanism enables recognition of conformationally aberrant proteins and their subsequent degradation, via autophagy and/or the ubiquitin proteasome system (UPS).

1.5.1 The unfolded protein response

The unfolded protein response (UPR) is a cellular stress response that is triggered by the accumulation of unfolded or misfolded proteins in the ER (Bakau et al., 2006). The UPR utilises three main sensors for monitoring folding, endoplasmic reticulum-to-nucleus signalling 1 (IRE1), ER membrane protein kinase (PERK) and transmembrane transcription factor ATF6 (activating transcription factor 6) (Bukau et al., 2006). Activation of the PERK kinase in the presence of ER stress causes inhibition of translation and the upregulation of transcription factor ATF6. The accumulation of misfolded proteins allows ATF6 to reach the Golgi where it is cleaved by transmembrane proteases, site 1 protease (S1P) and proteases site 2 protease (S2P), resulting in a cytosolic fragment. The cytosolic fragment then migrates to the nucleus to activate transcription. ER stress causes

autophosphorylation and subsequent activation of IRE1 RNase activity resulting in splicing of XBP1 (x-box binding protein 1) to generate mature XBP1 mRNA, mediating transcription of ER chaperones and the ERAD machinery. The ER chaperone BiP (immunoglobulin heavy chain binding protein1 or glucose regulated protein, Grp78) acts as the master regulator of IRE1, PERK and ATF6. ER stress causes BiP to bind to unfolded protein and results in its release from the UPR transducers, allowing for their subsequent activation and proteolysis. Prolonged UPR activation leads to apoptotic cell death and cell cycle arrest to prevent cells from progressing through the cell cycle (Liu & Kaufman., 2003).

1.5.2 ER associated degradation pathway

ERAD degrades proteins that are unable to achieve their native conformation. These misfolded polypeptides are recognised by molecular chaperones and targeted for degradation by the ubiquitin- proteasome machinery (Vembar & Brodsky, 2008).

Aberrantly folded proteins are recognised as ERAD substrates through the exposure of hydrophobic regions, which would otherwise have been buried within the native conformation of the polypeptide (Vembar & Brodsky, 2008). To prevent aggregation of these proteins molecular chaperones, such as Hsp70, regulated by Hsp40 and nucleotide exchange factors (NEFs), interacts with the misfolded protein in an ATP-dependant binding and release cycle (Vembar & Brodsky, 2008). The ER homologue of Hsp70, BiP and ER resident Hsp40 co-chaperones have been shown to maintain the solubility of misfolded proteins (Hegde et al., 2006). Prolonged association of Hsp70 with the aberrantly folded proteins causes polyubiquitination of the protein by E3 uibiquitin ligases. Aberrantly folded proteins are also targeted for ERAD by possible recognition of abnormal N-linked glycan status or disulphide bond status (Vembar & Brodsky, 2008).

Once substrates for ERAD have been identified they are targeted to the retrotranslocation channel and retrotranslocated back into the cytoplasm where

they are degraded by the UPS. Several ER resident proteins that target glycoproteins for retrotanslocation have been identified, including ER degradation-enhancing α-mannosidase-like lectins (EDEMs) and lectins that contain mannose-6-phosphate receptor-like domains, OS9 and XTP3-b (Vembar & Brodsky, 2008).

Prior to degradation by the proteasome, ERAD substrates are ubiquitylated by E1 ubiquitin-activating enzyme, E2 ubiquitin-conjugating enzymes and E3 ubiquitin ligases. In mammals E3s such as membrane associate RMA1 (RING-finger protein with membrane anchor-1) and cytoplasmic CHIP (C terminus of HSC70-interacting protein) have been shown to ubiquitylate the cystic transmembrane conductance regulator (CFTR), whilst another E3, Parkin, has been shown to ubiquitylate the Pael receptor GPCR (Imai et al., 2002).

1.5.3 Autophagy

In addition to ERAD, autophagy is another mechanism by which misfolded proteins are removed from the cellular environment. Three different types of autophagy have been described in mammalian cells: macroautophagy, microautophagy, and chaperone-mediated autophagy (CMA) (Martinez-Vicente & Cuervo, 2007). The induction of macroautophagy by the accumulation of misfolded proteins leads to the formation of *de novo* membranes in the cytoplasm (phagophores), which expands into a spherical double membrane bound structure known as the autophagosomes that engulf cargo for degradation and fuse with lysosomes (Nakatogawa et al., 2009). In microautophagy, substrates for degradation are directly internalised through invaginations of the lysosomal membrane. Whereas CMA involves selective degradation of substrate proteins, which after binding to lysosomal receptors are translocated to the lysosome for degradation (Martinez-Vicente & Cuervo, 2007). Hsc70, the constitutive member of 70kDa chaperone family, recognises the CMA substrate motif and delivers the substrate protein to the lysosome. Once at the lysosomal membrane each CMA substrates binds to

lysosome associated membrane protein type-2 (LAMP-2A) before translocation can occur (Cuervo, 2010).

1.6 Approaches to rescue the function of misfolded ER retained proteins

A number of other genetic diseases are linked to aberrant folding and ER retention of transmembrane proteins. These include cystic fibrosis, nephrogenic diabetes insipidus, and retinitis pigmentosa. A number of different therapeutic approaches have been tested to restore cell surface expression of intracellularly retained transmembrane proteins; the majority of these involve stabilising the misfolded protein. This has been achieved using three main approaches:

I. kosmotropes

II. small molecular ligands

III. manipulating the cellular molecular chaperone environment

1.6.1 The use of kosmotropes

Kosmotropes, such as dimethyl sulfoxide (DMSO), 4-phenly butric (4-PBA) and trimethyl N-oxide dihydrate (TMAO), are small molecular weight compounds that facilitate folding without direct specific binding to the mutant protein (Cohen & Kelly., 2003). Chemical chaperones have also been shown to improve transport and enhance stability of mutant α-glucosidases in glycogen storage disease type II (GSDII). GSDII, is an autosomal recessive disorder, caused by lysosomal acid α-glucosidase (AαGlu) deficiency resulting predominantly in skeletal muscle weakness. It was demonstrated that treatment of cultured fibroblasts, from GSDII patients, with 10 µl N-(n-butyl) α-glucosidasedeoxynojirimycin (NB-DNJ) promoted export of mutant AαGlu from the ER to the lysosomes, where normal activity was restored (Okumiya et al., 2007).

1.6.2 The use of small molecular ligands

Nephrogenic diabetes insipidus (NDI) a rare X-linked disease is caused by mutations within the GPCR V_2 vasopressin receptor. In most cases mutations within the receptor lead to the retention of the misfolded receptor in the ER. Affected patients suffer from an increased urinary output and infants are affected by severe episodes of dehydration resulting in growth and mental retardation (Robert et al., 2005). Previous studies have shown that treatment of cells, expressing the V_2 receptor, with non-peptidic V_2 receptor antagonists (SR121463, VPA985) are able to restore cell surface expression of mutated misfolded receptor (Bernier et al., 2004).

The gonadotophin-releasing hormone (GnRHR) provides another example of cell surface rescue of a misfolded GPCR by non-peptidic antagonists. In this case treatment with GnRHR selective antagonist IN3 restored cell surface expression of eleven misfolded mutants. Furthermore, the rescued mutant receptor, similar to WT GnRHR, exhibited agonist mediated endocytosis suggesting that the mutant receptor had normal pharmacological and biochemical properties once released from the ER (Leanos-Miranda., et al 2005).

1.6.3 Modulating the chaperone folding environment

Another approach to rescuing misfolded proteins trapped in the ER is to modulate the endogenous molecular chaperone machinery. To achieve this, the roles of specific chaperones involved in the folding and quality control of specific misfolded proteins need to be understood. For example, in the case of cystic fibrosis 80% of patients harbour a deletion of phenylalanine at position 508 (ΔF508) in the cystic fibrosis transmembrane conductance regulator (CFTR). By assessing proteins that interacted with CFTR a protein interaction map was determined and revealed that Hsp90 co-chaperones modulate the stability of CFTR in the ER. siRNA mediated knock-down of Aha1, a co-chaperone that regulates interactions of Hsp90 with CFTR, rescued mutant CFTR folding and export from the ER (Wang et al., 2006).

1.7 Aims of the research described in this thesis

The overall aims of this work were to develop and characterise cellular models to use in the identification of modulators of mutant MC4R functional expression. The work described in each chapter is summarised below:

- *Chapter 3-Development of a cellular model to monitor MC4R expression at the cell surface*

  In this chapter seven misfolding MC4R mutants were created using site directed mutagenesis. The localisation of the mutants was determined using confocal microscopy and the extent of ER retention was investigated. The MC4R mutants were characterised for cell surface expression using a rapid cell culture assay and for signalling function using a dual reporter luciferase assay.

- *Chapter 4-Kosmotropes as modulators of MC4R trafficking and functional expression*

  The data presented in chapter 4 investigates the effects of kosmotropes on mutant MC4R function. Kosmotropes, DMSO, trehalose and 4-PBA, were tested at varying concentrations, using the different assays established in chapter 3, for their effects on mutant MC4R cell surface expression and function.

- *Chapter 5-The effects of heat shock protein inducers and co-inducers on the cellular processing of MC4R*

  In Chapter 5 the cellular chaperone environment was manipulated by inhibiting Hsp90 and over-expressing Hsc70, and the effect on mutant MC4R function was investigated.

- *Chapter 6-Further strategies to promote cell surface expression of mutant MC4R*

  The final results chapter looked at the effects of autophagy inducer rapamycin, phytoalexin resveratrol and MC2R accessory protein MRAP, on the cell surface expression and function of mutant MC4R.

CHAPTER 2

Materials and Methods

2.1 Equipment, reagents and plasticware

Details of all laboratory equipment are listed in the Appendix 1. General laboratory reagents and chemicals were purchased from Sigma-Aldrich, UK and general plasticware from VWR, UK unless stated otherwise. General buffers and solutions were prepared in deionised water and autoclaved or filtered where necessary.

2.2 Nucleic acid amplification, extraction, purification and modification

2.2.1 Oligonucleotide design

After establishing the gene sequence of interest using internet databases NCBI and ENSEMBL, primer pairs were designed according to the basic principles listed below:

- Primers should ideally be 15-25 bp in length
- Sequences should be non-repetitive and non-palindromic
- G/C content should designed to be between 40-60%
- Forward and reverse primers should anneal at approximately the same temperature
- T_m should be between 58 and 68˚C and is calculated (approximately) as follows:

  Melting temperature (˚C) = (number of C/G bases) x 4 + (number of A/T bases) x 2
- Primers should not form secondary structures

Primers used in RT-PCR were intron-spanning to ensure the PCR reaction amplified only cDNA and not contaminating genomic DNA. Primers used for site-directed mutagenesis were created with the help of Stratagene's web-based

QuikChange® program (http://www.stratagene.com/qcprimerdesign). Primer sequences are shown below in table 2.1.

Table 2.1: List of primers

Primer name	Sequence (5'-3')	Genbank accession number
MC4R	F:GAATTCATGGTGAACTCCACCCACCGT	NM 005912
	R:TGCAGAATTCGCATATCTGCTAGACAAGTCACA	
HA-	F:GAATTCATGTACCCATACGAT	
MC4R	R: TGCAGAATTCGCATATCTGCTAGACAAGTCACA	
N62S	F:GTCATCAGCTTGTTGGAGAGTATCTTAGTGATTGTGGCA	
	R:TGCCACAATCACTAAGATACTCTCCAACAAGCTGATGAC	
P78L	F:AGAACAAGAATCTGCATTCACTCATGTACTTTTTCATCTGCAG	
	R:CTGCAGATGAAAAAGTACATGAGTGAATGCAGATTCTTGTTCT	
C271Y	F:CTCCACTTAATATTCTACATCTCTTATCCTCAGAATCCATATTGTG	
	R:CACAATATGGATTCTGAGGATAAGAGATGTAGAATATTAAGTGGAG	
P299H	F:GTGTAATTCAATCATCGATCATCTGATTTATGCACTCCGGA	
	R:TCCGGAGTGCATAAATCAGATGATCGATGATTGAATTACAC	
D90N	F:AGCTTGGCTGTGGCTAATATGCTGGTGAGCG	
	R:CGCTCACCAGCATATTAGCCACAGCCAAGCT	
S58C	F:TGACTCTGGGTGTCATCTGCTTGTTGGAGAATATC	
	R:GATATTCTCCAACAAGCAGATGACACCCAGAGTCA	
L106P	F:AGAAACCATTGTCATCACCCCATTAAACAGTACAGATACGG	
	R:CCGTATCTGTACTGTTTAATGGGGTGATGACAATGGTTTCT	
GAPDH	F:TGCACCACCAACTGCTTAG	NM 014364
	R:GGATGCAGGGATGATGTTC	
HOP	F: CTTCCAGAGAATAAGAAGCAG	NM 006819
	R:CTTTCTGAAAACACTCGTTGC	

2.2.2 Total RNA extraction from cells

RNA extraction was performed using the RNAeasy (Qiagen, UK) kit according to manufacturer's instructions (http://www.qiagen.com/literature). This extraction technique is based on selective binding of RNA to a silica gel based membrane, hence enabling wash steps to remove contaminants such as DNA and protein. In brief, the samples (approximately 700 µl) were applied to an RNAeasy mini column in a 2 ml collection tube and centrifuged for 15 sec at 15000 g. The flow-through was discarded and the column transferred to a new collection tube and washed with 700 µl of Buffer RW1 after transfer to a new collection tube. Subsequently, 500 µl of Buffer RPE was added and centrifuged for 2 min at 15000 g. This step was repeated, followed by centrifuging the column alone at 15000 g for 1 min to dry the silica-gel membrane. The RNA was eluted into a new 1.5 ml collection tube using 30-50 µl RNase-free water directly pipetted onto the membrane and left for 1 min before centrifuging at 15000 g for 1 min. RNA collected was quantified using the Nanodrop ND 1000 spectrophotometer (Labtech International, UK).

2.2.3 DNase treatment of RNA

To ensure that the RNA samples were not contaminated with genomic DNA, total RNA extracts underwent DNase treatment (reagents were obtained from Promega, UK unless specified). In brief, 2.5 µg total RNA was added to 2 µl 10x RQ1 DNase buffer, 0.75 µl (30 units) RNasin, 10 µl (10 units) DNAseI and made up to 20 µl total volume using RNase-free water. The mixture was incubated at 37°C for 1 hr. The samples were either frozen to stop the reaction or precipitated as described in section 2.2.8.

2.2.4 First strand cDNA synthesis

All reagents were purchased from Promega, UK. Subsequently, 2 µg of RNA was added to a sterile RNase-free microcentrifuge tube. Following this, 0.5 µg/1 µl of random primers was added and made up to a total volume of 15 µl with RNase-free water. The tube was heated to 70°C for 5 min to melt secondary structures within the template. The tube was cooled immediately on ice to prevent secondary structures reforming. It was spun briefly to collect the solution at the bottom of the tube. The following reagents were added to the mixture:

M-MLV 5X buffer	5 µl
dATP, 10 mM	1.25 µl
dCTP, 10 mM	1.25 µl
dGTP, 10 mM	1.25 µl
dTTP, 10 mM	1.25 µl
rRNasin ® ribonuclease inhibitor	25 units (1 µl)
M-MLV reverse transcriptase (Molony murine leukemia virus)	200 units (1µl)
Nuclease-free water to final volume	25 µl

The reaction was mixed gently, spun briefly and incubated at 37°C for 1hr. Samples were either stored at -20°C or used immediately.

2.2.5 Polymerase Chain Reaction (PCR)

PCR was performed to amplify genes of interest. The basic principle involves denaturing double stranded DNA at high temperatures, ~95°C. This is followed by annealing of sequence-specific oligonucleotide primers typically at temperatures 50-60°C before synthesis of complementary DNA strands from 5’ to 3’ by a thermostable polymerase. Repeated cycles allow exponential multiplication of a specific portion of DNA.

A PCR reaction mixture, typically in a total volume of 25 µl was as follows:

Template	0.5-1 µl
dH_2O	19.75-20.25 µl
10Xbuffer	2.5 µl
dNTPs (10 mM)	0.5 µl
Forward primer (10 µM)	0.5 µl
Reverse primer (10 µM)	0.5 µl
Taq DNA polymerase (5 U/µl)	0.25 µl
Total volume	25 µl

PCR automated cycling was typically carried out as follows. After initial denaturation at 95°C for 5 minutes, this was followed by 25 cycles of 95°C for 30 sec, 55°C for 30 sec and 72°C for 1 min, with a final extension step at 72°C for 5 min.

2.2.6 Agarose gel electrophoresis

All PCR products were run on 1-2% (w/v) agarose gel made in 1X TAE (40 mM Tris-acetate, 2 mM disodium ethylenediaminetetraacetate (Na_2EDTA), pH 8.3; National Diagnostics, UK), and visualised alongside DNA markers (GeneRuler^{TM} DNA Ladder Mix, 0.5 mg DNA/ml, Fermentas) with ethidium bromide (0.2 µg/ml) staining. 5 µl of each reaction was mixed with loading dye solution (40% w/v sucrose, 0.25% w/v bromophenol blue or Orange G, DEPC water) at a 1:5 ratio prior to loading the wells of a 1% (w/v) agarose gel. Electrophoresis was typically carried out at 120 V for 30 min or until clear separation of bands was achieved. Ethidium bromide intercalated into DNA fluoresces under UV light at 300 nm, allowing the DNA to be visualised. A transluminator (Uvitec, UK) was used to visualise bands, and capture an image of the resultant gel.

2.2.7 Extraction of DNA from agarose gels

DNA was extracted from gel slices using the QIAquick® Gel Extraction Kit (Qiagen, UK) according to the manufacturer's instructions (http://www.qiagen.com/literature). In brief, the DNA fragment of interest was visualised under UV light, and excised with a sharp clean blade. The gel slice was weighed in a microcentrifuge tube and the volume estimated, assuming 100 mg = 100 µl. 3 x volume of buffer QG (binding and solubilisation buffer) was added to 1 volume of gel. The sample was incubated at 50°C, vortexing intermittently until complete gel solubilisation was achieved. The sample was applied to the QIAquick column and centrifuged for 1 min at 15000 g. The flow-through was collected and discarded. The column was then washed with 0.75 ml of buffer PE and centrifuged at 15000 g for a further minute. The column was placed in a clean microcentrifuge tube and allowed to dry at room temperature for 2 min. Using 30-50 µl dH_2O applied to the membrane the DNA sample was eluted after centrifugation at 15000 g for 1 minute. The principle of QIAquick is based on binding properties of DNA to a silica membrane in the presence of high salt buffer. This allows washes with high salt buffers to remove impurities and contaminants, and elution of DNA from the membrane is then accomplished with low salt concentrations. Extracted DNA was stored at -20°C.

2.2.8 Nucleic acid precipitation

An equal volume of phenol was added to the nucleic acid solution. The sample was mixed vigorously to create an emulsion and centrifuged for 5 min at 15000 g to separate the nucleic acids (upper aqueous phase) from contaminating proteins, lipids and carbohydrates (in phenol phase). The transparent upper phase was carefully removed and placed in a new RNase/DNase-free microcentrifuge tube. Precipitation of nucleic acids was performed by the addition of 1/10th volume of 3 M sodium acetate pH 5.3, 2.5 volumes absolute ethanol and 1 µl glycogen (5 mg/ml). The solution was mixed, vortexed briefly and incubated at -70°C for a minimum of 15 min and a maximum overnight to precipitate nucleic acids. Precipitated nucleic acids were centrifuged at 15000 g for 10 min. After visualisation of the pellet, the supernatant was carefully removed by pipetting. The pellet was washed with 70% ethanol and centrifuged again for a further 10 min at maximum speed. After removal of the ethanol, the pellet was air-dried and resuspended in 10 µl of RNase/DNase-free water. The NanoDrop ND-100 spectrophotometer was also used to quantify nucleic acid concentration in accordance with the manufacturer's instructions.

2.2.9 DNA sequencing

Sequencing of PCR products or clones was performed to ensure that they were specific. Sequencing was performed by the Genome Centre (Bart's and The London, Queen Mary, University of London) using BigDye 3.1 chemistry (Applied Biosystems, UK), which is based on the Sanger dideoy-mediated chain termination method (Sanger et al., 1977). Analysis of sequence chromatograms was carried out using BioEdit (Hall, 1999).

2.3 Plasmid preparation, propagation and modification

2.3.1 Cloning constructs and design of oligonucleotides

Two sets of primers to human MC4R were designed, to introduce a GFP tag on the C-terminus and to remove the triple haemagglutinin (3xHA) tag on the N-terminus, to produce constructs, MC4R-GFP and HA-MC4R-GFP (Table 2.1). Enzyme cutting site *Eco*R1 was also incorporated into the primer sequences to enable direct cloning into pEGFP-N1 (Clontech). Restriction endonuclease digestion was performed with *Eco*R1 (NEB) and *Pst*1 (NEB) to ensure correct orientation of MC4R into vector pEGFP-N1.

Other basic vectors used in this study included pGEM®-T (Promega, UK) and pcDNA3.1 (+) (Invitrogen, Carlsbad, CA). Vector maps are shown in Appendix 3. Rod opsin, MRAP-FLAG, Aha1 and Hsc70 vectors were obtained from Professor Mike Cheetham, Dr. Tom Webb, Professor Paul Workman and Professor Harm Kampinga respectively (Saliba et al., 2002; Webb et al., 2009; Holmes et al., 2008; Hageman et al., 2007). MRAP-FLAG was constructed by directional cloning of human MRAPα into p3xFLAG-CMV-14 expression vector (Webb et al., 2009). The correct sequence of all constructs was confirmed by sequencing.

2.3.2 Restriction endonuclease digestion

Restriction endonuclease digestion was used as part of the cloning strategy, to linearise vectors and to verify the presence and orientation of a given insert in a particular vector. Enzymes were obtained from New England Biolabs (NEB) or Promega, UK. A typical reaction is shown below.

DNA	1 µg
10X reaction buffer	5 µl
Restriction enzyme (2-10U/µl)	1 µl
dH_2O to a final volume of	50 µl

Digests were typically performed for 2 hr at 37°C. The program NEB CUTTER V2.0 was used to determine enzyme restriction sites. Double digests were performed in a similar manner in either a one or two step procedure; the reaction buffers were selected using information available from manufacturers (http://www.promega.com/guides/re_guide/research.asp?search=buffer).

2.3.3 Ligations

Ligation reactions were set up as follows:

T4 DNA Ligase (1-3 U/µl ; Promega, UK)	1 µl
T4 DNA Ligase 10X buffer (Promega, UK)	1 µl
Vector	1 µl
Insert DNA	2 µl
dH_2O to a final volume of	10 µl

The vector was digested with relevant enzymes and run on an agarose gel to ensure linearisation. The digested vector was gel cleaned as described in section 2.2.7, prior to ligation. The ligation reaction was left overnight in an ice water bath prior to transforming competent bacteria.

2.3.4 Transformation of competent bacteria

Transformations were undertaken according to the protocol provided with JM109 *E-coli* competent cells (Promega, UK). For each transformation a 50 µl aliquot of competent cells was transferred to a sterile 1.5 ml eppendorf. 5 µl of ligation mixture was added to the cells. The sample was placed on ice for 10 min and swirled intermittently. The cells were heat shocked at 42°C for 47 secs and returned immediately to ice for 2 min. 950 µl of SOC (super optimal culture) medium (Invitrogen Ltd, UK) was added to each tube and incubated at 37°C for 1 hr at 225 rpm. Following this, the cells were centrifuged for 4 min at 1200 g.

Positioned next to a Bunsen burner, the supernatant was poured away and the remaining cells resuspended in the residual SOC media, normally 100 µl. This was plated using a sterile glass spreader onto a LB/agar plate with 100 µg/ml ampicillin plate (or 30 µg/ml kanamycin) and incubated overnight at 37°C. A positive control using the vector pGEM®-3Z (Promega, UK) was conducted for each set of ligations using control plasmid to assess transformation efficiency of cells.

2.3.5 Blue/white screening

In the case of the pGEM T vector, cells were plated onto agar plates previously coated with 50 µl of 50 mg/ml X-Gal (5-bromo-4-chloro-3-indolyl-beta-D-galactopyranoside, Promega, UK) and 100 µl of 0.1 M Isopropylβ-D-1-thiogalactopyranoside (IPTG) (Promega, UK). The pGEM T vector contains the LacZ gene coding for the β-galactosidase enzyme that converts X-Gal into a blue product. Insertion of a piece of DNA into the multiple cloning site, which lies within the LacZ gene, would result in disruption of this gene and therefore prevent the production of the β-galactosidase enzyme. Hence, bacteria with plasmids containing the desired DNA insert would fail to metabolise X-Gal and remain white. On this basis the white colonies were picked after overnight incubation.

2.3.6 Screening of colonies by PCR and restriction digests

The selected colonies were screened for the presence of an insert by restriction digestion of the plasmid followed by gel electrophoresis. After screening, sequencing across the cloning site was performed to confirm that the insert was correctly introduced into the vector, in frame and in the correct orientation.

2.3.7 Bacterial cultures

For each bacterial colony selected, 5 ml of sterile LB broth containing 100 µg/ml of ampicillin (or 30 µg/ml kanamycin) was poured into a 50 ml Falcon tube under sterile conditions. Colonies were selected (white colonies in the case of pGEM-T) from the LB/agar plate with a sterile pipette tip and transferred to the broth. The samples were incubated overnight at 37°C in a shaking incubator at 225 rpm.

2.3.8 Glycerol stocks

After overnight incubation 500 µl of the cultured transformed bacterial cells were pipetted into a sterile microcentrifuge tube. 500 µl of sterile glycerol (Sigma-Aldrich, UK) was added and mixed thoroughly. Glycerol stocks were stored at -70°C.

2.3.9 Preparation of LB-Agar plates

LB/Agar (10 g LB broth, 7.5 g agar, 500 ml water) was prepared and autoclaved. Once cooled to a temperature ~37°C, antibiotic was added to a total concentration of 100 µg/ml for ampicillin or 30 µg/ml for kanamycin. The mixture was poured into 10 cm petri dishes, in a sterile field created by a Bunsen burner and left to set at room temperature. Once set these were sealed, with parafilm and stored at 4°C or used immediately.

2.3.10 Plasmid DNA purification

Depending on the amount of plasmid DNA required, either Qiagen mini- or midi-preps (Qiagen, UK) were performed according to the protocol provided by the manufacturer (http://www.qiagen.com/literature). Although the exact compositions of the reagents are unavailable, the principle is based on alkaline lysis of bacterial

cells followed by absorption of plasmid DNA onto a silica membrane under high-salt conditions.

Miniprep for preparation of up to 20 µg of high-copy plasmid DNA

Plasmid DNA was recovered from cells using the Qiagen miniprep kit according to Qiagen protocol. Briefly, 5 ml of bacterial culture was centrifuged in a 50 ml Falcon tube for 15 min at 3000 g. After removing the culture media the cell pellet was resuspended in 250 µl ice-cold buffer P1 (cell resuspension solution). The cells were transferred into a 1.5 ml microcentrifuge tube and 250 µl of buffer P2 (cell lysis solution) was added. This was then mixed by inversion until homogenous. Immediately after this 350 µl of buffer N3 (neutralisation solution) was added and the sample mixed again. The microcentrifuge tube was then spun at 15000 g in a tabletop microcentrifuge for 10 min. The supernatant containing the plasmid DNA was applied to a QIAprep spin column and centrifuged for 30-60 sec. The flow-through was discarded and the column washed by adding 0.75 ml of buffer PE (wash buffer). The column was placed in a clean 1.5 ml microcentrifuge tube and the DNA eluted by the addition of 30-50 µl of dH_2O to the column, which was then centrifuged for 2 min at 15000 g.

Midiprep for preparation of up to 100 µg of high-copy plasmid DNA

Precisely 50 ml of bacterial cell culture was used for each midiprep. Bacterial cells were harvested after centrifugation at 3000 g for 15 min at 4˚C. The cell pellet was resuspended in 4 ml of buffer P1. Precisely 4 ml of lysis buffer was added and the tube inverted until thorough mixing was achieved. This was incubated at room temperature for 5 min. Subsequently 4 ml of neutralisation buffer was added and the solution mixed by inversion. The sample was then applied to a 20 ml syringe, having removed the plunger, and left for 10 min. In the meantime, the midi 100 column was equilibrated with 4 ml buffer QBT (equilibration buffer). Once buffer QBT had run through the column the supernatant from the syringe was applied to the column. This was allowed to flow through by gravity and the column was washed twice with wash buffer QC (2 x 10 ml). The DNA was eluted with 5 ml

buffer QF (elution buffer). DNA precipitation was performed by the addition of 0.7 volumes of isopropanol (Sigma-Aldrich, UK) at room temperature and centrifugation at 4000 g for 1 hr at 4°C. The supernatant was decanted and the pellet washed with 2 ml of 70% v/v ethanol at room temperature and recentrifuged at 4000 g for 1 hr at 4°C, after which the supernatant was discarded and the pellet air dried. The DNA was then dissolved in a suitable amount of water and stored at -20°C.

2.3.11 Site-directed mutagenesis of MC4R constructs

To create the seven selected MC4R mutants, primers (Table 2.1) were designed to introduce point mutations resulting in the required amino acid change. This was achieved by using the QuikChange II site-directed mutagenesis kit (Stratagene) and using MC4R-GFP or HA-MC4R-GFP or HA-MC4R constructs as template. The conditions for PCR are listed below:

10 x reaction buffer (Stratagene)	5 µl
construct template	125 ng
forward primer (100 ng/ul)	1.25 µl
reverse primer (100 ng/ul)	1.25 µl
dNTP mix (Stratagene)	0.2 nM
PfuUltra HF DNA polymerase (Stratagene)	1 µl
ddH_2O to a final volume of	50 µl

Cycling conditions:

1 cycle	95°C for 30 seconds
16 cycles	95°C for 30 seconds
	55°C for 1 minute
	68°C for 5 minutes and 40 seconds

Following the thermal cycling reaction the site-directed mutagenesis products were digested with 1 µl of *Dpn*1 restriction enzyme (10U/µl) at 37°C for 1 hour. This step

is necessary to digest the parental, non-mutated, supercoiled dsDNA. Plasmid DNA was then transformed as described in section 2.3.4 and signal colonies purified as described in section 2.3.10. DNA was sequenced (as described in section 2.2.9) to ensure that the plasmid contained the correct mutation.

2.4 Cell culture, transfection and the development of stable cell lines

2.4.1 Cell culture

Human neuroblastoma cell line (SK-N-SH) and Chinese hamster ovary (CHO) cells were grown in DMEM/F12 (Sigma) containing 10% heat inactivated foetal bovine serum (FBS, Invitrogen) with 50 U/ml penicillin and 50 µg/ml streptomycin (Invitrogen). Human embryonic kidney (HEK 293) cells were grown in Dulbecco's modified eagle's medium (DMEM) containing 10% v/v FBS with 50 U/ml penicillin and 50 µg/ml streptomycin. Cells were kept in a humidified atmosphere of 5% v/v CO_2 at 37°C.

2.4.2 Transfection of cells

Cells were seeded in 8, 12, 24, well cell culture plates or T25 cell culture flasks. After 48 hours or once cells had reached ~70% confluency, cells were transfected with the appropriate amount of plasmid DNA (Table 2.2) using Lipofectamine (Invitrogen) and Plus reagent (Invitrogen) in serum-free media for three hours according to manufacturer's instructions. Following transfection 20% v/v FBS media was added in equal volume in order to restore a 10% v/v FBS solution.

Table 2.2: Amount of reagents used for transfection of MC4R plasmids

Cell culture Vessel	DNA (ng/µl)	Lipofectamine (µl)	Plus reagent (µl)
24 well	200	1	2
12 well	400	2	4
8 well	800	4	8
T25 flask	2000	8	16

2.4.3 Preparation of stable cell lines expressing tagged WT and mutant MC4R

HEK 293 cells were seeded in a 6-well plate and allowed to grow to approximately 80% confluence. Cells were transfected with WT HA-MC4R and HA-MC4R (S58C, P78L, D90N and L106P) using the lipophilic agent Lipofectamine and Plus reagent (Invitrogen). To select for cells stably expressing MC4R Geneticin (G418) was utilised. Resistance to G418 is conferred by the neo gene from Tn5 encoding an aminoglycoside 3‘-phosphotransferase, APH 3‘II (Invitrogen). After optimisation of G418, transfectants were selected in G418 (1.5 mg/ml). After 14 days, cells were transferred to ninety-six well plate at a seeding density of 0.5 cells per well to achieve monoclonal MC4R expressing cell lines. The stable cell lines were gradually scaled up by transferring them to larger cell culture vessels once 100% confluence was achieved. HA-MC4R expression was tested by using Western blot analysis.

2.5 siRNA of Hop

siRNA transfections were carried out in 6 well cell culture dishes in triplicate for each siRNA duplex. Three Mission® siRNA duplexes (ID: 00126805, 00126806, 00126807) at a concentration of 10 nmol against *Hop* (NM 006819) were obtained from Sigma. The sequence of the Mission siRNA (Sigma) and the negative siRNA (control#1) (Ambion) were not disclosed by the manufacturer. Triplicate HEK 293 cells cultures were transfected individually with 150 nM of the siRNA duplexes using Lipofectamine and plus reagent prepared in OptiMEM following the manufacturer's instructions. RT-PCR was performed to confirm knockdown mRNA expression of *Hop*.

2.6 Drug treatments

All drug treatments were carried out upon the re-establishment of 10% v/v FBS solution, after the 3 hour serum free period, and incubated for 24 hours unless otherwise stated. Reagents used and the concentrations they were used at are detailed in Table 2.3.

Table 2.3: Reagent used in thesis

Reagent	Stock concentration	Supplier
NDP-MSH	10^{-5}M in dH_20	Bachem
AGRP	10^{-5}M in dH_20	Bachem
DMSO	>99%	Sigma
TMAO	1M in dH_20	Sigma
4-PBA	5M in dH_20	Sigma
Trehalose	0.3M in dH_20	Sigma
Geldanamycin	2mM in DMSO	Sigma
Rapmaycin	5mM in chloroform	Sigma
Resveratrol	10mM in ethanol	Sigma

2.7 Processing of cells for confocal microscopy

Cells were seeded on round 15mm coverslips (VWR), which were placed in the wells of a 12 well cell culture plate, prior to transfection. 24 hours post-transfection, tagged MC4R expressing cells were washed once with phosphate buffer saline (PBS) (Sigma) prior to fixation with 3.7% v/v formaldehyde (TABB Laboratories, UK) for 15 minutes at room temperature (RT). Cells were permabilised with 0.025% v/v Triton X-100 for 10 minutes and subsequently washed twice with PBS for 10 minutes. The cells were then blocked for 45 minutes in buffer A, which consisted of PBS containing 10% v/v donkey serum (Sigma) and 3% v/v albumin from bovine serum (BSA) (Sigma). To detect the N-terminal HA tag, cells were incubated for 1.5 hours in buffer A containing anti-HA monoclonal mouse antibody (Sigma) at a dilution of 1:500. Following this cells were washed with PBS, for a

duration of 10 minutes three times. Subsequently cells were incubated for a further hour in buffer A with cy3 conjugated anti-mouse secondary antibody at a dilution of 1:100 (Jackson laboratory). Cells were washed three times for 10 minutes with PBS and incubated with 2 µg/ml 4',6-Diamidino-2-phenylindole dihydrochloride (DAPI, Sigma) for two minutes. Cells were washed for five minutes with PBS and the round coverslips were mounted using florescent mounting media (Invitrogen) on glass slides (VWR) prior to imaging using a LSM 510 confocal microscope (Zeiss).

2.8 Processing of cells to assess cell surface expression

24 hours post-transfection, HA tagged MC4R expressing cells were washed once with PBS prior to fixation with 3.7% v/v formaldehyde for 15 minutes. To detect intracellular retained MC4R half the 24 well cell culture plate was permeabilised with 0.025% v/v triton X-100 for 10 minutes, leaving the remaining half non-permeabilised (Fig 2.1). Cells were washed with PBS for 10 minutes prior to 45 minutes incubation with blocking buffer (LI-COR). Following this cells were incubated for 1.5 hours with anti-HA monoclonal mouse antibody (Sigma) in blocking buffer at a dilution of 1:1000. Cells were washed with PBS, with three 10 minute washes. Cells were then incubated for 1 hour in blocking buffer with a dye that exists in the infrared spectrum (LI-COR) at a dilution of 1:1000 and SYTO 60 red fluorescent nucleic acid stain (Invitrogen) at a dilution of 1:10000 to account for variation in cell number. Finally cells were washed with PBS, with three 10 minutes before scanning the plate(s) at 800nm to detect the HA tag and 700 nm to detect the DNA stain on Odyssey® infrared imaging system (LI-COR).

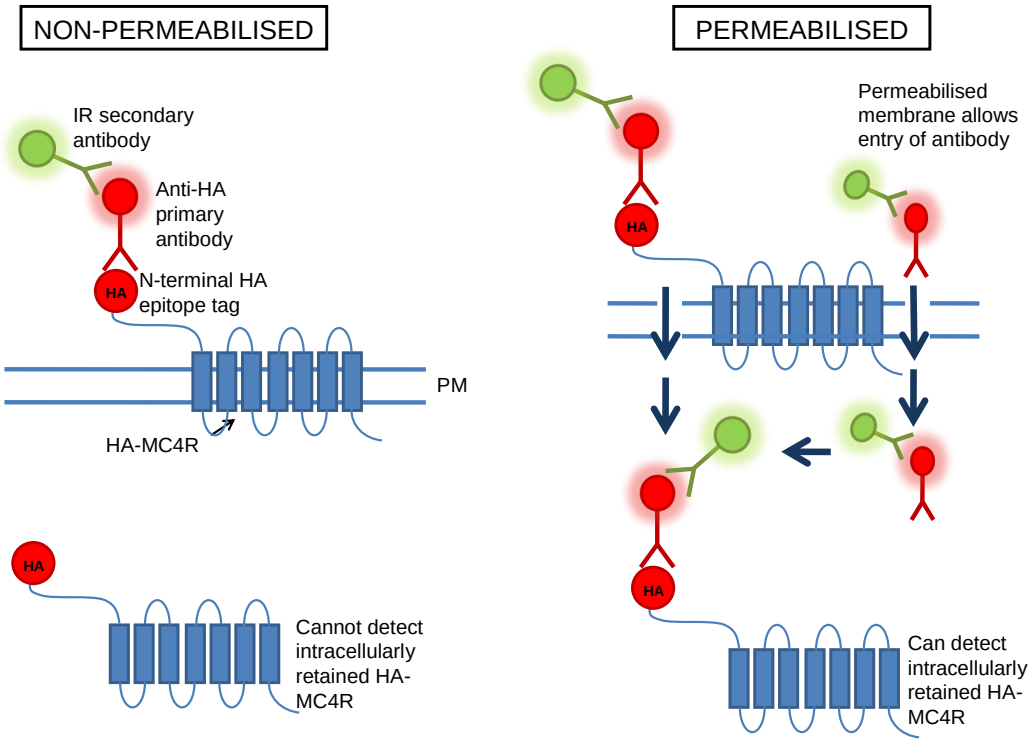

Figure 2.1: Schematic of immunocytochemistry staining to assess cell surface expression of MC4R

The IR secondary antibody is unable to penetrate non-permeabilised cells, therefore any intracellular retained MC4R is not detected and only MC4-receptor at the cell surface can be quantified. When cells are permeabilised IR secondary antibody is able to enter the cell and detect HA-primary antibody bound to the HA-epitope tag of MC4R. Therefore the total amount of MC4R, at the cell surface and intracellular, can be quantified and the percentage at the cell surface can be calculated.

2.9 Confocal microscopy and cell inclusion counting

SK-N-SH cells expressing MC4R-GFP were counted for inclusions using a 63x objective from a DMR Leica epifluorescence microscope. Cells were counted blind to experimental status in five different fields of view.

When imaging, to compare between cells treated with pharmacological reagents and control cells, the confocal microscope settings were kept constant.

MC4R expressing cells were visualised using a Zeiss LSM 510 microscope. The following excitations/emissions conditions were used in separate channels using the 63x objective: DAPI 364/475-525 nm, Cy2 488/505-530 nm, Cy3 543/560 nm.

2.10 SDS-polyacrylamide gel electrophoresis (SDS-PAGE)

T25 culture flasks were transfected with 2 µg of plasmid DNA. After 24 hours post transfection, MC4R expressing cells were washed twice with 4°C PBS before lysis. Cells were lysed using 250 µl Ripa buffer (Sigma) containing 0.1% v/v protease inhibitors (Sigma) and 0.1% v/v phosphatase inhibitors (Sigma). Cells were scraped on ice and collected in a 1.5 ml microcentrifuge tube. Cell lysates were incubated on ice for 30 minutes and subsequently centrifuged at 15000 g for 10 minutes. Subsequently, 200 µl of the supernatant was removed and placed in a sterile 1.5 ml microcentrige tube and an equal volume of laemmli buffer (Sigma) was added to the sample. The samples were run on a 12% v/v polyacrylamide gel. The resolving gel consisted of: 2.6 µl 4x ProtoGel resolving buffer (1.5 M Tris-HCL, 0.4% SDS, pH 8.8, National Diagnostics), 4.0µl 30% w/v acrylamide (National Diagnostics), 3.3 µl dH_2O, 100 µl of 10% v/v ammonium persulfate (Sigma) and 20 µl TEMED (Sigma). Once set the stacking gel was added and consisted of: 2.5 µl ProtoGel stacking buffer (0.5 M Tris-HCL, 0.4% SDS, pH 6.8, National Diagnostics), 1.3 µl 30% w/v acrylamide, 6.1 µl dH_2O, 100 µl of 10% v/v ammonium persulfate and 10 µl TEMED. Alternatively sample cell lysates were loaded into pre-cast 12% Nupage® Tris-HCl gels (Invitrogen).

Lysates were run alongside 5 µl of prestained protein marker (broad range 6-175 kDa, New England Biolabs, UK) to enable an approximation of the molecular weight of indentified proteins. Using a Mini-PROEAN 3 Electrophoresis system (Bio-Rad Laboratories Ltd, UK) or for pre-cast gels a X-Cell surelock system (Invitrogen, UK), proteins were separated by SDS-PAGE at 120 V until the dye front reached the bottom of the gel. The Tris-glycine running buffer contained 25 mM Tris-HCL, 250 mM Glycine and 0.1% v/v SDS.

2.10.1 Protein transfer

Proteins were transferred from 12% v/v polyacrylamide gels to Whatman® Protran® nitrocellulose transfer membrane (Sigma) using a semi dry electrophoretic transfer cell (Bio-Rad Laboratories Ltd, UK). The electrotransfer buffer was made up of 25 mM Tris, 192 mM glycine and 20% v/v methanol. Electrotransfer of proteins was carried out for 30 minutes at 15 V with a current of 0.4 A per gel.

2.10.2 Immunoblotting

The nitrocellulose membrane was incubated in blocking buffer (PBS, 5% w/v Marvel™, 0.1% v/v Tween-20 (polyoxyethylene (20) sorbitan monolaurate)) for 1 hour with gentle agitation. Membranes were subsequently incubated with primary antibody (Table 2.4) at a concentration of 1:1000, in blocking buffer and left overnight at 4°C with gentle agitation. This was followed by three 5 minute washes in wash buffer (PBS, 0.1% v/v Tween 20). The blot was subsequently incubated with dyes that exist in the infrared spectrum, goat anti-rabbit® IRDye® 800CW or anti-mouse® IRDye® 800CW (LI-COR Biosciences) at a dilution of 1:10,000 in blocking buffer for 1 hour. Incubation with the secondary antibody and subsequent steps were performed in the dark in a blacked-out box. Prior to scanning the nitrocellulose membrane an Odyssey Infrared Imagaing system (LI-COR) the nitrocellulose membrane was washed three times for 5 minutes in wash buffer.

Table 2.4: Antibodies used in this study

Primary antibody	Supplier
Mouse monoclonal antiHA clone HA-7	Sigma
Mouse monoclonal anti-Hsp70 clone BRM-22	Sigma
Rabbit monoclonal anti-V5	Sigma
Mouse monoclonal anti-FLAG	Sigma
Rabbit polycolonal to human Aha1	Professor Paul Workman, Institute of Cancer Research
ID4 Rhodopsin	Professor Mike Cheetham, Institute of Ophthalmology

2.10.3 Detection of MC4R glycoforms

The mobility of the different MC4R glycoforms were determined by digesting 10 µg of soluble cell lysates using Endoglycosidase H (EndoH) and Peptide N-glycosidase F (PNGaseF) (NEB) for 2 hours at 37°C. Following deglycosylation, the samples were run on a gel and Western blotted as described in sections 2.10

The deglycosylation reactions were as follows:

EndoH cloned from *Streptomyces plicatus* and over expressed in E.*coli* was supplied in 20 mM Tris-HCL (pH 7.5), 50 mM NaCl, 5 mM Na_2EDTA. 10x G5 buffer: 0.5 M sodium citrate (pH 5.5).

Triton-X soluble lysate	10 µg
10x G5 buffer	2 µl
EndoH (500 U/µl)	1 µl
ddH_2O to	20 µl
Total reaction volume:	20 µl

Reaction was incubated for 2 hours at 37°C

PNGaseF reaction:
PNGaseF purified from *Flavobacterium meningosepticum* was supplied in 20 mM Tris-HCL (pH 7.5 at 25°C), 50 mM NaCl, 5 mM Na_2EDTA and 50% glycerol. 10x G7 buffer: 0.5 M sodium phosphate (pH 7.5 at 25 °C).

Triton-X soluble lysate	10 µg
10x G7 buffer	2 µl
PNGaseF (500 U/µl)	1µl
ddH_2O to	20 µl
Total reaction volume:	20 µl

Reaction was incubated for 2 hours at 37°C

2.11 Co-immunoprecipitation

Cells lysates were prepared as previously described in section 2.10. Co-IP using anti-HA agarose conjugate, Clone HA-7 (Sigma-Aldrich, UK) was performed. For HA agarose, 40 µl agarose was placed into a 1.5 ml microcentrifuge tube. The agarose was washed five times in 1 ml PBS and after each wash the agarose was

centrifuged at 15000 g for 1 min. PBS was discarded carefully leaving the agarose intact. 700 µl of lysate was added to the agarose and placed on a rolling rotor overnight at 4°C. Following overnight incubation the agarose was washed five times with 1 ml PBS. On the last wash approximately 10 µl of supernatant was left on the agarose. 50 µl sample SDS buffer was added and the sample boiled for 3 min. The samples were then spun at 15000 g for 2 min. The supernatant was carefully removed, passed through a 0.22 µm filter (Millipore), before being used for Co-IP. Typically 20 µl of this sample was loaded alongside 20 µl of untreated protein lysate for comparison. Blotting was performed using rabbit anti-V5 antibody or rabbit anti-Aha1.

2.12 Measurement of MC4R signalling

2.12.1 Measurement of cAMP levels in cells expressing MC4R

The cAMP competitive binding assay is based on the competition between cAMP in the sample and [^{3}H] cAMP for the binding protein extracted from bovine adrenal glands. Any free [^{3}H] cAMP are absorbed by charcoal and removed by centrifugation and bound [^{3}H] cAMP that remains in the supernatant is determined by liquid scintillation counting (Brown et al., 1971).

After 24 hours post transfection, cells were starved for 30 minutes in serum free media and subsequently incubated with 1mM of IBMX for 60 minutes. After this period the cells were stimulated with 10^{-7} M NDP-MSH for 30 minutes. After stimulation, cells were harvested on ice by scraping them into the medium and harvested cells were placed in microcentifuge tubes. Cells were lysed by boiling for five minutes to release intracellular cAMP. The insoluble material was pelleted by centrifugation at 15000 g and the supernantant was transferred to fresh microcentrifuge tubes and stored at -20°C.

Serial dilution of stock cAMP was carried out to produce a standard curve with a range from 0.125 pmol to 64 pmol. Subsequently, 100 µl of each sample was placed into a separate 0.5 µl tube and was performed in duplicate. To the sample tubes, 50 µl of [^{3}H] cAMP was added followed by 100 µl of diluted binding protein, and the tubes were then vortexed. Several controls were also incorporated. To measure the total radioactivity possible, total count, 400 µl of assay buffer and 50 µl [^{3}H] cAMP was placed in a 0.5 µl tube with no cold cAMP. The non-specific binding control was prepared by adding 200 µl and 50 µl [^{3}H] cAMP, and was used to ensure that [^{3}H] cAMP does not bind to endogenous factors in the buffer. B_0 was prepared by adding 100 µl buffer, 100 µl binding protein and 50 µl [^{3}H] cAMP to a 0.5 µl tube. Individual B_0 controls were included for each batch of 16 samples centrifuged as to correct for any potential drift in B_0 with time, especially in cases where many samples were measured.

Calculation:

(X-NSB/ B_0-NSB) X 100 X = sample, NSB = Non specific binding

The count was expressed as a percentage of the total count. The percentage (y-axis) was plotted against cAMP content of the standards (x-axis) and the cAMP content for the unknown samples was then extrapolated from the standard curve.

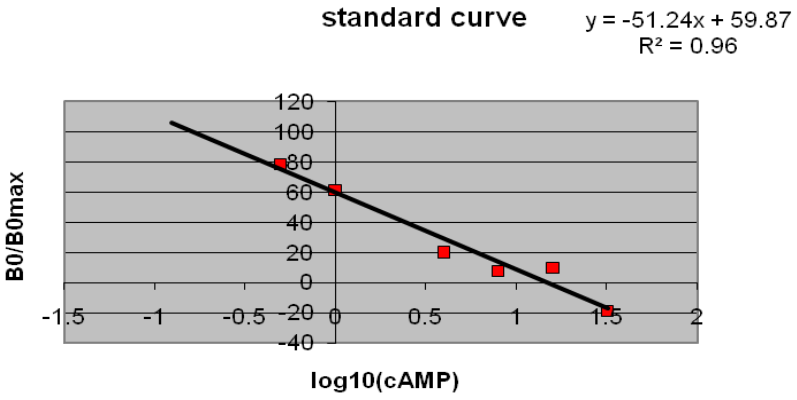

Figure 2.2: An example of the standard curve obtained from a cAMP assay

Inter-assay and Intra-assay coefficient of variance (CV) values were calculated using the equation: CV=SD/Mean. Inter-assay coefficient of variance: 12%, Intra-assay coefficient of variance: 15%.

2.12.2 Measurement of luciferase activity

Genetic reporter systems are widely used to study eukaryotic gene expression and cellular physiology. Applications include the study of receptor activity, transcription factors, intracellular signaling, mRNA processing and protein folding.

Dual-Luciferase Reporter assay (Promega) assays the activity of firefly (*Photinus pyralis*) and Renilla (*Renilla reniformis*) luciferases which are measured sequentially from a single sample (Fig.2.3).

Luciferase Assay Reagent II was prepared by re-suspending the lyophilized Luciferase Assay Substrate in 10 ml Luciferase Assay Buffer II (LAR II) and stored at -70°C. 1 volume of 50X Stop and Glo Substrate was added to 50 volumes of Stop and Glo Buffer and stored at -20°C.

Cells were co-transfected with a plasmid containing luciferase driven by the cAMP responsive promoter α-GSU-846 and pRL-CMV Renilla luciferase plasmid, which is driven by the CMV immediate-early enhancer/promoter. 24 hours post-transfection cells were washed with PBS and stimulated with 10^{-7}M NDP-MSH for 6 hours. Stimulation of the cells causes an increase of cAMP levels in the cells and this ultimately leads to the transcription of luciferase.

Cells were lysed with 100 µl of the the supplied Passive Lysis Buffer. The lysates were transferred to microcentrifuge tubes and incubated on ice for 15 minutes before centrifugation for 10 minutes at 15000 g. The supernantant was transferred to the fresh microcentrifuge tubes and stored at -20°C.

25 µl of the each sample was placed in a 96 well plate, and 80 µl of LAR II and 80 µl of Stop and Glo was automatically added to each sample. Luciferase and renilla activity was measured using a Polestar Omega illuminometer (BMG labtech).

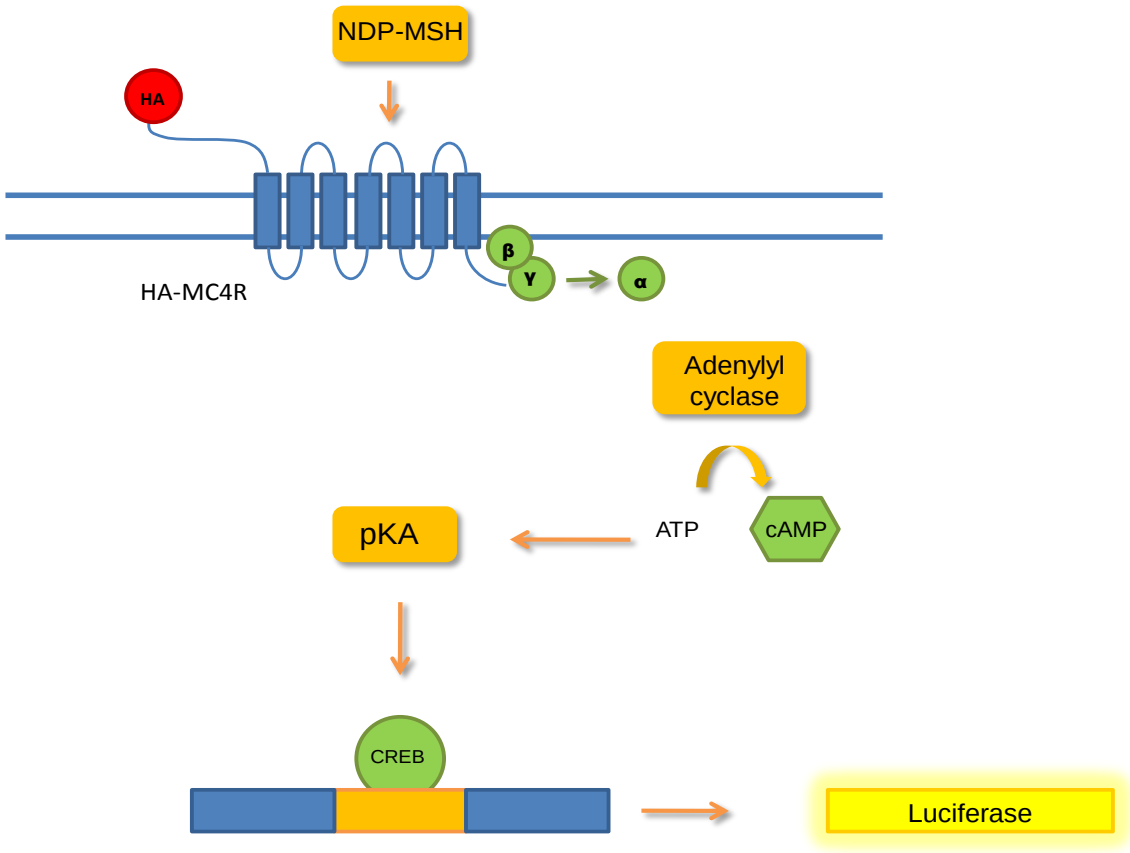

Figure 2.3: Activation of the cAMP signalling cascade

Agonist dependant stimulation of MC4R causes the dissociation of the α-subunit of the heterotrimeric G protein complex. The α-subunit then activates adenylyl cyclase which converts ATP to cAMP. cAMP in turn activates PKA (cAMP dependant protein kinase A) which phosphorylates the transcription factor CREB (cAMP response element binding protein) which regulates the activity of the luciferase gene containing CRE (cAMP response element).

2.13 Statistical analysis

All statistical analysis was performed using Microsoft Excel 2007. The determination of significance was performed using a student's t-test. In some instances, a one way analysis of variance (ANOVA) was performed followed by Dunnett's Multiple Comparison post-test using GraphPad PRISM2 (GraphPAD Software, San Diego, CA). In experiments where statistical analysis was used, experiments were performed with an n of 5 and represent at least 3 independent experiments. Error bars represent the mean standard deviation of the independent experiments. Statistical significance was taken as $p<0.05$.

CHAPTER 3

Development of a cellular model to monitor MC4R expression at the cell surface

3.1 Introduction

A number of Melanocortin 4 receptor (MC4R) mutations have been studied in detail at the biochemical and cellular level (Tao, 2010; Adan et al., 2006). These studies have suggested that MC4R mutations, like other naturally occurring mutations in GPCRs, can be divided into several categories on the basis of mechanisms of pathogenesis. A number of point mutations in MC4R have been classified as misfolding mutations based on the mutant receptor being intracellularly retained at the endoplasmic reticulum (ER), most likely due to the cells chaperone mediated quality control machinery detecting the mutant protein as aberrantly folded. One of the key aims of this study was to identify potential pharmacological modulators of MC4R folding and cell surface expression. In order to achieve this study aimed to identify ER retained MC4R misfolding mutants and develop a cell culture model designed to determine the cellular fate of wild-type and mutant MC4R.

The aim was to develop an assay suitable for screening molecules in the following classes of compounds i) chemical chaperones/kosmotropes and ii) inducers and inhibitors of molecular chaperones, for the ability to improve the processing of wild-type and mutant MC4R to the plasma membrane and to clarify the mechanism of action of any drugs identified as modulators of MC4R cell surface expression.

Previous studies have indicated a degree of variability in the severity of MC4R misfolding mutations with some mutants showing significant cell surface expression (Vaisse et al., 2000). Therefore, a cohort of MC4R mutations that had previously been suggested to be ER retained, were investigated. It was anticipated that these mutants would be defective in cell surface trafficking to varying degrees. In total seven MC4R misfolded mutations were selected and introduced into MC4R by site directed mutagenesis. The cellular localisation of each mutant was determined by confocal microscopy, and through the development of a cell culture assay, the cell surface expression of each mutant relative to wild-type MC4R was determined. This cell culture model was further used for the quantitative analysis

of the efficacy of drugs that may potentially improve cell surface trafficking of mutant MC4R proteins. Another aim was to monitor the levels of maturely glycosylated wild-type and mutant MC4R proteins as a metric for receptor maturation after drug treatment. As a GPCR, MC4R activation via ligand binding results in an increase of intracellular cAMP level. In this chapter cAMP was measured, after the addition of the agonist, to determine whether the compounds had improved the functionality of the mutant receptor compared to the wild-type receptor.

In summary the work described in this chapter represents the development of a cell culture model to monitor the trafficking and functional expression of wild-type (WT) and mutant MC4R to the plasma membrane.

3.2 Results

3.2.1 Expression of MC4R in SK-N-SH and HEK 293 cell lines

For this study it was intended to heterologously express wild-type and mutant MC4R in a cell line that did not express the endogenous protein. Previous studies of MC4R mutants have most commonly used HEK 293 cells (Tao & Segaloff, 2005; Shinyama et al., 2003). Using RT-PCR it was shown that HEK 293s did not have detectable levels of endogenous *MC4R* mRNA (Fig. 3.1). As MC4R is expressed in the brain, the use a neuronal cell line was also utilised. The neuroblastoma derived cell line, SK-N-SH, was selected. SK-N-SH cells were also found not to express any detectable levels of *MC4R* mRNA and were therefore used alongside HEK 293 cells in parts of this thesis (Fig. 3.1).

3.2.2 Generation of constructs

In order to investigate MC4R cellular localisation, a human MC4R cDNA clone that was tripled haemagglutinin (HA) tagged at the N-terminus in pcDNA 3.1 vector (HA-MC4R) was obtained from Missouri S&T cDNA Resource Center (www.cdna.org). From this construct MC4R-GFP and HA-MC4R-GFP fusion proteins were generated (chapter 2, section 2.3.1) (Fig. 3.2). The MC4R-GFP construct was generated to observe the cellular localisation of mutant MC4R, in HEK 293 and SK-N-SH cells, using confocal microscopy. The initial use for the HA-MC4R-GFP fusion protein was to easily quantify the proportion of the cell surface localised mutant MC4R and the proportion of intracellular localised mutant MC4R. In addition to using the HA-MC4R construct, which showed clear plasma membrane (PM) localisation (Fig. 3.3), the other HA-MC4R-GFP and MC4R-GFP constructs were also investigated.

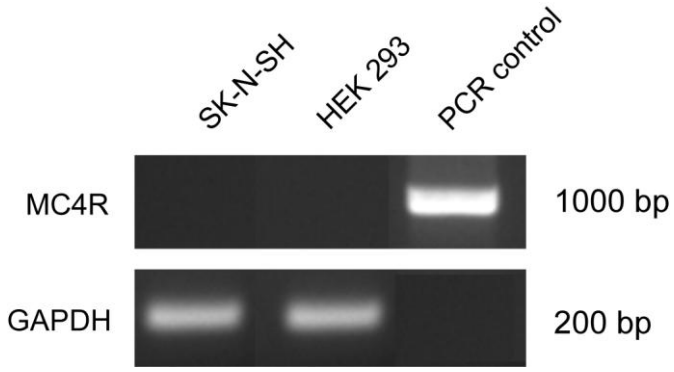

Figure 3.1: *MC4R* mRNA was not detected in HEK 293 or SK-N-SH cells

mRNA from SK-N-SH or HEK 293 cells was reverse transcribed to obtain cDNA. Primers for *MC4R* were used to amplify *MC4R* transcript from the cDNA obtained from each cell line. No endogenous expression of MC4R was observed in SK-N-SH or HEK 293 cell lines. GAPDH was used as a positive control for mRNA extraction and the RT reaction. Positive control for PCR shows amplification of MC4R from pcDNA3.1 3xHA-MC4R vector.

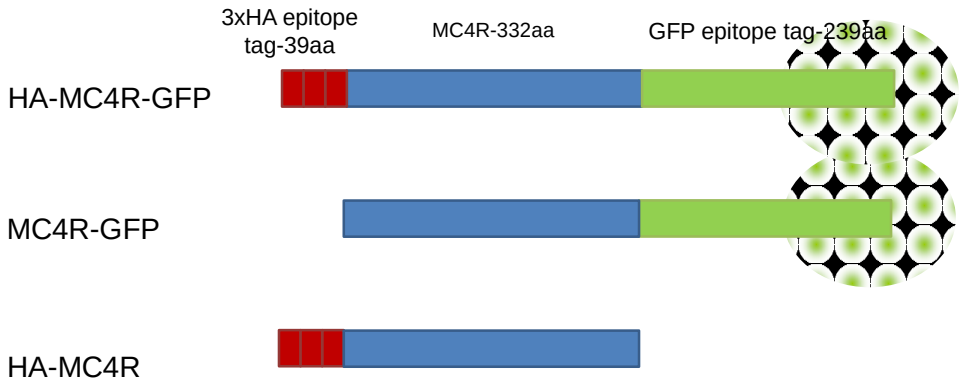

Figure 3.2: Schematic of the three WT MC4R construct used in this thesis
HA-MC4R was sub-cloned into pEGFP-N1 vector to generate the HA-MC4R-GFP fusion protein. MC4R-GFP was generated by PCR of the MC4R sequence from HA-MC4R pcDNA3.1 and sub-cloning the isolated MC4R insert into pEGFP-N1.

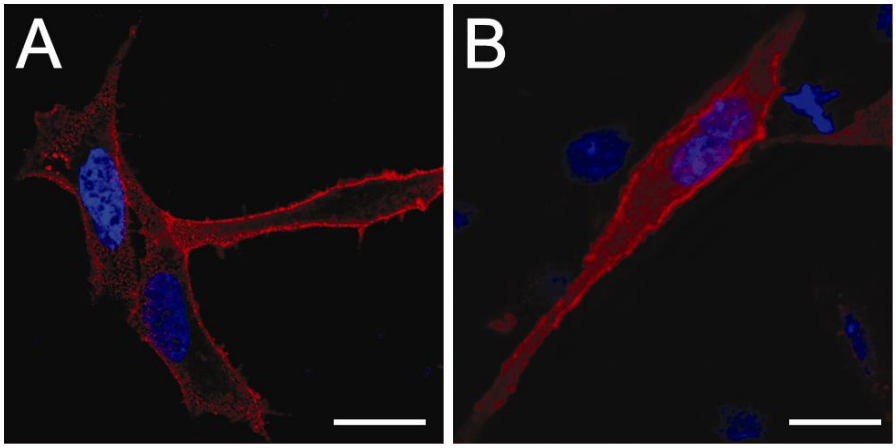

Figure 3.3: Wild-type HA-MC4R clearly localises to the plasma membrane (PM)

HEK 293 (A) or SK-N-SH (B) cells were transfected with WT HA-MC4R. 24 hours post transfection permeabilised cells were stained for the N-terminal HA tag (red) and nuclei (blue). Scale bar = 10 µM

3.2.3 Localisation of HA-MC4R-GFP

The HA-MC4R-GFP construct was designed to enable the quantification of cell surface and total levels of WT and mutant MC4R. The initial strategy was to measure cell surface levels of MC4R by immunostaining for the extracellular haemagglutinin (HA)-epitope tag, whilst total levels of the receptor were to be monitored by quantifying the GFP fluorescence. An added advantage of using a GFP-tagged construct was that the level of transfection efficiency could easily be determined by visualising the transfected cells using a fluorescent microscope before proceeding to subsequent assays.

HEK 293 cells were transfected with the wild-type construct HA-MC4R-GFP (WT HA-MC4R-GFP) and 24 hours post-transfection cells were fixed and stained for the HA-epitope tag. The sub-cellular localisation of HA-MC4R-GFP was then analysed by confocal microscopy. Interestingly, in a high proportion of transfected cells, MC4R staining was not predominantly at the plasma membrane (Fig. 3.4, C). With respect to the HA-MC4R-GFP construct, despite clear PM localization being observed in the permeabilised cells stained with anti-HA antibody (Fig. 3.4, A), the majority of GFP expression was observed intracellularly (Fig. 3.4, B). This suggests that only a small amount of the HA-MC4R-GFP fusion protein efficiently trafficked to the PM.

A possible reason for detecting the majority of HA-MC4R-GFP fusion protein as intracellular retained was that the amount of plasmid used in transfections, resulted in high levels of protein expression that saturated the cells ability to efficiently traffic MC4R. Therefore the amount of plasmid used to transfect cells was titred out resulting in a reduced level of protein being heterologously expressed. Visualisation of the cells transfected with a reduced amount of plasmid showed the majority of fusion protein still remained intracellularly localised (Fig. 3.4 D-E). In summary the WT HA-MC4R-GFP did not traffic efficiently to the PM with the majority of MC4R showing intracellular staining.

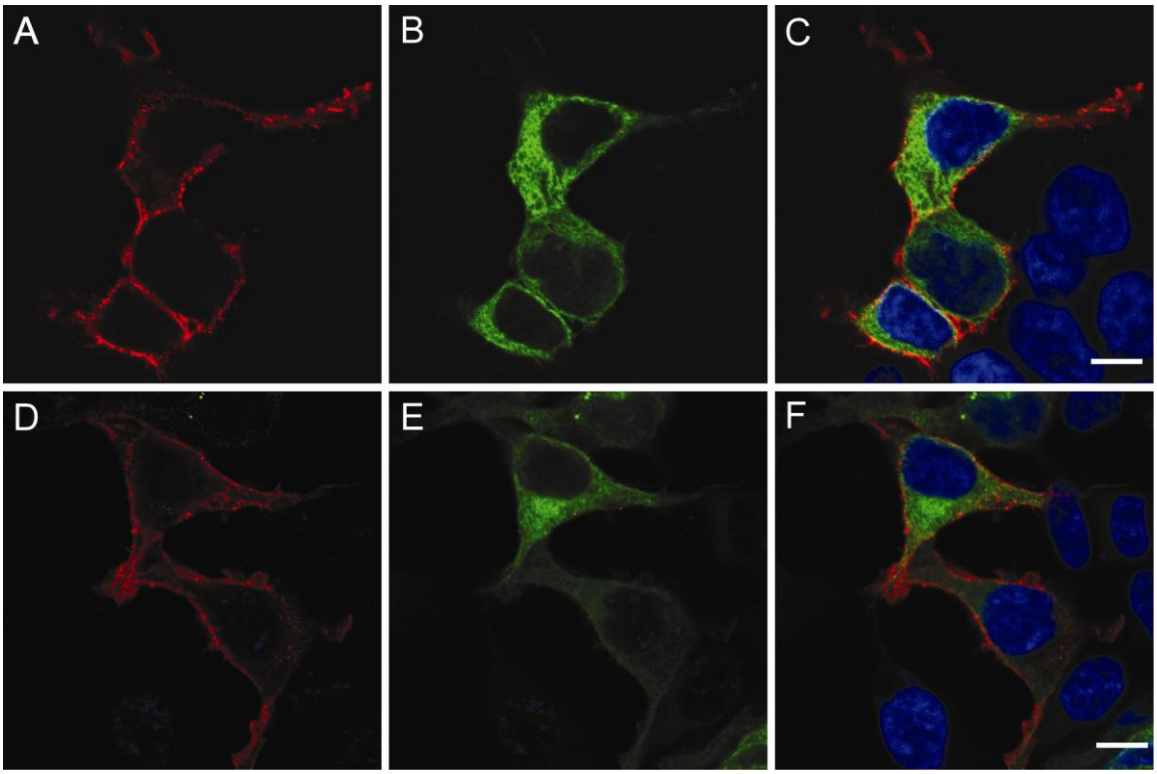

Figure 3.4: Localisation of HA-MC4R-GFP in HEK 293

HEK 293 cells were transiently transfected with HA-MC4R-GFP construct and 24 hours post-transfection were stained with primary anti-HA primary antibody and subsequently with Cy3 conjugated secondary antibody. Cell visualised by confocal microscopy showed PM localisation of N-terminal HA epitope tag (red) (A, D) intracellular localisation of C-terminal GFP tag (green) and (B, E) merged image with nuclei staining (blue). Although the amount of plasmid used for the transfection was reduced by half, the amount of HA-MC4R-GFP fusion protein at the cell surface did not increase suggesting that only a relatively small amount of protein was localized at the cell surface (D-F). Scale bar = 10 µM

3.2.4 Localisation of C-terminal tagged MC4R construct

To test if the GFP fusion was causing the intracellular retention of HA-MC4R-GFP, a construct solely tagged with GFP was synthesised. Wild-type MC4R was cloned into pEGF-N1 introducing a GFP tag on the C-terminus of the receptor. The selected mutations were then introduced by site directed mutagenesis and confirmed by sequencing. Wild-type MC4R-GFP was transiently transfected into HEK 293 cells and the WT fusion proteins localisation was observed by confocal microscopy. Once again little PM localisation of the GFP tagged MC4R protein was observed in fixed cells relative to intracellularly localised protein (Fig. 3.5). Furthermore, reducing the amount of plasmid DNA did not result in an increase in PM localisation of WT MC4R-GFP. In conclusion inefficient trafficking of C-terminal GFP tagged MC4R to the PM occurred in transfected HEK 293 cells.

3.2.5 Quantification of cell surface expression for epitope tagged MC4R

HEK 293 cells were transfected with all three WT constructs (HA-MC4R-GFP, MC4R-GFP, HA-MC4R), and 24 hours post transfection cells were fixed and stained. The number of cells with MC4R staining predominantly at the cell surface was quantified by blind counting after processing for immunofluorescence microscopy in 10 different fields of view. 70% of WT HA-MC4R transfected cells exhibited cell surface expression of the protein. However, HEK 293 cells transfected with GFP tagged MC4R had less than 20% of the cells predominantly expressing the receptor at the cell surface (Fig. 3.6). This may suggest that a C-terminal GFP tag on the receptor may hinder the receptors trafficking to the cell surface.

In order to investigate if inefficient trafficking of GFP tagged MC4R constructs was cell specific SK-N-SH cells were utilised.

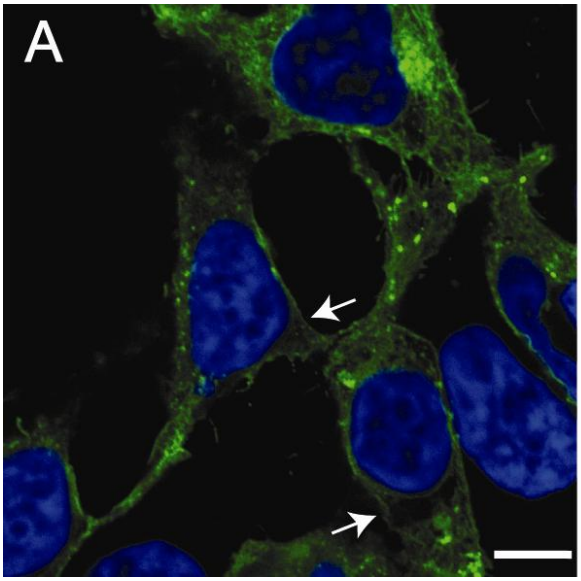

Figure 3.5: Localisation of WT MC4R-GFP in HEK 293 cells

HEK 293 cells were transiently transfected with WT MC4R-GFP (green), 24 hours post transfection cells were fixed and nuclei stained (blue). Cells were visualised by confocal microscopy. Arrows indicate areas of PM localisation. Scale bar = 10µM

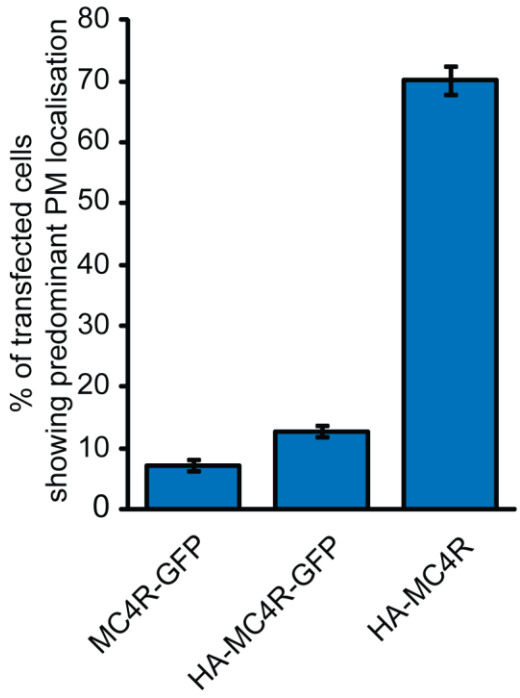

Figure 3.6: Quantification of cells showing PM localisation for epitope tagged MC4R

HEK 293 cells were transiently transfected with MC4R-GFP or HA-MCR-GFP or HA-MC4R. Cells were fixed and processed for immunofluorescence. The percentages of cells showing PM localisation were counted blind to experimental status in 10 different fields of view. Error bars represent the mean ±SD.

3.2.6 Localisation of WT MC4R in SK-N-SH cells

Localisation of MC4R fusion proteins was also analysed in SK-N-SH neuroblastoma cell line. The same amount of WT MC4R-GFP used in HEK 293 cells was used to transfect SK-N-SH cells. Interestingly no PM localisation of WT MC4R-GFP was observed in SK-N-SH cells (Fig.3.7, A). However, an increase in the number of cells exhibiting an abnormal morphology was observed in mutant MC4R expressing SK-N-SH cells (Fig.3.7 B). Perinuclear inclusions of mutant MC4R in SK-N-SH cells were also observed (Fig.3.7, B). Furthermore, cells expressing mutant MC4R-GFP showed an increased number of inclusions when compared WT MC4R-GFP expressing cells (Fig.3.7, B). The number of MC4R inclusions observed was quantified for both wild-type and mutant MC4R transfected SK-N-SH cells. A significant difference was observed in the percentage of inclusions for WT MC4R expressing SK-N-SH cells compared to mutant MC4R expressing SK-N-SH cells (Fig.3.7, C). Interestingly, severe mutant P78L (Lubrano-Berthelier et al., 2003) showed a higher incidence of inclusion formation compared to L106P, a mutation that has been previously described as a less severe mutation (retains partial function) (Tao & Segaloff, 2003). Therefore, the level of inclusion incidence may reflect the severity of MC4R mutations, with the more severe mutations such as MC4R-GFP (P78L) showing a higher incidence of inclusion formation than a less severe mutation such as MC4R-GFP (L106P). When SK-N-SH cells were transfected with HA-MC4R, clear PM localisation of the receptor was observed (Fig.3.3, B)

In summary the WT MC4R was most efficient at trafficking to the PM with an N-terminal HA epitope tag than a C-terminal GFP tag. Furthermore, mutant MC4R-GFP caused an increased incidence of inclusion formation. In conclusion SK-N-SH cells appear to be highly sensitive to expression of intracellularly retained MC4R mutants rapidly forming MC4R “aggresome” like inclusions. Aggresomes are accumulated insoluble protein aggregates formed in a microtubule dependant fashion (Johnston et al., 1998) and have been previously described in intranuclear

and perinuclear inclusions *in vitro* models of Retinitis Pigmentosa disease (Mendes & Cheetham et al., 2008). Furthermore, as HA tagged MC4R localised at the cell surface, this suggests that the presence of the C-terminal GFP tag may inhibit MC4R trafficking to the PM. Therefore in all subsequent experiments HA-MC4R was the construct used for heterologous expression of MC4R.

3.2.7 Expression analyses of MC4R expression in cells transfected with HA-MC4R

MC4R mutants HA-MC4R (D90N, S58C, P78L, L106P, C271Y, N62S, and P299H) were introduced into the triple HA tagged WT MC4R vector by site directed mutagenesis. HEK 293 cells were transfected with vectors for the expression WT HA-MC4R or mutant HA-MC4R and 24 hours post transfection cell lysates were collected and resolved on an SDS-PAGE gel. For both WT and mutant HA-MC4R high molecular weight smears and a band of approximately 32.5kD in size were observed (Fig. 3.8). Although the same amount of WT and mutant MC4R plasmids were used during transfection and the same amount of total protein was loaded, higher cellular levels were observed for some mutant constructs (e.g.HA-MC4R (S58C), HA-MC4R (P78L), HA-MC4R (C271Y), and HA-MC4R (P299H)). Whilst HA-MC4R (L106P) and HA-MC4R (D90N) showed lower band intensities when compared to the other constructs (Fig. 3.8). For mutant HA-MC4R (N62S) an additional lower molecular weight band of approximately 16.5kD was observed (Fig. 3.8). This may represent a degradation product of mutant MC4R.

As HA- MC4R was detected in HEK 293 cells by western analysis, the next step was to investigate MC4R sub-cellular localisation.

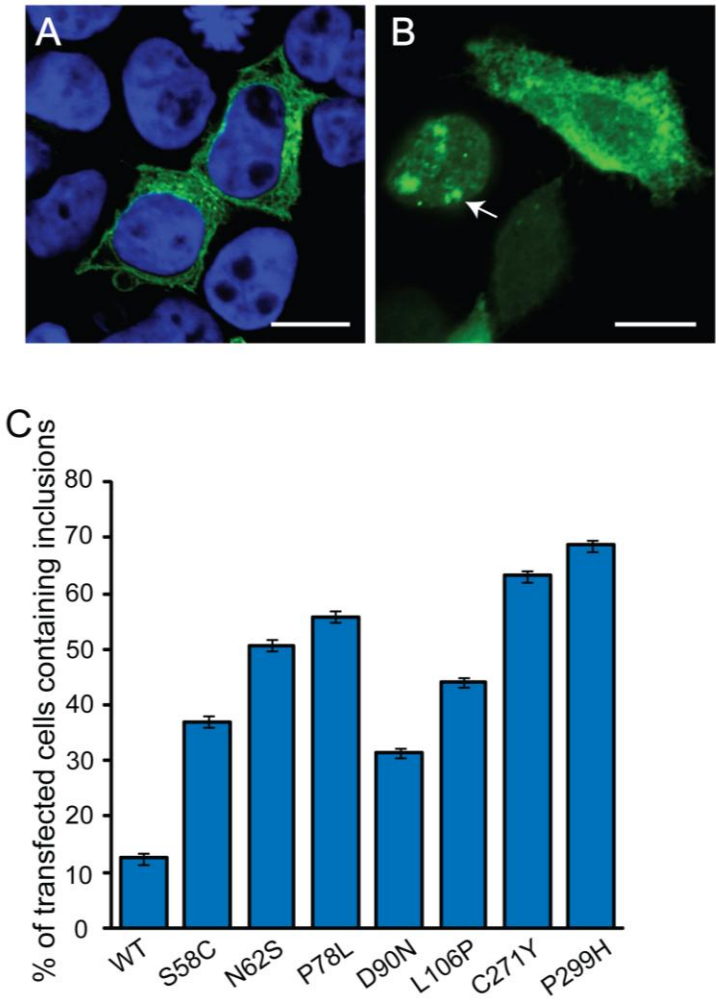

Figure 3.7: Immunofluorescence of wild-type and mutant MC4R-GFP constructs in SK-N-SH cells and quantification of MC4R inclusions

SK-N-SH cells transfected with WT MC4R-GFP exhibited PM and intracellular localisation (A). SK-N-SH cells transfected with mutant MC4R-GFP (L106P) formed inclusions. Arrow shows MC4R inclusions scale bar = 10µM (B). 24-hours post transfection cell were fixed and stained. The percentage of cells with fluorescent intracellular inclusions were counted blind in 5 different fields of view (C). Using a student's t-test P <0.001 for all mutants compared with WT. Using one way ANOVA and Dunnett's Multiple Comparison post-test P <0.0001 for all mutants compared with WT. Error bars represent the mean ±SD.

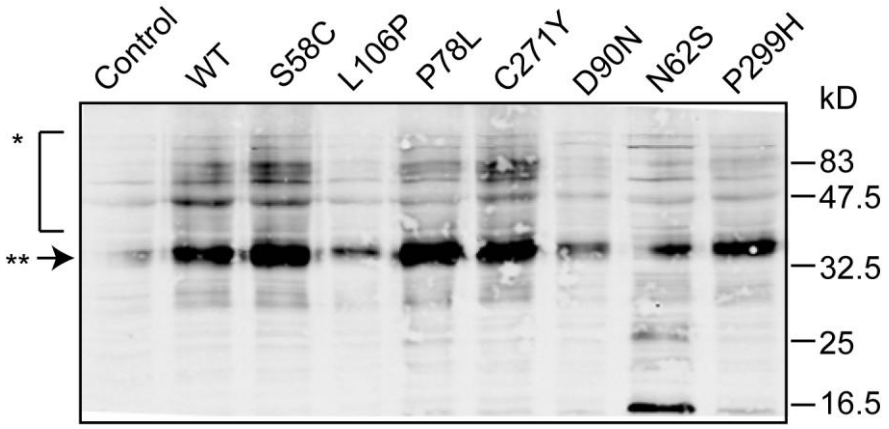

Figure 3.8: WT and mutant MC4R protein expression in HEK 293 cells

HEK 293 cells were transfected with WT or mutant HA-MC4R. 24 hours post transfection cells were lysed in RIPA buffer containing phosphotase and protease inhibitors. Samples were resolved on a 12% SDS-PAGE gel and immunoblotted with anti-HA antibody and IRDye® 800CW secondary antibody. The membrane was scanned on a LI-COR infrared scanner detecting infrared fluorescence from the secondary antibody. *High molecular weight bands and ** distinct MC4R band size of ~ 32.5kD was observed.

3.2.8 Localisation of N-terminal HA-epitope tagged WT MC4R and mutant MC4R in HEK 293 cells

Treatment of cells with detergent triton X-100 to permeabilise the PM, as would be predicted, showed some WT HA-MC4R protein was localised intracellularly (Fig. 3.3). Varying degrees of PM localisation was observed for HA-MC4R mutant proteins, with HA-MC4R (L106P) showing partial PM localisation and HA-MC4R (P78L) no PM localisation (Fig. 3.9). Triton X-100 treatment of cells expressing HA-MC4R mutant proteins showed that the majority of mutants had an intracellular localisation, with all mutants showing reduced PM localisation when compared to the WT receptor (Fig. 3.9). In summary the immunofluorescence data shows that HA-MC4R (P78L) and HA-MC4R (P299H) are completely intracellular retained, with HA-MC4R (C271Y), HA-MC4R (N62S) and HA-MC4R (D90N) showing a small amount of PM localisation compared to HA-MC4R (L106P) which shows the most PM localisation.

To investigate whether the misfolding mutants were retained intracellularly within the ER additional staining with an antibody against ER retention peptide motif KDEL (lys-asp-glu-leu) was carried out. Some overlap between KDEL and WT HA-MC4R was observed (Fig. 3.10). Furthermore, an apparent increase in overlap was observed for the more severe misfolding mutants, HA-MC4R (P78L), compared to less severe mutants HA-MC4R (L106P) (Fig. 3.10). Therefore it is likely that the selected MC4R misfolding mutants are intracellular retained at the ER.

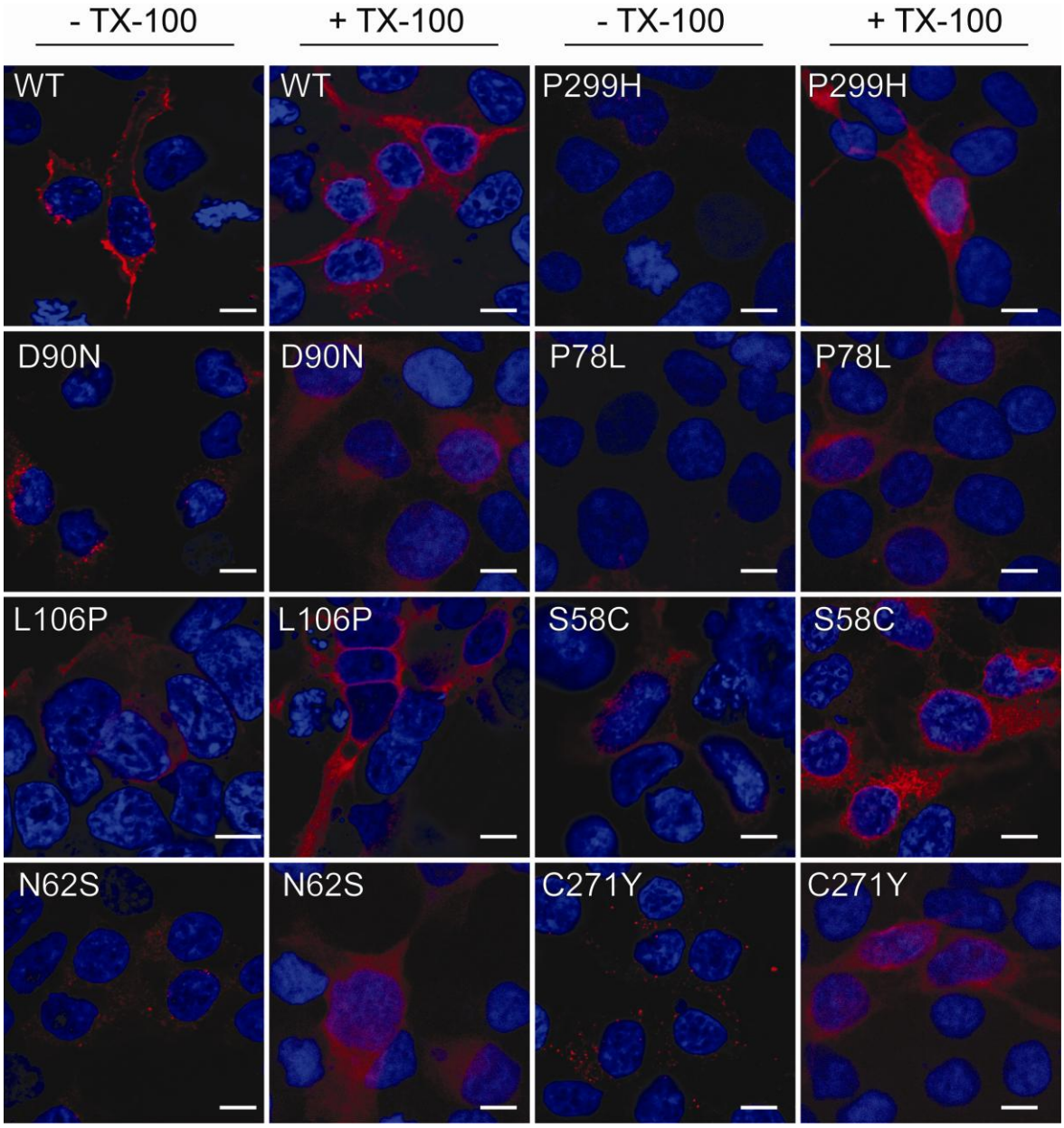

Figure 3.9: Identification of ER retained MC4R mutants by confocal microscopy

HEK 293 cells were transfected with either WT or mutant HA-MC4R. 24 hours post transfection cell staining for the N-terminal HA tag (red) and nuclei (blue) was carried out in permeabilised and non-permeabilised cells. Scale bar = 10 µM

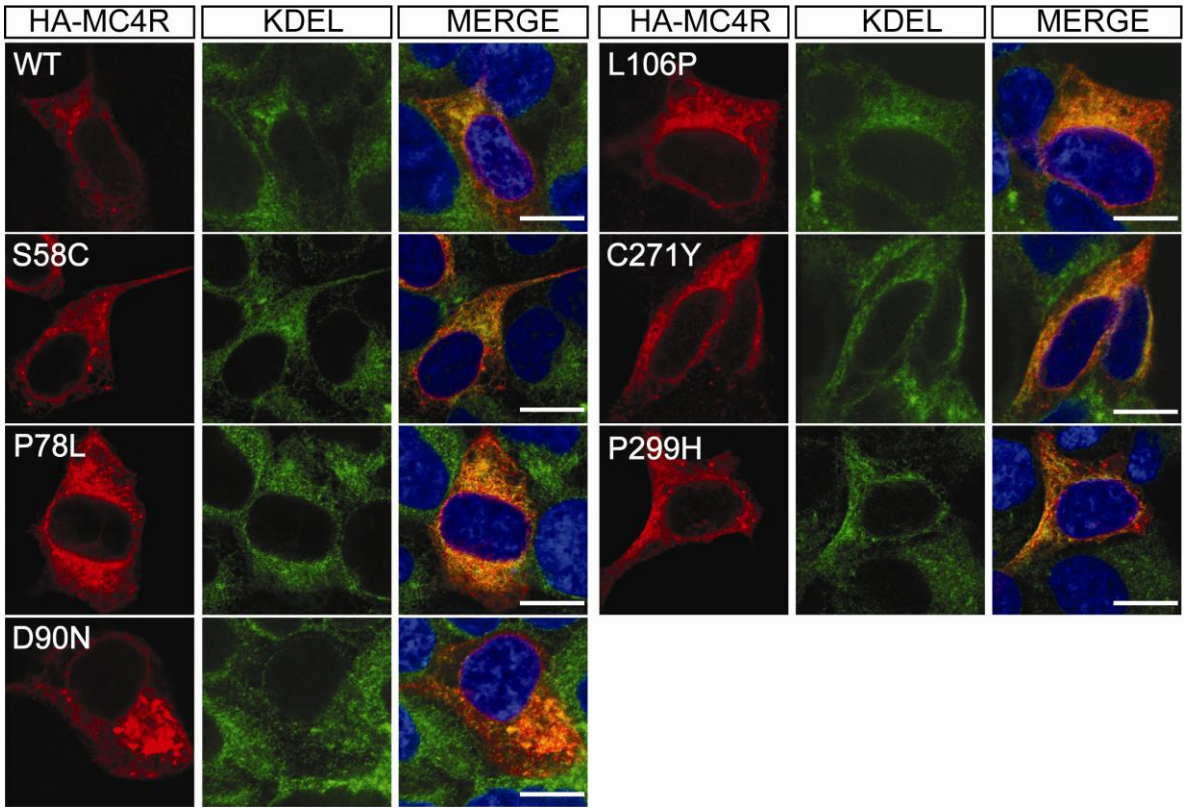

Figure 3.10: Co-localisation of ER retained mutants with ER marker KDEL

HEK 293 cells were transfected with WT or mutant HA-MC4R. 24 hours post transfection cell staining for the N-terminal HA-tag (red), ER marker KDEL (green) and nuclei (blue) was carried out in permeabilised cells. Scale bar = 10 µM

3.2.9 Measurement of WT and mutant MC4R signalling at the cell surface using Luciferase assay

Confocal microscopy demonstrated that WT HA-MC4R could traffic to the cell surface in our model but mutant MC4R was retained at the ER. Therefore, a luciferase reporter construct, which regulates the activity of the luciferase gene (Fowkes et al., 2003), was utilised to measure WT and mutant HA-MC4R signal transduction. The luciferase reporter construct (αGSU) was transiently co-expressed with MC4R in HEK 293 cells. It was hypothesised that variability in activity for the different misfolded mutant MC4R would be observed, as some mutants are more intracellular retained than others.

The results showed that WT HA-MC4R had more functional activity than mutant HA-MC4R (Fig.3.11). Furthermore, the data indicated that the more intracellular retained mutants e.g. HA-MC4R (P78L) were less capable of signalling than partially retained mutants e.g. HA-MC4R (L106P) (Fig.3.11). This assay was used to determine the efficacy of selected compounds on rescuing mutant function at the cell surface.

As the bioluminescence measured in this assay is downstream from receptor, to confirm that WT MC4R does indeed have a greater functional activity than MC4R mutant protein a cAMP assay was also carried out. This data was concurrent with the luciferase assay clearly indicating that WT HA-MC4R is more functionally active than mutant HA-MC4R (P78L) (Fig.3.12).

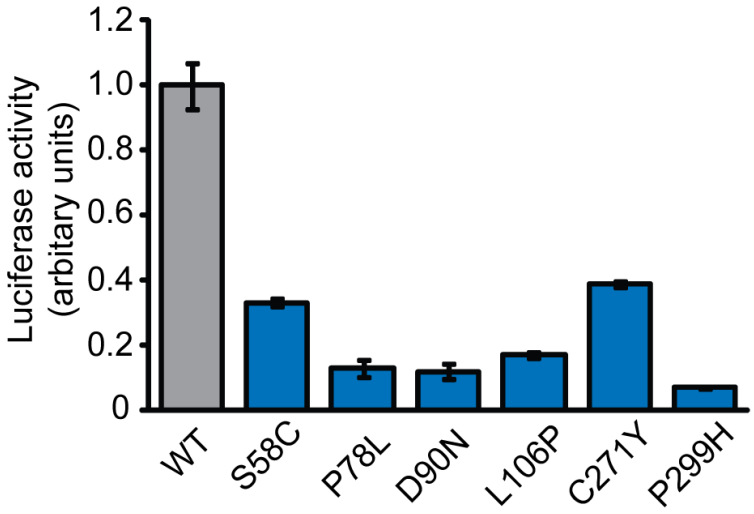

Figure 3.11: Misfolding mutant MC4R is unable to signal as well as wild-type MC4R transducing receptor

Using a luciferase reporter system for cAMP activity signalling was quantified for wild-type and mutant HA-MC4Rs. HEK 293 cells were transfected with equal concentrations of plasmids for expression of WT or mutant HA-MC4R, or empty control vector. Cells were co-transfected with a luciferase reporter construct for MC4R signalling, and a vector for renilla expression. 16 hours post transfection cells were stimulated with 10^{-7}M NDP-MSH for 6 hours and luciferase activity was measured. Values were normalised to renilla activity to control for variability in transfection. $P<0.05$ for all mutants compared with WT. Error bars represent the mean ±SD.

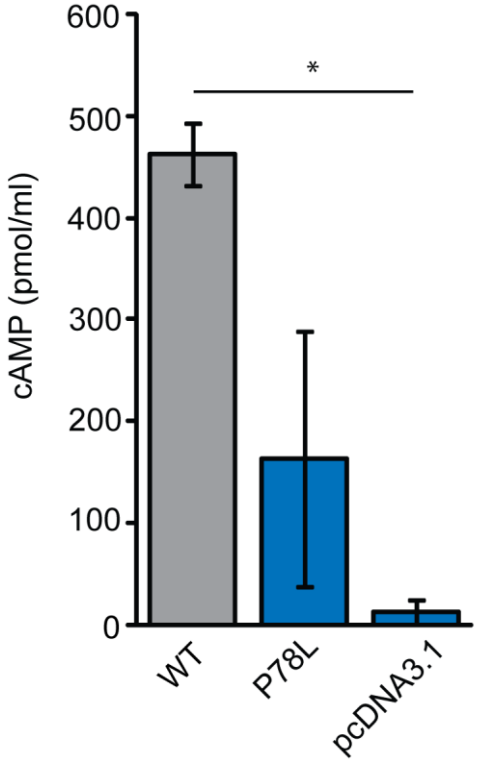

Figure 3.12: HA-MC4R (P78L) is unable to signal as well as normal WT transducing receptor

HEK 293 cells were transfected with WT HA-MC4R, severe misfolding mutant HA-MC4R (P78L) or empty vector (pcDNA3.1). 24 hours post- transfection cells were stimulated with 10^{-7}M NDP-MSH for 30 minutes, cell lysates were obtained and intracellular cAMP was measured. WT HA-MC4R shows a significant increase in cAMP production compared with the misfolding mutant HA-MC4R (P78L). $P<0.05$. Error bars represent the mean ±SD.

3.2.10 Development of a rapid throughput assay to monitor MC4R cell surface expression

The construct HA-MC4R-GFP was initially intended to be used to measure the cell surface expression of wild-type and mutant MC4R. However due to the lack of cell surface expression an (Fig.3.9) in cell western assay was developed using HA-MC4R. The assay was designed to detect the HA tagged N-terminus of MC4R, which is localised extracellularly when the receptor is correctly trafficked to the PM. To obtain cell surface expression values, HA-MC4R localised at the PM in non-permeabilised HEK 293 cells, was detected by immunofluorescence using an anti-HA primary antibody and an infrared dye conjugated secondary antibody. This fluorescence staining was detected on an infrared scanner (Odyssey, LI-COR). Total cellular levels of MC4R were quantified in cells permeabilised (as antibody cannot enter non-permeabilised cells) with triton X-100 and also stained with an anti-HA primary antibody and an infrared dye conjugated secondary antibody (Fig.3.13, A). MC4R trafficking values were obtained by dividing integrated intensity values for each non-permeabilised well by the average integrated intensity value obtained for the matching permeabilised well. The values were normalised against WT HA-MC4R and a DNA stain to correct for any difference in cell number.

Immunofluorescence data indicated reduced staining for MC4R mutant proteins compared to WT HA-MC4R in non-permeabilised cells, with more severely intracellulary retained mutants, e.g. HA-MC4R (P78L), showing a more dramatic percentage reduction (71.47±3.39%) when compared to less severe mutants e.g. HA-MC4R (L106P) (33.63±6.81%) (Fig.3.13, B). Similar to previous studies there was variability in the severity of cell surface expression of MC4R misfolding mutants. For example mutant HA-MC4R (D90N) showed a more pronounced reduction in cell surface expression (55.22±15.17%) than HA-MC4R (P299H) (8.45±3.72%) (Fig.3.13, B). With the development of this assay the degree of cell surface expression of WT HA-MC4R and mutant MC4R can be quantified, and the effect of modulators of MC4R cell surface expression analysed.

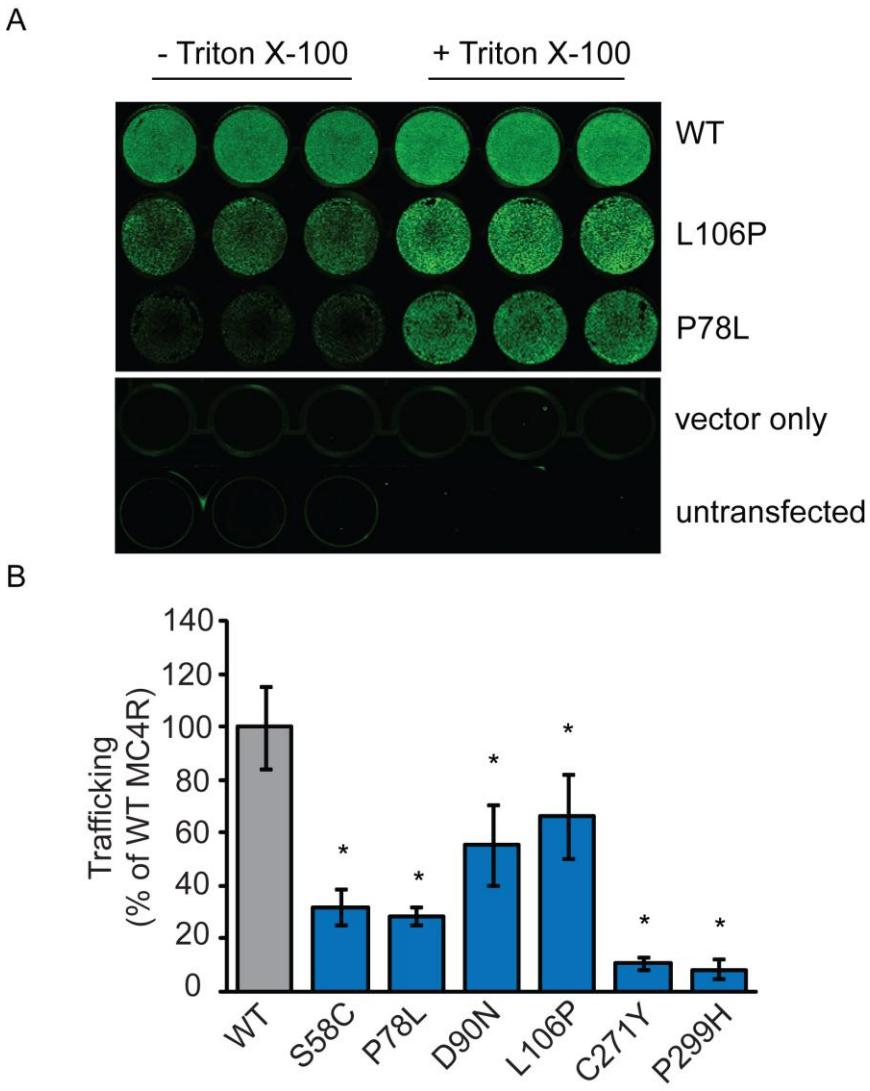

Figure 3.13: Quantification of levels of cell surface expression of WT and mutant HA-MC4R using a rapid throughput cell surface assay

Representative image of a culture plate containing HEK 293 cells expressing HA-MC4R stained with an anti-HA primary antibody and IRDye® 800CW secondary antibody. The tissue culture plate was scanned on a LI-COR infrared scanner. Cell surface expression was detected in non-permeabilised cells and total expression in triton X-100 treated permeabilised cells (A). Comparison of the trafficking levels of WT HA-MC4R and MC4R harbouring clinically occurring mutations that are predicted to cause the protein to aberrantly fold (B). *P<0.05. Error bars represent the mean ±SD.

3.2.11 Development of HEK 293 cell lines stably expressing MC4R

To further investigate the *in vitro* trafficking of MC4R mutants we developed HEK 293 cell lines stably expressing WT HA-MC4R, HA-MC4R (L106P), HA-MC4R (D90N), HA-MC4R (S58C) and HA-MC4R (P78L) (Fig.3.13). Stable cell lines were also developed because of the limitations of transient transfections, such as variable transfection efficiency between experiments and were subsequently used as a complementary approach.

Monoclonal stable cell lines under the selection of Geneticin (G418) were created. To determine the expression levels between the different clones the cell lysates were collected and run on an SDS-PAGE gel. Differential expression was observed for clones of the same mutant and the following clones that were easily detectable on an SDS-PAGE gel were selected and propagated; WT HA-MC4R clone 3, HA-MC4R (D90N) clone 3, HA-MC4R (P78L) clone 6, HA-MC4R (S58C) clone 5 and HA-MC4R (L106P) clone 4 (Fig.3.14, A). To confirm the sub-cellular localisation of the receptor in the stably expressing HEK 293 cell lines, immunofluorescence was carried out using a primary antibody detecting the N-terminal HA tag. Localisation of WT HA-MC4R was visible at the cell surface (Fig.3.14, B). Mutant HA-MC4R (D90N) was partially localised at the cell surface but with the majority of the mutant receptor localised intracellularly (Fig.3.14, B).

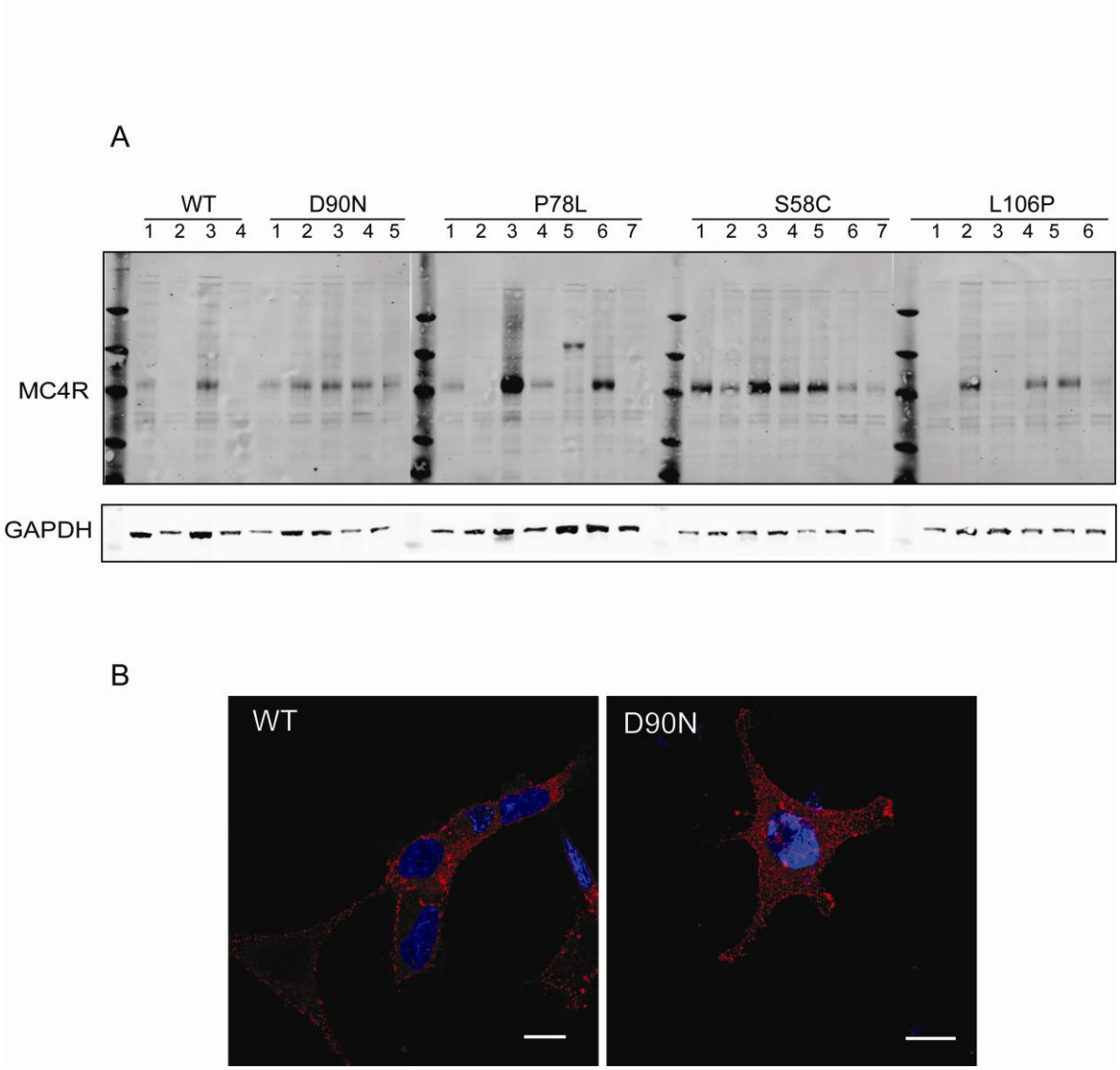

Figure 3.14: Analysis of expression of HEK 293 cells stably expressing WT and mutant MC4R

MC4R cell lysate samples were resolved on a 12% SDS-PAGE gel and immunblotted for MC4R with anti-HA antibody (A). Immunofluorescence of HEK 293 cells stably expressing WT HA-MC4R or mutant HA-MC4R (D90N) (B). Scale bar = 10μM

3.2.12 Analysis of WT and mutant MC4R glycosylation status

Most GPCRs are glycosylated proteins and require this post-translational modification in order to reach the cell surface (Lanctot et al., 2006). In order to determine the extent of N-linked glycosylation, the selected MC4R mutant's cell lysates were collected and treated with Endoglycosidase H (EndoH) or Peptide N-glycosidase F (PNGaseF). EndoH is an enzyme that specifically cleaves high mannose oligosaccharides from N-linked glycoproteins and therefore will only cleave sugars from ER resident proteins. PNGaseF cleaves all oligosaccharides that are added in the secretory pathway, resulting in the unglycosylated form of the protein (Alberts et al., 2002).

After PNGaseF treatment a band of approximately 30 kD was observed and levels of higher weight species were decreased (Fig.3.15, A). This suggested that sugars added to the glycosylated protein were effectively cleaved resulting in a lower molecular weight unglycosylated MC4R. WT HA-MC4R showed little resistance to EndoH digestion, producing a band of slightly higher molecular weight of ~ 31 kD in size (Fig.3.15, A). The same pattern of mobility was observed for the severe mutants HA-MC4R (P78L) and HA-MC4R (P299H) when treated with EndoH or PNGaseF (Fig.3.15, A).

The majority of WT HA-MC4R appeared not to be maturely glycosylated in this model, particularly as functional WT HA-MC4R was observed at the cell surface (Fig.3.11). If levels of transfected MC4R were too high the endogenous cellular machinery could possibly fail to fully process all the heterologously expressed protein. To address this issue reduced amounts of plasmid was used in subsequent transfections. However, the same results were observed with the WT receptor showing little resistance to EndoH digestion (Fig.3.15, B). To ensure that the enzymes were functioning effectively two controls (rod opsin and MRAP 2) were also treated with EndoH and PNGaseF and analysed by western blot. Although the expected glycosylation states for both rod opsin and MRAP 2 were observed, WT MC4R continued to be digested with EndoH (Fig.3.15, C).

3.2.13 Effects of agonists on MC4R trafficking

To investigate the practicality of testing the efficacy of different agonists and antagonists on MC4R trafficking, the in cell western assay was utilised to test MC4R agonist α-melanocyte-stimulating hormone (α-MSH) and agouti related peptide (AGRP) on MC4R trafficking.

(α-MSH) synthetic analogue [Nle^4-D-Phe^7]-α-melanocyte-stimulating hormone (NDP-MSH) was used in the cell culture assay. NDP-MSH has similar binding affinity for MC4R compared to α-MSH and contains the minimal core sequence required for α-MSH biological activity (His-Phe-Arg-Trp) (Nargund et al., 2006).

HEK 293 cells were seeded in a 24 well plate, transfected with WT HA-MC4R and incubated overnight with or without NDP-MSH. It was hypothesised that ligand binding at the ER may stabilise MC4R and promote cell surface expression. Because ligand binding at the cell surface causes receptor internalisation media was replaced, to remove NDP-MSH before assaying for cell surface expression of MC4R. However, even when NDP-MSH was removed from the cells 4 hours before assaying for cell surface expression, reduced cell surface levels of MC4R were observed suggesting that MC4R recycling was limited in HEK 293 cells (Fig.3.16, A).

Therefore, it was hypothesised that it would be possible quantify the effects of agonist on MC4R trafficking if internalisation was blocked. It had been reported that agonist dependent internalisation of MC4R could be blocked with the pre-incubation of cells with internalisation inhibitors (Hansen et al., 1993). The experiment was repeated again with a one hour pre-incubation of cells with an internalisation blocker methyl dansyl codavarine (MDC). It was observed that concentrations of MDC above 10 μM resulted in toxicity. The concentration of MDC pre-incubation was subsequently reduced to 5 μM and 2.5 μM, with 2.5 μM concentration of MDC showing no cell death and no reduction in cell surface expression of MC4R after 24 hour incubation with NDP-MSH (Fig.3.16, B).

In summary the cell culture plate based assay, developed in this study, confirmed previous findings that MC4R undergoes agonist dependent internalisation and inefficiently recycles back to the PM after agonist removal. Internalisation of NDP-MSH was successfully blocked using the lowest concentration of MDC. This approach could be used if this type of assay was used to determine the effects of agonists on MC4R trafficking.

3.2.14 The effect of antagonists on MC4R trafficking

To investigate the practicality of testing the efficacy of different antagonists a similar approach to testing for agonist (above) was utilised. HEK 293 cells were seeded in a 24 well plate and transiently transfected with WT HA-MC4R or mutant HA-MC4R (L106P) and subsequently incubated overnight with or without MC4R antagonist agouti related peptide (AGRP) (18-132) at concentrations of 1nM, 10nM and 100nM. 24 hours post transfection the cells were fixed and stained and cell surface expression of MC4R was quantified. In HEK 293 cells, expressing WT or mutant HA-MC4R, overnight exposure to 1-10 nM AGRP (18-132) caused a concentration dependant increase in cell surface levels of MC4R (Fig.3.17). At 100 nM a slight decrease in cell surface levels was observed for both WT and mutant MC4R compared to concentrations of 1-10 nM (Fig.3.17).

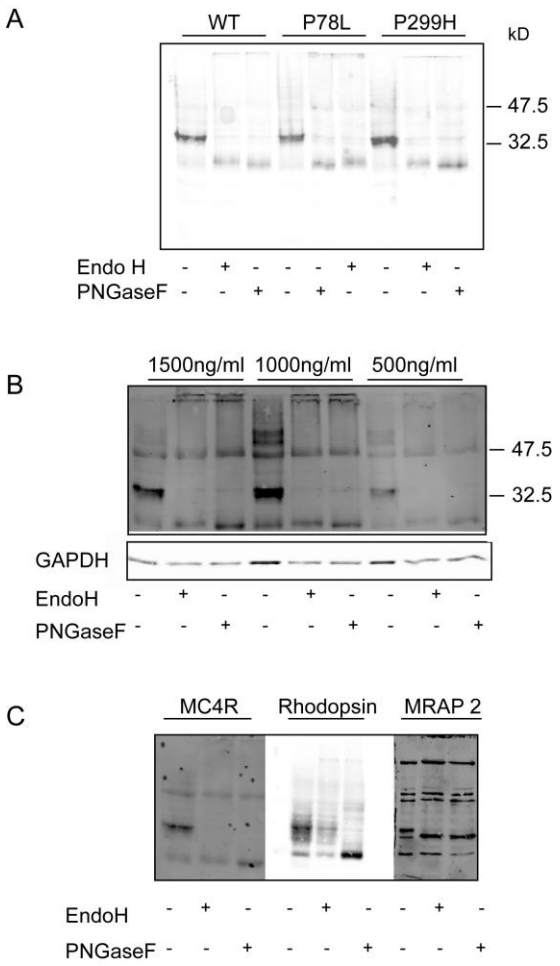

Figure 3.15: Analysis of the glycosylation state of WT HA-MC4R suggests that the majority of the receptor is not maturely glycosylated

HEK 293 cells were transfected with WT HA-MC4R or mutant HA-MC4R (P78L, P299H) (A), reduced concentrations of WT HA-MC4R (B), or WT HA-MC4R, Rod opsin and MRAP 2 (C). Cell lysates were collected for each transfection and treated with or without EndoH or PNGaseF for 2 hours at 37°C. Cell lysate samples were resolved on a 12% SDS-PAGE gel and immunblotted for MC4R with anti-HA antibody, for rod opsin with ID4 anti-rhodopsin antibody and for MRAP with anti FLAG-antibody. Digestion with EndoH produce a band of ~31 kD for both WT and mutant MC4R and a consistent band of ~30 kD was produced after digestion with PNGaseF.

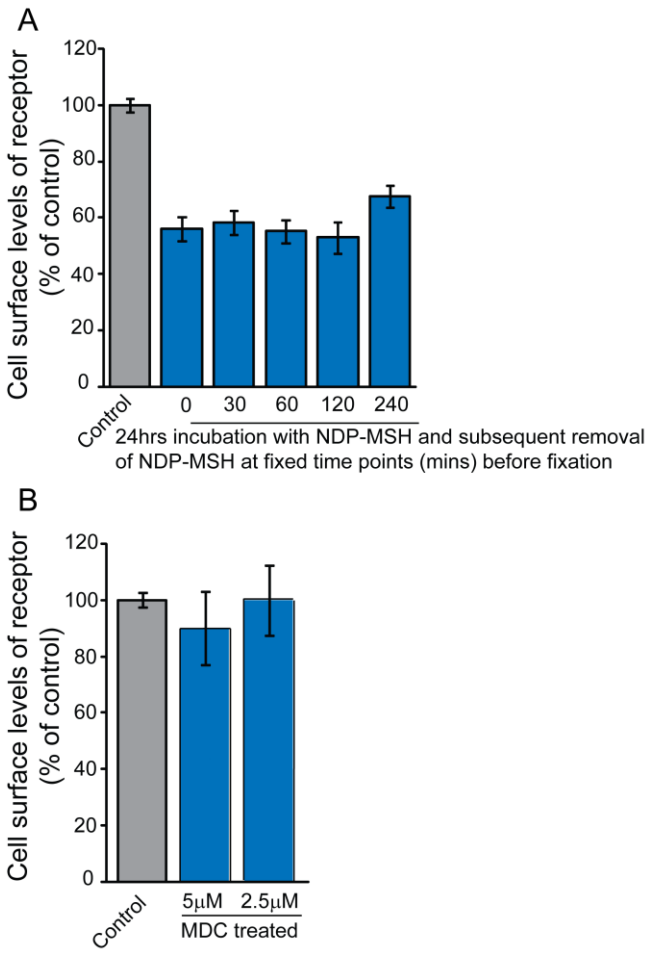

Figure 3.16: Agonist dependent internalisation affects cell surface levels of MC4R

HEK 293 cells were transfected with WT HA-MC4R and exposed to NDP-MSH for 24 hours. NDP-MSH was then removed and cells were left incubating at 37°C before fixation at time points of 0, 30, 60, 120 and 240 minutes. Cell surface expression was measured for MC4R at each time point. $P<0.05$ for all time points compared to control (A). HEK 293 cells were transfected with WT HA-MC4R, and incubated with 10^{-7}M NDP-MSH and in addition with indicated concentrations of MDC for 24 hours. 24 hours post-transfection cells were fixed and stained and cell surface expression was obtained for MC4R at each concentration (B). Error bars represent the mean ±SD.

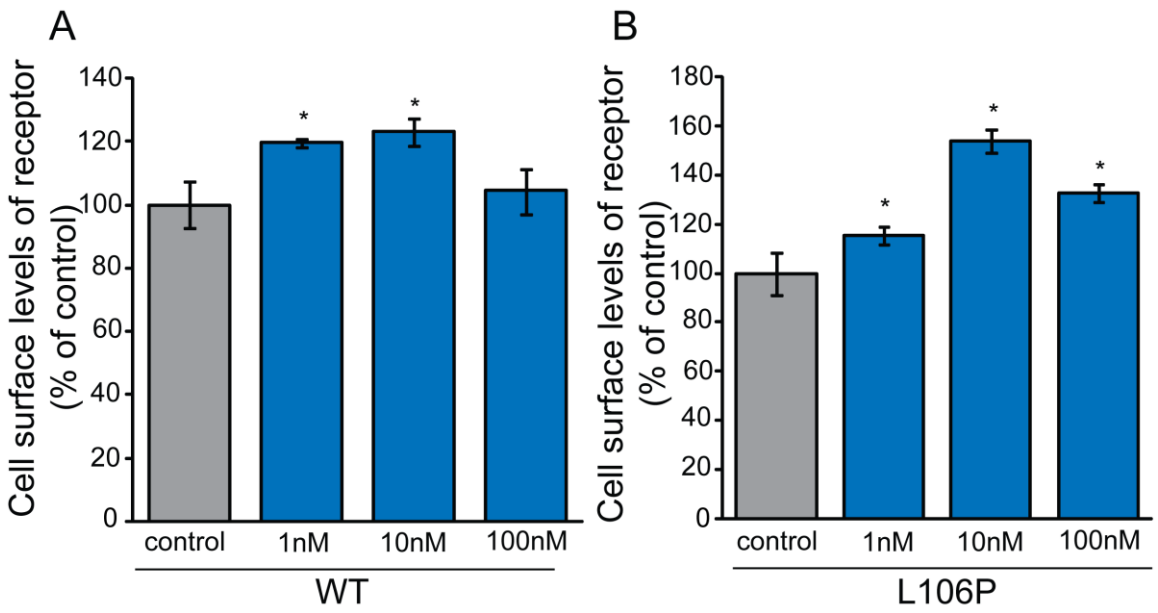

Figure 3.17: AGRP (18-132) causes an increase in cell surface expression of MC4R in HEK 293 cells

HEK 293 cells were transfected with WT (A), or mutant HA-MC4R (L106P) (B), and were exposed to 1, 10 or 100 nM AGRP (18-132) for 24 hours. Cell surface HA-antigen was measured using the cell culture plate based assay to obtain cell surface expression levels of HA-MC4R. *P<0.05. Error bars represent the mean ±SD.

3.3 Discussion

Consistent with previous findings, the MC4R mutations selected for this study disrupt MC4R normal cellular trafficking, with the majority of the receptors retained intracellularly and not expressed at the cell surface in transiently transfected HEK 293 cells. Using confocal analysis it has been shown that some misfolding mutants show more PM localisation than others, indicating that there is variability in the severity of trafficking defects among MC4R misfolding mutants, and that the majority of the mutants are ER retained. In agreement with confocal analysis, quantification of MC4R immunofluorescence, using the in cell western assay, indicated variability in trafficking between MC4R mutants to the cell surface. Using the dual reporter luciferase assay and consistent with previous published data, variability between the capabilities of mutant MC4R to signal was observed.

To visualise the sub-cellular localisation of WT and mutant MC4R, constructs for expression of MC4R-GFP were generated. However, WT MC4R-GFP expressing protein in HEK 293 and SK-N-SH cells did not traffic efficiently to the PM. Furthermore, mutant C-terminal GFP tagged expressing SK-N-SH cells showed a high incidence of inclusion formation. Previously it has been reported that the expression of ER retained mutants of some GPCRs, for example rhodopsin, can result in cell death in neuronal cell types (Saliba et al., 2002). Furthermore, similar to SK-N-SH cells expressing MC4R mutant protein, mutant rhodopsin (P23H) expressing SK-N-SH cells, formed inclusions near the centrosome (Saliba et al., 2002). As N-terminal HA tagged MC4R was capable of trafficking more efficiently to the PM it was concluded that the C-terminal GFP tag was disrupting the cellular trafficking of MC4R. Although GFP has been commonly used to monitor the biological functions of proteins, including MC4R, it has been reported to disrupt the localisation of MC2R (Roy et al., 2007). Roy et al (2007) reported that MC2R-GFP fusion protein impaired cell membrane localisation and signalling in the presence of its accessory protein MRAP (Roy et al., 2007). The carboxy-terminus of MCRs contain a conserved dihydrophobic sequence composed of leucine, isoleucine,

phenylalanine, valine or methionine, preceded by an acidic glutamate or aspartate. For MC4R the motif consists of di-isoleucine at codons 316/317 and disruption of either codon 316 or 317 have been shown to cause decreased cell surface expression and function (VanLeeuwen et al., 2003). Previous studies have shown that the di-leucine motif in the C-terminus of the vasopressin V_2 receptor is required for exit of the receptor from the ER (Schulein et al., 1998). Although this has not been shown for MC4R, it can be hypothesised that the large GFP tag causes steric hindrance of the di-isoleucine motif at the C-terminus and disrupts its function decreasing MC4R trafficking.

N-terminal tagged MC4R was expressed in HEK 293 cells and on SDS-PAGE ran as high molecular weight bands and one sharper band. The high molecular weight bands may represent different glycoforms of MC4R, with an additional smaller band observed for HA-MC4R (N62S) as a cleaved degradation product. The lower band intensities for HA-MC4R (D90N) and HA-MC4R (L106P) may be due to the mutants being targeted for degradation and therefore lower cellular levels were observed for these mutants. The glycosylation experiments revealed that the majority of WT HA-MC4R was not maturely glycosylated *in vitro* and that the sharp band identified at 32.5kD may be the MC4R ER resident glycoform.

Unlike C-terminal tagged MC4R, WT N-terminal tagged HA-MC4R was able to reach the PM more efficiently. Concurrent with previous research the confocal images show that some MC4R misfolding mutations, such as HA-MC4R (L106P), are partially localised at the cell surface whereas other misfolding mutations, such as HA-MC4R (P78L), are more intracellularly localised (Tao & Segaloff, 2003). The immunofluorescence data therefore confirms that some MC4R mutations are more intracellular retained than others.

Treatment of MC4R expressing HEK 293 with NDP-MSH caused internalisation of MC4R. This data suggests that after removal of NDP-MSH MC4R fails to recycle back from the endosome to the cell surface. It has been previously reported that MC4R undergoes slow recycling back to the cell surface in HEK 293 cells (Gao et

al., 2003). Many GPCRs such as the β_2-adrenergic receptor, thyrotropin-releasing receptor type A, C5a anaphylatoxin receptor and cholecystokinin receptor have been shown to recycle back to the cell surface in approximately 20-60 minutes (Gao et al., 2003). Although uncommon in GPCRs, it has been shown that the choriogonadotropin receptor/luteinizing hormone (hCG/LH) receptor and the thrombin receptor do not recycle back to the cell surface but are targeted to the lysosome mediated degradative pathway (Wong and Minchin, 1996). It has also been shown that MC1R expressing B16 melanoma cells treated with NDP-MSH undergo agonist mediated internalisation. In this case MC1R does not recycle back to the PM but is targeted to the lysosome compartment resulting in a down-regulation of the MC1R at the cell surface (Wong and Minchin, 1996). Therefore in this *in vitro* model, after agonist mediated internalisation the majority of MC4R may be targeted to lysosomes instead of recycling back to the cell surface.

It has been reported that a proportion of MC4R expressed in HEK 293 cells internalises spontaneously even in the absence of agonist, and that AGRP (18-132) may inhibit the internalisation or facilitate the recruitment of internalised receptor to the cell membrane (Shinyama et al., 2003). However, to differentiate between AGRP stabilising existing MC4R at the cell surface or AGRP improving the recruitment of internalised receptor to the cell membrane would not be possible to decipher using the current in cell western assay.

This chapter established a cellular model to monitor MC4R cell surface expression. The experimental approach used in subsequent chapters, to elucidate the efficacy of pharmacological reagents on MC4R cell surface expression, are outlined below (Fig. 3.18).

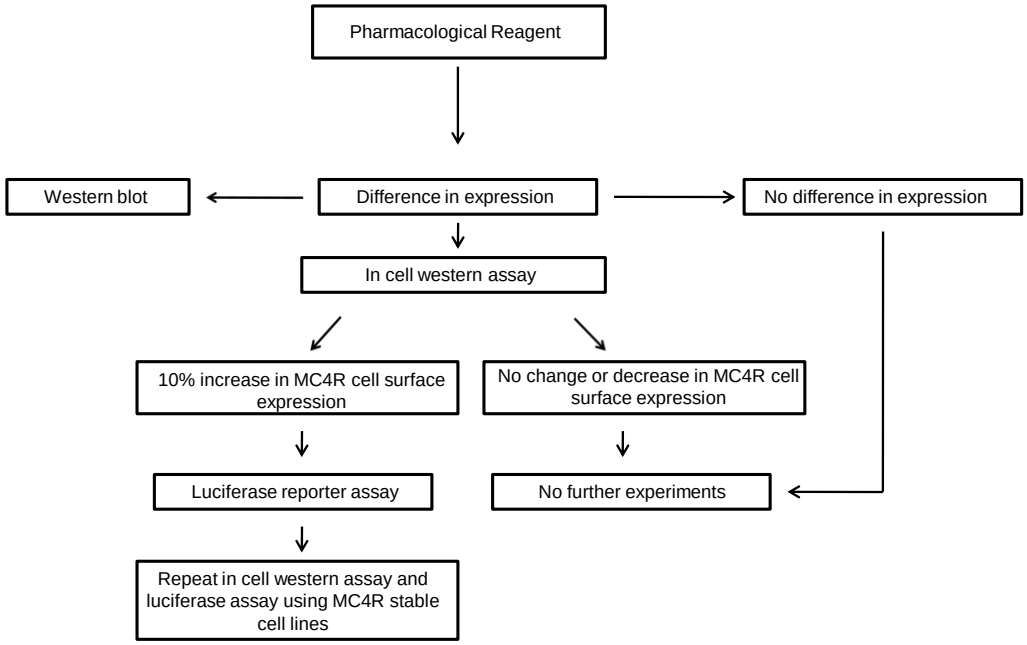

Figure 3.18: Flow diagram to illustrate experimental approach

Flow chart to describe the experiments carried out to elucidate the action of pharmacological reagents on the regulation of MC4R folding and cell surface expression.

CHAPTER 4

Kosmotropes as modulators of MC4R trafficking and functional expression

4.1 Introduction

A number of studies have shown that low molecular weight compounds, known as chemical chaperones/kosmotropes, have potential therapeutic benefit in models of conformational diseases (Powers et al., 2009; Chaudhuri & Paul, 2006). Chemicals with kosmotropic activity include polyols such as glycerol; solvents such as dimethyl sulfoxide (DMSO); methylamines such as trimethylamine-N-oxide (TMAO); fatty acids such as 4-phenylbutyric acid (4-PBA); and simple sugars such as trehalose. Kosmotropes affect protein folding via two different mechanisms. Firstly, kosmotropes promote protein stabilization by increasing the free-energy difference between a partially folded protein and its more compact native structure (Arakawa et al., 2006). Secondly, kosmotropes reduce the free movement of proteins to prevent aggregation of partially folded molecules (Papp & Csermely, 2006).

Kosmotropes have been tested in a number of disease models where transmembrane proteins are aberrantly folded and intracellularly retained, for example, cystic fibrosis. Mouse NIH 3T3 cells expressing the most common clinically occurring cystic fibrosis transmembrane conductance regulator (CFTR) mutation (ΔF508) were treated with either 1.25 M glycerol or 100 mM TMAO for three days. Treatment with the kosmotropes restored the ability of the mutant expressing protein to traffic to the plasma membrane where it was functionally similar to the WT protein, in mediating chloride transport (Brown et al., 1996).

Another example where kosmotropes have been used to rescue endoplasmic reticulum (ER) retention of misfolded proteins was explored in the disease model of Familial Hypercholesterolemia (FH). This disease is caused by mutation in the low-density lipoprotein receptor (LDLR). At a concentration of 5 mM, and incubation time of 24 hours, 4-PBA was shown to mediate a 13 fold increase in the cell surface localisation of G544V-mutant LDLR in stably transfected CHO cells (Tveten et al., 2007). Furthermore, the authors demonstrated that once at the cell

surface the mutant receptor was able to bind and internalise LDL with similar efficacy to WT receptor (Tveten et al., 2007).

Kosmotropes have not only been shown to be successful in reducing intracellular retention of misfolded proteins, but also reduce aggregate formation of proteins associated with neurodegeneration. Trehalose is a promising kosmotrope because of its lack of toxicity and high solubility. *In vitro* studies suggest that trehalose has the ability to bind and stabilize polyglutamine containing proteins and therefore may be incorporated into a treatment strategy for polyglutamine diseases such as Huntington disease (HD) and spinocerebellar ataxia 1 and 3 (Ignatova & Gierasch, 2006). Supporting this idea, in transgenic HD mice, oral administration of trehalose decreased polyglutamine aggregates in the cerebrum and liver, improved motor dysfunction, and increased life span (Tanaka et al*.,* 2004).

Based on these studies it is clear that kosmotropes have the potential to be beneficial in the treatment of diseases caused by conformational defective proteins such as CFTR, LDLR. Kosmotropes have been shown to have some effect for, α_1-Antitrypsin (Burrows et al., 2000), Aquaporin-2 (Tamarappoo et al., 1999) and the glucocorticoid receptor (Baskakov et al., 1999). However chemical chaperones lack specificity, and are only effective at relatively high concentrations. These factors may limit their therapeutic value for some conditions (Ulloa-Aguirre et al., 2004).

In this chapter the potential of kosmotropes, DMSO, TMAO, 4-PBA, and trehalose (Fig.4.1), to rescue the functional expression of mutant MC4R and promote trafficking of the wild-type protein is investigated.

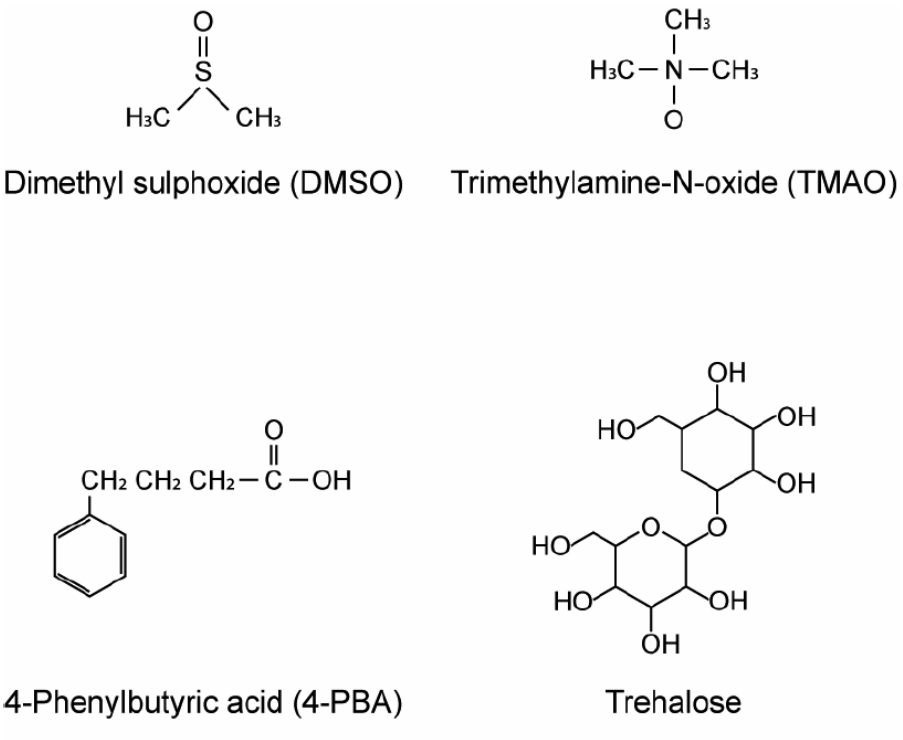

Figure 4.1: Graphical representation of the molecular structure of the chemical chaperones used in this study

4.2 Results

4.2.1 The effect of DMSO on the cellular trafficking of MC4R

Immediately after transfection with plasmids for the expression of WT or mutant HA-MC4R, HEK 293 cells were treated with kosmotropes for 24 hours (described in Chapter 2, section 2.6). After treatment cells were assessed for changes in cell surface expression and trafficking of MC4R (using the in cell western assay, described in Chapter 2, section 2.8). Changes in the total cellular level of MC4R (by western analysis, described in Chapter 2, section 2.10) and its functional activity (by the luciferase reporter assay), as described in Chapter 2, section 2.12.2, were also monitored. The flow diagram outlined in Chapter 3 was followed to analyse the effects, if any, observed for each kosmotrope. When treatment of WT HA-MC4R or HA-MC4R (L106P) expressing cells, with a specific kosmotrope, resulted in an increase in total or cell surface levels of the receptor the compound was tested on cells expressing the other intracellular retained mutants. The concentration of kosmotrope used corresponded to that which most affected HA-MC4R (L106P).

No significant changes in the cell surface levels of WT or HA-MC4R (L106P) were observed after treatment with 0.1%-1.0% DMSO (Fig.4.2, A). However, a significant increase (24.13±2.79%) in the total cellular level of WT HA-MC4R was observed but no changes were observed for the mutant receptor (Fig.4.2, B). When cell surface levels of MC4R were normalised to total levels of expression (Chapter 2, section 2.8), to reflect changes in trafficking of the receptor, no change was detected in trafficking of the WT HA-MC4R or mutant HA-MC4R (L106P) (Fig.4.2, C). Concentrations of DMSO above 1% caused cells to become rounded and detached from the cell culture plate, possibly due to the cells suffering from osmotic shock. Therefore concentrations above 1% DMSO were not tested.

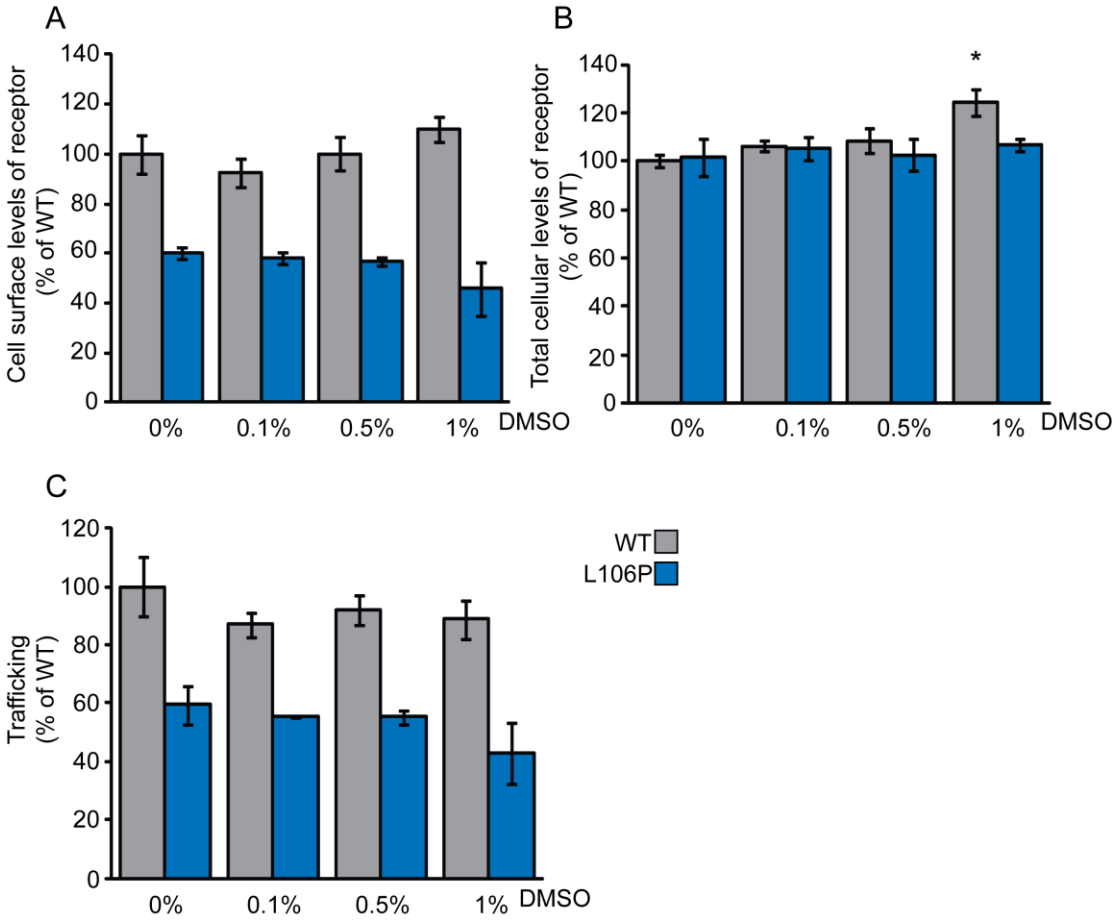

Figure 4.2: Treatment with DMSO increased total cellular levels of WT HA-MC4R

HEK 293 cells were transfected with plasmids for expression of WT HA-MC4R or mutant L106P HA-MC4R, 3 hours after transfection cells were incubated with 0, 0.1, 0.5 or 1% DMSO for 24 hours prior to in cell western analysis. MC4R cell surface expression (A), total cellular levels (B), and trafficking to the cell surface (C) was quantified at each concentration of DMSO. *P<0.05. Error bars represent the mean ±SD.

4.2.2 The effect of TMAO on the cellular trafficking of MC4R

The concentrations of TMAO used in this study (10-100 mM) did not result in any significant changes in MC4R cell surface expression or total cellular levels of the protein (Fig.4.3, A, B). A small but significant decrease in the percentage of WT and mutant HA-MC4R (L106P) receptor trafficking to the PM, after treatment with 100 mM TMAO, was observed (Fig.4.3, C). For WT HA-MC4R a decrease in trafficking of 3.35±1.32% after treatment with 10 mM TMAO was observed, relative to untreated control cells. Treatment with TMAO to a final concentration of 100 mM further decreased trafficking, (5.07±3.53% decrease). For mutant L106P, a decrease in trafficking of 5.14±1.15% was observed after treatment with 100 mM TMAO (Fig.4.3, C). Concentrations of TMAO above 100 mM caused the cells to become rounded and detached from the cell culture plate (not shown).

4.2.3 The effect of Trehalose on the cellular trafficking of MC4R

100 mM trehalose increased total receptor levels of WT HA-MC4R and mutant HA-MC4R (L106P), with the concentration of 100 mM proving to be the most effective (an increase of 56.04±19.16% and 42.04±16.06% for WT HA-MC4R and HA-MC4R (L106P) respectively) (Fig.4.4, B). However, no corresponding significant changes were detected in the cell surface levels of HA-MC4R (L106P), but cell surface levels of WT HA-MC4R increased (43.42±20.43%) after treatment with 100 mM trehalose (Fig.4.4, A). Therefore, the overall percentage of the receptor trafficking to the PM did not increase, and when expressed as a percentage of total cellular levels remained unchanged. (Fig.4.4, C).

To further confirm the increase in total levels of MC4R, after treatment with 1mM or 100 mM trehalose, western analysis was performed (Fig.4.5). An increase in levels of both WT and mutant HA-MC4R (L106P) was detected (Fig.4.5).

As trehalose increased the total cellular levels of HA-MC4R (L106P), presumably by stabilising the mutant receptor at the ER, it was further investigated whether trehalose could mediate the stabilisation of a more severe intracellular retained mutant HA-MC4R (P78L). Interestingly although 100 mM trehalose had no significant effect on the cell surface levels or trafficking of HA-MC4R (P78L) (Fig.4.6, A, C), similar to WT HA-MC4R and HA-MC4R (L106P), trehalose increased (41.23±22.30%) total cellular levels of HA-MC4R (P78L) (Fig.4.6, B).

After detecting an increase in total cellular levels of protein in HEK 293 cells immunostaining of WT and mutant HA-MC4R was performed to investigate the localisation of the receptor after trehalose treatment (Fig.4.7). The confocal images suggested that there was indeed an increase in the total cellular levels of WT HA-MC4R and mutant HA-MC4R (P78L and L106P) and that the localisation of MC4R was not altered after trehalose treatment (Fig.4.7 & Fig.4.8), supporting the finding from the previous experiment (Fig.4.6, B).

4.2.4 The effect of 4-PBA on the cellular trafficking of MC4R

Treatment with 5 mM 4-PBA, was explored for the other MC4R trafficking mutants in this study utilising the in cell western assay. Furthermore, as 4-PBA had better efficacy in a rhodopsin retinitis pigmentosa model compared to trehalose (Mendes & Cheetham, 2008), it was decided to test all the mutants utilised in this study instead of solely limiting it the least severe mutant HA-MC4R (L106P).

After 24 hours treatment with 5 mM 4-PBA a small, yet significant, increase in cell surface levels of HA-MC4R (D90N) and HA-MC4R (P299H) was observed, 13.20±1.13% and 6.22±4.18% respectively (Fig.4.9, A). Furthermore, a significant increase in total receptor levels was observed for HA-MC4R (S58C), HA-MC4R

(P78L) and HA-MC4R (L106P) (19.45±3.23%, 7.60±2.62% and 10.33±3.73%), however no change was detected for the WT receptor (Fig.4.9, B). The only mutant to show an increase in trafficking to the cell surface was HA-MC4R (D90N), with 19.65±7.60% more receptor trafficking to the cell surface after 4-PBA treatment (Fig.4.9, C). WT and HA-MC4R (L106P) both showed a decrease in trafficking to the cell surface (Fig.4.9, C).

Surprisingly in contrast to the in cell western assay, after treatment with 5mM 4-PBA, a large increase in cellular levels of WT HA-MC4R was detected by western analysis (Fig.4.10). However, consistent with the in cell western analysis an increase in the cellular levels of mutant HA-MC4R (L106P, P78L) was observed (Fig.4.10).

Once it was identified that 4-PBA did have a positive effect on some of the mutants tested, immunostaining of WT and mutant HA-MC4R was performed to investigate the localisation of the receptor after 4-PBA treatment. The confocal images revealed an increase in the total cellular levels of MC4R after 4-PBA treatment (Fig.4.11). Furthermore, an increase in the cell surface localisation of HA-MC4R (D90N) was observed in the confocal analysis (Fig.4.12).

As an increase in total cellular levels for some MC4R mutants and an increase in trafficking of HA-MC4R (D90N) was observed, it was investigated whether 4-PBA treatment increased receptor signaling in response to α-MSH stimulation. This was carried out using the luciferase reporter system (Chapter 2, section 2.12.2). For WT HA-MC4R and HA-MC4R (L106P), in agreement with the observation that 4-PBA treatment did not promote trafficking, no increase in receptor signaling at the PM was observed in cells treated with 4-PBA. However, a significant increase in luciferase activity was observed for severely misfolded mutants HA-MC4R (P78L), HA-MC4R (D90N) and HA-MC4R (P299H) (Fig.4.8).

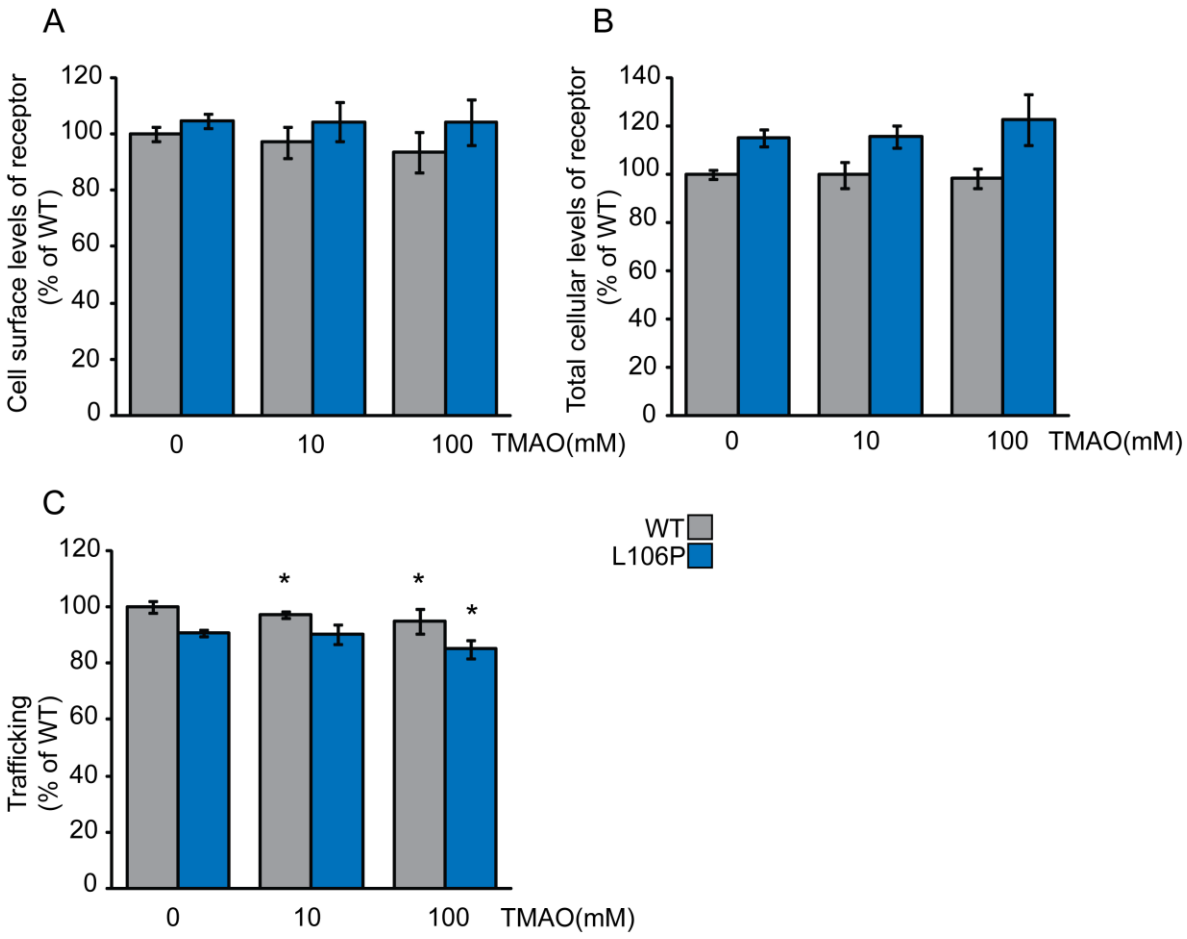

Figure 4.3: Treatment with TMAO causes a reduction of MC4R trafficking to the cell surface

HEK 293 cells were transfected with plasmids for expression of WT HA-MC4R or mutant HA-MC4R (L106P), 3 hours after transfection cells were incubated with 0, 10, or 100 TMAO for 24 hours prior to in cell western analysis. MC4R cell surface expression (A), total cellular levels (B), and trafficking to the cell surface (C) was quantified at each concentration of TMAO. *P<0.05. Error bars represent the mean ±SD.

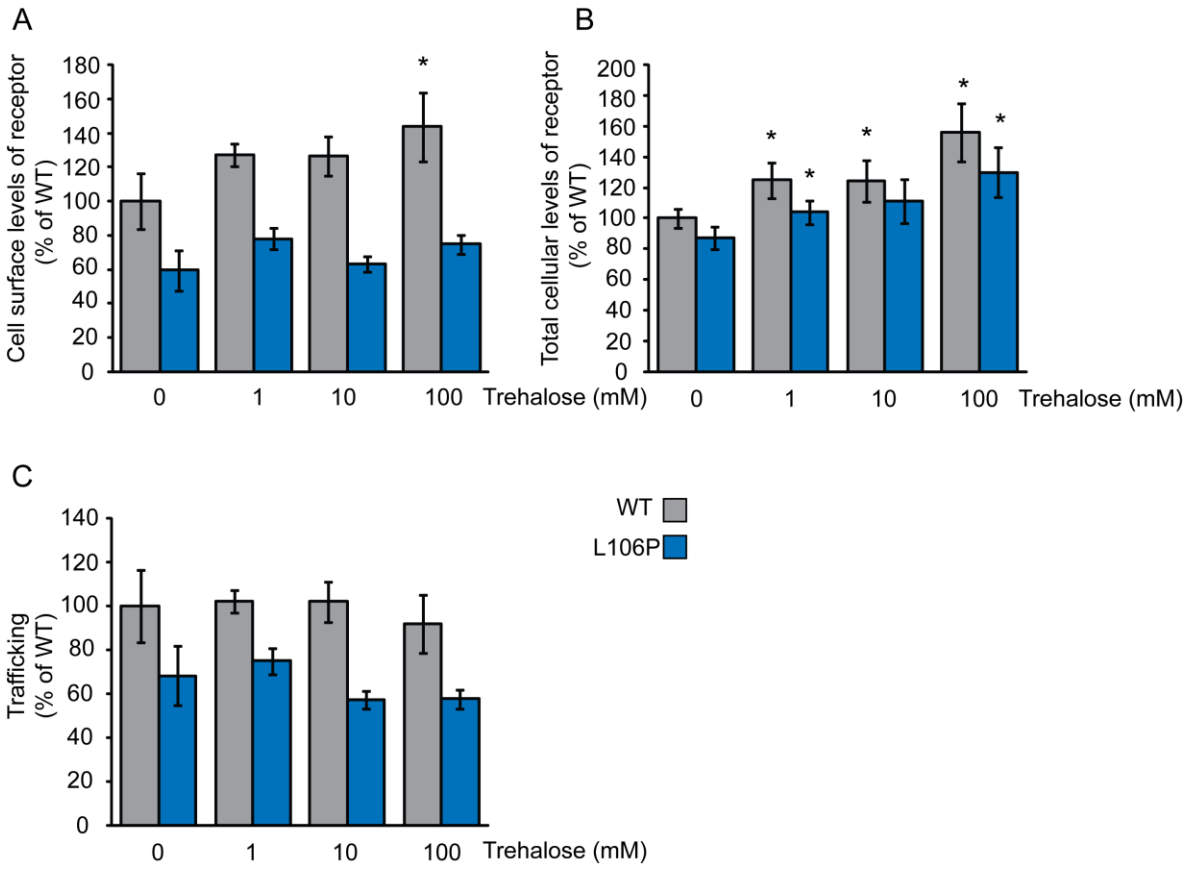

Figure 4.4: Trehalose treatment increased total cellular levels but not trafficking of WT and HA-MC4R (L106P)

HEK 293 cells were transfected with plasmids for expression of WT HA-MC4R or mutant HA-MC4R (L106P), 3 hours after transfection cells were incubated with 0, 1, 10 or 100 mM Trehalose for 24 hours prior to in cell western analysis. MC4R cell surface expression (A), total cellular levels (B) and trafficking to the cell surface (C) was quantified at each concentration of trehalose. *P<0.05. Error bars represent the mean ±SD.

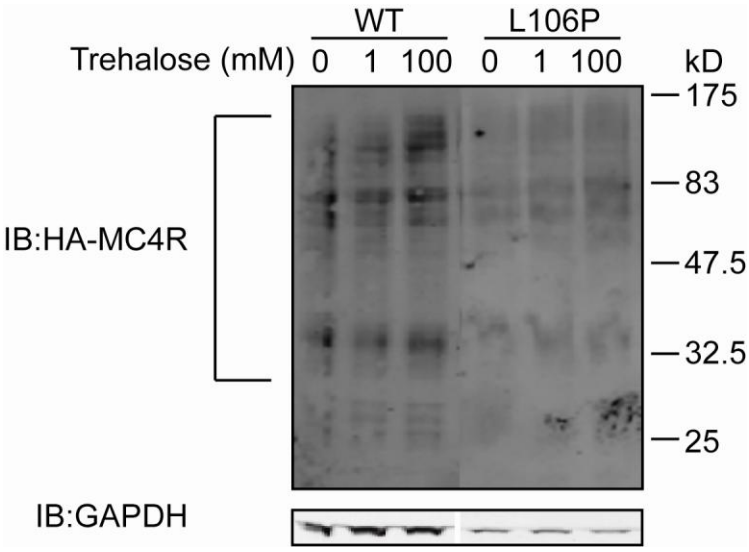

Figure 4.5: Treatment of cells with kosmotrope trehalose increases total levels of MC4R

Treatment of HEK 293 cells with indicated concentrations of trehalose, for 24 hours after transfection with plasmids for wild-type or mutant HA-MC4R expression, resulted in an increase in total levels of MC4R.

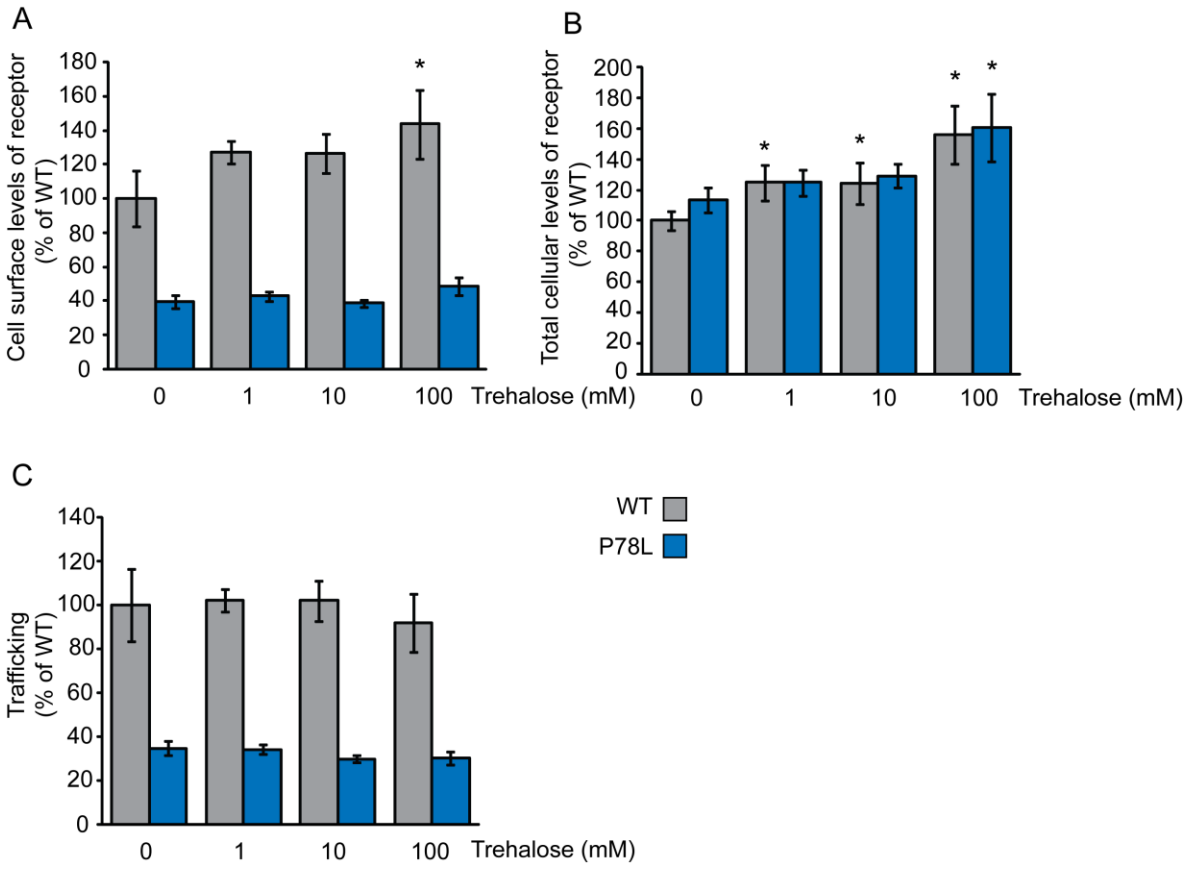

Figure 4.6: Trehalose treatment increased total cellular levels but not trafficking of WT and intracellular retained HA-MC4R (P78L)

HEK 293 cells were transfected with plasmids for expression of WT HA-MC4R or mutant HA-MC4R (P78L), 3 hours after transfection cells were incubated with 0, 1, 10 or 100 mM Trehalose for 24 hours prior to in cell western analysis. MC4R cell surface expression (A) or total cellular levels (B) and trafficking to the cell surface (C) was quantified at each concentration of trehalose. *P<0.05. Error bars represent the mean ±SD.

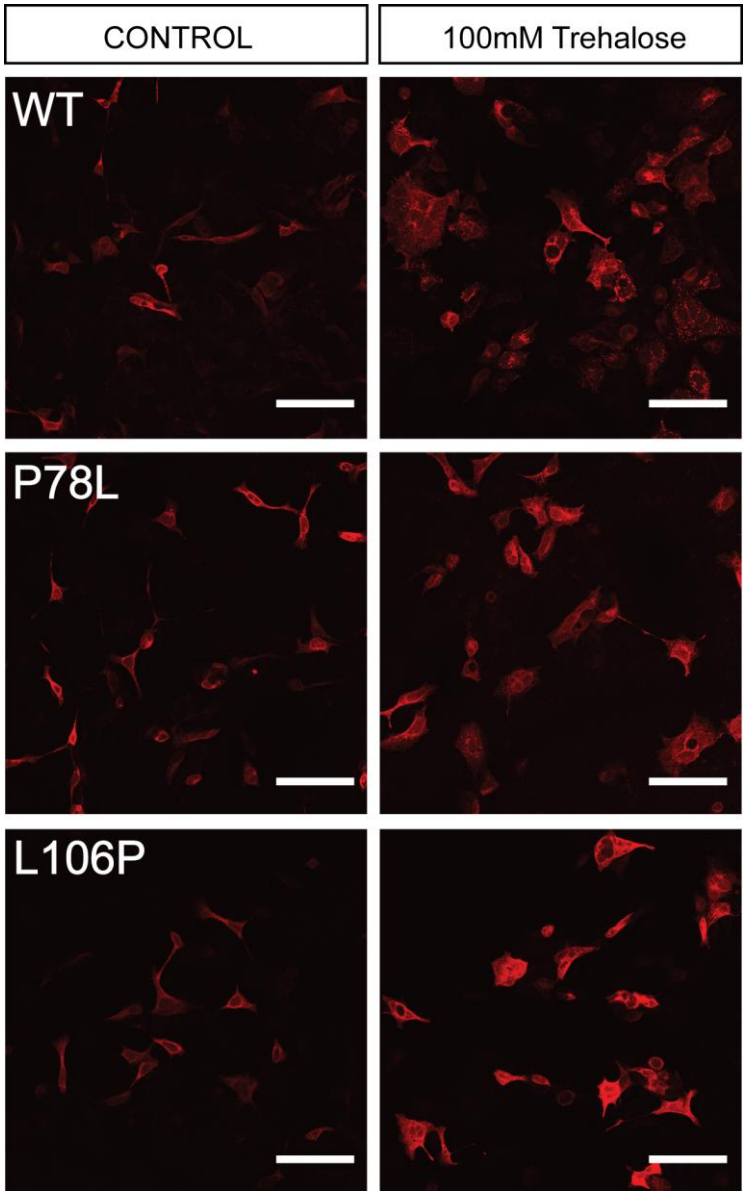

Figure 4.7: Trehalose increases total cellular levels of MC4R

HEK 293 cells were transfected with plasmids for expression of WT HA-MC4R or mutant HA-MC4R, 3 hours after transfection cells were incubated with 100mM trehalose for 24 hours prior to confocal analysis. 24 hours post transfection cells were formaldehyde fixed and immunostained with primary anti HA-antibodies, to detect the N-terminal HA-tagged MC4R, and Cy3 fluorescent secondary antibodies. Confocal settings including detector gain, amplifier offset and pinhole were constant for all imaging. Scale bar = 100 µM

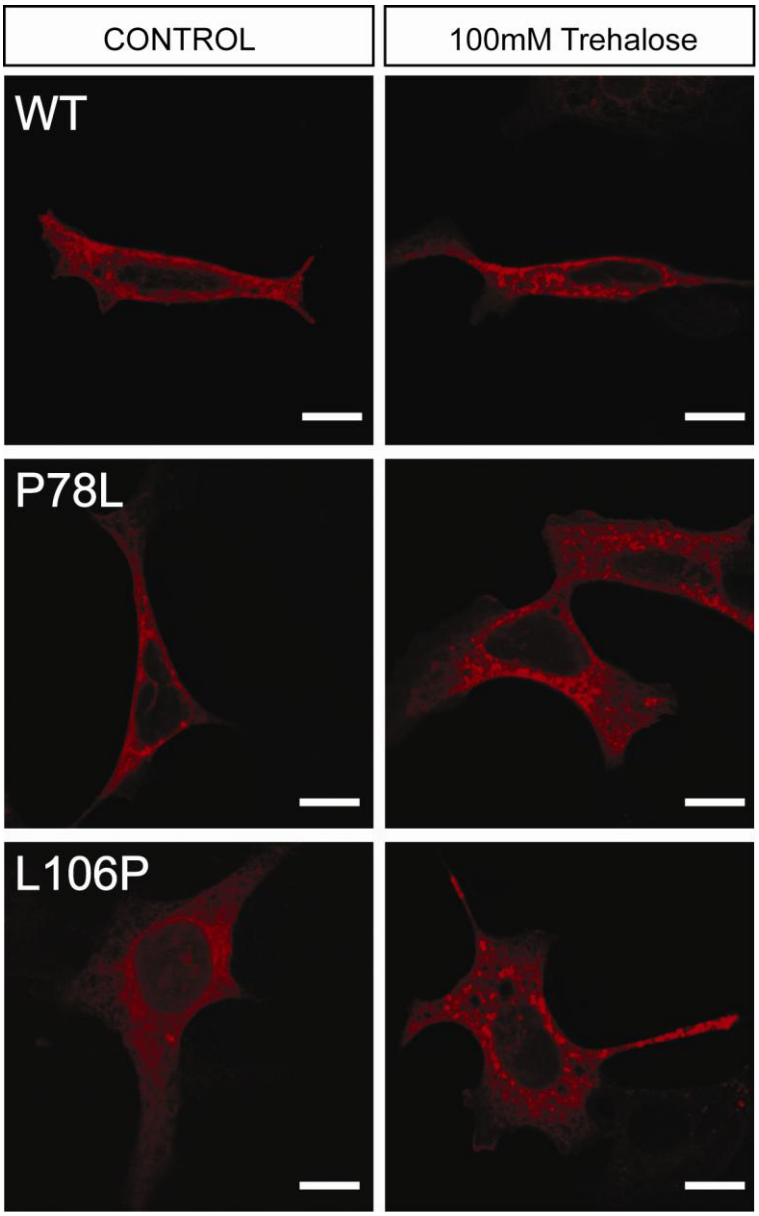

Figure 4.8: Trehalose does not alter the localisation of MC4R

HEK 293 cells were transfected with plasmids for expression of WT HA-MC4R or mutant HA-MC4R, 3 hours after transfection cells were incubated with 100mM trehalose for 24 hours prior to confocal analysis. 24 hours post transfection cells were formaldehyde fixed and immunostained with primary anti HA-antibodies, to detect the N-terminal HA-tagged MC4R, and Cy3 fluorescent secondary antibodies. Confocal settings including detector gain, amplifier offset and pinhole were constant for all imaging. Scale bar = 10 µM

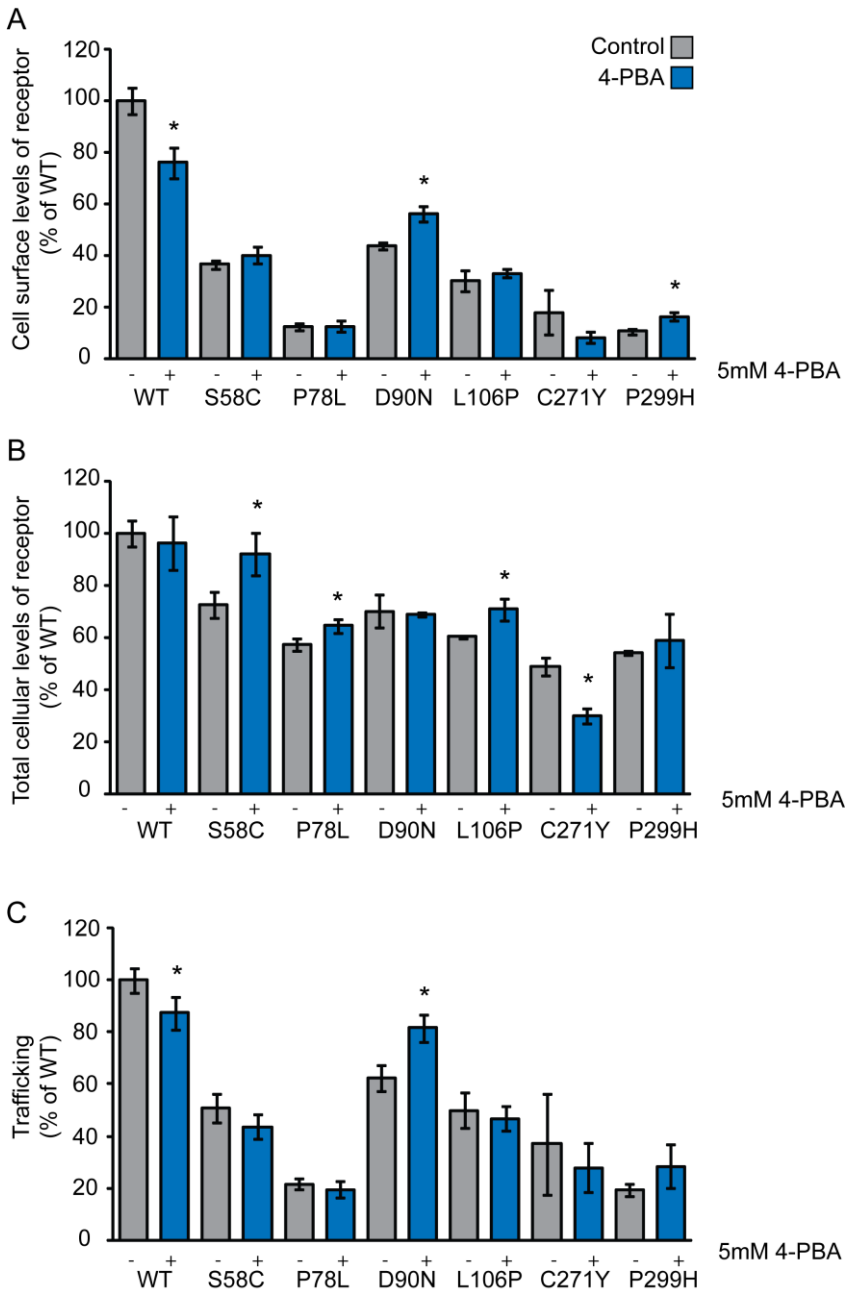

Figure 4.9: 4-PBA promotes cell surface expression of HA-MC4R (D90N)

HEK 293 cells were transfected with plasmids for expression of WT HA-MC4R or mutant HA-MC4R, 3 hours after transfection cells were incubated with 5mM 4-PBA for 48 hours prior to in cell western analysis. MC4R cell surface expression (A), total cellular levels (B), and trafficking to the cell surface (C) was quantified at each concentration of 4-PBA. *P<0.05. Error bars represent the mean ±SD.

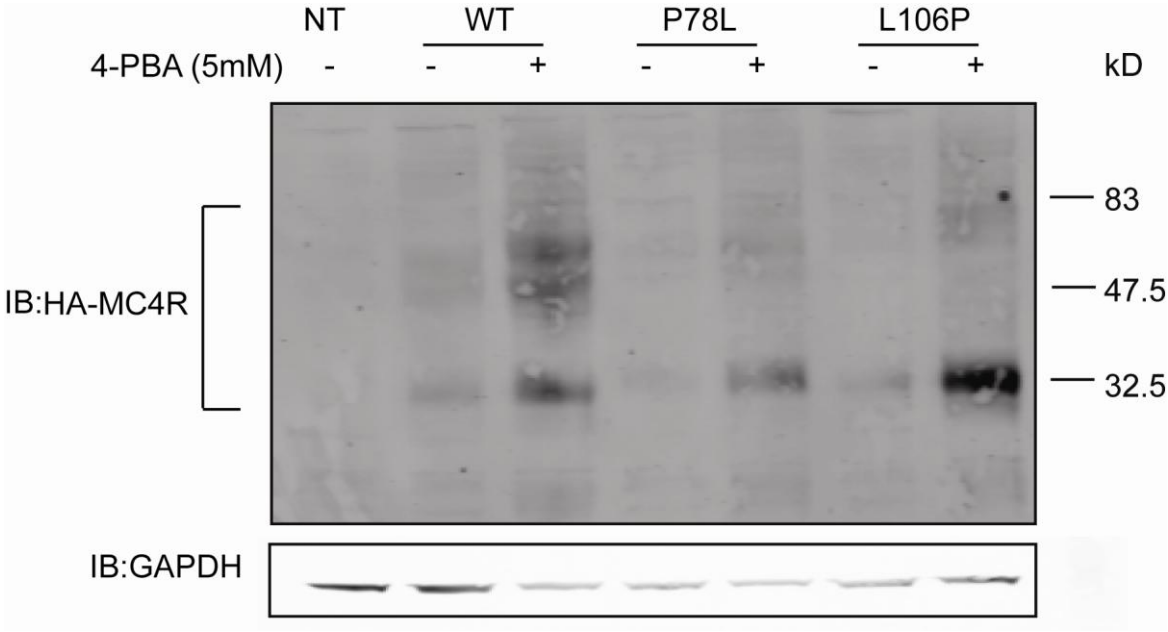

Figure 4.10: Treatment of cells with kosmotrope 4-PBA increases total levels of MC4R detected by western blotting

Treatment of HEK 293 cells with 5 mM, for 48 hours after transfection with plasmids for wild-type or mutant HA-MC4R expression, resulted in an increase in total cellular levels of MC4R.

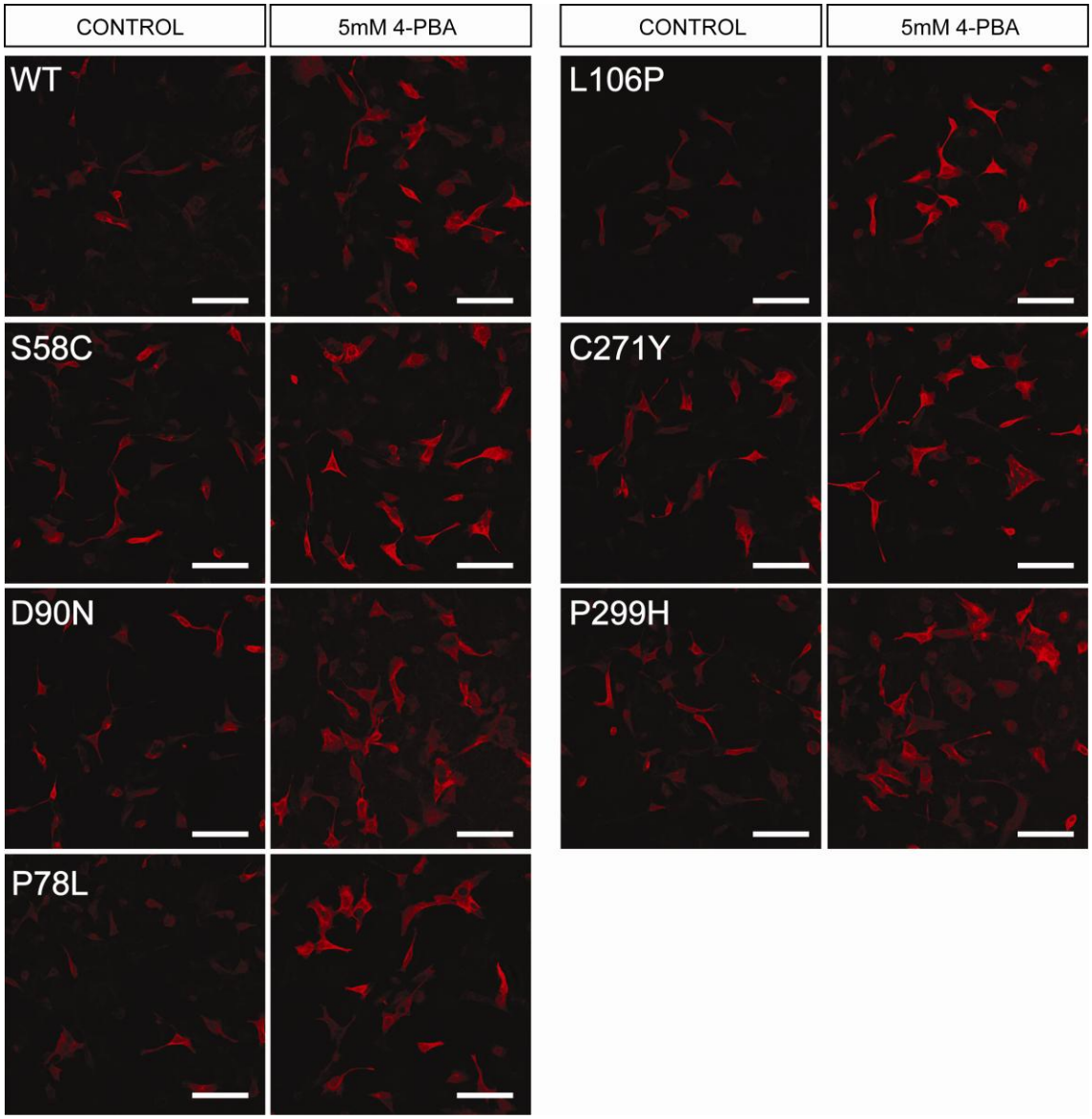

Figure 4.11: 4-PBA increases total cellular levels of MC4R

HEK 293 cells were transfected with plasmids for expression of WT HA-MC4R or mutant HA-MC4R, 3 hours after transfection cells were incubated with 5 mM 4-PBA for 48 hours prior to confocal analysis. 48 hours post transfection cells were formaldehyde fixed and immunostained with primary anti HA-antibodies, to detect the N-terminal HA-tagged MC4R, and fluorescent Cy3 secondary antibodies. Confocal settings including detector gain, amplifier offset and pinhole were constant for all imaging. Scale bar = 100 µM

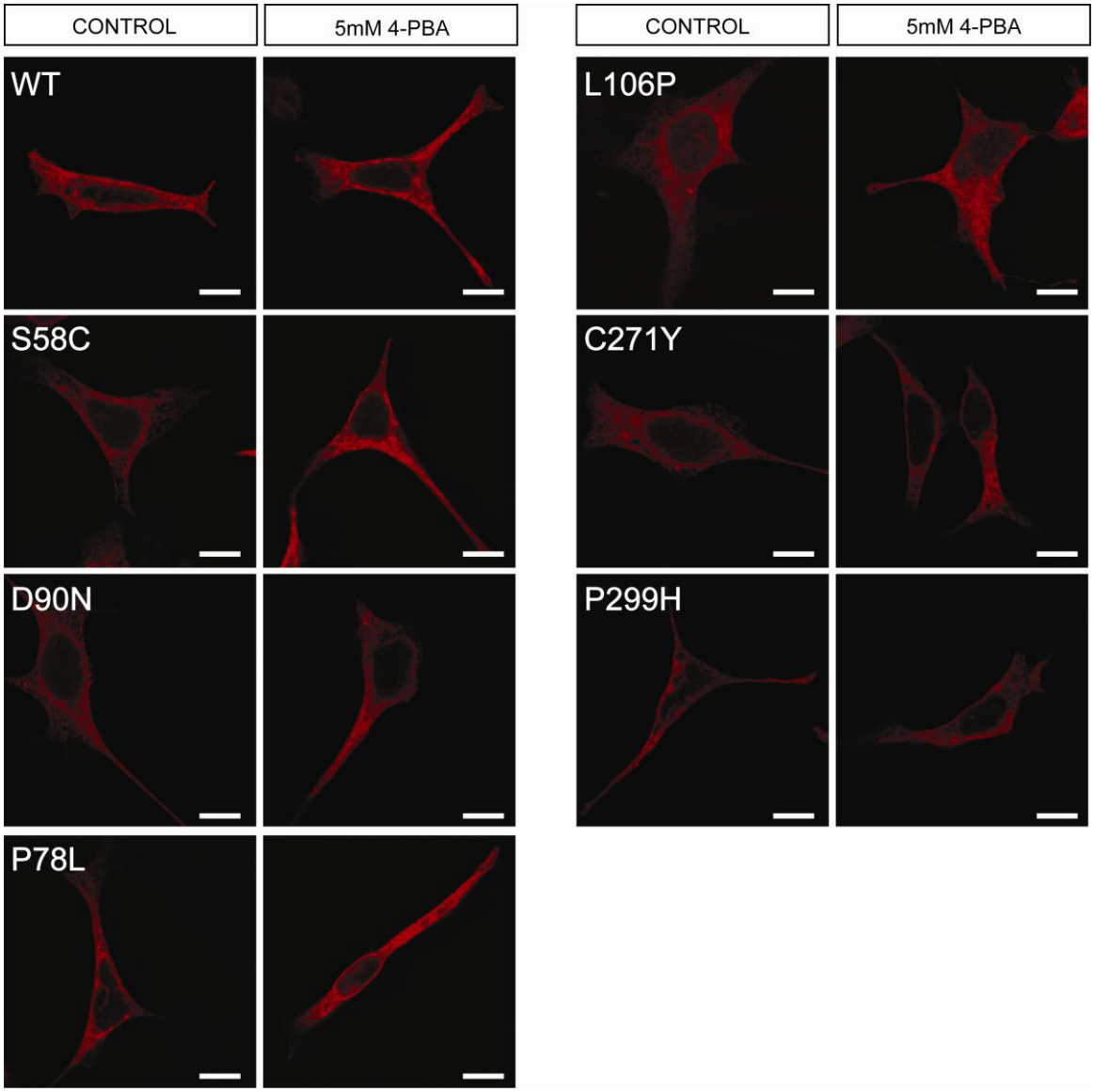

Figure 4.12: 4-PBA does not alter the cellular localisation of MC4R

HEK 293 cells were transfected with plasmids for expression of WT HA-MC4R or mutant HA-MC4R, 3 hours after transfection cells were incubated with 5 mM 4-PBA for 48 hours prior to confocal analysis. 48 hours post transfection cells were formaldehyde fixed and immunostained with primary anti HA-antibodies, to detect the N-terminal HA-tagged MC4R, and fluorescent Cy3 secondary antibodies. Confocal settings including detector gain, amplifier offset and pinhole were constant for all imaging. Scale bar = 10 µM

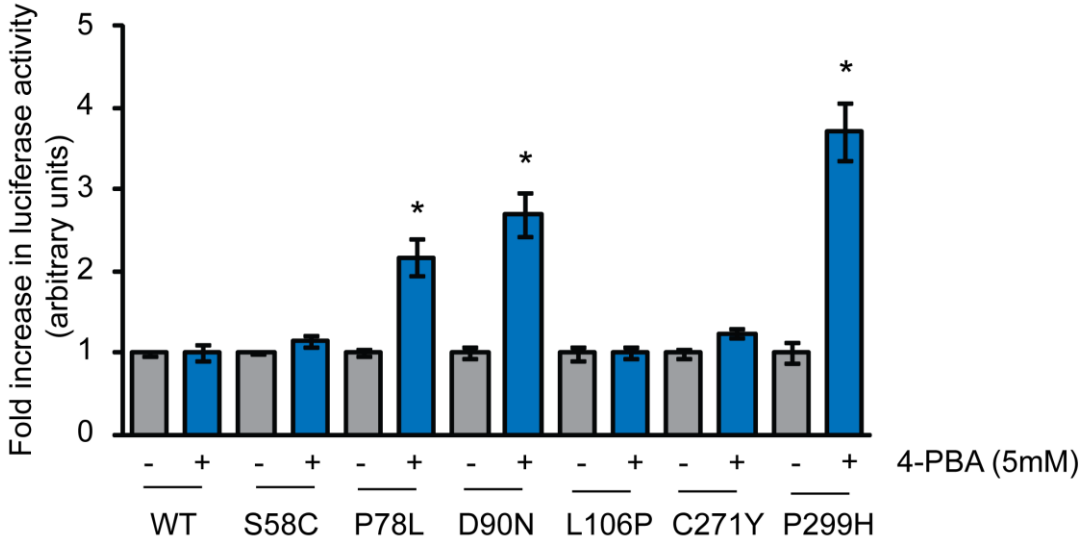

Figure 4.13: 4-PBA promotes functional expression of intracellular retained mutants

Using a luciferase reporter system for cAMP activity MC4R signalling was quantified for wild-type and mutant HA-MC4Rs. Cells were co-transfected with plasmids for expression of wild-type or mutant MC4R, a luciferase reporter construct for MC4R signalling, and a vector for renilla expression. 3 hours post-transfection cells were incubated with 5 mM 4-PBA. 48 hours post transfection cells were stimulated with 10^{-7}M NDP-MSH for 6 hours and luciferase activity was measured. Values were normalised to renilla activity of control to account for variability in transfection efficiency. Data is shown as fold increases in luciferase activity relative to untreated controls. *P<0.05. Error bars represent the mean ±SD.

4.3 Discussion

In summary, 100 mM trehalose significantly increased the total cellular levels of both WT HA-MC4R and some MC4R mutants. Whilst treatment with 5mM 4-PBA increased the trafficking and increased the signalling of some MC4R mutants. Contrasting results were obtained for WT HA-MC4R after 4-PBA treatment, with the in cell western showing a reduction in total cellular levels of the WT receptor. Unfortunately due to time constraints this inconsistency was not fully resolved.

The concentrations of kosmotropes used in this study that proved to be effective are similar to those used in other studies. For example, Oculopharyngeal musculardystrophy (OPMD) is caused by the abnormal expansion of a polyalanine tract within the coding region of poly (A) binding protein nuclear 1 (PABPN1). Abnormal PABPN1 forms aggregates within the nuclei of skeletal muscle fibres (Davies et al., 2006). Treatment of COS-7 cells expressing mutant PABPN1 with 100mM trehalose, reduced aggregate formation and toxicity of mutant PABPN1. Furthermore, oral administration of trehalose in an OPMD transgenic mouse model attenuated muscle weakness and reduced aggregate formation (Davies et al., 2006). In a different study, the kosmotrope 4-PBA was shown to be an effective treatment in reducing aggregate formation of mutant HFE, a type I transmembrane glycoprotein (de Almeida et al., 2007). The C287Y mutation of the HFE protein is associated with hereditary haemochromatosis, and similar to MC4R, the misfolded mutant protein is retained in the ER and fails to traffic to the cell surface. Treatment of HEK 293 cells expressing C287Y HFE with 5 mM 4-PBA prevented aggregate formation of the mutant protein (de Almeida et al., 2007).

Osmolytes such as DMSO and TMAO are thought to stabilise misfolded proteins by increasing the relative hydration around the polypeptide and decreasing the surface area of the polypeptide (Gekko & Timasheff, 1981). For example, the formation of fibrils by amyloid-β is characteristic of Alzheimer's disease. TMAO (150 μM) and glycerol (6.0 M) were found to accelerate amyloid-β random coils into more complex β-sheet formation, a conformational change required for fiber

formation associated with Alzheimer's disease (Yang et al., 1999). This indicates that osmolytes such as TMAO and glycerol are capable of stabilising and promoting the folding of unfolded proteins. Although the osmolytes used in this study did not prove to be very effective in improving MC4R trafficking they have been shown to have some effect in other disease paradigms associated with aberrantly folded proteins. For example, the most commonly inherited disorder in sulfur metabolism is caused by mutations in the cystathionine beta-synthase (*CBS*) gene, resulting in a loss/decrease in enzyme activity due to misfolding of the enzyme (Singh et al., 2007). Kosmotropes, glycerol, DMSO and TMAO, were able to promote folding of the enzyme and restore function of human CBS enzyme in *Saccharomyces cerevisiae* and *Escherichia coli* models. Furthermore, by combining different kosmotropes together they were able to rescue enzyme function using lower concentrations of the reagents (Singh et al., 2007). With respect to MC4R, this experiment could be tested by combining different kosmotropes DMSO and TMAO together at a range of different concentrations to determine if it would promote MC4R folding and possibly trafficking.

It seems likely that the increase in total cellular levels of mutant MC4R, seen after treatment with trehalose or 4-PBA, may reflect that the receptor is stabilised at the ER and is not being sent for degradation. However, with the exception of HA-MC4R (D90N), stabilisation of the misfolded protein at the ER does not appear sufficient to allow the mutant proteins to exit from the ER.

Interestingly, in addition to HA-MC4R (D90N), mutants HA-MC4R (P78L) and HA-MC4R (P299H) showed an increase in functional activity after 4-PBA treatment (Fig.4.13). Although no increase in trafficking for HA-MC4R (P78L) or HA-MC4R (P299H) was observed, an increase in cell surface expression was detected for HA-MC4R (P299H) (Fig.4.9). This increase in cell surface expression for HA-MC4R (P299H) may be the reason why an increase in functional activity was observed, as more protein may be present at the cell surface resulting in an increase in receptor signaling. For HA-MC4R (P78L) a slight, but not significant,

increase was observed in trafficking of the mutant and this was sufficient to cause an increase in functional activity of the mutant receptor.

However, it is important to note that although the fold increase in signaling is more than WT MC4R the absolute levels of mutant receptor signaling after 4-PBA treatment are still not comparable to WT MC4R. This observation with 4-PBA is not unique to MC4R. In a model of Fabry disease, caused by deficiency of α-galactosidases, 1 mM 4-PBA was found to improve trafficking of mutant α-galactosidases in human fibroblasts, but did not restore functionality (Yam et al., 2007).

An alternative mechanism of action has been previously described for 4-PBA. It has been shown that exposure of IB3-1 cystic fibrosis epithelial cells to 4-PBA upregulates chaperones and co-chaperones involved in protein folding and trafficking, suggesting a potential role of 4-PBA acting as a transcriptional regulator (Singh et al., 2006). Furthermore, microarray analysis on 4-PBA treated IB3-1 showed an upregulation of transcript levels of heat shock proteins (Hsp) 90 and 70, both of which are involved in protein folding (Wright et al., 2004). 4-PBA may be exerting a similar effect in HEK 293 cells expressing MC4R by altering the expression of key chaperones and co-chaperones allowing the stabilisation of mutant MC4R, thus increasing total levels of the receptor. The potential up-regulation of heat shock proteins could be tested by treating WT HA-MC4R and mutant MC4R expressing HEK 293 cells with 4-PBA, and subsequently immunoblotting the lysates with antibodies against Hsp70, Hsp90 and other chaperones.

The data presented in this chapter provides proof-of-principle that the kosmotropes 4-PBA and trehalose are able to stabilise the protein structure of MC4R and increase total cellular levels of a misfolded potein. Furthermore, 4-PBA may be useful in improving the trafficking and function of some clinically occurring MC4R mutants (HA-MC4R (P78L), HA-MC4R (D90N), and HA-MC4R (P299H)). Both 4-PBA, and trehalose (a natural sugar), are non-toxic to cells. Indeed 4-PBA has been approved by the U.S. Food and Drug Administration for use in urea-cycle

disorders in children, sickle cell disease and thalassemia (Qi et al., 2004). However, the direct use of kosmotropes to treat MC4R monogenic obesity may be effective as the effects observed, at the concentrations tested, were minimal.

CHAPTER 5

The effects of heat shock protein inducers and co-inducers on the cellular processing of MC4R

5.1 Introduction

Heat shock proteins (Hsp) are a highly conserved functional class of proteins that are transcriptionally upregulated under conditions of cellular stress, such as exposure to elevated temperatures, heavy metals and oxygen free radicals (De Maio, 1999). Furthermore, under normal cellular conditions Hsp are involved in *de novo* protein folding, protein degradation and protein complex assembly. Hsps are part of a group of proteins known as molecular chaperones. Molecular chaperones are a large and diverse group of proteins that share the property of assisting the folding and unfolding and the assembly and disassembly of other macromolecular structures, but are not permanent components of these structures when they are performing their normal biological functions (Ellis, 2006). Molecular chaperones are also involved in numerous specific cellular functions such as, clathrin uncoating, exocytosis, mitochondrial protein import and intermediate filament organisation (Young et al., 2003).

Hsp90 is one of the most abundant proteins in eukaryotic cells comprising 1-2% of total proteins under non-stress conditions (Marcos-Carcavilla et al., 2008). Under normal cellular conditions, Hsp90 is bound to the transcription factor, heat shock factor 1 (HSF-1) (Morimoto, 2002), forming part of a larger complex with histone deacetylase 6 (HDAC6) and its partner p97/VCP (Boyault et al., 2007). Under cellular stress, HDAC6 through its ubiquitin binding activity, binds to ubiquitinated proteins and becomes dissociated from p97/VCP. This in turn leads to p97/VCP using its segregase activity to release HSF-1 from Hsp90 (Boyault et al., 2007). Phosphorylation and trimerisation of dissociated HSF-1 enables activated HSF-1 to bind to DNA within the nucleus resulting in the upregulation of cytoplasmic Hsp70, Hsp40 and Hsp90 expression (Westerheide & Morimoto, 2005). Geldanamycin (GA), a natural occurring benzoquinone ansamycin antibiotic found in *Streptomyces hygroscopicus* var. *geldanus* (BeBoer et al., 1976), has been shown to bind specifically to Hsp90 inhibiting its function (Smith et al., 1995; Prodromou et al., 1997). Therefore, inhibition of Hsp90 by GA causes Hsp90 to dissociate from

the HSF-1 complex resulting in the induction of the expression of Hsp70 and Hsp40 (Thomas et al., 2006). Interestingly, because of its ability to inhibit Hsp90, GA is being investigated as a therapeutic drug against cancer. This is because Hsp90 is required for the stability and folding of many oncoproteins, including protein kinases such as ErbB2, EGFR, Bcr-Abl tyrosine kinase, Met tyrosine kinase, PKB/Akt, c-Raf and b-Raf, androgen and oestrogen receptors, HIF-1*α* (hypoxia-inducible factor-1*α*) and telomerase (Pearl et al., 2008). Therefore, inhibition of Hsp90 leads to the protesomal degradation of numerous oncogenic client proteins thus affecting numerous oncogenic pathways including proliferation, evasion of apoptosis, immortalization, invasion, angiogenesis and metastasis (Pearl et al., 2008).

The therapeutic potential of GA, in diseases where normal proteostasis is disrupted, has been most extensively explored in the context of neurodegeneration. For example, in an *in vitro* model of Huntington's disease, COS-1 cells were treated with 360 nM GA, which resulted in a 3-4 fold up-regulation of Hsp40, Hsp70 and Hsp90 when compared to untreated controls (Sittler et al., 2001). In addition, when the GA treated cells were analysed for the presence of aggregated huntingtin protein, an 80% reduction of aggregates was observed (Stittler et al., 2001). Similar to the GA effects, overexpression of Hsp70 and Hsp40 independently or collectively, also inhibited huntingtin protein aggregation in COS-1 cells by 30-40% or 60-80% respectively (Stittler et al., 2001).

Other examples of GA inducing Hsp70 and preventing neurotoxicity have been reported. In a cell culture model of Parkinson's disease, human neuroglioma cells were pre-treated with 200 nM GA for 16-18 hours resulting in a 50 % reduction in α-synuclein inclusions (Mclean et al., 2004). In addition pre-treatment of cells with GA showed a 20% reduction in α-synuclein induced toxicity compared to untreated cells (Mclean et al., 2004). In an *in vivo* rodent model of Parkinson's disease, intracerebral ventricular injection of 10 µg/kg GA into the rodent's brain protected

against 1-methyl-4-pheny 1,2,3,6-tetrahydropyridine (MPTP)-induced neurotoxicity by induction of Hsp70 (Shen et al., 2005).

These examples and others indicate that pharmacological induction of Hsp70 by GA can promote the clearance of misfolded proteins that manifest as aggregates. Furthermore, direct overexpression of Hsp70, or the use of agents that induce Hsp70 expression, have also proved to be effective in improving the trafficking of misfolded proteins. For example, overexpression of Hsp70 in IB3-1 cells expressing mutant ΔF508 CFTR, resulted in a 2 fold increase in the mature 180kD form of the protein when compared to mock transfected cells (Choo-Kang et al., 2001). Whilst the non-essential amino acid glutamine, an inducer of Hsp70, also caused a ~2.5 fold increase of the mature 180kD form of the mutant CFTR protein when IB3-1 cells were treated with 50 nM glutamine (Choo-Kang et al., 2001).

There is growing evidence that molecular chaperones that reside in the cytosol interact with the cytoplasmic domains of GPCRs and can promote their processing to the plasma membrane (PM) and functional expression (Meimaridou et al., 2009). For example, Hsc70/HspA8 has been demonstrated to interact with the cytoplasmic domains of non-glycosylated angiotensin II type 1 receptor (Lanctot et al., 2006), whilst the DnaJ protein, hlj1/DnaJB4 has been shown to interact with the human mu opioid receptor via binding to its C-terminal domain (Ancevska-Taneva et al., 2006). Some of the examples above demonstrate that Hsp70 can also promote the inhibition of a toxic gain of function caused by misfolded proteins. In light of these advances, in this chapter manipulation of the cellular chaperone environment and its affect on misfolded MC4R is investigated.

Experiments involving Hsc70 were carried out with the assistance of Dr. Eirini Meimaridou.

5.2 Results

5.2 The effect of geldanamycin on the cellular trafficking of MC4R

Geldanamycin (Sigma) was used to induce Hsp70 expression. HEK 293 cells were seeded at equal density and treated with concentrations of GA ranging from 0-1000 nM for 24 hours prior to cell lysis. To determine the degree of Hsp70 induction western analyses for Hsp70 and GAPDH was performed (Fig.5.1, A). As expected, an increase in Hsp70 expression was observed in cells treated with GA. A concentration of 0.4 µM GA proved to be most effective, causing an approximate 10 fold increase in Hsp70 levels (Fig.5.1, B). Hsp70 was also induced in HEK 293 cells expressing WT HA-MC4R or mutant HA-MC4R (L106P) after treatment with 0.4 µM GA (Fig.5.1, C). Interestingly, the basal level (control untreated cells) of Hsp70 in MC4R (L106P) expressing cells appeared higher than WT HA-MC4R expressing cells (Fig.5.1, C).

The effect of increasing cellular levels of Hsp70 via GA treatment, on MC4R expression was investigated using GA concentrations of 0.4 µM and 1.0 µM. GA was added to HEK 293 cells straight after transfection with plasmids for expression of WT or mutant HA-MC4R. After 24 hours of treatment, cells were assessed for changes in cell surface expression and trafficking of MC4R (using the in cell western assay, described in Chapter 2, section 2.8). Changes in the total cellular level of MC4R (by western analysis, described in Chapter 2, section 2.10) and its functional activity (by the luciferase reporter assay), as described in Chapter 2, section 2.12.2, were also monitored. Surprisingly, a significant decrease in the cell surface and total cellular levels of both WT and mutant receptor was observed after treatment with GA. (Fig.5.2, A, B). Importantly, the amount of WT and mutant receptor trafficking to the cell surface was decreased upon pharmacological induction of Hsp70 (Fig.5.2, C). In addition, confocal images of cells transiently expressing WT or mutant receptor treated with GA also suggested a decrease in

total levels of the GPCR (Fig.5.3). These results indicated that the Hsp90 chaperone machinery may have a role to play in MC4R trafficking as treatment with GA also inhibits Hsp90.

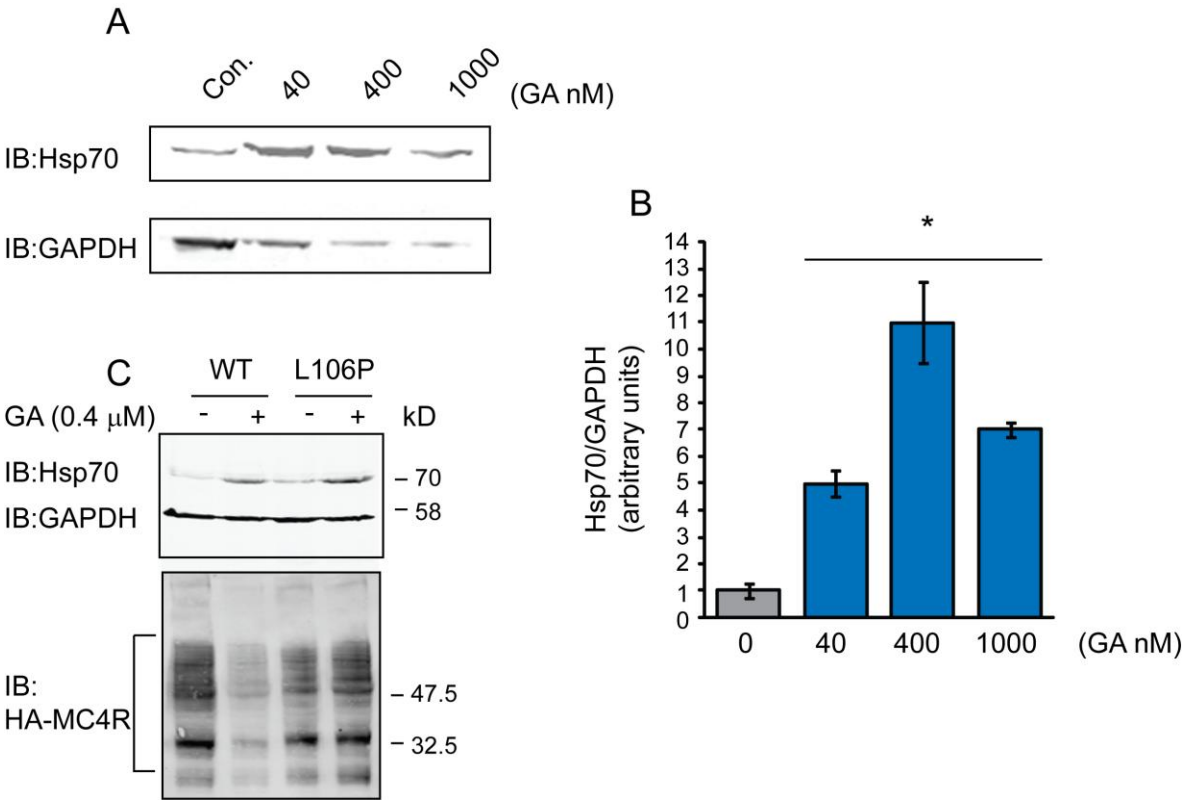

Figure 5.1: 400nM GA induces expression of Hsp70

After treatment with varying concentrations of GA for 24 hours HEK 293 lysates were collected and immunoblotted for Hsp70 and housekeeping protein GAPDH. Western analysis showed an induction in the expression of Hsp70 with GA (representative image) (A). Densitometric analysis of immunoblot A and 3 other immunoblots were performed. An approximate 10 fold increase in Hsp70 induction was observed with 400 nM GA treatment (B). *P< 0.05. Western analysis showed an induction in the expression of Hsp70 after GA treatment (C).

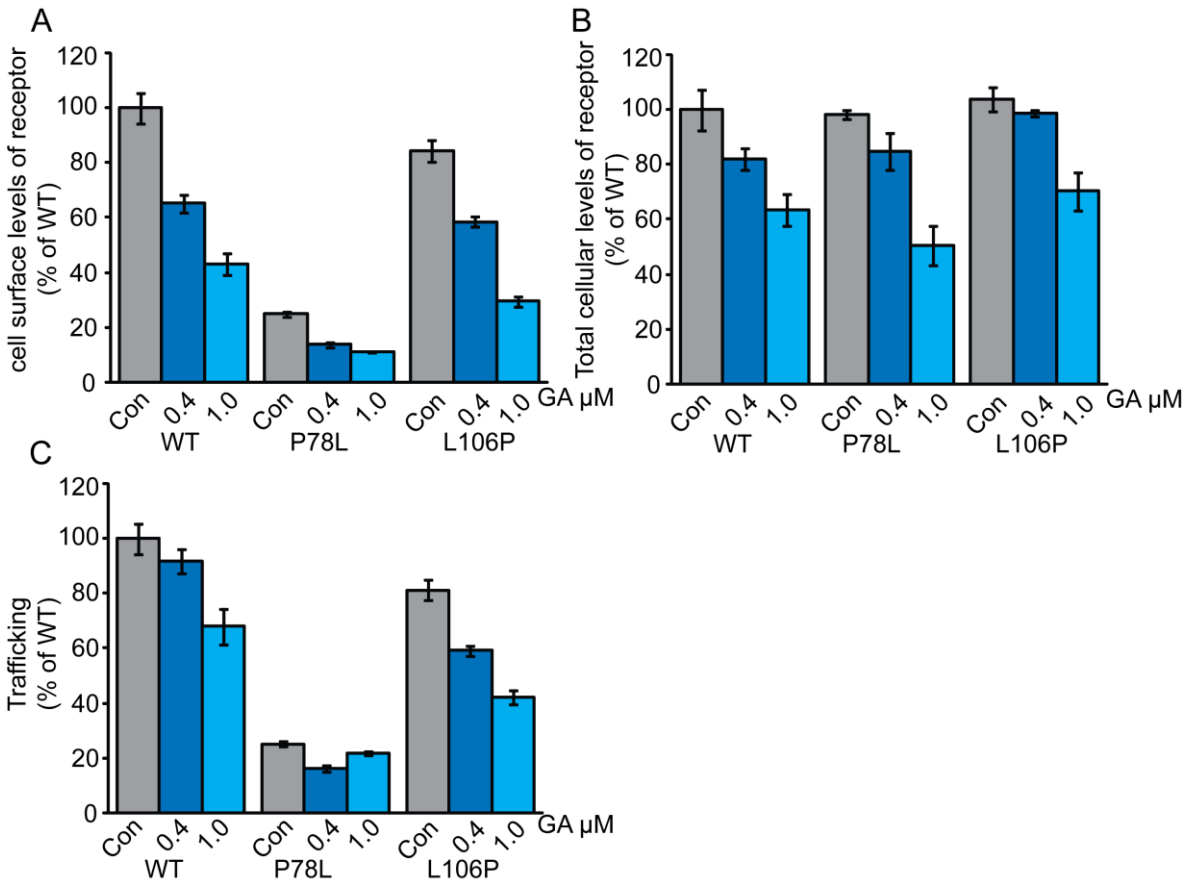

Figure 5.2: Treatment of cells with the pharmacological inducer of Hsp70 geldanamycin reduces cellular levels of MC4R

HEK 293 cells were transfected with plasmids for expression of WT or mutant, HA-MC4R (L106P or P78L). Immediately after transfection cells were incubated with 0, 0.4, 1.0 µM GA for 24 hours prior to in cell western analysis. MC4R cell surface levels (A), total cellular levels (B), and trafficking to the cell surface (C) was quantified at each concentration of GA. *P< 0.05 for all GA treated cells compared to control cells. Error bars represent ±SD.

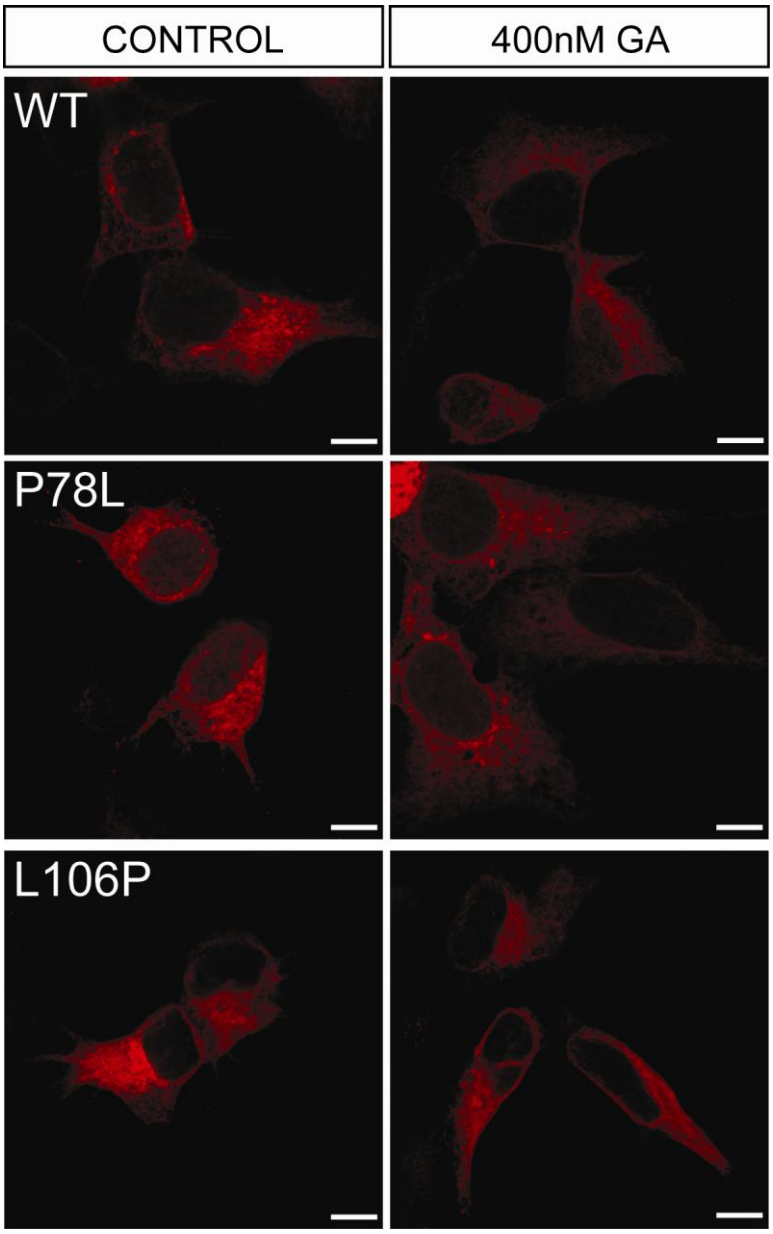

Figure 5.3: GA treated HEK 293 cells have lower cellular levels of HA-MC4R
HEK 293 cells transiently expressing WT or mutant HA-MC4R were treated with 0.4 µM GA for 24 hours. Cells were then fixed and stained with a monoclonal anti-HA mouse primary antibody and a secondary Cy3 conjugated antibody. Cells were imaged using a Zeiss LSM confocal microscope keeping all settings between control and non-treated cells the same. Scale bar = 10µm

5.3 The effect of Hsp90 co-chaperone Aha1 on MC4R trafficking

Unexpectedly, inhibition of Hsp90, decreased cell surface expression and total cellular levels of MC4R. This might indicate that inhibiting Hsp90 may be detrimental to MC4R processing. Therefore, it was hypothesised that upregulation of Hsp90 would increase MC4R expression levels. However, Hsp90 is an abundant protein and it has previously proved difficult to significantly increase cellular levels by heterologous expression (Chapple, personal communication), therefore the rate of Hsp90 client protein binding and release was targeted using activator of Hsp90 ATPase (Aha1). Aha1 is a co-chaperone of Hsp90 that binds to the middle domain of Hsp90 and stimulates its ATPase activity (Panaretou et al., 2002; Lotz et al., 2003).

HEK 293 cells were transiently co-transfected with plasmids encoding WT HA-MC4R and Aha1 or an empty control vector at a 1:1, 1:5 or 1:10 ratio. Aha1 expression significantly increased the cell surface expression of WT HA-MC4R at the 1:1 ratio (by 56.14±3.05%) and the 1:5 ratios (by 65.32±12.23%) (Fig.5.4, A). However, once the MC4R/Aha1 plasmid ratio was increased to a ratio 1:10 the level of receptor at the cell surface was not significantly different from the untreated control (Fig.5.4, A). Total cellular levels of WT HA-MC4R also increased in the presence of Aha1 with a significant increase at a 1:1 ratio (108.22±5.96%) and a 1:5 ratio (134.16±4.21%)(Fig.5.4, B). Transfecting the cells with MC4R:Aha1 plasmids at a ratio exceeding 1:5 led to a reduction in MC4R levels (Fig.5.4, B).

Based on the above findings, the effect of Aha1 (used at a 1:1 ratio to MC4R) on mutant MC4R processing was further investigated. Co-transfection with Aha1 caused a significant increase in cell surface expression of mutant MC4R, with the exception of mutant HA-MC4R (C271Y) (Fig.5.18, A). The greatest increase in cell surface expression was observed for mutant receptor HA-MC4R (S58C) (26.17±8.78%) (Fig.5.18, A). Similar to the WT receptor, the total cellular levels of

MC4R mutants also significantly increased upon Aha1 expression, with the exception of HA-MC4R (C271Y) (this may have been due to reduced transfection efficiency for this mutant) (Fig.5.18, B). In contrast, the level of receptor trafficking to the PM was not improved in cells over-expressing Aha1 for either the WT or mutant MC4R and once again a reduction in the proportion of receptor trafficking to the PM was observed (Fig.5.18, C). These findings suggests that Aha1, and thus Hsp90 stimulation, increase total cellular levels of WT and mutant MC4R but does not improve trafficking of the receptor to the PM.

To further confirm the increase in total levels of MC4R after treatment with Aha1, western analysis was performed (Fig.5.19). An increase in total levels of both WT and mutant HA-MC4R (L106P, P78L) were detected (Fig.5.19).

Confocal imaging of HEK 293 cells heterologously co-expressing MC4R and Aha1 also suggested an increase in total cellular levels of the receptor. However, there was minimal evidence of co-localisation between the co-chaperone and GPCR (Fig.5.7). Furthermore, no co-immunoprecipitation of Aha1 with MC4R was detected (Fig.5.8, C). Together these results suggest that Aha1 does not interact directly with MC4R.

To further investigate the effects of Aha1 on MC4R a functional assay was performed. HA-MC4R expressing HEK 293 cells, co-transfected with Aha1, showed a slight, but not significant increase, in signalling. HA-MC4R (D90N) was the only mutant to show a significant increase in reporter gene activity (8.46±1.90%), as detected by a luciferase reporter construct in the presence of Aha1 (Fig.5.9). This is consistent with Aha1 stabilising MC4R at the ER, and thus causing an increase in cellular levels, but not promoting trafficking of the mutant receptor.

To further investigate the effects of Aha1 on MC4R cell surface expression the stable cell lines described in Chapter 3 were utilised. Similar to the transient MC4R expression system an increase in MC4R cell surface and total cellular levels were

observed when the mutant MC4R stable cell lines were transiently transfected for Aha1 expression (Fig.5.10, A, B). Unexpectedly, a slight but significant decrease (0.23±0.06) was observed for cell surface expression of the WT receptor in cells hetrologously over-expressing Aha1.

Comparable to the transiently expressing MC4R cells, Aha1 did not promote the ratio of the receptor trafficking to the cell surface in the MC4R stable cell lines (Fig.5.10, C).

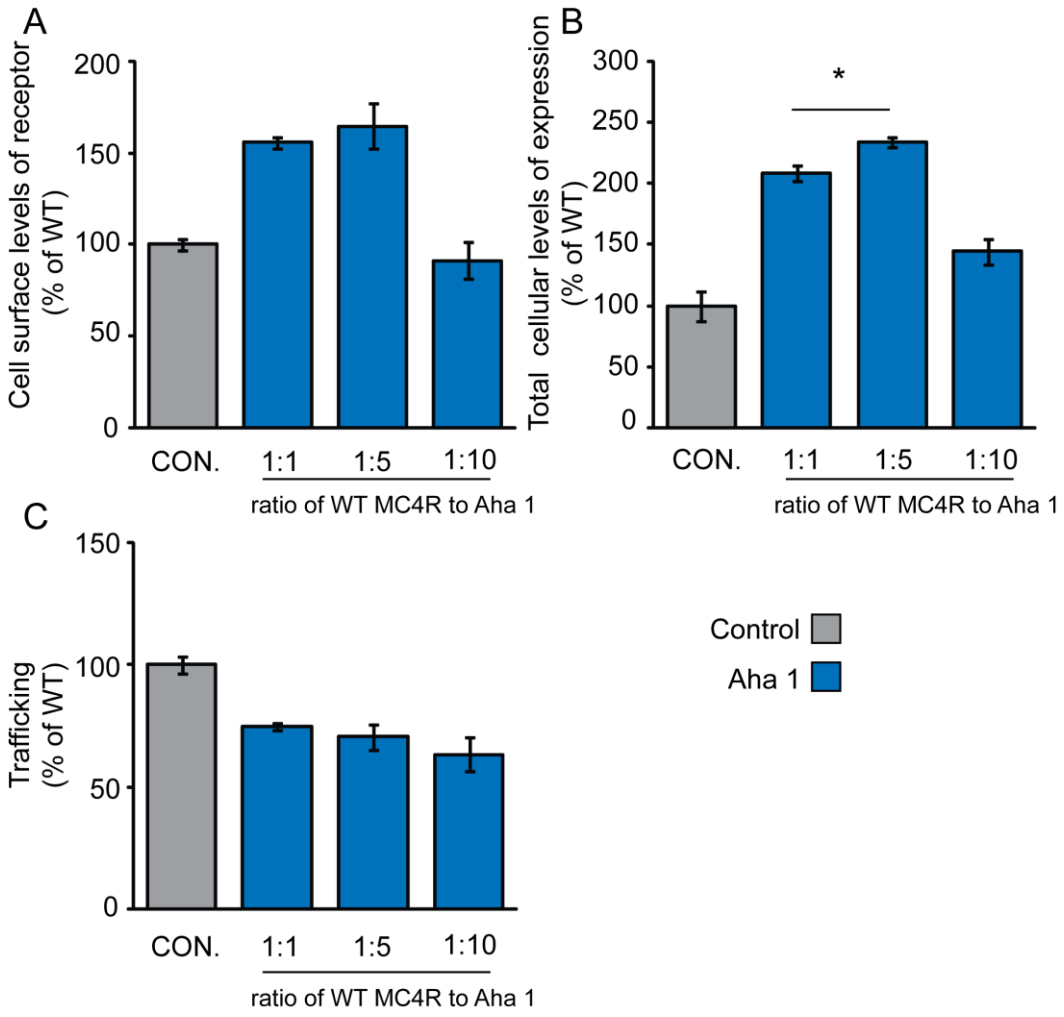

Figure 5.4: Increasing the ratio of Aha1 to HA-MC4R decreases cellular levels of MC4R

HEK 293 cells were transiently co-transfected with plasmids encoding WT HA-MC4R and increasing concentrations of plasmid for expression of Aha1. The total amount of DNA used in each transfection was kept constant by using empty control vector pcDNA3.1. 24 hours post transfection in cell western analysis was performed. Aha1 expression elevated cell surface levels of WT MC4R, but no further increase was observed with increased Aha1 expression (A). Increasing Aha1 expression increased total receptor levels (B). WT receptor trafficking to the cell surface slightly decreased with increased Aha1 expression (C). *P<0.05. Error bars represent ±SD

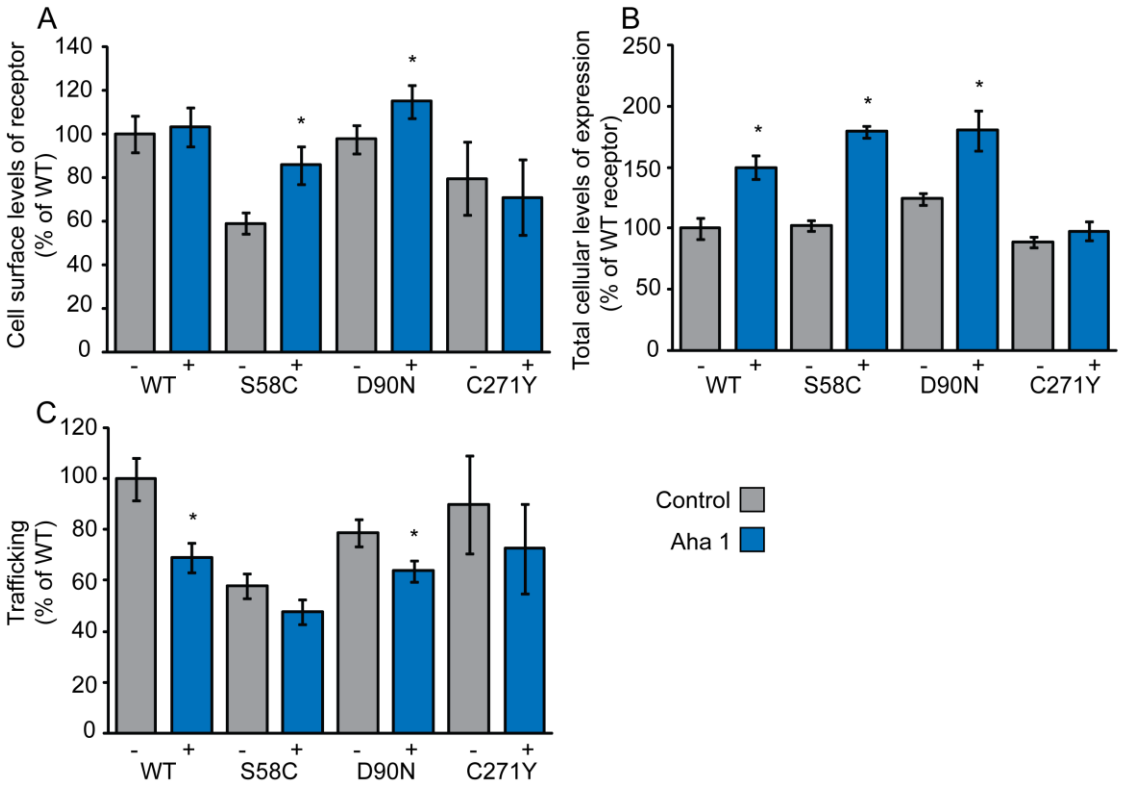

Figure 5.18: Over-expression of Hsp90 co-chaperone Aha1 causes a significant increase in the total cellular levels of MC4R

HEK 293 cells were co-transfected with plasmids for expression of WT HA-MC4R or mutant MC4R with equal amounts of plasmid encoding Aha1 or empty control vector (pcDNA3.1). 24 hours post-transfection cells were fixed and stained and in cell western analysis performed. MC4R cell surface levels (A), total cellular levels (B), and trafficking to the cell surface (C) was quantified for cells co-expressing Aha1 and control cells. *P<0.05. Error bars represent ±SD.

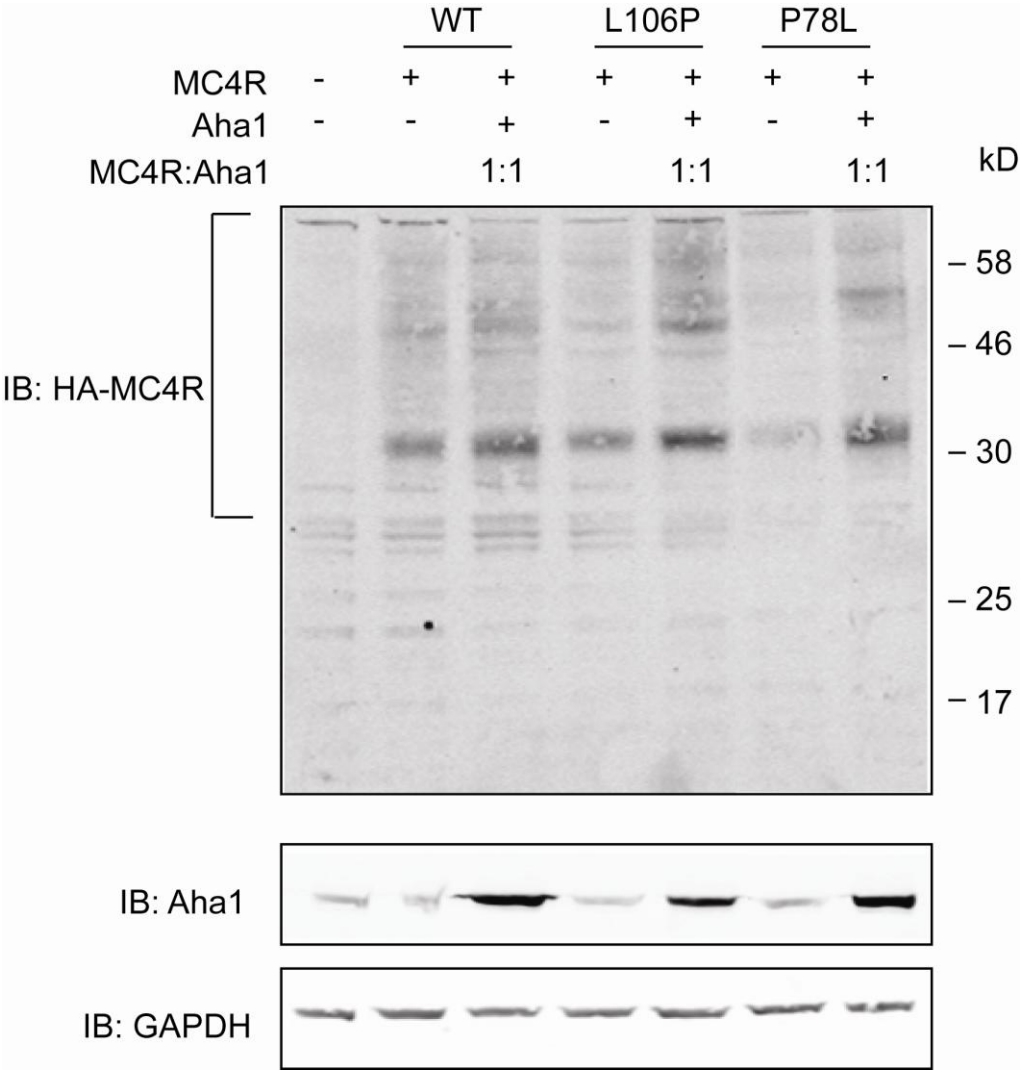

Figure 5.19: Over-expression of Hsp90 co-chaperone Aha1 causes an increase in the total levels of MC4R

HEK 293 cells were co-transfected with plasmids for expression of WT HA-MC4R or mutant MC4R with plasmid encoding Aha1 or empty control vector. 24 hours post-transfection cells were lysed and collected lysates were run on a 12% SDS-PAGE gel followed by immunoblotting for HA-MC4R, Aha1 and GAPDH.

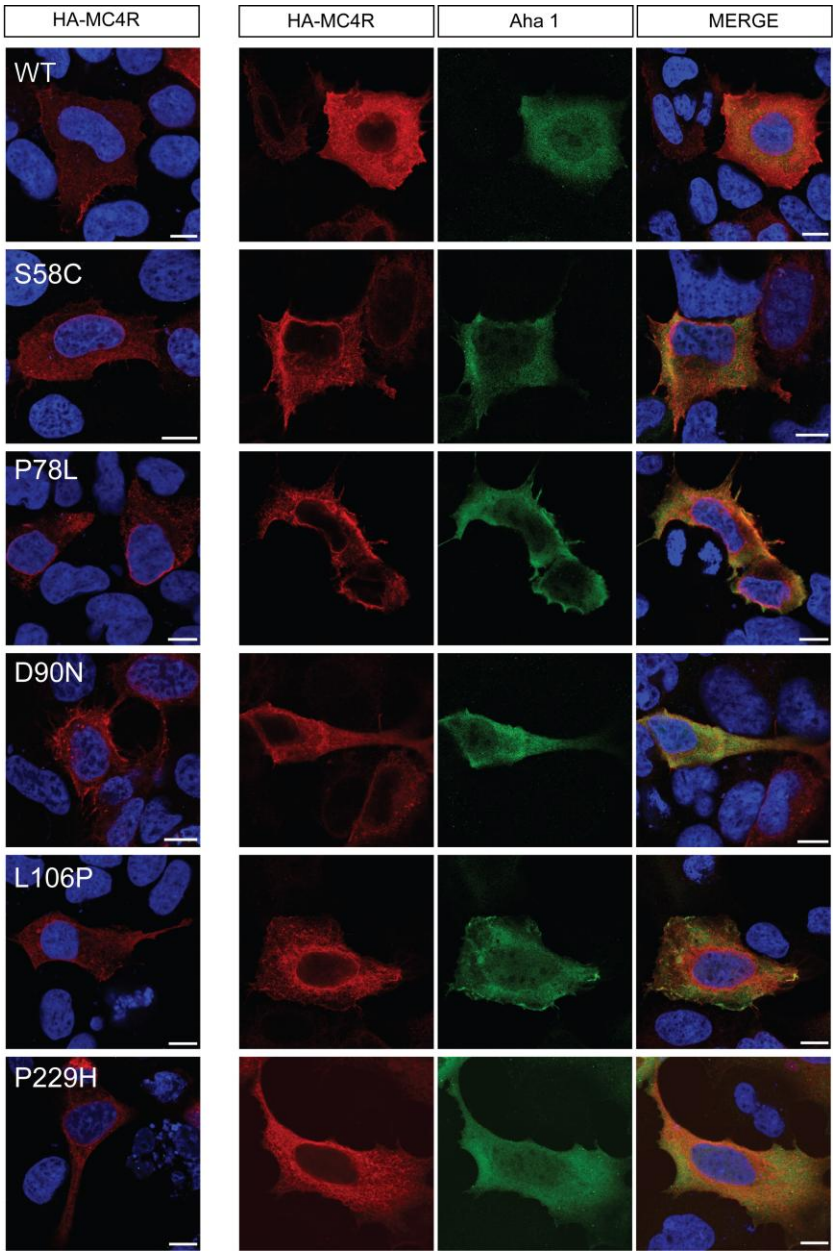

Figure 5.7: Aha1 over-expression in HEK 293 cells increases MC4R cellular levels

HEK 293 cells were co-transfected with plasmids expressing MC4R and Aha1 or control empty vector. 24 hours post transfection cells were fixed and stained with antibodies detecting HA-MC4R (red) and/or Aha1 (green) with nuclei staining (blue). Cells were imaged using a Zeiss Confocal LSM 510 confocal microscope. Scale bar = 10µm

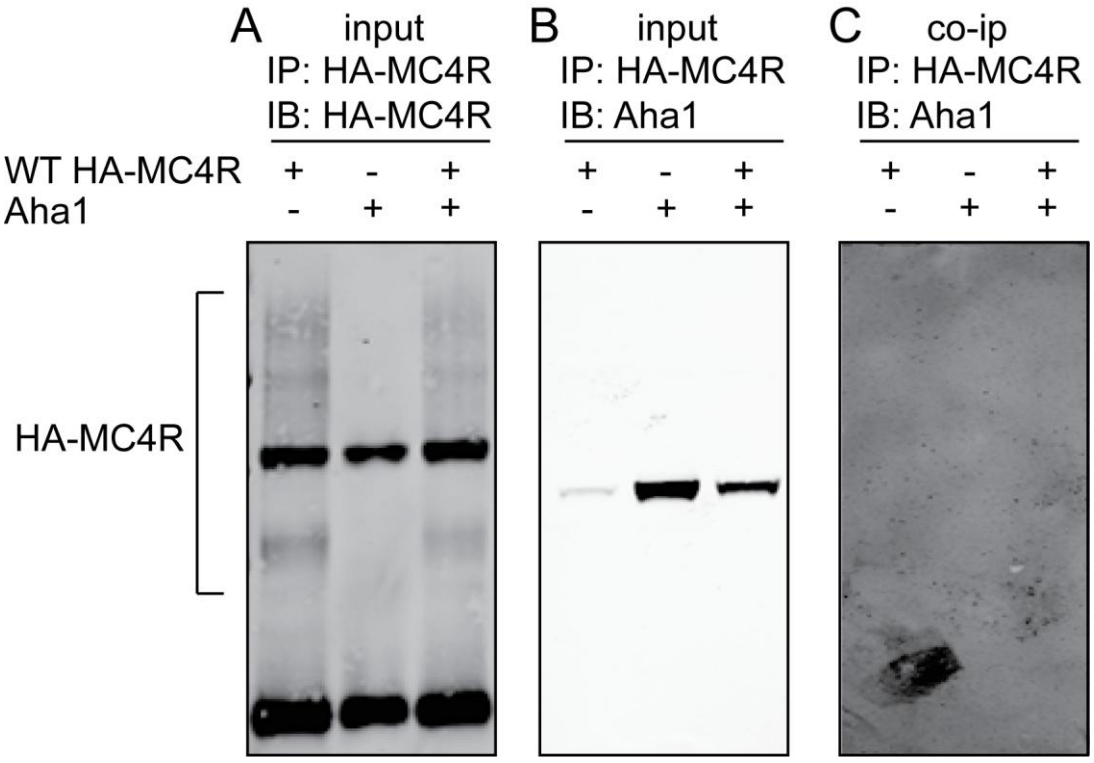

Figure 5.8: Aha1 does not co-immunoprecipitate with MC4R

WT HA-MC4R and Aha1 were immunoprecipitated from a RIPA buffer (Sigma) soluble cell lysate and immunoblotted with monoclonal anti HA antibody and HA-MC4R proteins (A), or immunoblotted with anti-Aha1 antibody (B).

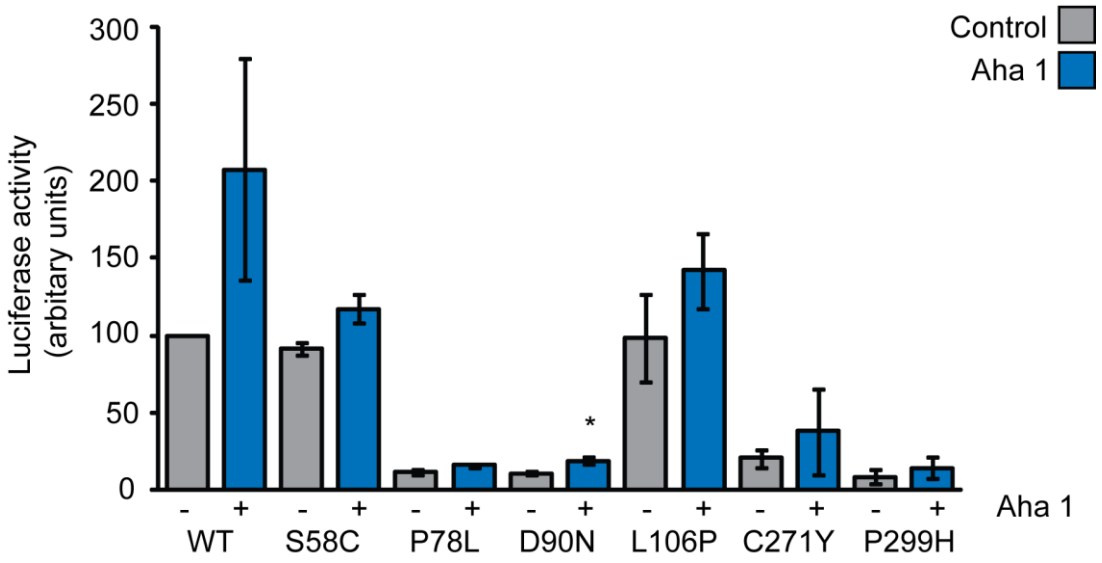

Figure 5.9: Over-expression of Aha1 promotes MC4R signalling

Using a luciferase reporter system for cAMP activity MC4R signalling was quantified for WT and mutant HA-MC4Rs co-transfected with Aha1. HEK 293 cells were co-transfected with equal concentrations of plasmids for expression of WT or mutant HA-MC4R with Aha1 or empty control vector. Cells were also co-transfected with a luciferase reporter construct for MC4R signalling, and a vector for renilla expression. 16 hours post transfection cells were stimulated with 10^{-7}M NDP-MSH for 6 hours and luciferase activity was measured. Values were normalised to renilla activity to control for variability in transfection. *P<0.05. Error bars represent ±SD.

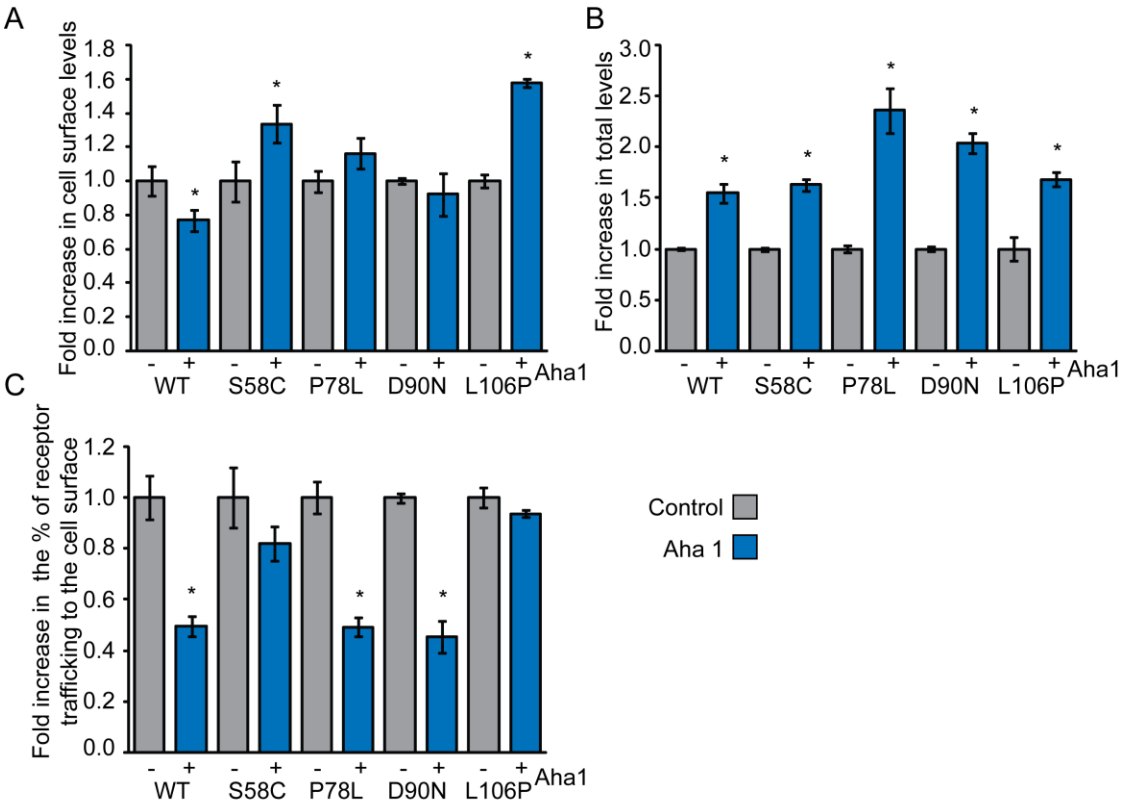

Figure 5.10: Over-expression of Aha1 increases total cellular MC4R levels

HEK 293 cells stably expressing HA-MC4R were co-transfected with equal amounts of plasmid encoding Aha1 or control empty vector (pcDNA3.1). 24 hours post-transfection cells were fixed and stained and in cell western analysis performed. MC4R cell surface levels (A), total cellular levels (B), and trafficking to the cell surface (C) was quantified for cells co-expressing Aha1 and control cells. Data is shown as fold increases in MC4R expression relative to untreated controls. *P<0.05. Error bars represent ±SD.

5.2.3 The effect of Hsc70 on the cellular trafficking of MC4R

Hsc70 has been shown to be involved in the folding of both WT and mutant proteins, and in some paradigms of protein misfolding disease has been shown to rescue cellular phenotypes (Spooner et al., 2008). Therefore it was decided that further investigation of the effects of Hsc70 on MC4R processing was required. After transfection of cells (with equal amounts) of Hsc70, HEK 293 cells were assessed for changes in cell surface expression and trafficking of MC4R (described in Chapter 2, section 2.8). Changes in the total cellular level of MC4R (by western analysis, described in Chapter 2, section 2.10) and its functional activity, as described in Chapter 2, section 2.12.2, were analysed.

Except for the severe mutant HA-MC4R (P78L) Hsc70 expression increased the cell surface expression of WT HA-MC4R and the intracellular retained mutants (Fig.5.11, A). In addition Hsc70 expression increased the total cellular levels of both WT HA-MC4R and mutant receptor and interestingly promoted a more significant increase in the intracellular mutants compared to the WT receptor (Fig.5.11, B). Except for the severe intracellular retained mutant HA-MC4R (P78L), Hsc70 expression also elevated trafficking levels of WT and mutant MC4R.

To further confirm the increase in total levels of MC4R after Hsc70 over-expression western analysis was performed (Fig.5.12). An increase in levels of both WT and mutant HA-MC4R was detected (Fig.5.12).

After detecting an increase in total cellular levels of protein in HEK 293 cells, immunostaining of WT and mutant HA-MC4R (P78L) mutant was performed to obtain a visual image of the localisation of the receptor after Hsc70 over-expression (Fig.5.13). Although not detected in the in cell western assay, upon Hsc70 expression cell surface expression of HA-MC4R (P78L) did improve in a sub-population of the transfected cells (Fig.5.13).

To determine if there was a direct interaction between MC4R and Hsc70 *in vitro*, a co-immunoprecipitation experiment was carried out using a cell lysate from cells

expressing V5-tagged Hsc70 and HA tagged MC4R. The results clearly indicated that Hsc70 co-immunoprecipitates with WT HA-MC4R (Fig.5.14).

As an increase in trafficking levels for most MC4R mutants was observed, it was investigated whether Hsc70 expression would increase receptor signalling in response to NDP-MSH stimulation. This was done using the luciferase reporter system (described in Chapter 2). In agreement with the observation that Hsc70 did promote trafficking, an increase in receptor signalling at the PM was observed in cells expressing WT and mutant HA-MC4R (Fig.5.15). A fold increase of 1.21±0.02, 3.17±0.62, 2.51±0.07 and 1.02±0.05 was measured for mutants HA-MC4R (S58C), HA-MC4R (P78L), HA-MC4R (D90N) and HA-MC4R (L106P) respectively.

Over-expression of Hsc70 in stable HA-MC4R cell lines increased cell surface levels of mutant MC4R. A significant fold increase of 1.90±0.29, 6.01±1.34, 4.28±0.52 was measured for stably expressing mutants HA-MC4R (S58C), HA-MC4R (P78L) and HA-MC4R (L106P) (Fig.5.16, A). Similar to the transiently transfected cells, expression of Hsc70 in MC4R stable cell lines increased total cellular levels of MC4R (Fig.5.16, B), however due to the reduced effect of Hsc70 on cell surface levels of MC4R, Hsc70 did not promote the ratio of MC4R trafficking to the cell surface to the same extent as observed in transiently transfected cells. Only HA-MC4R (P78L) showed a significant fold increase (3.64±0.88) in trafficking to the cell surface (Fig.5.16, C).

As an increase in MC4R functional expression was observed upon NDP-MSH stimulation in the transiently transfected cells it was decided to determine if this also occurred in the MC4R stable expressing cell lines. Hsc70 expression did promote both WT and mutant MC4R signalling but to a lesser degree when compared to the transiently transfected HEK 293 cells (1.02±0.59, 0.84±0.07, 1.11±0.14, 1.06±0.15 for HA-MC4R (S58C), HA-MC4R (P78L), HA-MC4R (D90N) and HA-MC4R (L106P) respectively) (Fig.5.17).

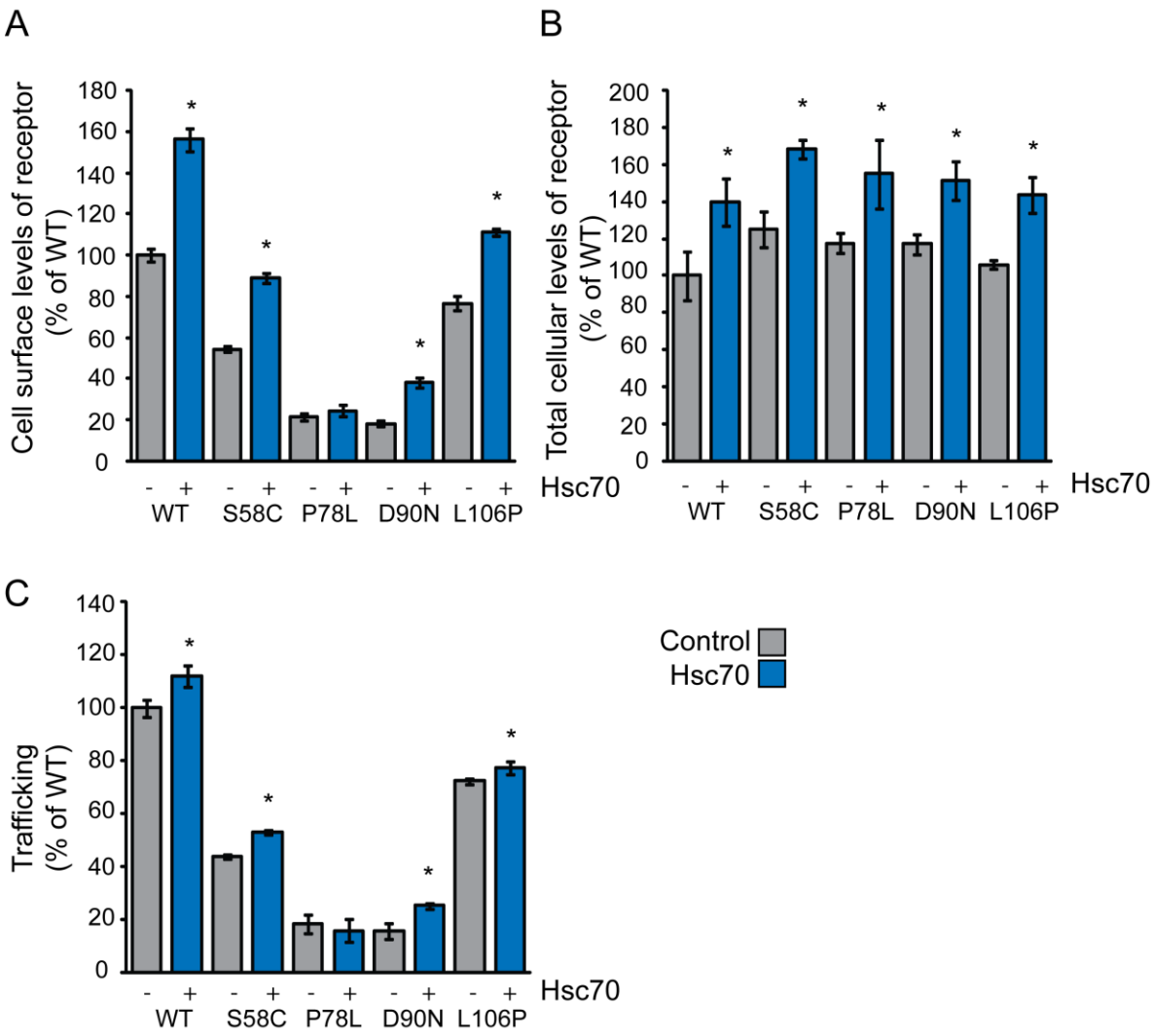

Figure 5.11: Expression of Hsc70 increases the trafficking of heterologous MC4R to the cell surface

HEK 293 cells were co-transfected with plasmids for expression of WT HA-MC4R or mutant MC4R with equal amounts of plasmid encoding Hsc70 or control empty vector (pcDNAfrt/20). 24 hours post-transfection cells were fixed and stained and in cell western analysis was performed. MC4R cell surface expression (A), total cellular levels (B), and trafficking to the cell surface (C) was quantified for cell co-expressing Hsc70 and control cells. *P<0.05. Error bars represent ±SD.

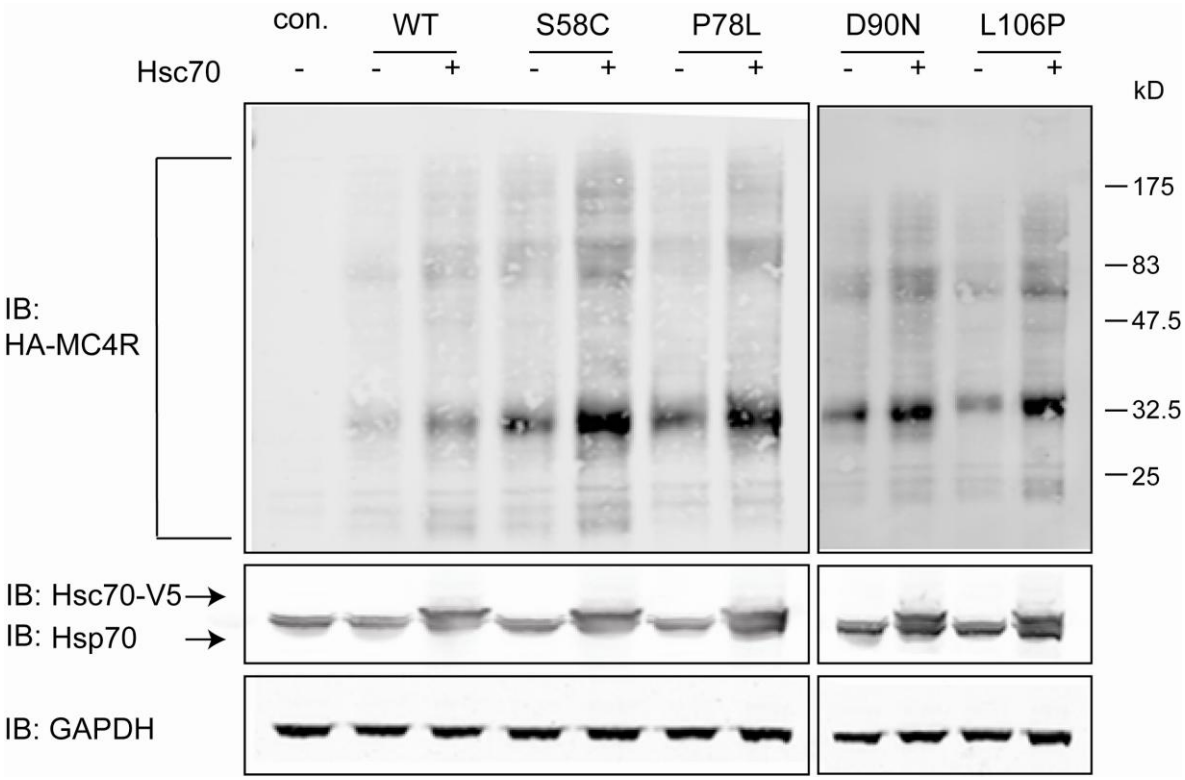

Figure 5.12: Expression of Hsc70 increases the total cellular expression of MC4R

HEK 293 cells were transiently co-transfected with plasmids expressing WT or mutant HA-MC4R and Hsc70 or control empty vector (pcDNAfrt/20). 24 hours post-transfection lysates were collected and resolved on a 12% SDS-PAGE gel prior to immunoblotting for HA tagged MC4R, V5 tagged Hsc70, endogenous Hsp70 and housekeeping protein GAPDH.

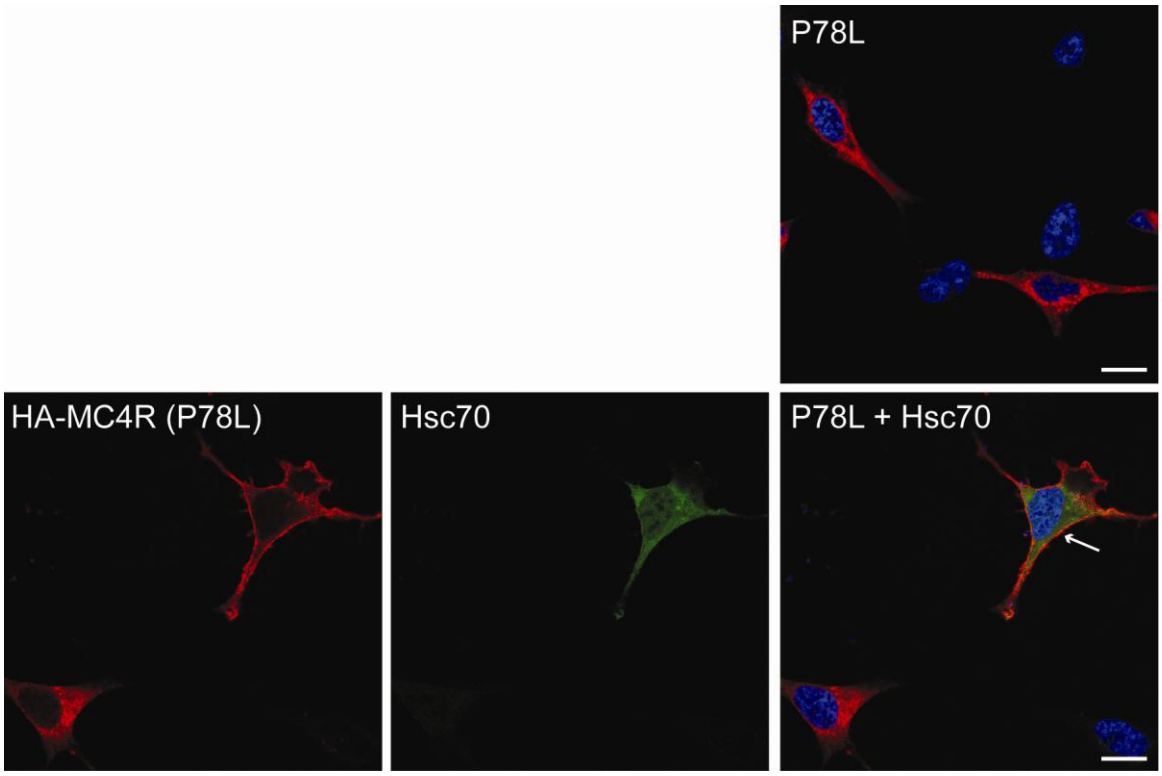

Figure 5.13: Hsc70 expression increases intracellular retained HA-MC4R (P78L) cell surface expression

HEK 293 cells were co-transfected with plasmids expressing MC4R and Hsc70 or control empty vector. 24 hours post transfection cells were fixed and stained with antibodies detecting HA-MC4R (red) and/or Hsc70 (green) with nuclei staining (blue). Cells were imaged using a Zeiss Confocal LSM 510 confocal microscope. Arrow shows increase in cell surface expression of HA-MC4R (P78L) for cell transfected with Hsc70. Scale bar = 10 µm

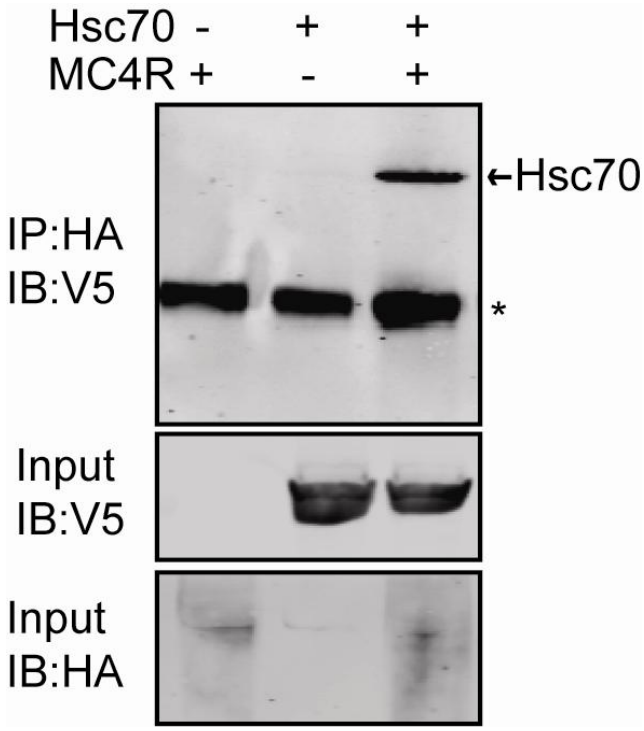

Figure 5.14: Hsc70 co-immunoprecipitates with MC4R

HEK 293 cells were transiently co-transfected with plasmids for the expression of WT HA-MC4R and Hsc70 or control empty vector (pcDNAfrt/20). 24 hours post-transfection, WT HA-MC4R and Aha1 were immunoprecipitated from a RIPA buffer (Sigma) soluble cell lysate and immunoblotting against V5 tagged Hsc70 using an anti-V5 antibody. Both the input and Co-IP gels were run and blotted at the same time.

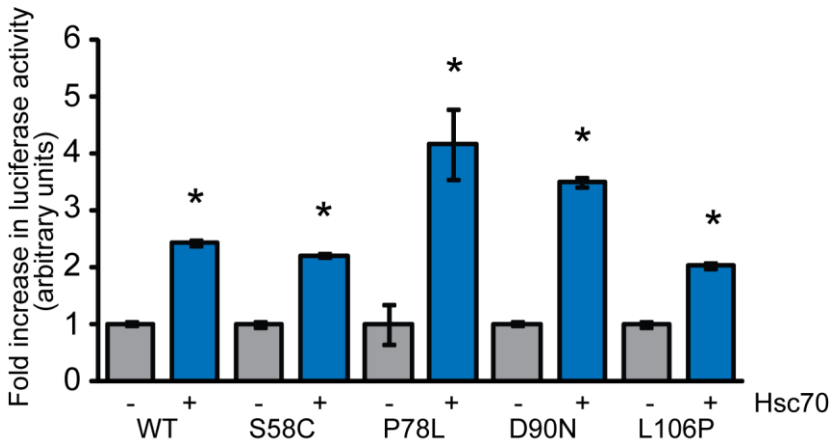

Figure 5.15: Over-expression of Hsc70 in HEK 293 increases functional expression of MC4R

HEK 293 cells heterologously expressing WT or mutant MC4R were co-transfected with plasmids encoding Hsc70 or a control empty vector and plasmid for a luciferase reporter and a vector for renillia expression. 16 hours post transfection cell were stimulated with 10^{-7}M NDP-MSH for 6 hours and luciferase activity was measured. Values were normalised to renilla activity to control for variability in transfection. Data is shown as fold increases in luciferase activity relative to untreated controls. *P<0.05. Error bars represent ±SD.

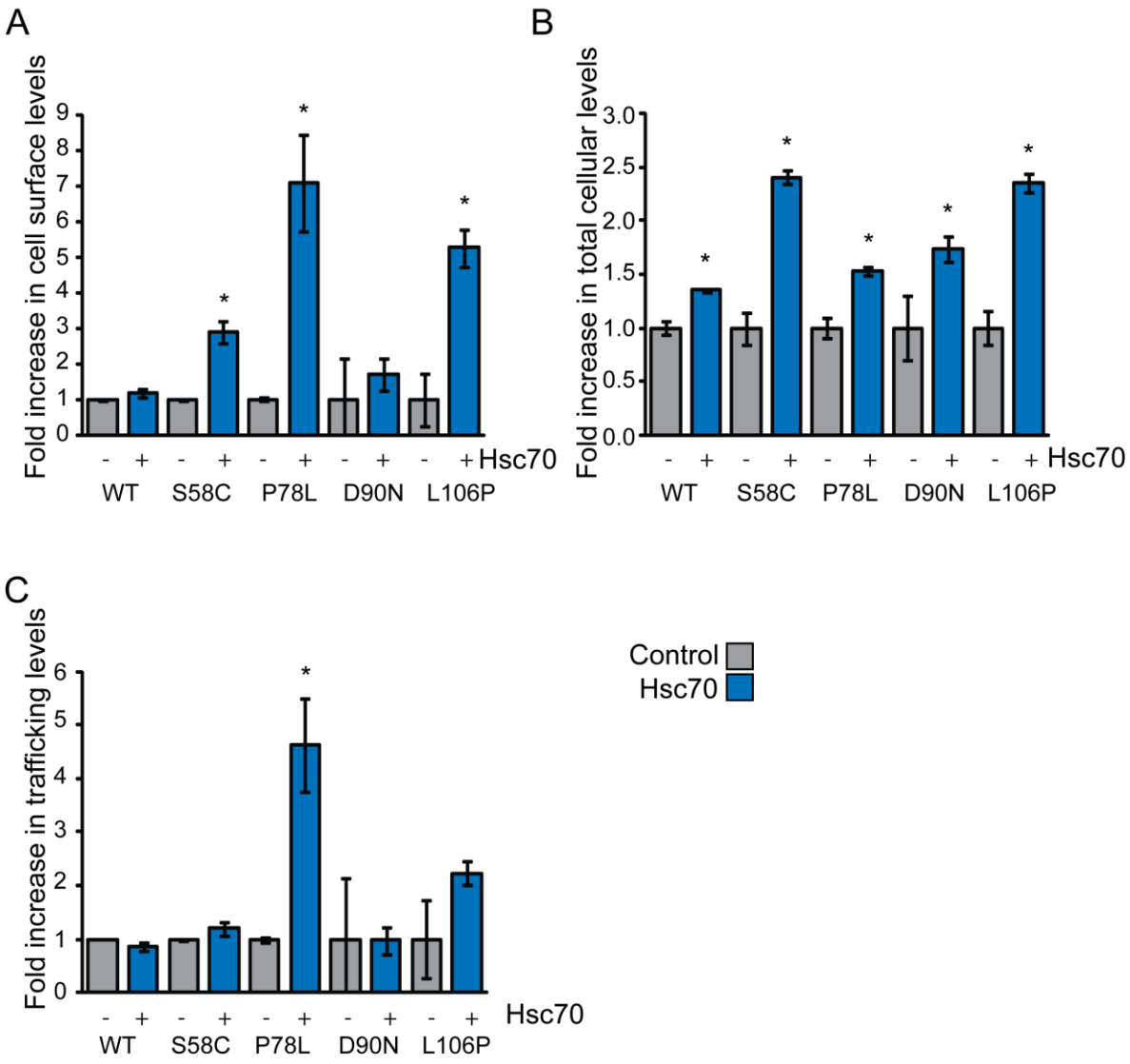

Figure 5.16: Over-expression of Hsc70 increases trafficking of stably expressing HA-MC4R (P78L)

HEK 293 cells stably expressing HA-MC4R were co-transfected with equal amounts of plasmid for the expression of Aha1 or control empty vector (pcDNA3.1). 24 hours post-transfection cells were fixed and stained and in cell western analysis was performed. MC4R cell surface levels (A), total cellular levels (B), and trafficking to the cell surface (C) was quantified for cell co-expressing Hsc70 and control cells. Data is shown as fold increases in MC4R expression relative to untreated controls. *P<0.05. Error bars represent the ±SD.

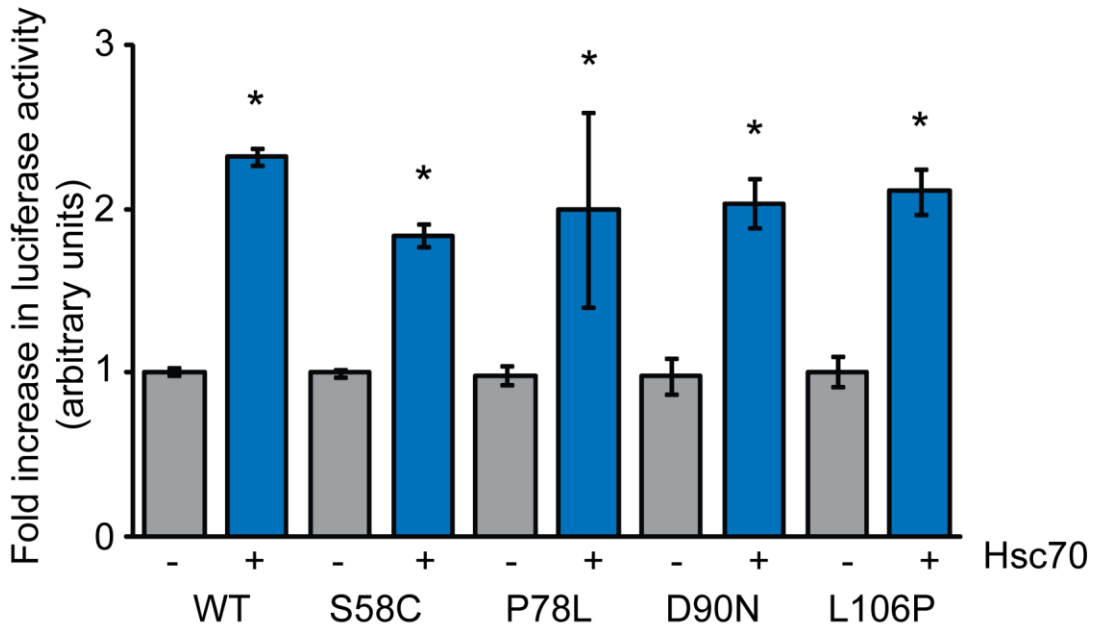

Figure 5.17: Over-expression of Hsc70 promotes stably expressing MC4R functional expression

Using a luciferase reporter system for cAMP activity MC4R signalling was quantified for wild-type and mutant HA-MC4Rs transfected with Hsc70. HEK 293 cells stably expressing HA-MC4R were transfected with plasmids for the expression of Hsc70 or control empty vector. Cells were also co-transfected with a luciferase reporter construct for MC4R signalling, and a vector for renilla expression. 16 hours post transfection cells were stimulated with 10^{-7}M NDP-MSH for 6 hours and luciferase activity was measured. Values were normalised to renilla activity to control for variability in transfection. Data is shown as fold increases in luciferase activity relative to untreated controls. *P<0.05. Error bars represent ±SD.

5.2.4 Synergistic effect of Aha1 and Hsc70

As both Aha1 and Hsc70 improved the functional expression of mutant MC4R independently it was hypothesised that the two combined would further magnify any MC4R signalling. Indeed, the data indicates that Aha1 and Hsc70 work synergistically and enhance MC4R functional activity compared to when acting independently of each other (Fig.5.18). Upon NDP-MSH stimulation, Hsc70 and Aha1 collectively caused a significant (*P<0.05) fold increase of MC4R functional expression compared to either Aha1 alone or Hsc70 alone. For the intracellular mutant tested, HA-MC4R (S58C), a greater fold increase in the synergistic effect was observed compared to WT HA-MC4R.

The data presented thus far indicates that the two different chaperone machineries, namely Hsc70 and Hsp90, are important in the regulation of MC4R processing. It is known that Hsp90 and Hsp70 chaperone machineries play a vital role in the folding and maturation of key regulatory proteins such as kinases, steroid hormones and transcription factors (Wegele et al., 2004). Furthermore, it has been demonstrated that a third protein, the Hsp organiser protein (Hop) interacts with both Hsp90 and Hsp70 and functions as an adaptor protein (Chen & Smith, 1998). Therefore knockdown of Hop would potentially disrupt the functional interaction of the Hsp70 and Hsp90 chaperone systems resulting in a decrease in MC4R signalling. This hypothesis was tested by selectively knocking down *Hop*, using siRNA oligos (1 in combination with siRNA oligo 3) targeted to Hop sequence in HEK 293 cells transiently expressing MC4R (Fig. 5.19, A). As predicted a reduction in MC4R signalling was observed but only for the intracellular retained mutants (0.17±0.08 and 0.10±0.06 for HA-MC4R (S58C) and HA-MC4R (P78L) respectively) tested and not for the WT receptor (Fig.5.19, B).

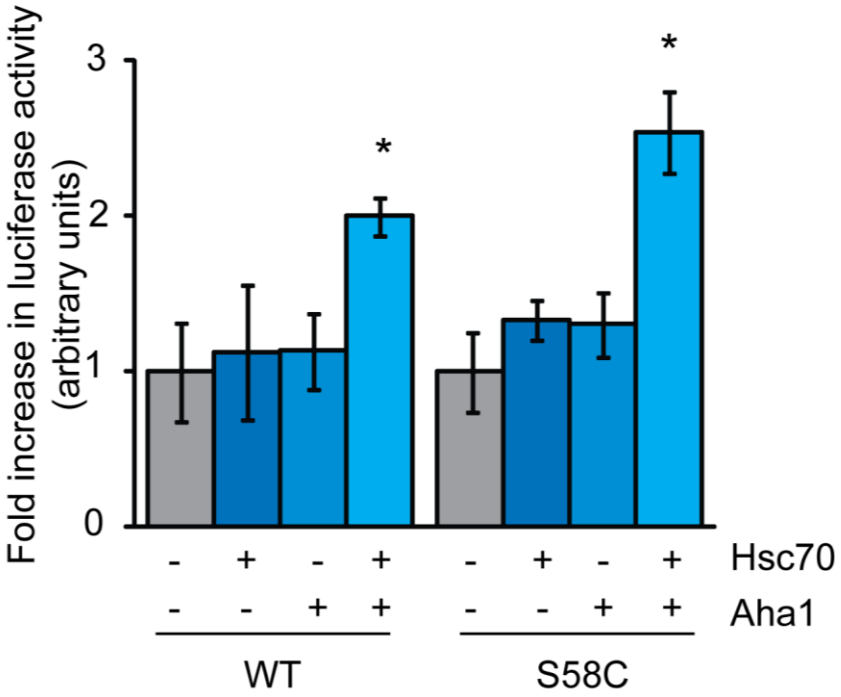

Figure 5.18: Hsc70 and Aha1 have a synergistic effect on the functional expression of MC4R

HEK 293 cells stably expressing WT HA-MC4R and intracellular retained mutant HA-MC4R (S58C) were transfected with plasmids for the expression of Hsc70, Aha1 or both Hsc70 and Aha1. Cells were also co-transfected with a luciferase reporter construct for MC4R signalling, and a vector for renilla expression. 16 hours post transfection cells were stimulated with 10^{-7}M NDP-MSH for 6 hours and luciferase activity was measured. Values were normalised to renilla activity to control for variability in transfection. Data is shown as fold increases in luciferase activity relative to untreated controls. *P<0.05. Error bars represent the mean ±SD.

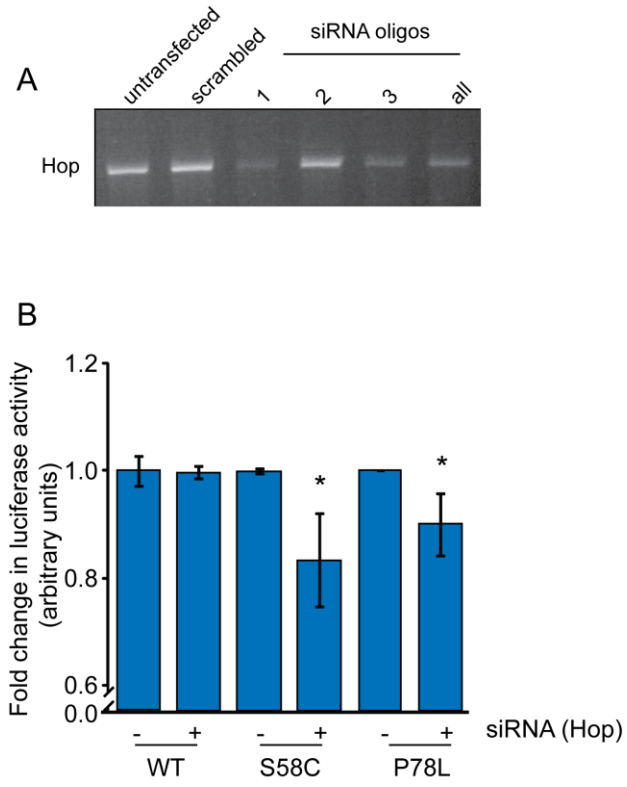

Figure 5.19: Knockdown of *Hop* causes a reduction in mutant HA-MC4R (S58C, P78L) functional expression

siRNA peptide oligos targeted for *Hop* were transfected into HEK 293 cells. mRNA from the cells was reverse transcribed to obtain cDNA. Primers for *Hop* were used to amplify *Hop* transcript from the cDNA obtained. siRNA oligos 1 and 3 proved to be the most successful for effective knockdown of *Hop* (A). Using a luciferase reporter system for cAMP activity MC4R signalling was quantified for WT and mutant HA-MC4Rs co-transfected with either siRNA against a scrambled sequence or siRNA against Hop. Cells were also co-transfected with a luciferase reporter construct for MC4R signalling, and a vector for renilla expression. 16 hours post transfection cells were stimulated with 10^{-7}M NDP-MSH for 6 hours and luciferase activity was measured. Values were normalised to renilla activity to control for variability in transfection (B). Data is shown as fold increases in luciferase activity relative to untreated controls. *P<0.05. Error bars represent the mean ±SD.

5.3 Discussion

In summary, these results strongly implicate a role for the Hsp90 and Hsc70 chaperone systems in MC4R processing. In agreement with previous *in vitro* (retinal epithelium cells) and *in vivo* (mouse brains) studies, treatment of HEK 293 cells with 400 nM GA caused an ~10 fold induction in Hsp70 expression (Fig.5.1, B) (Wu et al., 2007; Kwon et al., 2009). However, Hsp70 pharmacological inducer GA did not promote MC4R trafficking or cell surface levels of MC4R. Therefore, this suggests that inhibition of Hsp90 with GA is not a potential method to rescue MC4R misfolding mutants. Hsp90 has been shown to interact with nascent CFTR polypeptide, with GA mediated inhibition of Hsp90 preventing nascent CFTR folding and promoting its degradation by the proteasome (Loo et al., 1998). Furthermore, disruption to Hsp90 function leads to the degradation of multiple steroid hormone receptors (Segnitz et al., 1997) and tyrosine kinases (Schnaider et al., 200) by the proteasome. Although not directly tested, the interpretation of the reduction of MC4R expression levels when treated with GA, may suggest that there may be a direct association of Hsp90 with the cytoplasmic domains of MC4R. If so, acting at the cytoplasmic face of the endoplasmic reticulum (ER), cytosolic Hsp90 may potentially interact with the cytoplasmic domains of ER retained MC4R mutants thereby possibly counteracting their susceptibility to become degraded by the proteasome. This data may also suggest that native MC4R may be a possible client protein of Hsp90, and that Hsp90 is required for its folding, and stability. GA inhibition of Hsp90 does not block the formation of Hsp90 complexes with folded or misfolded proteins, nor will it disrupt any existing complexes (Panaretou et al., 1998; Obermann et al., 1998). However, as GA binds to the ATP binding site of Hsp90, it will reduce the ability of Hsp90 to bind and release client proteins and therefore reduce the rate of Hsp90 natural chaperone cycle possibly resulting in the degradation of MC4R. GA also inhibits the glucose regulated protein (GRP94), the ER luminal homologue of Hsp90, and this data may also suggest that GRP94 is required for MC4R processing, possibly by stabilising the receptor. In fact GRP94 and another ER luminal chaperone, calnexin, have been shown to stabilise

and promote the mobility of both native and misfolded human insulin receptor (Ramos et al., 2007).

Therefore it was hypothesised that, stimulation of Hsp90 chaperone cycle would promote MC4R's folding and functional expression of the receptor at the cell surface. The activator of the ATPase activity of Hsp90, Aha1 was used to increase the natural chaperone cycling activity of Hsp90 (Lotz et al., 2003). However, Aha1 over-expression did not significantly increase MC4R functional expression at the PM. These results suggest that although Aha1 is able to increase the total levels of both WT and mutant MC4R it is not able to efficiently increase MC4R's trafficking to the cell surface.

It is not surprising that a partial positive effect of Aha1 was observed for the WT receptor, as confocal imaging indicated that a proportion of the WT receptor was localised intracellularly in transiently transfected HEK 293 cells. The data presented here leads to the speculation that, Hsp90 possibly binds to the cytosolic domains of mutant MC4R polypeptide intermediates and manages to stabilise them effectively at the ER.

It could also be hypothesised that stabilisation of MC4R at the ER may allow mutant protein to escape from the cellular quality control machineries and therefore not become retro-translocated for degradation. However, the data suggests that only a minority of misfolded receptors possibly achieve a more native conformation to enter the secretory pathway and reach the cell surface.

In contrast to the data obtained for Hsp90 and MC4R, for CFTR expressing cells, Aha1 knockdown increased trafficking of misfolded (ΔF508 mutant) protein to the cell surface (Wang et al., 2006). The authors demonstrated that silencing of Aha1 reduced endoplasmic reticulum associated degradation (ERAD) of the mutant protein whereas over-expression of Aha1 destabilised both the WT and mutant ΔF508 CFTR protein and promoted their ER-associated degradation (Wang et al., 2006). Further investigations suggested that the C-terminal domain of Aha1 helps

the dimerisation of Hsp90 N-terminal domains (Koulov et al., 2010) and the N-terminal domain of Aha1 binds to the middle domain of Hsp90 (Meyer et al., 2004). With at least one Aha1 monomer interacting with one Hsp90 dimer, Aha1 bridges the Hsp90 dimer interface (Koulov et al., 2010). In the case of CFTR, it has been suggested that reduction of Aha1 levels possibly decreases Hsp90 ATPase activity thereby increasing client protein (ΔF508 CFTR) 'dwell time' with Hsp90 (Koulov et al., 2010). An increase in 'dwell time' potentially allows for increase association of client protein with Hsp90 and possibly the generation of more kinetically stable ΔF508 CFTR fold, resulting in export of the mutant protein from the ER (Koulov et al., 2010). This suggests that differential chaperone cellular environments may be required for different proteins.

Heterologous expression of Hsc70 was successful in enhancing mutant MC4R functional expression. Cytoplasmic chaperones have been shown to influence the folding and processing of other GPCRs. For example, DnaJ proteins HSJ1a and HSJ1b regulate the ATPase activity and substrate binding of Hsp70. HSJ1b has been shown to modulate the processing of GPCR rhodopsin at the cytoplasmic face of the ER (Chapple et al., 2003). In another example, disruption of GPCR angiotensin II type I receptor (AT_1) glycosylation, causes the receptor to become retained in the ER and associate with the cytosolic chaperone Hsp70 (Lanctot et al., 2005). Hsc70 has also been shown to interact with the N-terminal cytosolic nucleotide-binding domain (NBD1) of CFTR and assists in the folding of NBD1 (Meacham et al., 1999). Furthermore, Hsc70 with co-chaperone CHIP forms part of a multisubunit CHIP E3 ubiquitin ligase complex that ubiquitinates cytosolic regions of CFTRΔF508 targeting it for proteasomal degradation (Younger et al., 2006). This demonstrates that CHIP can convert Hsc70s function from a protein folding machine into a degradation component (Meacham et al., 2001).

The data presented here strongly indicates a role for the Hsc70 and Hsp90 chaperone machineries in MC4R processing; supporting this functional expression of MC4R was further elevated in cells expressing both Hsc70 and Aha1. In

addition, siRNA downregulation of the Hsp70/Hsp90 organising protein (Hop) caused a decrease in mutant MC4R signalling. One of the functions of Hop is to act as an adaptor protein, providing a physical link between chaperone machineries Hsc70/Hsp70 and Hsp90, and mediates the transfers of protein substrates from Hsp70 to Hsp90 (Wegele et al., 2006). Potentially acting as a monomer, Hop binds to the C-terminus of Hsp70 and one of the two TPR domains on Hsp90 (Yi et al., 2009). Interestingly, probable disruption of the Hsp70/Hsp90 chaperone complex by knockdown of Hop causes a decrease in the functional expression of mutant HA-MC4R (S58C, P78L) but not the WT receptor. This data further indicates that the cytosolic chaperones Hsc70 and Hsp90 are involved in the processing of misfolded MC4R. Possible greater knockdown of Hop may effect WT receptor functional expression.

CHAPTER 6

Further strategies to promote cell surface expression of mutant MC4R

6.1 Introduction

The experiments described in this chapter have been undertaken to investigate the effects of two compounds that are known modulators of cellular proteostasis, rapamycin and resveratrol, and melanocortin-2-accessory protein (MRAP) on the cell surface expression of mutant MC4R.

6.1 Autophagy inducer, rapamycin

As discussed in chapter 1, the ubiquitin-proteasome system and autophagy are the two major mechanisms responsible for the clearance of cellular proteins. Autophagy can be induced by inhibiting the mammalian target of rapamycin (mTOR), a negative regulator of autophagy (Winslow & Rubinsztein, 2008). mTOR is a well conserved 270kD phosphatidylinositol kinase-related kinase (Diaz-Troya et al., 2008). Rapamycin, a U.S. Food and Drug Administration approved lipophilic macrolide antibiotic, forms a complex with the immunophilin FK506-binding protein 12 (FKBP12), which in turns binds to and inactivates mTOR thereby inducing autophagy (Ravikumar et al., 2006).

Numerous studies have investigated the induction of autophagy, using chemicals including rapamycin, in order to remove potential toxic aggregated proteins formed in neurodegenerative disorders. For example, the use of rapamycin or the rapamycin ester CCI-779 reduced aggregate formation and toxicity in mouse and drosophila models expressing mutant huntingtin (Ravikumar et al., 2004). Furthermore, inhibition of autophagy with bafilomycin A1 increased the percentage of cells containing aggregated Olfactory GPCRs (Lu et al., 2003).

Therefore it was hypothesised that induction of autophagy by rapamycin would possibly promote the clearance of misfolded MC4R leading to a reduction in the concentration of aberrantly folded MC4R. This in turn may improve the cellular protein homeostasis enabling any partially folded mutant MC4R to achieve a

more native conformation, thus allowing it to pass to the endoplasmic reticulum (ER) quality control resulting in an increase in MC4R trafficking and function.

6.2 Resveratrol

Resveratrol a naturally occurring molecule, classified as a polyphenol, is synthesized by plants in response to biological attack from fungi, bacteria or other injurious substances (Sadruddin et al., 2009). Found at a naturally high concentration in red grapes and red wine, resveratrol has been shown to have protective effects against a number of diseases including cancer, neurodegenerative diseases, and metabolic syndromes (Saiko et al., 2008).

The effects of Resveratrol have been analyzed in various models of protein misfolding disease. For example, administration of 0.2% resveratrol for 45 days to Alzheimer's disease (AD) transgenic mice reduced plaque counts (caused by aggregated beta amyloid deposits) in the medial cortex, striatum and hypothalamus regions of the brain (Karuppagounder et al., 2008). In a yeast model of Huntington's disease (HD), misfolded/aggregated huntingtin was thought to be abnormally interacting with mitochondrial membranes resulting in disturbances to mitochondrial distribution and function leading to an increase in reactive oxygen species (ROS) (Solans et al., 2006). Treatment with 10-50 μM of the antioxidant resveratrol for 10-20 hours partially prevented the cells respiration dysfunction and cell death (Solan et al., 2006). Therefore, the effect of resveratrol on MC4R processing was investigated. It was hypothesised that resveratrol would reduce the concentration of intracellular misfolded protein, modulating cellular proteostasis and possibly increasing the cell surface expression and function of mutant MC4R.

6.1.3 MC2R accessory protein MRAP

Previous studies have shown that in non-adrenal cell lines MC2R is retained in the ER (Noon et al., 2002). Later studies identified that MRAP, a small transmembrane protein, is required for the functional expression of MC2R (Metherell et al., 2005). MRAP is required to facilitate the trafficking of MC2R from the ER to the plasma membrane. Mutations in MRAP cause ER retention of MC2R and result in glucocorticoid deficiency type 2 (Metherell et al., 2005). MRAP has also been shown to be expressed in the hypothalamus by *in situ* hybridisation (Gardiner et al., 2002), interestingly this is the same localisation for MC4R expression (Balthasar et al., 2005). Recently, the MRAP homologue MRAP2 has been identified and characterized (Chan et al., 2009). MRAP2 has also been shown to be expressed in the hypothalamus (Lein et al., 2007). Furthermore, recent work has shown that both MRAP and MRAP2 are able to interact with WT MC4R and moderately attenuate its signalling in CHO cells (Chan et al., 2009).

It was postulated that MRAP would also be able to bind to ER retained mutant MC4R, and may possibly stabilise it sufficiently to promote a degree of functional cell surface expression of the mutant receptor.

6.3 Results

6.5 Effect of rapamycin on MC4R processing

HEK 293 cells transiently expressing WT HA-MC4R or HA-MC4R (L106P) were treated with 1, 5 or 10 µM rapamycin or a vehicle control for 24 hours. Cell surface levels of WT HA-MC4R increased with increasing concentrations of rapamycin, with 10 µM causing an increase of 27.78%±12.81 (Fig.6.1, A). Cell surface levels of the mutant receptor HA-MC4R (L106P) remained unchanged (Fig.6.1, A). No change in total cellular levels of the WT or mutant receptor was observed after rapamycin treatment (Fig.6.1, B). Although, an increase of 16.52±11.69% was observed for the proportion of WT receptor trafficking to the cell surface after treatment with 10 µM of rapamycin (Fig.6.1, C). However, the ratio of mutant receptor trafficking to the cell surface remained unchanged with increasing concentrations of rapamycin (Fig.6.1, C).

After 48 hours treatment with rapamycin the same trends were observed for the WT receptor but more positive changes were seen for the mutant receptor. A significant but minimal increase of HA-MC4R (L106P) cell surface receptor levels was seen with increasing concentrations of rapamycin, with 10 µM causing an increase of 7.04±0.57% (Fig.6.2, A). Total cellular levels of the mutant receptor also increased with increasing concentration of rapamycin, with 10 µM causing an increase of 11.68±4.09% (Fig.6.2, B). However, rapamycin did not cause any large changes in the proportion of MC4R trafficking to the cell surface after 48 hours treatment.

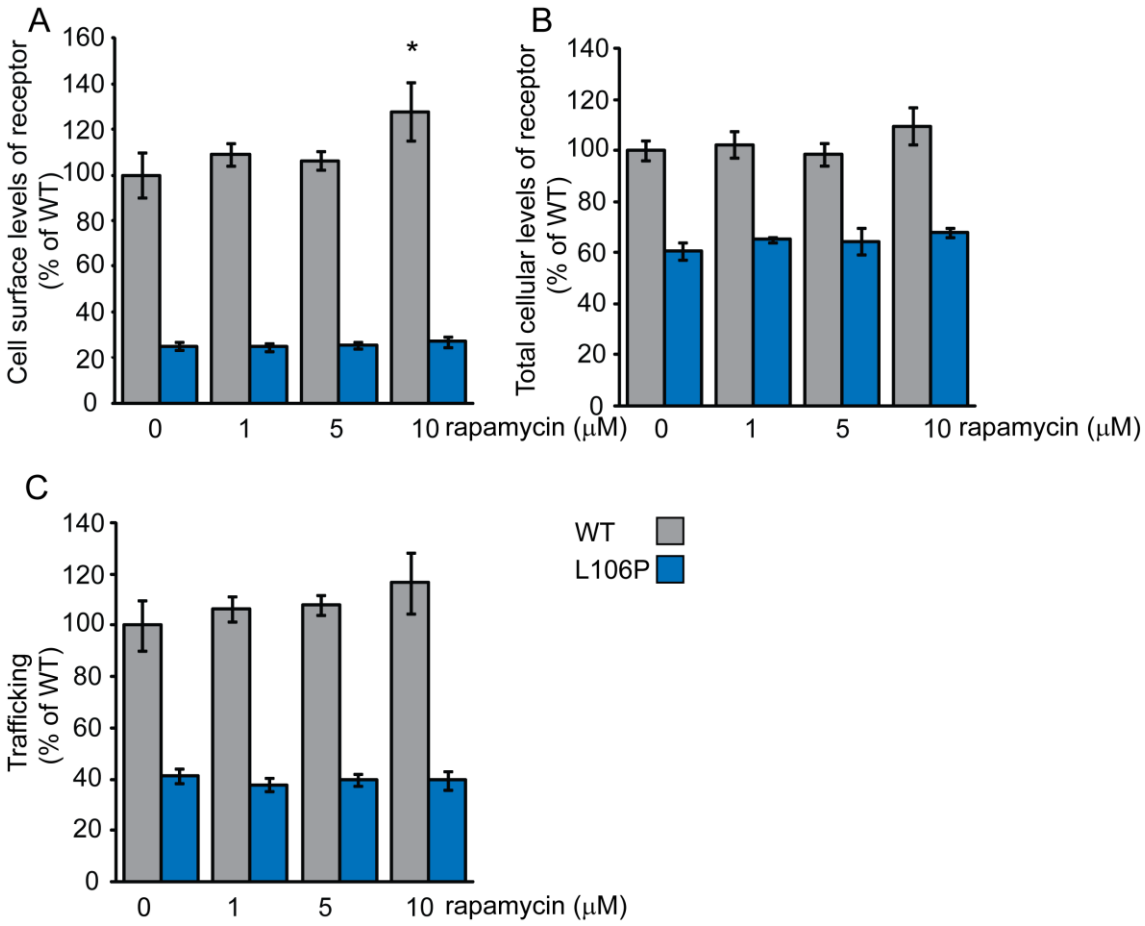

Figure 6.1: 24 hours treatment with rapamycin causes an increase in cell surface expression of WT MC4R

HEK 293 cells were transfected with plasmids for the expression of WT HA-MC4R or mutant HA-MC4R (L106P). Immediately after transfection cells were incubated with 1, 5 or 10 μM rapamycin or vehicle control for 24 hours prior to in cell western analysis. MC4R cell surface levels (A), total cellular levels (B), and trafficking to the cell surface (C) was quantified for MC4R at each concentration of rapamycin. *P<0.05. Error bars represent the mean ±SD.

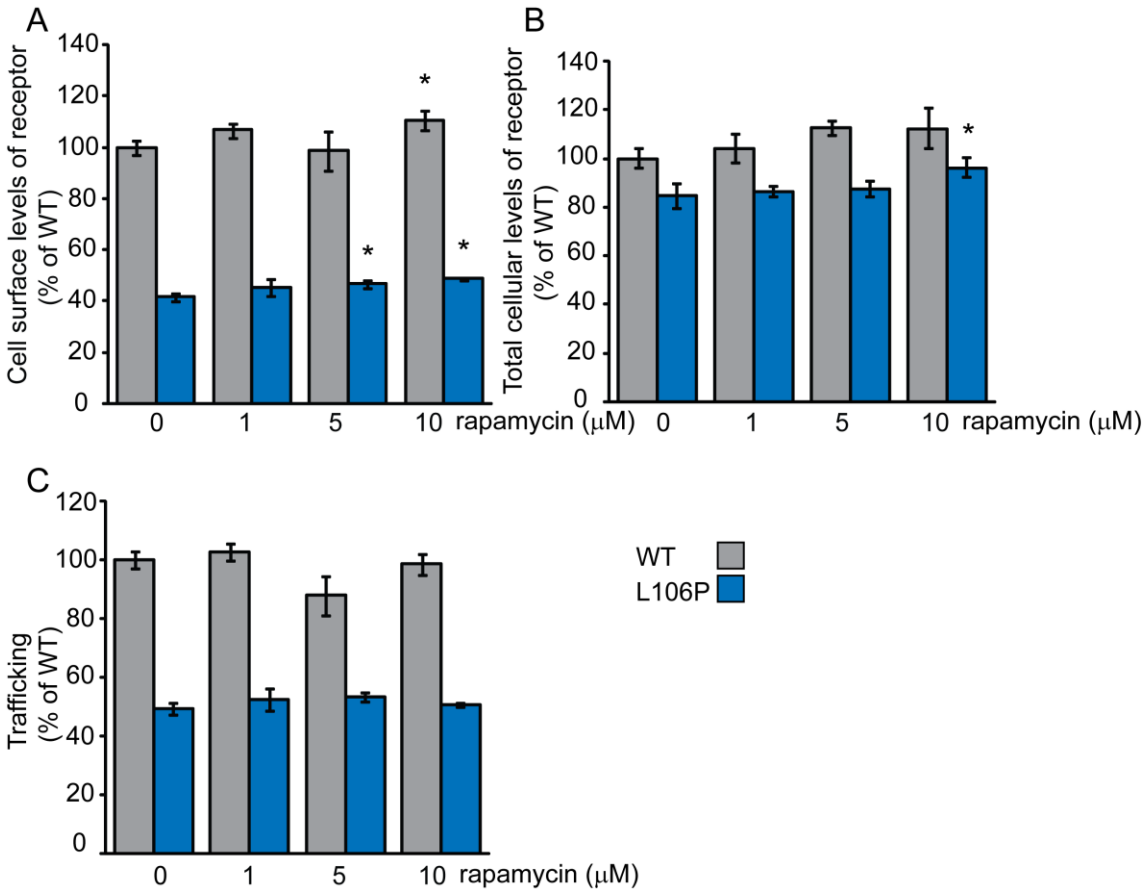

Figure 6.2: 48 hours treatment with rapamycin does not promote trafficking of MC4R to the cell surface

HEK 293 cells were transfected with plasmids for the expression of WT HA-MC4R or mutant HA-MC4R (L106P). Immediately after transfection cells were incubated with 1, 5 or 10 μM rapamycin or vehicle control for 48 hours prior to in cell western analysis. MC4R cell surface levels (A), total cellular levels (B), and trafficking to the cell surface (C) was quantified for MC4R at each concentration of rapamycin. *P<0.05. Error bars represent the mean ±SD.

6.6 Effect of resveratrol on MC4R processing

HEK 293 cells transiently expressing WT HA-MC4R or HA-MC4R (L106P) were treated with 1, 10 or 100 µM resveratrol or vehicle control. Surprisingly a significant reduction in cell surface levels of WT HA-MC4R were observed with increasing concentrations of resveratrol (Fig.6.3, A). A reduction of 19.71±3.40% in cell surface levels of MC4R was recorded between control and 100µM resveratrol treated cells expressing WT protein. However no reduction in cell surface levels of HA-MC4R (L106P) expressing cells was observed for resveratrol concentrations above 1µM compared to control cells. Total cellular levels of WT HA-MC4R and mutant HA-MC4R (L106P) were unaffected (Fig.6.3, B). In contrast to our hypothesis that resveratrol may be advantageous for MC4R trafficking to the PM, increasing concentrations of resveratrol caused a reduction in the proportion WT receptor trafficking to the PM, although no difference was observed for partially intracellular retained mutant HA-MC4R (L106P) (Fig.6.3, C).

A longer incubation period of 48 hours did not change the pattern of WT HA-MC4R expression levels when compared to 24 hours of treatment with resveratrol (Fig.6.4). After treatment with 10 µM resveratrol, a similar reduction in cell surface levels of WT receptor was observed after 24 hours (15.16±4.57%) and 48 hours (13.20±3.33%) (Fig.6.4, A). WT MC4R total cellular levels were not affected with increasing concentrations of resveratrol after 48 hours of treatment (Fig.6.4, B). Similar to results at 24 hours, 48 hour treatment with resveratrol caused a decrease in the proportion of WT receptor trafficking to the cell surface (Fig.6.4, C). In addition, similar to the WT receptor 48 hours exposure to resveratrol reduced the proportion of mutant MC4R (L106P) trafficking to the cell surface at resveratrol concentrations of 1 µM (7.12±1.66%) and 10 µM (8.85±3.44%) (Fig. 6.4, C).

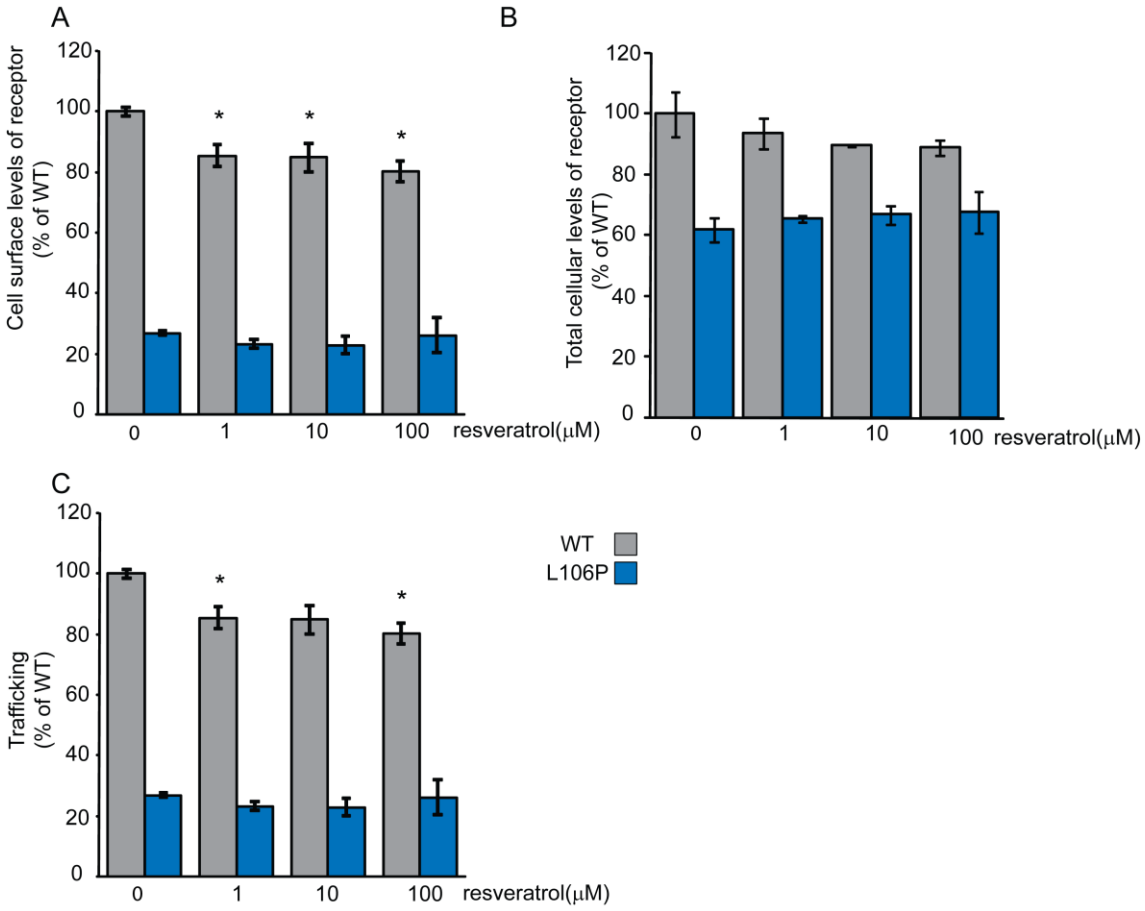

Figure 6.3: 24 hours treatment with resveratrol causes a reduction in WT MC4R cell surface expression

HEK 293 cells were transfected with plasmids for the expression of WT HA-MC4R or mutant HA-MC4R (L106P). Immediately after transfection cells were incubated with 1, 10 or 100 μM resveratrol or vehicle control for 24 hours prior to in cell western analysis. MC4R cell surface levels (A), total cellular levels (B), and trafficking to the cell surface (C) was quantified for MC4R at each concentration of resveratrol. *P<0.05. Error bars represent the mean ±SD.

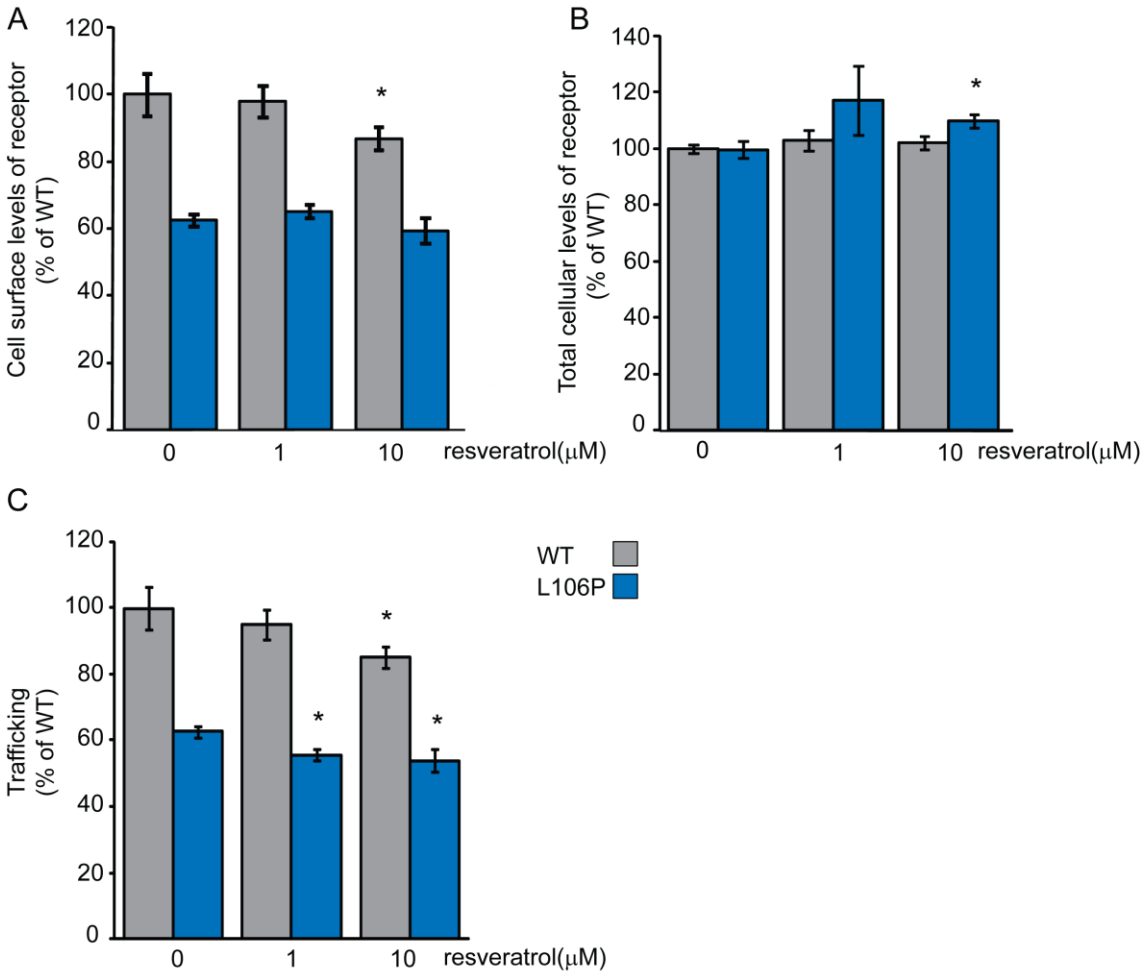

Figure 6.4: 48 hours treatment with resveratrol does not improve the proportion of MC4R trafficking to the cell surface

HEK 293 cells were transfected with plasmids for the expression of WT HA-MC4R or mutant HA-MC4R (L106P). Immediately after transfection cells were incubated with 1, 5 or 10 μM resveratrol or vehicle control for 48 hours prior to in cell western analysis. MC4R cell surface levels (A), total cellular levels (B), and trafficking to the cell surface (C) was quantified for MC4R at each concentration of resveratrol. *P<0.05. Error bars represent the mean ±SD.

6.7 Effect of MRAP on the cellular trafficking and function of MC4R

MRAP expression had no effect on WT HA-MC4R cell surface expression, but significantly improved the cell surface expression of all intracellular retained MC4R mutants. Surprisingly, the most severe mutant in the cohort HA-MC4R (P78L), showed the largest fold increase in cell surface expression (1.77±0.08) (Fig.6.5, A). Both WT and mutant HA-MC4R total cellular expression levels were slightly increased in MRAP expressing cells. Mutants HA-MC4R (D90N) and HA-MC4R (L106P) showed the largest fold increase of 0.34±0.023 and 0.73±0.18 respectively (Fig.6.5, B). Interestingly, cells expressing MRAP had an increase in the proportion of mutant MC4R trafficking to the cell surface but a decrease in ratio of WT receptor trafficking to the cell surface. MRAP promoted the trafficking of the most severe mutant HA-MC4R (P78L) to the cell surface, resulting in a fold increase of 1.39±0.15 (Fig.6.5, C).

Confocal analysis also suggested there was indeed an increase in the trafficking of misfolding MC4R mutants in the presence of MRAP supporting the findings from the in cell western assay (Fig.6.6).

Measurements of reporter gene activity, using a luciferase reporter assay, revealed that MRAP expression improved the signalling and function of mutant HA-MC4R (P78L) but had no effect on WT signalling (Fig.6.7). Mutant HA-MC4R (P78L) signalling improved 3.71±0.37 fold in cells co-transfected for MRAP expression (Fig. 6.7).

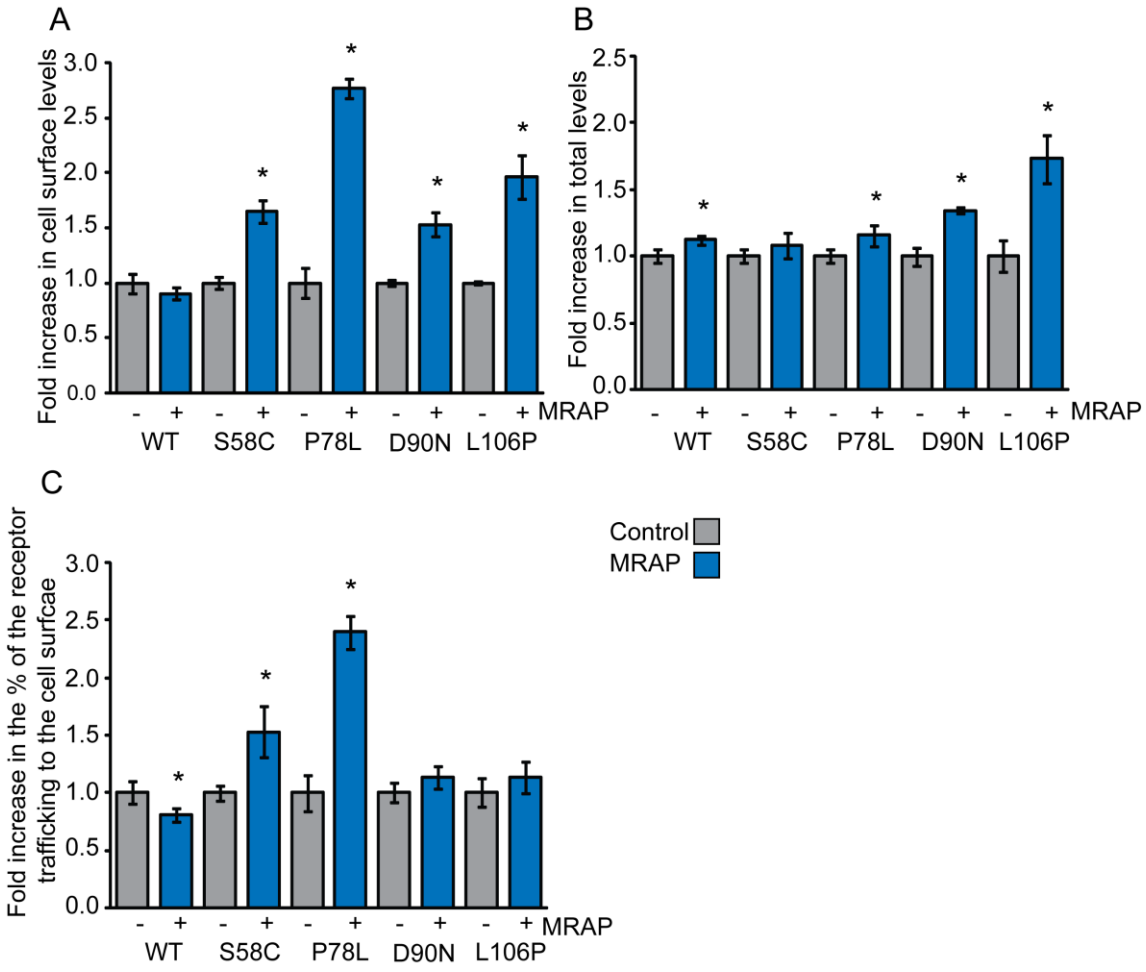

Figure 6.5: MRAP promotes the trafficking of mutant receptor to the cell surface

HEK293 cells were transiently co-transfected with equal amounts of plasmid for the expression of MC4R and MRAP or MC4R and empty vector for 24 hours prior to in cell western analysis. MC4R cell surface levels (A), total cellular levels (B), and trafficking to the cell surface (C) was quantified for cells co-expressing MRAP and control cells. *P<0.05. Error bars represent the mean ±SD.

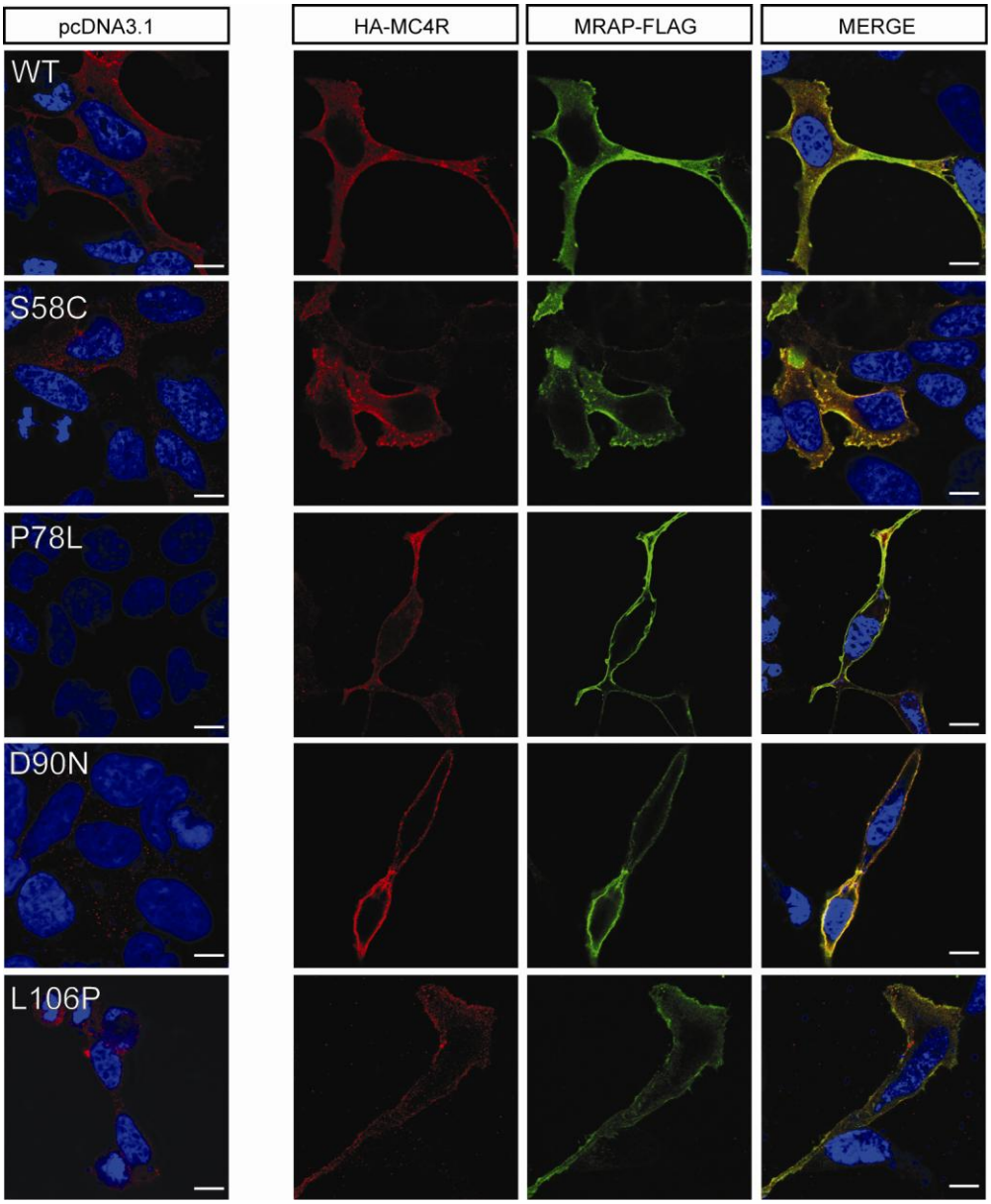

Figure 6.6: MRAP promotes the cell surface expression of mutant MC4R

HEK293 cells were transfected with plasmids for expression of WT HA-MC4R or mutant HA-MC4R and MRAP-FLAG or empty vector. 24 hours post transfection cells were formaldehyde fixed and immunostained with primary anti HA-antibodies, to detect the N-terminal HA-tagged MC4R (red), primary anti-FLAG to detect the C-terminal FLAG tagged MRAP (green) with nuclei staining (blue) and Cy3 and Cy2 fluorescent secondary antibodies. Scale bar = 10 µM

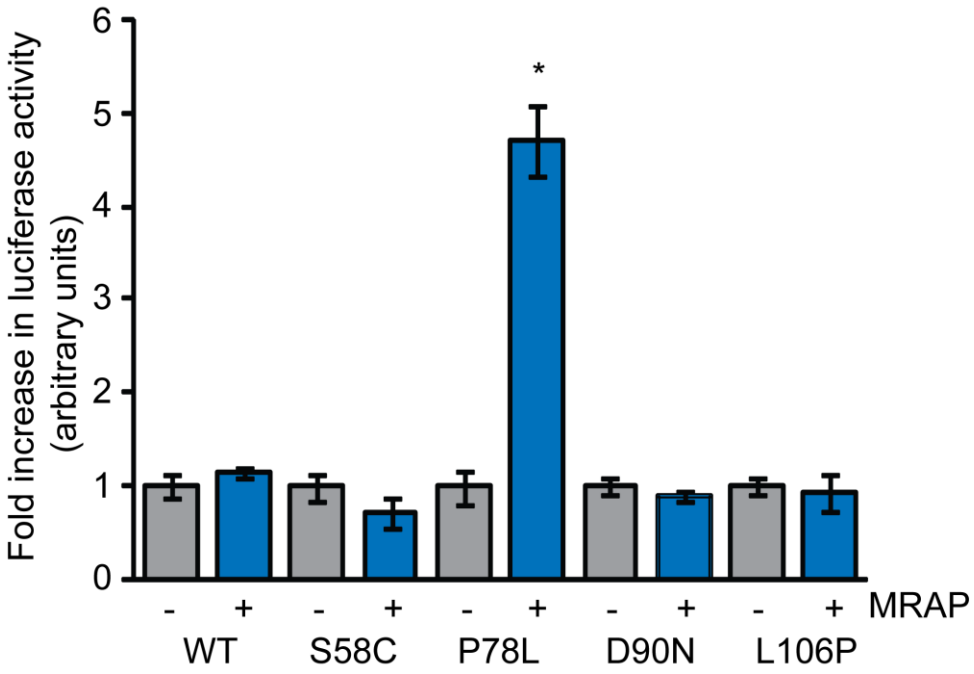

Figure 6.7: MRAP promotes the functional expression of mutant HA-MC4R (P78L) MC4R at the cell surface

Using a luciferase reporter system for cAMP activity MC4R signalling was quantified for wild-type and mutant HA-MC4Rs. Cells were co-transfected with plasmids for expression of WT or mutant MC4R and MRAP-FLAG, a luciferase reporter construct for MC4R signalling, and a vector for renilla expression. 16 hours post transfection cells were stimulated with 10^{-7}M NDP-MSH for 6 hours and luciferase activity was measured. Values were normalised to renilla activity to control for variability in transfection. *P<0.05. Error bars represent the mean ±SD

6.4 Discussion

6.4.1 Rapamycin

In summary a minimal effect was observed with mTOR inhibitor rapamycin on MC4R processing. After 24 hours treatment with rapamycin, no effect was observed for the relative amount of HA-MC4R (L106P) trafficking to the cell surface and the same was observed for WT MC4R. Interestingly, after 48 hours treatment with 5 µM rapamycin, a small increase in the proportion of HA-MC4R (L106P) trafficking to the cell surface was observed. This may indicate that prolonged incubation with rapamycin may be advantageous for mutant MC4R trafficking.

In this study the concentrations of rapamycin that showed some effect on MC4R processing are similar to those used in other cellular models of disease where aberrant protein folding is a feature. For example, rapamycin used at a concentration of ~0.2 µM was found to promote the clearance of cellular inclusions caused by non-HD polyglutamine expansions in COS-7 cells (Berger et al., 2006). Furthermore, it was demonstrated that rapamycin could clear aggregated mutant proteins in an *in vivo* Drosophila model (Berger et al., 2006). In a separate study, mutations within the collagen gene caused mutant procollagens to become misfolded and aggregate in the ER (Ishida et al., 2009). In mouse embryonic fibroblasts, activation of autophagy with ~10 µM rapamycin resulted in a reduction of aggregated procollagen trimers in the ER (Ishida et al., 2009).

The above examples demonstrate that rapamycin is able to promote the clearance of toxic aggregates from cells. Although aggregated mutant MC4R was observed when heterologously expressed in neuronal SK-N-SH cells, in HEK 293 cells misfolded MC4R does not seem to become aggregated in the cytosol or ER, and intracellularly retained MC4R does not seem to result in cell death and therefore is not toxic to HEK 293 cells. This may explain why

rapamycin is not as effective in this MC4R model compared to other published studies. In addition, different readouts were utilised to measure the reduction of toxic aggregates, however these were not used in this study. Therefore similar to soluble human misfolded α-antitrypsin Z variant, the majority of MC4R could be degraded by endoplasmic reticulum associated degradation (ERAD) rather than macroautophagy, reserving macroautophagy solely for the clearance of aggregated misfolded proteins localised in the cytosol (Kruse et al., 2006).

6.4.2 Resveratrol

Resveratrol did not increase the proportion of WT or mutant HA-MC4R trafficking to the cell surface after 24 or 48 hours treatment.

The concentrations of resveratrol used in this study are comparable to those used in other *in vitro* models. For example, Transthyretin (TTR) is a tetrameric protein that can dissociate into amyloidogenic monomers. Engineered monomeric M-TTR, has the same tertiary structure as the subunits of the wild-type protein, but can achieve a misfolded state more easily since prior tetramer dissociation, the limiting step in the fibril formation process, is not required (Reixach et al., 2006). Resveratrol concentrations of 2 and 4 μM inhibited M-TTR-induced cytotoxicity after 5 days in human neuroblastoma IMR-32 cells (Reixach et al., 2006). It would therefore be interesting to investigate if an incubation period longer than 48 hours, with resveratrol, would have a more dramatic effect on mutant MC4R folding.

In a separate study the, human neuroblastoma SK-N-BE cell line, expressing aggregated proteins such as amyloid β-peptide (Aβ42), associated with AD or α-synuclein peptide (α-syn A30P), associated with Parkinson's disease was treated with resveratrol. The study showed that 15 μM resveratrol protected the cells from the toxicity caused by the cellular aggregates (Albani et al., 2009). However, as no obvious cellular aggregated MC4R was observed in HEK 293

cells this may explain why incubation with resveratrol did not dramatically affect mutant MC4R cellular levels.

A resveratrol concentration of 10 µM has also been shown to cause cell cycle arrest and proliferation inhibition via induction of unfolded protein response (UPR) in the human leukemia K562 cell line after 24 hours of treatment (Liu et al., 2010). In this MC4R model a small reduction in the proportion of MC4R trafficking to the cell surface was observed after 48 hours of 1-10 µM resveratrol treatment. Similar to the K562 cell line, resveratrol may cause HEK 293 cells to arrest in the G1 phase and result in a decrease in the overall rate of protein synthesis (Liu et al., 2010).

6.4.3 MRAP

In agreement with previous research, MRAP decreases the trafficking of WT MC4R to the cell surface (Chan et al., 2009). Interestingly, MRAP is able to increase the trafficking levels of mutant HA-MC4R (S58C, P78L) and can promote the signalling of mutant HA-MC4R (P78L).

Unlike MC2R, no accessory proteins are required for the trafficking of MC4R to the cell surface. Here, MRAP may possibly be functioning as a chaperone for mutant MC4R. Other studies have shown accessory proteins interacting with other GPCRs. For example, the Dopamine receptor interacting protein 78 (DRiP78) is an accessory protein and required for the trafficking of the D1 dopamine receptor (Bermak et al., 2001). However, DRiP78 has demonstrated to have a role in the trafficking of AT1 angiotensin II receptors and M2 muscarinic acetylcholine receptors to the cell surface (Leclerc et al., 2002). Furthermore, DRiP78 also plays a role as a molecular chaperone in the assembly of the G protein subunits Gβ/γ by protecting Gγ from degradation until it associates appropriately with the Gβ subunit (Dupre et al., 2007).

As the total cellular levels of mutant MC4R improves when co-expressed with MRAP, it is reasonable to assume that MRAP may possibly stabilise mutant MC4R at the ER and prevent its degradation. Furthermore, as more mutant MC4R is also observed at the cell surface in the presence of MRAP this may indicate that MRAP not only stabilises mutant MC4R at the ER but may allow it to traffic through the secretory pathway to the cell surface. Interestingly, the effects of MRAP on mutant MC4R processing are most obvious with the more severely intracellular retained mutant HA-MC4R (P78L) used in this study and suggests that MRAP possibly enables HA-MC4R (P78L), to achieve a native conformational structure at the cell surface, enabling it to bind and become activated by MC4R agonist NDP-MSH. Although it has been shown that MRAP is a negative modulator of WT MC4R signalling (Chan et al., 2009), this data suggests that MRAP may prove to be an effective modulator of mutant MC4R signalling.

CHAPTER 7
General Discussion

7.1 Discussion

In summary a rapid throughput cell surface assay was designed to test the efficacy of compounds and molecular chaperones on the trafficking of mutant MC4R to the cell surface. A luciferase reporter assay was used in conjunction to test if an increase in levels of mutant MC4R at the cell surface, lead to an increase in MC4R functional activity. This data shows a limited effect of kosmotropes, a small positive effect with MRAP, and a role for the Hsp90/70 chaperone machineries in MC4R processing and trafficking (Table 7.1).

Table 7.1: Table to show the effects of different pharmacological agents and proteins used in this study

Pharmacological reagent	Cell surface expression level	Total cellular levels	Trafficking levels	Functional expression
DMSO	No effect	Increase (WT)	No effect	ND
TMAO	No effect	No effect	Decrease	ND
Trehalose	Increase	Increase	No effect	ND
4-PBA	Increase	Increase	Increase	Increase
Geldanamycin	Decrease	Decrease	Decrease	ND
Rapamycin	No effect	No effect	No effect	ND
Resveratrol	Decrease	Decrease	Decrease	ND
Aha1	Increase	Increase	Decrease	No effect
Hsc70	Increase	Increase	Increase	Increase
MRAP	Increase	Increase	Increase	Increase (P78L)

ND = Not determined

The work presented in this thesis indicates a limited role for the use of kosmotropes in rescuing mutant MC4R function. Although an increase in total cellular levels of mutant MC4R was observed after treatment with trehalose and 4-PBA, limited increase in the trafficking levels of the mutant receptors were quantified after 4-PBA treatment. This work would possibly benefit from treating mutant MC4R expressing cells with both 4-PBA and trehalose.

MC2R accessory protein MRAP may have a promising role in improving mutant MC4R function. The data presented in chapter 6 suggests that MRAP improves trafficking levels of only a subset of the MC4R mutations selected for this study, possibly due to their differential conformations. This suggests that MRAP is unable to interact with some of the mutants, possibly due to their folding defect preventing MRAP interaction. However, MRAP may bind to all the MC4R mutants but possibly fails to stabilise them at the ER. MRAP also improved P78L functional activity which indicates that MRAP remains bound to P78L at the cell surface, allowing P78L to adopt a conformation that enables it to interact with NDP-MSH and signal. However more experimental work would be required to determine how and where MRAP interacts with MC4R mutants. It would also be interesting to explore the effects of MRAP homolog MRAP2 on mutant MC4R processing. Interestingly, MRAP2 is expressed in the ventromedial hypothalamus in the brain (Lein et al., 2007), a site where MC4R is also expressed (Balthasar et al., 2005). MRAP2 shares 27% homology with the MRAP splice variant, MRAPα (Webb & Clark, 2010). MRAP2 may therefore bind differently to MC4R compared to MRAPα and may have the potential to improve the trafficking levels of a larger subset of MC4R ER retained mutants.

However, the most significant work presented here is the manipulation of Hsp90 and Hsc70 cellular molecular chaperone machineries to improve the signalling capability of mutant MC4R. It would be interesting to determine if the synergistic effect of Aha1/Hsc70 on increasing HA-MC4R (S58C) functional expression extends to the other MC4R mutants within this cohort. In this study the

manipulation of cytosolic chaperones on endoplasmic reticulum (ER) retained mutant MC4R was investigated. ER chaperones should also modulate MC4R processing. For example, ER chaperones calnexin, calreticulin and BiP have been shown to interact with a number of GPCRs including angiotensin II type 1 receptor (AT1R), thyrotropin receptor and luteinizing hormone receptor (LHR) (Dong et al., 2007). It would therefore be interesting to compare the effects of ER chaperones to cytosolic chaperones. It has been shown that intracellular retained proteins can associate with different chaperones compared to their cognate WT proteins, due to the intracellular proteins being exposed to different chaperone networks involved in degradation (Mizrachi & Segaloff, 2004). For the glycoprotein hormone receptors, which are structurally related GPCRs, ER retained mutant forms of the protein were found to be associated with BiP (Mizrachi & Segaloff, 2004). It has been demonstrated that when antisense genes for the ER chaperone BiP were introduced into CHO cells, a 2-3 fold increase in the amount of variant protein was secreted from the cells rather than remaining ER retained (Welch, 2004). However, global knockdown of an important molecular chaperone involved in protein folding and quality control may in fact be detrimental to the cell. The approach of manipulating key chaperones via their co-chaperones may possibly prove to be a better alternative. As a member of the Hsp70 protein family, a number of proteins that stimulate BiP's ATPase activity have been identified, including nucleotide exchange factor (NEF) BAP (Chung et al., 2002), and ER DNAJ homologues, ERdj1 (Chevalier et al., 2000), ERdj3 (Shen & Hendershot, 2005), ERdj4 (Shen et al., 2002), ERdj5 (Ushioda et al., 2008). Either silencing of these co-chaperones or over-expression may prove to be an effective approach at rescuing the function of misfolded proteins. Alternatively, BiP inducers such as BiP inducer X (BIX) have been shown to prevent neuronal cell death by ER stress through pretreatment of neuroblastoma cells with BIX (Kudo et al., 2008). If the same approach was used against misfolded proteins, that possibly cause ER stress, it would be interesting to see if an increase in cell surface expression of the aberrantly folded proteins would be observed.

Therefore it would be interesting to test if ER stress was induced by MC4R misfolding mutants by measuring the transcriptional levels of ER stress markers such as BiP (Gething, 1999) or CHOP (Kaufman, 1999) and to test any reduction in their levels upon treatment with the compounds used in this study.

As a complex metabolic disorder, obesity contributes to a number of other complications (e.g. insulin resistance and diabetes) and has been associated with low grade chronic inflammation, characterised by elevated levels of inflammation markers (Bastard et al., 2000). Further studies have implicated c-Jun N-terminal kinase (JNK) activation as a mediator of insulin resistance and have shown ER stress as a potential mechanism leading to JNK activation and insulin resistance in obese animal models (Hotamisligil et al., 2005). Some of the compounds utilised in this study have been used to alleviate ER stress and/or treat insulin resistance in obese mice.

For example Ozcan et al (2006) have demonstrated that treatment of obese and diabetic mice with, 4-PBA, resulted in normalisation of hyperglycemia, restoration of systemic insulin sensitivity, resolution of fatty liver disease, and enhancement of insulin action in liver, muscle and adipose tissues. In summary, they established 4-PBA as a potential therapeutic agent for the treatment of type 2 diabetes (Ozcan et al., 2006). More recently, Ozcan et al (2009) have shown that 4-PBA can also act as a leptin-sensitising agent and may be used as a novel treatment for obesity. For high fat diet-induced obese mice, administration of leptin resulted in an initial reduction in body weight but this weight loss was rapidly regained. However, pretreatment of these mice with 4-PBA resulted in a significant weight loss thus increasing leptin sensitivity (Ozcan et al., 2009). This indicates that 4-PBA may target several different pathways in obesity. It is therefore important that it also targets MC4R folding.

In another example, research on type II diabetes and obesity, have shown that mTOR may have a role to play in the development of insulin resistance and obesity (Harrington et al., 2004; Um et al., 2004). Work carried out by Harrington et al

(2004) indicated that protein kinase S6K1, positively regulated by mTOR, inactivates insulin receptor substrate (IRS) function, by downregulation of IRS-1 transcription and via direct phosphorylation of IRS-1 (Harrington et al., 2004). Another study has also shown that mTOR activity may be linked to obesity (Mori et al., 2009). Mice with deleted Tsc1, an upstream inhibitory regulator of mTOR signaling developed hyperphagia and obesity. These mice displayed increased mTOR signaling and enlarged neuronal cell size, including POMC neurons (Mori et al., 2009). Treatment with rapamycin (autophagy inducer) ameliorated the hyperphagia and obesity phenotypes (Mori et al., 2009). In a separate study, although administration of rapamycin reduced adiposity in diet-induced obese mice, long-term administration of rapamycin resulted in glucose intolerance (Chang et al., 2009).

Resveratrol has also been found to protect against metabolic disease. Acting as an activator of the protein deacetylase, SIRT1, resveratrol treated mice showed an induction of genes for oxidative phosphorylation and mitochondrial biogenesis (Lagouge et al., 2006). Treatment with resveratrol in obese high-fat diet mice improved both muscle oxidation and sensitivity to insulin (Lagouge et al., 2006). Furthermore, resveratrol treated mice had reduced fat pad mass and reduction in adipocyte size (Lagouge et al., 2006). Consistent with the above findings, resveratrol treated adipocytes displayed increased apoptosis and reduced adipogenesis, as well as upregulating the expression of genes regulating mitochondrial activity (Rayalam, 2008).

Hsp70 family member, Hsp72 has also been implicated to have a protective effect in obesity induced insulin resistance (Chung et al., 2008). Obese insulin resistant humans were shown to have reduced Hsp72 protein expression furthermore, elevated Hsp72 protein levels in skeletal muscles of mice was shown to protect against obesity-induced insulin resistance (Chung et al., 2008). This raises the interesting question of whether reduced Hsp70 in these animals could be altering MC4R processing *in vivo*.

Due to time limitations the effects of small molecular ligands on mutant MC4R trafficking were not investigated. The use of small molecular ligands in the treatment of aberrantly folded proteins is expanding and has proven successful for *in vitro* disease models of retinitis pigmentosa (Noorwez et al., 2008), nephrogenic diabetes insipidus (Morello et al., 2000; Hawtin, 2006; Robben et al., 2007), and diseases caused by mutation within the δ-opioid receptor (Leskela et al., 2007). A number of small molecular ligands have also been synthesised for MC4R, and provide new therapeutic agents against monogenic obesity (Joseph et al., 2008; Wang & Richards, 2005). Exciting data from Xiang et al (2007) demonstrated that peptides (e.g. NDP-MSH, MTII) and small molecular ligands (e.g. AMW3-130, THIQ, and AMW3-106) used at nanomolar to subnanomolar concentrations were able to rescue the functional activity of 13 human MC4R polymorphisms (Xiang et al., 2007). In addition, the MC4R inverse agonist ML00253764 has also been shown to be effective at rescuing the cell surface expression and function of MC4R intracellular retained mutants C84R and W174C (Fan & Tao, 2009).

Importantly, the success of these emerging pharmacological chaperones on rescuing function of aberrantly folded proteins may critically depend on how effectively they can bind to the mutant protein and provide a folding template for the protein to escape the cellular QCS. For the human gonadotropin-releasing hormone receptor (hGnRHR) pharmacological chaperones in two different chemical classes (Indoles and Quinolones) were able to bind to a range of mutants by stabilizing them at the ER and creating a ligand mediated bridge stabilizing the interaction between TM2 and TM3, thereby allowing the stabilised mutant protein to pass the cellular quality control system (Janovick et al., 2009). The mechanism applied by the other pharmacological reagents used in this study in stabilizing MC4R, may be similar to that applied by small molecular ligands in the hGnRHR paradigm.

The body of work described here primarily utilises heterologous expression of MC4R. Antibodies for MC4R are commercially available and protein has been

detected in astrocytes, the most abundant glial cell type in the brain (Caruso et al., 2007). However, when using the hypothalamic cell line GT1-7, where MC4R mRNA message and cAMP response to agonist stimulation has been previously shown (Buch et al., 2009); no MC4R protein was detected using commercial MC4R antibodies (abcam). This work would benefit from the production of an antibody against the N-terminus of MC4R and finding/generating a cell line with endogenous MC4R expression. This would avoid the need to employ transfections and cell lines stably expressing MC4R were the levels of MC4R expression can vary between experiments or over time.

Ultimately, animal models of MC4R point mutations should be employed to test the efficacy of emerging pharmacological reagents on MC4R signaling. To date two mice lines have been identified with MC4R point mutations, namely *fatboy* (I194T) and *southbeach* (L300P). Both mutations cause a reduction in MC4R signaling (Meehan et al., 2006). It would therefore be exciting to test if pharmacological reagents on these mice changed their fat mass by improving MC4R function.

To conclude, this study has characterised and developed a cell model that mimics the mechanism of intracellular retention of clinically occurring MC4R misfolding mutations. This has resulted in the creation of an assay that allows for the rapid identification of drugs for the treatment of monogenic obesity caused by MC4R dysfunction. Furthermore this study provides 'proof of principle' that class II MC4R mutations can be manipulated through stablisation of the mutant receptor. For the pharmacological agents tested, that proved to be effective in improving mutant MC4R function, it would be interesting to test these *in vivo* prior to potential translation into the clinic.

References

Adan,R.A., Tiesjema,B., Hillebrand,J.J., la Fleur,S.E., Kas,M.J., and de Krom,M. (2006). The MC4 receptor and control of appetite. Br. J. Pharmacol. *149*, 815-827.

Albani,D., Polito,L., Batelli,S., De Mauro,S., Fracasso,C., Martelli,G., Colombo,L., Manzoni,C., Salmona,M., Caccia,S., Negro,A., and Forloni,G. (2009). The SIRT1 activator resveratrol protects SK-N-BE cells from oxidative stress and against toxicity caused by alpha-synuclein or amyloid-beta (1-42) peptide. J. Neurochem. *110*, 1445-1456.

Alberts,B., Johnson,A., Lewis,J., Raff,M., Roberts,K., Walter,D. (2002). Molecular biology of the cell. 4th Edition.

Ancevska-Taneva,N., Onoprishvili,I., Andria,M.L., Hiller,J.M., and Simon,E.J. (2006). A member of the heat shock protein 40 family, hlj1, binds to the carboxyl tail of the human mu opioid receptor. Brain Res. *1081*, 28-33.

Arakawa,T., Ejima,D., Kita,Y., and Tsumoto,K. (2006). Small molecule pharmacological chaperones: From thermodynamic stabilization to pharmaceutical drugs. Biochim. Biophys. Acta *1764*, 1677-1687.

Balthasar,N., Dalgaard,L.T., Lee,C.E., Yu,J., Funahashi,H., Williams,T., Ferreira,M., Tang,V., McGovern,R.A., Kenny,C.D., Christiansen,L.M., Edelstein,E., Choi,B., Boss,O., Aschkenasi,C., Zhang,C.Y., Mountjoy,K., Kishi,T., Elmquist,J.K., and Lowell,B.B. (2005). Divergence of melanocortin pathways in the control of food intake and energy expenditure. Cell *123*, 493-505.

Barker,P.A. and Salehi,A. (2002). The MAGE proteins: emerging roles in cell cycle progression, apoptosis, and neurogenetic disease. J. Neurosci. Res. *67*, 705-712.

Baskakov,I.V., Kumar,R., Srinivasan,G., Ji,Y.S., Bolen,D.W., and Thompson,E.B. (1999). Trimethylamine N-oxide-induced cooperative folding of an intrinsically unfolded transcription-activating fragment of human glucocorticoid receptor. J. Biol. Chem. *274*, 10693-10696.

Bastard,J.P., Jardel,C., Bruckert,E., Vidal,H., and Hainque,B. (2000). Variations in plasma soluble tumour necrosis factor receptors after diet-induced weight loss in obesity. Diabetes Obes. Metab *2*, 323-325.

BeBoer,C. and Dietz,A. (1976). The description and antibiotic production of Streptomyces hygroscopicus var. Geldanus. J. Antibiot. (Tokyo) *29*, 1182-1188.

Bell,C.G., Walley,A.J., and Froguel,P. (2005). The genetics of human obesity. Nat. Rev. Genet. *6*, 221-234.

Ben Sefer,E., Ben Natan,M., and Ehrenfeld,M. (2009). Childhood obesity: current literature, policy and implications for practice. Int. Nurs. Rev. *56*, 166-173.

Berger,Z., Ravikumar,B., Menzies,F.M., Oroz,L.G., Underwood,B.R., Pangalos,M.N., Schmitt,I., Wullner,U., Evert,B.O., O'Kane,C.J., and Rubinsztein,D.C. (2006). Rapamycin alleviates toxicity of different aggregate-prone proteins. Hum. Mol. Genet. *15*, 433-442.

Bermak,J.C., Li,M., Bullock,C., and Zhou,Q.Y. (2001). Regulation of transport of the dopamine D1 receptor by a new membrane-associated ER protein. Nat. Cell Biol. *3*, 492-498.

Bernier,V., Lagace,M., Lonergan,M., Arthus,M.F., Bichet,D.G., and Bouvier,M. (2004). Functional rescue of the constitutively internalized V2 vasopressin receptor mutant R137H by the pharmacological chaperone action of SR49059. Mol. Endocrinol. *18*, 2074-2084.

Biebermann,H., Krude,H., Elsner,A., Chubanov,V., Gudermann,T., and Gruters,A. (2003). Autosomal-dominant mode of inheritance of a melanocortin-4 receptor mutation in a patient with severe early-onset obesity is due to a dominant-negative effect caused by receptor dimerization. Diabetes *52*, 2984-2988.

Boyault,C., Zhang,Y., Fritah,S., Caron,C., Gilquin,B., Kwon,S.H., Garrido,C., Yao,T.P., Vourc'h,C., Matthias,P., and Khochbin,S. (2007). HDAC6 controls major cell response pathways to cytotoxic accumulation of protein aggregates. Genes Dev. *21*, 2172-2181.

Breit,A., Wolff,K., Kalwa,H., Jarry,H., Buch,T., and Gudermann,T. (2006). The natural inverse agonist agouti-related protein induces arrestin-mediated endocytosis of melanocortin-3 and -4 receptors. J. Biol. Chem. *281*, 37447-37456.

Brown,B.L., Albano,J.D., Ekins,R.P., and Sgherzi,A.M. (1971). A simple and sensitive saturation assay method for the measurement of adenosine 3':5'-cyclic monophosphate. Biochem. J. *121*, 561-562.

Brown,C.R., Hong-Brown,L.Q., Biwersi,J., Verkman,A.S., and Welch,W.J. (1996). Chemical chaperones correct the mutant phenotype of the delta F508 cystic fibrosis transmembrane conductance regulator protein. Cell Stress. Chaperones. *1*, 117-125.

Buch,T.R., Heling,D., Damm,E., Gudermann,T., and Breit,A. (2009). Pertussis toxin-sensitive signaling of melanocortin-4 receptors in hypothalamic GT1-7 cells defines agouti-related protein as a biased agonist. J. Biol. Chem. *284*, 26411-26420.

Bukau,B., Weissman,J., and Horwich,A. (2006). Molecular chaperones and protein quality control. Cell *125*, 443-451.

Burrows,J.A., Willis,L.K., and Perlmutter,D.H. (2000). Chemical chaperones mediate increased secretion of mutant alpha 1-antitrypsin (alpha 1-AT) Z: A

potential pharmacological strategy for prevention of liver injury and emphysema in alpha 1-AT deficiency. Proc. Natl. Acad. Sci. U. S. A *97*, 1796-1801.

Butler,A.A. (2006). The melanocortin system and energy balance. Peptides *27*, 281-290.

Calton,M.A., Ersoy,B.A., Zhang,S., Kane,J.P., Malloy,M.J., Pullinger,C.R., Bromberg,Y., Pennacchio,L.A., Dent,R., McPherson,R., Ahituv,N., and Vaisse,C. (2009). Association of functionally significant Melanocortin-4 but not Melanocortin-3 receptor mutations with severe adult obesity in a large North American case-control study. Hum. Mol. Genet. *18*, 1140-1147.

Caruso,C., Durand,D., Schioth,H.B., Rey,R., Seilicovich,A., and Lasaga,M. (2007). Activation of melanocortin 4 receptors reduces the inflammatory response and prevents apoptosis induced by lipopolysaccharide and interferon-gamma in astrocytes. Endocrinology *148*, 4918-4926.

Chagnon,Y.C., Chen,W.J., Perusse,L., Chagnon,M., Nadeau,A., Wilkison,W.O., and Bouchard,C. (1997). Linkage and association studies between the melanocortin receptors 4 and 5 genes and obesity-related phenotypes in the Quebec Family Study. Mol. Med. *3*, 663-673.

Chambers,J.C., Elliott,P., Zabaneh,D., Zhang,W., Li,Y., Froguel,P., Balding,D., Scott,J., and Kooner,J.S. (2008). Common genetic variation near MC4R is associated with waist circumference and insulin resistance. Nat. Genet. *40*, 716-718.

Chan,L.F., Webb,T.R., Chung,T.T., Meimaridou,E., Cooray,S.N., Guasti,L., Chapple,J.P., Egertova,M., Elphick,M.R., Cheetham,M.E., Metherell,L.A., and Clark,A.J. (2009). MRAP and MRAP2 are bidirectional regulators of the melanocortin receptor family. Proc. Natl. Acad. Sci. U. S. A *106*, 6146-6151.

Chang,G.R., Wu,Y.Y., Chiu,Y.S., Chen,W.Y., Liao,J.W., Hsu,H.M., Chao,T.H., Hung,S.W., and Mao,F.C. (2009). Long-term administration of rapamycin reduces adiposity, but impairs glucose tolerance in high-fat diet-fed KK/HlJ mice. Basic Clin. Pharmacol. Toxicol. *105*, 188-198.

Chapple,J.P. and Cheetham,M.E. (2003). The chaperone environment at the cytoplasmic face of the endoplasmic reticulum can modulate rhodopsin processing and inclusion formation. J. Biol. Chem. *278*, 19087-19094.

Chaudhuri,T.K. and Paul,S. (2006). Protein-misfolding diseases and chaperone-based therapeutic approaches. FEBS J. *273*, 1331-1349.

Chen,S. and Smith,D.F. (1998). Hop as an adaptor in the heat shock protein 70 (Hsp70) and hsp90 chaperone machinery. J. Biol. Chem. *273*, 35194-35200.

Chevalier,M., Rhee,H., Elguindi,E.C., and Blond,S.Y. (2000). Interaction of murine BiP/GRP78 with the DnaJ homologue MTJ1. J. Biol. Chem. *275*, 19620-19627.

Chini,B. and Parenti,M. (2009). G-protein-coupled receptors, cholesterol and palmitoylation: facts about fats. J. Mol. Endocrinol. *42*, 371-379.

Choo-Kang,L.R. and Zeitlin,P.L. (2001). Induction of HSP70 promotes DeltaF508 CFTR trafficking. Am. J. Physiol Lung Cell Mol. Physiol *281*, L58-L68.

Chung,J., Nguyen,A.K., Henstridge,D.C., Holmes,A.G., Chan,M.H., Mesa,J.L., Lancaster,G.I., Southgate,R.J., Bruce,C.R., Duffy,S.J., Horvath,I., Mestril,R., Watt,M.J., Hooper,P.L., Kingwell,B.A., Vigh,L., Hevener,A., and Febbraio,M.A. (2008). HSP72 protects against obesity-induced insulin resistance. Proc. Natl. Acad. Sci. U. S. A *105*, 1739-1744.

Chung,K.T., Shen,Y., and Hendershot,L.M. (2002). BAP, a mammalian BiP-associated protein, is a nucleotide exchange factor that regulates the ATPase activity of BiP. J. Biol. Chem. *277*, 47557-47563.

Cohen,F.E. and Kelly,J.W. (2003). Therapeutic approaches to protein-misfolding diseases. Nature *426*, 905-909.

Conn,P.M. and Ulloa-Aguirre,A. (2010). Trafficking of G-protein-coupled receptors to the plasma membrane: insights for pharmacoperone drugs. Trends Endocrinol. Metab *21*, 190-197.

Cuervo,A.M. (2010). Chaperone-mediated autophagy: selectivity pays off. Trends Endocrinol. Metab *21*, 142-150.

Cummings,D.E., Clement,K., Purnell,J.Q., Vaisse,C., Foster,K.E., Frayo,R.S., Schwartz,M.W., Basdevant,A., and Weigle,D.S. (2002). Elevated plasma ghrelin levels in Prader Willi syndrome. Nat. Med. *8*, 643-644.

Davenport,J.R., Watts,A.J., Roper,V.C., Croyle,M.J., van Groen,T., Wyss,J.M., Nagy,T.R., Kesterson,R.A., and Yoder,B.K. (2007). Disruption of intraflagellar transport in adult mice leads to obesity and slow-onset cystic kidney disease. Curr. Biol. *17*, 1586-1594.

Davies,J.E., Sarkar,S., and Rubinsztein,D.C. (2006). Trehalose reduces aggregate formation and delays pathology in a transgenic mouse model of oculopharyngeal muscular dystrophy. Hum. Mol. Genet. *15*, 23-31.

de Almeida,S.F., Picarote,G., Fleming,J.V., Carmo-Fonseca,M., Azevedo,J.E., and de Sousa,M. (2007). Chemical chaperones reduce endoplasmic reticulum stress and prevent mutant HFE aggregate formation. J. Biol. Chem. *282*, 27905-27912.

De Maio,A. (1999). Heat shock proteins: facts, thoughts, and dreams. Shock *11*, 1-12.

Diaz-Troya,S., Perez-Perez,M.E., Florencio,F.J., and Crespo,J.L. (2008). The role of TOR in autophagy regulation from yeast to plants and mammals. Autophagy. *4*, 851-865.

Dong,C., Filipeanu,C.M., Duvernay,M.T., and Wu,G. (2007). Regulation of G protein-coupled receptor export trafficking. Biochim. Biophys. Acta *1768*, 853-870.

Dubern,B., Clement,K., Pelloux,V., Froguel,P., Girardet,J.P., Guy-Grand,B., and Tounian,P. (2001). Mutational analysis of melanocortin-4 receptor, agouti-related protein, and alpha-melanocyte-stimulating hormone genes in severely obese children. J. Pediatr. *139*, 204-209.

Dupre,D.J., Robitaille,M., Richer,M., Ethier,N., Mamarbachi,A.M., and Hebert,T.E. (2007). Dopamine receptor-interacting protein 78 acts as a molecular chaperone for Ggamma subunits before assembly with Gbeta. J. Biol. Chem. *282*, 13703-13715.

Duvernay,M.T., Filipeanu,C.M., and Wu,G. (2005). The regulatory mechanisms of export trafficking of G protein-coupled receptors. Cell Signal. *17*, 1457-1465.

Ellis,R.J. (2006). Protein folding: inside the cage. Nature *442*, 360-362.

Elsner,A., Tarnow,P., Schaefer,M., Ambrugger,P., Krude,H., Gruters,A., and Biebermann,H. (2006). MC4R oligomerizes independently of extracellular cysteine residues. Peptides *27*, 372-379.

Fan,Z.C. and Tao,Y.X. (2009). Functional characterization and pharmacological rescue of melanocortin-4 receptor mutations identified from obese patients. J. Cell Mol. Med. *13*, 3268-3282.

Farooqi,I.S., Yeo,G.S., Keogh,J.M., Aminian,S., Jebb,S.A., Butler,G., Cheetham,T., and O'Rahilly,S. (2000). Dominant and recessive inheritance of morbid obesity associated with melanocortin 4 receptor deficiency. J. Clin. Invest *106*, 271-279.

Farooqi,I.S., Keogh,J.M., Yeo,G.S., Lank,E.J., Cheetham,T., and O'Rahilly,S. (2003). Clinical spectrum of obesity and mutations in the melanocortin 4 receptor gene. N. Engl. J. Med. *348*, 1085-1095.

Farooqi,I.S. and O'Rahilly,S. (2009). Leptin: a pivotal regulator of human energy homeostasis. Am. J. Clin. Nutr. *89*, 980S-984S.

Fischer,J., Koch,L., Emmerling,C., Vierkotten,J., Peters,T., Bruning,J.C., and Ruther,U. (2009). Inactivation of the Fto gene protects from obesity. Nature *458*, 894-898.

Fowkes,R.C., Desclozeaux,M., Patel,M.V., Aylwin,S.J., King,P., Ingraham,H.A., and Burrin,J.M. (2003). Steroidogenic factor-1 and the gonadotrope-specific element enhance basal and pituitary adenylate cyclase-activating polypeptide-

stimulated transcription of the human glycoprotein hormone alpha-subunit gene in gonadotropes. Mol. Endocrinol. *17*, 2177-2188.

Frayling,T.M., Timpson,N.J., Weedon,M.N., Zeggini,E., Freathy,R.M., Lindgren,C.M., Perry,J.R., Elliott,K.S., Lango,H., Rayner,N.W., Shields,B., Harries,L.W., Barrett,J.C., Ellard,S., Groves,C.J., Knight,B., Patch,A.M., Ness,A.R., Ebrahim,S., Lawlor,D.A., Ring,S.M., Ben Shlomo,Y., Jarvelin,M.R., Sovio,U., Bennett,A.J., Melzer,D., Ferrucci,L., Loos,R.J., Barroso,I., Wareham,N.J., Karpe,F., Owen,K.R., Cardon,L.R., Walker,M., Hitman,G.A., Palmer,C.N., Doney,A.S., Morris,A.D., Smith,G.D., Hattersley,A.T., and McCarthy,M.I. (2007). A common variant in the FTO gene is associated with body mass index and predisposes to childhood and adult obesity. Science *316*, 889-894.

Gantz,I., Miwa,H., Konda,Y., Shimoto,Y., Tashiro,T., Watson,S.J., DelValle,J., and Yamada,T. (1993). Molecular cloning, expression, and gene localization of a fourth melanocortin receptor. J. Biol. Chem. *268* , 15174-15179.

Gao,Q.B. and Wang,Z.Z. (2006). Classification of G-protein coupled receptors at four levels. Protein Eng Des Sel *19*, 511-516.

Gao,Z., Lei,D., Welch,J., Le,K., Lin,J., Leng,S., and Duhl,D. (2003). Agonist-dependent internalization of the human melanocortin-4 receptors in human embryonic kidney 293 cells. J. Pharmacol. Exp. Ther. *307* , 870-877.

Gardiner,K., Slavov,D., Bechtel,L., and Davisson,M. (2002). Annotation of human chromosome 21 for relevance to Down syndrome: gene structure and expression analysis. Genomics *79*, 833-843.

Gekko,K. and Timasheff,S.N. (1981). Mechanism of protein stabilization by glycerol: preferential hydration in glycerol-water mixtures. Biochemistry *20*, 4667-4676.

Gething,M.J. (1999). Role and regulation of the ER chaperone BiP. Semin. Cell Dev. Biol. *10*, 465-472.

Gurevich,V.V. and Gurevich,E.V. (2008). GPCR monomers and oligomers: it takes all kinds. Trends Neurosci. *31*, 74-81.

Hageman,J., Vos,M.J., van Waarde,M.A., and Kampinga,H.H. (2007). Comparison of intra-organellar chaperone capacity for dealing with stress-induced protein unfolding. J. Biol. Chem. *282*, 34334-34345.

Hamma,T. and Ferre-D'Amare,A.R. (2010). The box H/ACA ribonucleoprotein complex: interplay of RNA and protein structures in post-transcriptional RNA modification. J. Biol. Chem. *285*, 805-809.

Hansen,S.H., Sandvig,K., and van Deurs,B. (1993). Molecules internalized by clathrin-independent endocytosis are delivered to endosomes containing transferrin receptors. J. Cell Biol. *123*, 89-97.

Harrington,L.S., Findlay,G.M., Gray,A., Tolkacheva,T., Wigfield,S., Rebholz,H., Barnett,J., Leslie,N.R., Cheng,S., Shepherd,P.R., Gout,I., Downes,C.P., and Lamb,R.F. (2004). The TSC1-2 tumor suppressor controls insulin-PI3K signaling via regulation of IRS proteins. J. Cell Biol. *166*, 213-223.

Harville,H.M., Held,S., Diaz-Font,A., Davis,E.E., Diplas,B.H., Lewis,R.A., Borochowitz,Z.U., Zhou,W., Chaki,M., MacDonald,J., Kayserili,H., Beales,P.L., Katsanis,N., Otto,E., and Hildebrandt,F. (2010). Identification of 11 novel mutations in eight BBS genes by high-resolution homozygosity mapping. J. Med. Genet. *47*, 262-267.

Hawtin,S.R. (2006). Pharmacological chaperone activity of SR49059 to functionally recover misfolded mutations of the vasopressin V1a receptor. J. Biol. Chem. *281*, 14604-14614.

Heard-Costa,N.L., Zillikens,M.C., Monda,K.L., Johansson,A., Harris,T.B., Fu,M., Haritunians,T., Feitosa,M.F., Aspelund,T., Eiriksdottir,G., Garcia,M., Launer,L.J., Smith,A.V., Mitchell,B.D., McArdle,P.F., Shuldiner,A.R., Bielinski,S.J., Boerwinkle,E., Brancati,F., Demerath,E.W., Pankow,J.S., Arnold,A.M., Chen,Y.D., Glazer,N.L., McKnight,B., Psaty,B.M., Rotter,J.I., Amin,N., Campbell,H., Gyllensten,U., Pattaro,C., Pramstaller,P.P., Rudan,I., Struchalin,M., Vitart,V., Gao,X., Kraja,A., Province,M.A., Zhang,Q., Atwood,L.D., Dupuis,J., Hirschhorn,J.N., Jaquish,C.E., O'Donnell,C.J., Vasan,R.S., White,C.C., Aulchenko,Y.S., Estrada,K., Hofman,A., Rivadeneira,F., Uitterlinden,A.G., Witteman,J.C., Oostra,B.A., Kaplan,R.C., Gudnason,V., O'Connell,J.R., Borecki,I.B., Van Duijn,C.M., Cupples,L.A., Fox,C.S., and North,K.E. (2009). NRXN3 is a novel locus for waist circumference: a genome-wide association study from the CHARGE Consortium. PLoS. Genet. *5*, e1000539.

Hegde,N.R., Chevalier,M.S., Wisner,T.W., Denton,M.C., Shire,K., Frappier,L., and Johnson,D.C. (2006). The role of BiP in endoplasmic reticulum-associated degradation of major histocompatibility complex class I heavy chain induced by cytomegalovirus proteins. J. Biol. Chem. *281*, 20910-20919.

Hinney,A., Schmidt,A., Nottebom,K., Heibult,O., Becker,I., Ziegler,A., Gerber,G., Sina,M., Gorg,T., Mayer,H., Siegfried,W., Fichter,M., Remschmidt,H., and Hebebrand,J. (1999). Several mutations in the melanocortin-4 receptor gene including a nonsense and a frameshift mutation associated with dominantly inherited obesity in humans. J. Clin. Endocrinol. Metab *84*, 1483-1486.

Hinney,A. and Hebebrand,J. (2009). Three at one swoop! Obes. Facts. *2*, 3-8.

Hofmann,K.P., Scheerer,P., Hildebrand,P.W., Choe,H.W., Park,J.H., Heck,M., and Ernst,O.P. (2009). A G protein-coupled receptor at work: the rhodopsin model. Trends Biochem. Sci. *34*, 540-552.

Holmes,J.L., Sharp,S.Y., Hobbs,S., and Workman,P. (2008). Silencing of HSP90 cochaperone AHA1 expression decreases client protein activation and increases cellular sensitivity to the HSP90 inhibitor 17-allylamino-17-demethoxygeldanamycin. Cancer Res. *68*, 1188-1197.

Hotamisligil,G.S. (2005). Role of endoplasmic reticulum stress and c-Jun NH2-terminal kinase pathways in inflammation and origin of obesity and diabetes. Diabetes *54 Suppl 2*, S73-S78.

Huszar,D., Lynch,C.A., Fairchild-Huntress,V., Dunmore,J.H., Fang,Q., Berkemeier,L.R., Gu,W., Kesterson,R.A., Boston,B.A., Cone,R.D., Smith,F.J., Campfield,L.A., Burn,P., and Lee,F. (1997). Targeted disruption of the melanocortin-4 receptor results in obesity in mice. Cell *88*, 131-141.

Ichihara,S. and Yamada,Y. (2008). Genetic factors for human obesity. Cell Mol. Life Sci. *65*, 1086-1098.

Ignatova,Z. and Gierasch,L.M. (2006). Inhibition of protein aggregation in vitro and in vivo by a natural osmoprotectant. Proc. Natl. Acad. Sci. U. S. A *103*, 13357-13361.

Imai,Y., Soda,M., Hatakeyama,S., Akagi,T., Hashikawa,T., Nakayama,K.I., and Takahashi,R. (2002). CHIP is associated with Parkin, a gene responsible for familial Parkinson's disease, and enhances its ubiquitin ligase activity. Mol. Cell *10*, 55-67.

Ishida,Y. and Nagata,K. (2009). Autophagy eliminates a specific species of misfolded procollagen and plays a protective role in cell survival against ER stress. Autophagy. *5*, 1217-1219.

Jalink,K. and Moolenaar,W.H. (2010). G protein-coupled receptors: the inside story. Bioessays *32*, 13-16.

Janovick,J.A., Patny,A., Mosley,R., Goulet,M.T., Altman,M.D., Rush,T.S., III, Cornea,A., and Conn,P.M. (2009). Molecular mechanism of action of pharmacoperone rescue of misrouted GPCR mutants: the GnRH receptor. Mol. Endocrinol. *23*, 157-168.

Johnston,J.A., Ward,C.L., and Kopito,R.R. (1998). Aggresomes: a cellular response to misfolded proteins. J. Cell Biol. *143*, 1883-1898.

Joseph,C.G., Wilson,K.R., Wood,M.S., Sorenson,N.B., Phan,D.V., Xiang,Z., Witek,R.M., and Haskell-Luevano,C. (2008). The 1,4-benzodiazepine-2,5-dione

small molecule template results in melanocortin receptor agonists with nanomolar potencies. J. Med. Chem. *51*, 1423-1431.

Kaufman,R.J. (1999). Stress signaling from the lumen of the endoplasmic reticulum: coordination of gene transcriptional and translational controls. Genes Dev. *13*, 1211-1233.

Kobilka,B.K. (2007). G protein coupled receptor structure and activation.

Biochim. Biophys. Acta. *1768*, 794-807.

Koulov,A.V., LaPointe,P., Lu,B., Razvi,A., Coppinger,J., Dong,M.Q., Matteson,J., Laister,R., Arrowsmith,C., Yates,J.R., III, and Balch,W.E. (2010). Biological and structural basis for Aha1 regulation of Hsp90 ATPase activity in maintaining proteostasis in the human disease cystic fibrosis. Mol. Biol. Cell *21*, 871-884.

Kovacs,J.J., Hara,M.R., Davenport,C.L., Kim,J., and Lefkowitz,R.J. (2009). Arrestin development: emerging roles for beta-arrestins in developmental signaling pathways. Dev. Cell *17*, 443-458.

Kruse,K.B., Brodsky,J.L., and McCracken,A.A. (2006). Characterization of an ERAD gene as VPS30/ATG6 reveals two alternative and functionally distinct protein quality control pathways: one for soluble Z variant of human alpha-1 proteinase inhibitor (A1PiZ) and another for aggregates of A1PiZ. Mol. Biol. Cell *17*, 203-212.

Kudo,T., Kanemoto,S., Hara,H., Morimoto,N., Morihara,T., Kimura,R., Tabira,T., Imaizumi,K., and Takeda,M. (2008). A molecular chaperone inducer protects neurons from ER stress. Cell Death. Differ. *15*, 364-375.

Kwon,H.M., Kim,Y.J., Ryu,S., Yang,S.I., Lee,S.H., and Yoon,B.W. (2009). Differential expression of HSP70 mRNA in the mouse brain after treatment with geldanamycin. Neurol. Res. *31*, 541-544.

Lagouge,M., Argmann,C., Gerhart-Hines,Z., Meziane,H., Lerin,C., Daussin,F., Messadeq,N., Milne,J., Lambert,P., Elliott,P., Geny,B., Laakso,M., Puigserver,P., and Auwerx,J. (2006). Resveratrol improves mitochondrial function and protects against metabolic disease by activating SIRT1 and PGC-1alpha. Cell *127*, 1109-1122.

Lanctot,P.M., Leclerc,P.C., Escher,E., Leduc,R., and Guillemette,G. (1999). Role of N-glycosylation in the expression and functional properties of human AT1 receptor. Biochemistry *38*, 8621-8627.

Lanctot,P.M., Leclerc,P.C., Clement,M., Auger-Messier,M., Escher,E., Leduc,R., and Guillemette,G. (2005). Importance of N-glycosylation positioning for cell-

surface expression, targeting, affinity and quality control of the human AT1 receptor. Biochem. J. *390*, 367-376.

Lasaga,M., Debeljuk,L., Durand,D., Scimonelli,T.N., and Caruso,C. (2008). Role of alpha-melanocyte stimulating hormone and melanocortin 4 receptor in brain inflammation. Peptides *29*, 1825-1835.

Leanos-Miranda,A., Ulloa-Aguirre,A., Janovick,J.A., and Conn,P.M. (2005). In vitro coexpression and pharmacological rescue of mutant gonadotropin-releasing hormone receptors causing hypogonadotropic hypogonadism in humans expressing compound heterozygous alleles. J. Clin. Endocrinol. Metab *90*, 3001-3008.

Leclerc,P.C., Auger-Messier,M., Lanctot,P.M., Escher,E., Leduc,R., and Guillemette,G. (2002). A polyaromatic caveolin-binding-like motif in the cytoplasmic tail of the type 1 receptor for angiotensin II plays an important role in receptor trafficking and signaling. Endocrinology *143*, 4702-4710.

Lee,Y.S., Poh,L.K., Kek,B.L., and Loke,K.Y. (2008). Novel melanocortin 4 receptor gene mutations in severely obese children. Clin. Endocrinol. (Oxf) *68*, 529-535.

Lein,E.S., Hawrylycz,M.J., Ao,N., Ayres,M., Bensinger,A., Bernard,A., Boe,A.F., Boguski,M.S., Brockway,K.S., Byrnes,E.J., Chen,L., Chen,L., Chen,T.M., Chin,M.C., Chong,J., Crook,B.E., Czaplinska,A., Dang,C.N., Datta,S., Dee,N.R., Desaki,A.L., Desta,T., Diep,E., Dolbeare,T.A., Donelan,M.J., Dong,H.W., Dougherty,J.G., Duncan,B.J., Ebbert,A.J., Eichele,G., Estin,L.K., Faber,C., Facer,B.A., Fields,R., Fischer,S.R., Fliss,T.P., Frensley,C., Gates,S.N., Glattfelder,K.J., Halverson,K.R., Hart,M.R., Hohmann,J.G., Howell,M.P., Jeung,D.P., Johnson,R.A., Karr,P.T., Kawal,R., Kidney,J.M., Knapik,R.H., Kuan,C.L., Lake,J.H., Laramee,A.R., Larsen,K.D., Lau,C., Lemon,T.A., Liang,A.J., Liu,Y., Luong,L.T., Michaels,J., Morgan,J.J., Morgan,R.J., Mortrud,M.T., Mosqueda,N.F., Ng,L.L., Ng,R., Orta,G.J., Overly,C.C., Pak,T.H., Parry,S.E., Pathak,S.D., Pearson,O.C., Puchalski,R.B., Riley,Z.L., Rockett,H.R., Rowland,S.A., Royall,J.J., Ruiz,M.J., Sarno,N.R., Schaffnit,K., Shapovalova,N.V., Sivisay,T., Slaughterbeck,C.R., Smith,S.C., Smith,K.A., Smith,B.I., Sodt,A.J., Stewart,N.N., Stumpf,K.R., Sunkin,S.M., Sutram,M., Tam,A., Teemer,C.D., Thaller,C., Thompson,C.L., Varnam,L.R., Visel,A., Whitlock,R.M., Wohnoutka,P.E., Wolkey,C.K., Wong,V.Y., Wood,M., Yaylaoglu,M.B., Young,R.C., Youngstrom,B.L., Yuan,X.F., Zhang,B., Zwingman,T.A., and Jones,A.R. (2007). Genome-wide atlas of gene expression in the adult mouse brain. Nature *445*, 168-176.

Leskela,T.T., Markkanen,P.M., Pietila,E.M., Tuusa,J.T., and Petaja-Repo,U.E. (2007). Opioid receptor pharmacological chaperones act by binding and stabilizing newly synthesized receptors in the endoplasmic reticulum. J. Biol. Chem. *282*, 23171-23183.

Liu,B.Q., Gao,Y.Y., Niu,X.F., Xie,J.S., Meng,X., Guan,Y., and Wang,H.Q. (2010). Implication of unfolded protein response in resveratrol-induced inhibition of K562 cell proliferation. Biochem. Biophys. Res. Commun. *391*, 778-782.

Liu,C.Y. and Kaufman,R.J. (2003). The unfolded protein response. J. Cell Sci. *116*, 1861-1862.

Liu,Y.Z., Pei,Y.F., Liu,J.F., Yang,F., Guo,Y., Zhang,L., Liu,X.G., Yan,H., Wang,L., Zhang,Y.P., Levy,S., Recker,R.R., and Deng,H.W. (2009). Powerful bivariate genome-wide association analyses suggest the SOX6 gene influencing both obesity and osteoporosis phenotypes in males. PLoS. One. *4*, e6827.

Loo,M.A., Jensen,T.J., Cui,L., Hou,Y., Chang,X.B., and Riordan,J.R. (1998). Perturbation of Hsp90 interaction with nascent CFTR prevents its maturation and accelerates its degradation by the proteasome. EMBO J. *17*, 6879-6887.

Loos,R.J., Lindgren,C.M., Li,S., Wheeler,E., Zhao,J.H., Prokopenko,I., Inouye,M., Freathy,R.M., Attwood,A.P., Beckmann,J.S., Berndt,S.I., Jacobs,K.B., Chanock,S.J., Hayes,R.B., Bergmann,S., Bennett,A.J., Bingham,S.A., Bochud,M., Brown,M., Cauchi,S., Connell,J.M., Cooper,C., Smith,G.D., Day,I., Dina,C., De,S., Dermitzakis,E.T., Doney,A.S., Elliott,K.S., Elliott,P., Evans,D.M., Sadaf,F., I, Froguel,P., Ghori,J., Groves,C.J., Gwilliam,R., Hadley,D., Hall,A.S., Hattersley,A.T., Hebebrand,J., Heid,I.M., Lamina,C., Gieger,C., Illig,T., Meitinger,T., Wichmann,H.E., Herrera,B., Hinney,A., Hunt,S.E., Jarvelin,M.R., Johnson,T., Jolley,J.D., Karpe,F., Keniry,A., Khaw,K.T., Luben,R.N., Mangino,M., Marchini,J., McArdle,W.L., McGinnis,R., Meyre,D., Munroe,P.B., Morris,A.D., Ness,A.R., Neville,M.J., Nica,A.C., Ong,K.K., O'Rahilly,S., Owen,K.R., Palmer,C.N., Papadakis,K., Potter,S., Pouta,A., Qi,L., Randall,J.C., Rayner,N.W., Ring,S.M., Sandhu,M.S., Scherag,A., Sims,M.A., Song,K., Soranzo,N., Speliotes,E.K., Syddall,H.E., Teichmann,S.A., Timpson,N.J., Tobias,J.H., Uda,M., Vogel,C.I., Wallace,C., Waterworth,D.M., Weedon,M.N., Willer,C.J., Wraight, Yuan,X., Zeggini,E., Hirschhorn,J.N., Strachan,D.P., Ouwehand,W.H., Caulfield,M.J., Samani,N.J., Frayling,T.M., Vollenweider,P., Waeber,G., Mooser,V., Deloukas,P., McCarthy,M.I., Wareham,N.J., Barroso,I., Jacobs,K.B., Chanock,S.J., Hayes,R.B., Lamina,C., Gieger,C., Illig,T., Meitinger,T., Wichmann,H.E., Kraft,P., Hankinson,S.E., Hunter,D.J., Hu,F.B., Lyon,H.N., Voight,B.F., Ridderstrale,M., Groop,L., Scheet,P., Sanna,S., Abecasis,G.R., Albai,G., Nagaraja,R., Schlessinger,D., Jackson,A.U., Tuomilehto,J., Collins,F.S., Boehnke,M., and Mohlke,K.L. (2008). Common variants near MC4R are associated with fat mass, weight and risk of obesity. Nat. Genet. *40*, 768-775.

Lotz,G.P., Lin,H., Harst,A., and Obermann,W.M. (2003). Aha1 binds to the middle domain of Hsp90, contributes to client protein activation, and stimulates the ATPase activity of the molecular chaperone. J. Biol. Chem. *278*, 17228-17235.

Lu,M., Echeverri,F., and Moyer,B.D. (2003). Endoplasmic reticulum retention, degradation, and aggregation of olfactory G-protein coupled receptors. Traffic. *4*, 416-433.

Lubrano-Berthelier,C., Durand,E., Dubern,B., Shapiro,A., Dazin,P., Weill,J., Ferron,C., Froguel,P., and Vaisse,C. (2003). Intracellular retention is a common characteristic of childhood obesity-associated MC4R mutations. Hum. Mol. Genet. *12*, 145-153.

Marcos-Carcavilla,A., Calvo,J.H., Gonzalez,C., Moazami-Goudarzi,K., Laurent,P., Bertaud,M., Hayes,H., Beattie,A.E., Serrano,C., Lyahyai,J., Martin-Burriel,I., and Serrano,M. (2008). Structural and functional analysis of the HSP90AA1 gene: distribution of polymorphisms among sheep with different responses to scrapie. Cell Stress. Chaperones. *13*, 19-29.

Martinez-Vicente,M. and Cuervo,A.M. (2007). Autophagy and neurodegeneration: when the cleaning crew goes on strike. Lancet Neurol. *6*, 352-361.

McLean,P.J., Klucken,J., Shin,Y., and Hyman,B.T. (2004). Geldanamycin induces Hsp70 and prevents alpha-synuclein aggregation and toxicity in vitro. Biochem. Biophys. Res. Commun. *321*, 665-669.

Meacham,G.C., Lu,Z., King,S., Sorscher,E., Tousson,A., and Cyr,D.M. (1999). The Hdj-2/Hsc70 chaperone pair facilitates early steps in CFTR biogenesis. EMBO J. *18*, 1492-1505.

Meacham,G.C., Patterson,C., Zhang,W., Younger,J.M., and Cyr,D.M. (2001). The Hsc70 co-chaperone CHIP targets immature CFTR for proteasomal degradation. Nat. Cell Biol. *3*, 100-105.

Meehan,T.P., Tabeta,K., Du,X., Woodward,L.S., Firozi,K., Beutler,B., and Justice,M.J. (2006). Point mutations in the melanocortin-4 receptor cause variable obesity in mice. Mamm. Genome *17*, 1162-1171.

Meimaridou,E., Gooljar,S.B., and Chapple,J.P. (2009). From hatching to dispatching: the multiple cellular roles of the Hsp70 molecular chaperone machinery. J. Mol. Endocrinol. *42*, 1-9.

Mendes,H.F. and Cheetham,M.E. (2008). Pharmacological manipulation of gain-of-function and dominant-negative mechanisms in rhodopsin retinitis pigmentosa. Hum. Mol. Genet. *17*, 3043-3054.

Metherell,L.A., Chapple,J.P., Cooray,S., David,A., Becker,C., Ruschendorf,F., Naville,D., Begeot,M., Khoo,B., Nurnberg,P., Huebner,A., Cheetham,M.E., and Clark,A.J. (2005). Mutations in MRAP, encoding a new interacting partner of the ACTH receptor, cause familial glucocorticoid deficiency type 2. Nat. Genet. *37*, 166-170.

Meyer,P., Prodromou,C., Hu,B., Vaughan,C., Roe,S.M., Panaretou,B., Piper,P.W., and Pearl,L.H. (2003). Structural and functional analysis of the middle segment of hsp90: implications for ATP hydrolysis and client protein and cochaperone interactions. Mol. Cell *11*, 647-658.

Meyre,D., Delplanque,J., Chevre,J.C., Lecoeur,C., Lobbens,S., Gallina,S., Durand,E., Vatin,V., Degraeve,F., Proenca,C., Gaget,S., Korner,A., Kovacs,P., Kiess,W., Tichet,J., Marre,M., Hartikainen,A.L., Horber,F., Potoczna,N., Hercberg,S., Levy-Marchal,C., Pattou,F., Heude,B., Tauber,M., McCarthy,M.I., Blakemore,A.I., Montpetit,A., Polychronakos,C., Weill,J., Coin,L.J., Asher,J., Elliott,P., Jarvelin,M.R., Visvikis-Siest,S., Balkau,B., Sladek,R., Balding,D., Walley,A., Dina,C., and Froguel,P. (2009). Genome-wide association study for early-onset and morbid adult obesity identifies three new risk loci in European populations. Nat. Genet. *41*, 157-159.

Milligan,G. (2008). A day in the life of a G protein-coupled receptor: the contribution to function of G protein-coupled receptor dimerization. Br. J. Pharmacol. *153 Suppl 1*, S216-S229.

Milligan,G. (2010). The role of dimerisation in the cellular trafficking of G-protein-coupled receptors. Curr. Opin. Pharmacol. *10*, 23-29.

Mizrachi,D. and Segaloff,D.L. (2004). Intracellularly located misfolded glycoprotein hormone receptors associate with different chaperone proteins than their cognate wild-type receptors. Mol. Endocrinol. *18*, 1768-1777.

Mok,C.A., Heon,E., and Zhen,M. (2010). Ciliary dysfunction and obesity. Clin. Genet. *77*, 18-27.

Montague,C.T., Farooqi,I.S., Whitehead,J.P., Soos,M.A., Rau,H., Wareham,N.J., Sewter,C.P., Digby,J.E., Mohammed,S.N., Hurst,J.A., Cheetham,C.H., Earley,A.R., Barnett,A.H., Prins,J.B., and O'Rahilly,S. (1997). Congenital leptin deficiency is associated with severe early-onset obesity in humans. Nature *387*, 903-908.

Morello,J.P., Salahpour,A., Laperriere,A., Bernier,V., Arthus,M.F., Lonergan,M., Petaja-Repo,U., Angers,S., Morin,D., Bichet,D.G., and Bouvier,M. (2000). Pharmacological chaperones rescue cell-surface expression and function of misfolded V2 vasopressin receptor mutants. J. Clin. Invest *105*, 887-895.

Mori,H., Inoki,K., Masutani,K., Wakabayashi,Y., Komai,K., Nakagawa,R., Guan,K.L., and Yoshimura,A. (2009). The mTOR pathway is highly activated in diabetic nephropathy and rapamycin has a strong therapeutic potential. Biochem. Biophys. Res. Commun. *384*, 471-475.

Morimoto,R.I. (2002). Dynamic remodeling of transcription complexes by molecular chaperones. Cell *110*, 281-284.

Mutch,D.M. and Clement,K. (2006). Unraveling the genetics of human obesity. PLoS. Genet. *2*, e188.

Naidoo,N. (2009). ER and aging-Protein folding and the ER stress response. Ageing Res. Rev. *8*, 150-159.

Nakatogawa,H., Suzuki,K., Kamada,Y., and Ohsumi,Y. (2009). Dynamics and diversity in autophagy mechanisms: lessons from yeast. Nat. Rev. Mol. Cell Biol. *10*, 458-467.

Nargund,R.P., Strack,A.M., and Fong,T.M. (2006). Melanocortin-4 receptor (MC4R) agonists for the treatment of obesity. J. Med. Chem. *49*, 4035-4043.

Ni,M. and Lee,A.S. (2007). ER chaperones in mammalian development and human diseases. FEBS Lett. *581*, 3641-3651.

Nijenhuis,W.A., Garner,K.M., van Rozen,R.J., and Adan,R.A. (2003). Poor cell surface expression of human melanocortin-4 receptor mutations associated with obesity. J. Biol. Chem. *278*, 22939-22945.

Noon,L.A., Franklin,J.M., King,P.J., Goulding,N.J., Hunyady,L., and Clark,A.J. (2002). Failed export of the adrenocorticotrophin receptor from the endoplasmic reticulum in non-adrenal cells: evidence in support of a requirement for a specific adrenal accessory factor. J. Endocrinol. *174* , 17-25.

Noorwez,S.M., Ostrov,D.A., McDowell,J.H., Krebs,M.P., and Kaushal,S. (2008). A high-throughput screening method for small-molecule pharmacologic chaperones of misfolded rhodopsin. Invest Ophthalmol. Vis. Sci. *49*, 3224-3230.

Obermann,W.M., Sondermann,H., Russo,A.A., Pavletich,N.P., and Hartl,F.U. (1998). In vivo function of Hsp90 is dependent on ATP binding and ATP hydrolysis. J. Cell Biol. *143*, 901-910.

Okumiya,T., Kroos,M.A., Vliet,L.V., Takeuchi,H., Van der Ploeg,A.T., and Reuser,A.J. (2007). Chemical chaperones improve transport and enhance stability of mutant alpha-glucosidases in glycogen storage disease type II. Mol. Genet. Metab *90*, 49-57.

Oswal,A. and Yeo,G.S. (2007). The leptin melanocortin pathway and the control of body weight: lessons from human and murine genetics. Obes. Rev. *8*, 293-306.

Ozcan,L., Ergin,A.S., Lu,A., Chung,J., Sarkar,S., Nie,D., Myers,M.G., Jr., and Ozcan,U. (2009). Endoplasmic reticulum stress plays a central role in development of leptin resistance. Cell Metab *9*, 35-51.

Ozcan,U., Yilmaz,E., Ozcan,L., Furuhashi,M., Vaillancourt,E., Smith,R.O., Gorgun,C.Z., and Hotamisligil,G.S. (2006). Chemical chaperones reduce ER stress

and restore glucose homeostasis in a mouse model of type 2 diabetes. Science *313*, 1137-1140.

Palczewski,K., Kumasaka,T., Hori,T., Behnke,C.A., Motoshima,H., Fox,B.A., Le,T., I, Teller,D.C., Okada,T., Stenkamp,R.E., Yamamoto,M., and Miyano,M. (2000). Crystal structure of rhodopsin: A G protein-coupled receptor. Science *289*, 739-745.

Panaretou,B., Prodromou,C., Roe,S.M., O'Brien,R., Ladbury,J.E., Piper,P.W., and Pearl,L.H. (1998). ATP binding and hydrolysis are essential to the function of the Hsp90 molecular chaperone in vivo. EMBO J. *17*, 4829-4836.

Panaretou,B., Siligardi,G., Meyer,P., Maloney,A., Sullivan,J.K., Singh,S., Millson,S.H., Clarke,P.A., Naaby-Hansen,S., Stein,R., Cramer,R., Mollapour,M., Workman,P., Piper,P.W., Pearl,L.H., and Prodromou,C. (2002). Activation of the ATPase activity of hsp90 by the stress-regulated cochaperone aha1. Mol. Cell *10*, 1307-1318.

Papp,E. and Csermely,P. (2006). Chemical chaperones: mechanisms of action and potential use. Handb. Exp. Pharmacol. 405-416.

Pearl,L.H., Prodromou,C., and Workman,P. (2008). The Hsp90 molecular chaperone: an open and shut case for treatment. Biochem. J. *410*, 439-453.

Powers,E.T., Morimoto,R.I., Dillin,A., Kelly,J.W., and Balch,W.E. (2009). Biological and chemical approaches to diseases of proteostasis deficiency. Annu. Rev. Biochem. *78*, 959-991.

Prodromou,C., Roe,S.M., O'Brien,R., Ladbury,J.E., Piper,P.W., and Pearl,L.H. (1997). Identification and structural characterization of the ATP/ADP-binding site in the Hsp90 molecular chaperone. Cell *90*, 65-75.

Qanbar,R. and Bouvier,M. (2003). Role of palmitoylation/depalmitoylation reactions in G-protein-coupled receptor function. Pharmacol. Ther. *97*, 1-33.

Qi,X., Hosoi,T., Okuma,Y., Kaneko,M., and Nomura,Y. (2004). Sodium 4-phenylbutyrate protects against cerebral ischemic injury. Mol. Pharmacol. *66*, 899-908.

Ramos,R.R., Swanson,A.J., and Bass,J. (2007). Calreticulin and Hsp90 stabilize the human insulin receptor and promote its mobility in the endoplasmic reticulum. Proc. Natl. Acad. Sci. U. S. A *104*, 10470-10475.

Rankinen,T., Zuberi,A., Chagnon,Y.C., Weisnagel,S.J., Argyropoulos,G., Walts,B., Perusse,L., and Bouchard,C. (2006). The human obesity gene map: the 2005 update. Obesity. (Silver. Spring) *14*, 529-644.

Rasmussen,S.G., Choi,H.J., Rosenbaum,D.M., Kobilka,T.S., Thian,F.S., Edwards,P.C., Burghammer,M., Ratnala,V.R., Sanishvili,R., Fischetti,R.F., Schertler,G.F., Weis,W.I., and Kobilka,B.K. (2007). Crystal structure of the human beta2 adrenergic G-protein-coupled receptor. Nature *450*, 383-387.

Ravikumar,B., Vacher,C., Berger,Z., Davies,J.E., Luo,S., Oroz,L.G., Scaravilli,F., Easton,D.F., Duden,R., O'Kane,C.J., and Rubinsztein,D.C. (2004). Inhibition of mTOR induces autophagy and reduces toxicity of polyglutamine expansions in fly and mouse models of Huntington disease. Nat. Genet. *36*, 585-595.

Ravikumar,B., Berger,Z., Vacher,C., O'Kane,C.J., and Rubinsztein,D.C. (2006). Rapamycin pre-treatment protects against apoptosis. Hum. Mol. Genet. *15*, 1209-1216.

Rayalam,S., Yang,J.Y., Ambati,S., Della-Fera,M.A., and Baile,C.A. (2008). Resveratrol induces apoptosis and inhibits adipogenesis in 3T3-L1 adipocytes. Phytother. Res. *22*, 1367-1371.

Reixach,N., Adamski-Werner,S.L., Kelly,J.W., Koziol,J., and Buxbaum,J.N. (2006). Cell based screening of inhibitors of transthyretin aggregation. Biochem. Biophys. Res. Commun. *348*, 889-897.

Renstrom,F., Payne,F., Nordstrom,A., Brito,E.C., Rolandsson,O., Hallmans,G., Barroso,I., Nordstrom,P., and Franks,P.W. (2009). Replication and extension of genome-wide association study results for obesity in 4923 adults from northern Sweden. Hum. Mol. Genet. *18*, 1489-1496.

Riemer,J., Bulleid,N., and Herrmann,J.M. (2009). Disulfide formation in the ER and mitochondria: two solutions to a common process. Science *324*, 1284-1287.

Ritter,S.L. and Hall,R.A. (2009). Fine-tuning of GPCR activity by receptor-interacting proteins. Nat. Rev. Mol. Cell Biol. *10*, 819-830.

Robben,J.H. and Deen,P.M. (2007). Pharmacological chaperones in nephrogenic diabetes insipidus: possibilities for clinical application. BioDrugs. *21*, 157-166.

Robert,J., Auzan,C., Ventura,M.A., and Clauser,E. (2005). Mechanisms of cell-surface rerouting of an endoplasmic reticulum-retained mutant of the vasopressin V1b/V3 receptor by a pharmacological chaperone. J. Biol. Chem. *280*, 42198-42206.

Rosenbaum,D.M., Rasmussen,S.G., and Kobilka,B.K. (2009). The structure and function of G-protein-coupled receptors. Nature *459*, 356-363.

Roy,S., Rached,M., and Gallo-Payet,N. (2007). Differential regulation of the human adrenocorticotropin receptor [melanocortin-2 receptor (MC2R)] by human MC2R accessory protein isoforms alpha and beta in isogenic human embryonic kidney 293 cells. Mol. Endocrinol. *21*, 1656-1669.

Rubinsztein,D.C. and Carmichael,J. (2003). Huntington's disease: molecular basis of neurodegeneration. Expert. Rev. Mol. Med. *5*, 1-21.

Ruddock,L.W. and Molinari,M. (2006). N-glycan processing in ER quality control. J. Cell Sci. *119*, 4373-4380.

Saliba,R.S., Munro,P.M., Luthert,P.J., and Cheetham,M.E. (2002). The cellular fate of mutant rhodopsin: quality control, degradation and aggresome formation. J. Cell Sci. *115*, 2907-2918.

Sanger,F., Nicklen,S., and Coulson,A.R. (1977). DNA sequencing with chain-terminating inhibitors. Proc. Natl. Acad. Sci. U. S. A *74*, 5463-5467.

Schmauss,C., Brines,M.L., and Lerner,M.R. (1992). The gene encoding the small nuclear ribonucleoprotein-associated protein N is expressed at high levels in neurons. J. Biol. Chem. *267*, 8521-8529.

Schnaider,T., Somogyi,J., Csermely,P., and Szamel,M. (2000). The Hsp90-specific inhibitor geldanamycin selectively disrupts kinase-mediated signaling events of T-lymphocyte activation. Cell Stress. Chaperones. *5*, 52-61.

Schulein,R., Hermosilla,R., Oksche,A., Dehe,M., Wiesner,B., Krause,G., and Rosenthal,W. (1998). A dileucine sequence and an upstream glutamate residue in the intracellular carboxyl terminus of the vasopressin V2 receptor are essential for cell surface transport in COS.M6 cells. Mol. Pharmacol. *54*, 525-535.

Segnitz,B. and Gehring,U. (1997). The function of steroid hormone receptors is inhibited by the hsp90-specific compound geldanamycin. J. Biol. Chem. *272*, 18694-18701.

Seo,S., Guo,D.F., Bugge,K., Morgan,D.A., Rahmouni,K., and Sheffield,V.C. (2009). Requirement of Bardet-Biedl syndrome proteins for leptin receptor signaling. Hum. Mol. Genet. *18*, 1323-1331.

Seo,S., Baye,L.M., Schulz,N.P., Beck,J.S., Zhang,Q., Slusarski,D.C., and Sheffield,V.C. (2010). BBS6, BBS10, and BBS12 form a complex with CCT/TRiC family chaperonins and mediate BBSome assembly. Proc. Natl. Acad. Sci. U. S. A *107*, 1488-1493.

Sevier,C.S., Qu,H., Heldman,N., Gross,E., Fass,D., and Kaiser,C.A. (2007). Modulation of cellular disulfide-bond formation and the ER redox environment by feedback regulation of Ero1. Cell *129*, 333-344.

Shen,H.Y., He,J.C., Wang,Y., Huang,Q.Y., and Chen,J.F. (2005). Geldanamycin induces heat shock protein 70 and protects against MPTP-induced dopaminergic neurotoxicity in mice. J. Biol. Chem. *280*, 39962-39969.

Shen,Y., Meunier,L., and Hendershot,L.M. (2002). Identification and characterization of a novel endoplasmic reticulum (ER) DnaJ homologue, which stimulates ATPase activity of BiP in vitro and is induced by ER stress. J. Biol. Chem. *277*, 15947-15956.

Shen,Y. and Hendershot,L.M. (2005). ERdj3, a stress-inducible endoplasmic reticulum DnaJ homologue, serves as a cofactor for BiP's interactions with unfolded substrates. Mol. Biol. Cell *16*, 40-50.

Shinyama,H., Masuzaki,H., Fang,H., and Flier,J.S. (2003). Regulation of melanocortin-4 receptor signaling: agonist-mediated desensitization and internalization. Endocrinology *144*, 1301-1314.

Singh,L.R., Chen,X., Kozich,V., and Kruger,W.D. (2007). Chemical chaperone rescue of mutant human cystathionine beta-synthase. Mol. Genet. Metab *91*, 335-342.

Sittler,A., Lurz,R., Lueder,G., Priller,J., Lehrach,H., Hayer-Hartl,M.K., Hartl,F.U., and Wanker,E.E. (2001). Geldanamycin activates a heat shock response and inhibits huntingtin aggregation in a cell culture model of Huntington's disease. Hum. Mol. Genet. *10*, 1307-1315.

Smith,D.F., Whitesell,L., Nair,S.C., Chen,S., Prapapanich,V., and Rimerman,R.A. (1995). Progesterone receptor structure and function altered by geldanamycin, an hsp90-binding agent. Mol. Cell Biol. *15*, 6804-6812.

Spooner,R.A., Hart,P.J., Cook,J.P., Pietroni,P., Rogon,C., Hohfeld,J., Roberts,L.M., and Lord,J.M. (2008). Cytosolic chaperones influence the fate of a toxin dislocated from the endoplasmic reticulum. Proc. Natl. Acad. Sci. U. S. A *105*, 17408-17413.

Srinivasan,S., Vaisse,C., and Conklin,B.R. (2003). Engineering the melanocortin-4 receptor to control G(s) signaling in vivo. Ann. N. Y. Acad. Sci. *994*, 225-232.

Stratigopoulos,G., Padilla,S.L., LeDuc,C.A., Watson,E., Hattersley,A.T., McCarthy,M.I., Zeltser,L.M., Chung,W.K., and Leibel,R.L. (2008). Regulation of Fto/Ftm gene expression in mice and humans. Am. J. Physiol Regul. Integr. Comp Physiol *294*, R1185-R1196.

Stutzmann,F., Vatin,V., Cauchi,S., Morandi,A., Jouret,B., Landt,O., Tounian,P., Levy-Marchal,C., Buzzetti,R., Pinelli,L., Balkau,B., Horber,F., Bougneres,P., Froguel,P., and Meyre,D. (2007). Non-synonymous polymorphisms in melanocortin-4 receptor protect against obesity: the two facets of a Janus obesity gene. Hum. Mol. Genet. *16*, 1837-1844.

Sun,Y., Huang,J., Xiang,Y., Bastepe,M., Juppner,H., Kobilka,B.K., Zhang,J.J., and Huang,X.Y. (2007). Dosage-dependent switch from G protein-coupled to G protein-independent signaling by a GPCR. EMBO J. *26*, 53-64.

Tamarappoo,B.K., Yang,B., and Verkman,A.S. (1999). Misfolding of mutant aquaporin-2 water channels in nephrogenic diabetes insipidus. J. Biol. Chem. *274*, 34825-34831.

Tan,K., Pogozheva,I.D., Yeo,G.S., Hadaschik,D., Keogh,J.M., Haskell-Leuvano,C., O'Rahilly,S., Mosberg,H.I., and Farooqi,I.S. (2009). Functional characterization and structural modeling of obesity associated mutations in the melanocortin 4 receptor. Endocrinology *150*, 114-125.

Tanaka,M., Machida,Y., Niu,S., Ikeda,T., Jana,N.R., Doi,H., Kurosawa,M., Nekooki,M., and Nukina,N. (2004). Trehalose alleviates polyglutamine-mediated pathology in a mouse model of Huntington disease. Nat. Med. *10*, 148-154.

Tansky,M.F., Pothoulakis,C., and Leeman,S.E. (2007). Functional consequences of alteration of N-linked glycosylation sites on the neurokinin 1 receptor. Proc. Natl. Acad. Sci. U. S. A *104*, 10691-10696.

Tao,Y.X. and Segaloff,D.L. (2003). Functional characterization of melanocortin-4 receptor mutations associated with childhood obesity. Endocrinology *144*, 4544-4551.

Tao,Y.X. (2005). Molecular mechanisms of the neural melanocortin receptor dysfunction in severe early onset obesity. Mol. Cell Endocrinol. *239*, 1-14.

Tao,Y.X. (2010). The Melanocortin-4 Receptor: Physiology, Pharmacology, and Pathophysiology. Endocr. Rev.

Tarnow,P., Schoneberg,T., Krude,H., Gruters,A., and Biebermann,H. (2003). Mutationally induced disulfide bond formation within the third extracellular loop causes melanocortin 4 receptor inactivation in patients with obesity. J. Biol. Chem. *278*, 48666-48673.

Tatro,J.B. (1996). Receptor biology of the melanocortins, a family of neuroimmunomodulatory peptides. Neuroimmunomodulation. *3*, 259-284.

Thomas,M., Harrell,J.M., Morishima,Y., Peng,H.M., Pratt,W.B., and Lieberman,A.P. (2006). Pharmacologic and genetic inhibition of hsp90-dependent trafficking reduces aggregation and promotes degradation of the expanded glutamine androgen receptor without stress protein induction. Hum. Mol. Genet. *15*, 1876-1883.

Thorleifsson,G., Walters,G.B., Gudbjartsson,D.F., Steinthorsdottir,V., Sulem,P., Helgadottir,A., Styrkarsdottir,U., Gretarsdottir,S., Thorlacius,S., Jonsdottir,I., Jonsdottir,T., Olafsdottir,E.J., Olafsdottir,G.H., Jonsson,T., Jonsson,F., Borch-Johnsen,K., Hansen,T., Andersen,G., Jorgensen,T., Lauritzen,T., Aben,K.K., Verbeek,A.L., Roeleveld,N., Kampman,E., Yanek,L.R., Becker,L.C., Tryggvadottir,L., Rafnar,T., Becker,D.M., Gulcher,J., Kiemeney,L.A., Pedersen,O., Kong,A., Thorsteinsdottir,U., and Stefansson,K. (2009). Genome-wide association

yields new sequence variants at seven loci that associate with measures of obesity. Nat. Genet. *41*, 18-24.

Tobin,A.B., Butcher,A.J., and Kong,K.C. (2008). Location, location, location...site-specific GPCR phosphorylation offers a mechanism for cell-type-specific signalling. Trends Pharmacol. Sci. *29*, 413-420.

Tobin,A.B. (2008). G-protein-coupled receptor phosphorylation: where, when and by whom. Br. J. Pharmacol. *153 Suppl 1*, S167-S176.

Tveten,K., Holla,O.L., Ranheim,T., Berge,K.E., Leren,T.P., and Kulseth,M.A. (2007). 4-Phenylbutyrate restores the functionality of a misfolded mutant low-density lipoprotein receptor. FEBS J. *274*, 1881-1893.

Ulloa-Aguirre,A., Janovick,J.A., Brothers,S.P., and Conn,P.M. (2004). Pharmacologic rescue of conformationally-defective proteins: implications for the treatment of human disease. Traffic. *5*, 821-837.

Um,S.H., Frigerio,F., Watanabe,M., Picard,F., Joaquin,M., Sticker,M., Fumagalli,S., Allegrini,P.R., Kozma,S.C., Auwerx,J., and Thomas,G. (2004). Absence of S6K1 protects against age- and diet-induced obesity while enhancing insulin sensitivity. Nature *431*, 200-205.

Ushioda,R., Hoseki,J., Araki,K., Jansen,G., Thomas,D.Y., and Nagata,K. (2008). ERdj5 is required as a disulfide reductase for degradation of misfolded proteins in the ER. Science *321*, 569-572.

Vaisse,C., Clement,K., Guy-Grand,B., and Froguel,P. (1998). A frameshift mutation in human MC4R is associated with a dominant form of obesity. Nat. Genet. *20*, 113-114.

Vaisse,C., Clement,K., Durand,E., Hercberg,S., Guy-Grand,B., and Froguel,P. (2000). Melanocortin-4 receptor mutations are a frequent and heterogeneous cause of morbid obesity. J. Clin. Invest *106*, 253-262.

VanLeeuwen,D., Steffey,M.E., Donahue,C., Ho,G., and MacKenzie,R.G. (2003). Cell surface expression of the melanocortin-4 receptor is dependent on a C-terminal di-isoleucine sequence at codons 316/317. J. Biol. Chem. *278*, 15935-15940.

Vembar,S.S. and Brodsky,J.L. (2008). One step at a time: endoplasmic reticulum-associated degradation. Nat. Rev. Mol. Cell Biol. *9*, 944-957.

Waelter,S., Boeddrich,A., Lurz,R., Scherzinger,E., Lueder,G., Lehrach,H., and Wanker,E.E. (2001). Accumulation of mutant huntingtin fragments in aggresome-like inclusion bodies as a result of insufficient protein degradation. Mol. Biol. Cell *12*, 1393-1407.

Walley,A.J., Blakemore,A.I., and Froguel,P. (2006). Genetics of obesity and the prediction of risk for health. Hum. Mol. Genet. *15 Spec No 2*, R124-R130.

Wang,D., Ma,J., Zhang,S., Hinney,A., Hebebrand,J., Wang,Y., and Wang,H.J. (2010). Association of the MC4R V103I polymorphism with obesity: a Chinese Case-control study and meta-analysis in 55,195 individuals. Obesity. (Silver. Spring) *18*, 573-579.

Wang,X. and Richards,N.G. (2005). Computer-based strategy for modeling the interaction of AGRP and related peptide ligands with the AGRP-binding site of murine melanocortin receptors. Curr. Pharm. Des *11*, 345-356.

Wang,X., Venable,J., LaPointe,P., Hutt,D.M., Koulov,A.V., Coppinger,J., Gurkan,C., Kellner,W., Matteson,J., Plutner,H., Riordan,J.R., Kelly,J.W., Yates,J.R., III, and Balch,W.E. (2006). Hsp90 cochaperone Aha1 downregulation rescues misfolding of CFTR in cystic fibrosis. Cell *127*, 803-815.

Webb,T.R., Chan,L., Cooray,S.N., Cheetham,M.E., Chapple,J.P., and Clark,A.J. (2009). Distinct melanocortin 2 receptor accessory protein domains are required for melanocortin 2 receptor interaction and promotion of receptor trafficking. Endocrinology *150*, 720-726.

Webb,T.R. and Clark,A.J. (2010). Minireview: the melanocortin 2 receptor accessory proteins. Mol. Endocrinol. *24*, 475-484.

Wegele,H., Muller,L., and Buchner,J. (2004). Hsp70 and Hsp90--a relay team for protein folding. Rev. Physiol Biochem. Pharmacol. *151*, 1-44.

Welch,W.J. (2004). Role of quality control pathways in human diseases involving protein misfolding. Semin. Cell Dev. Biol. *15*, 31-38.

Westerheide,S.D. and Morimoto,R.I. (2005). Heat shock response modulators as therapeutic tools for diseases of protein conformation. J. Biol. Chem. *280*, 33097-33100.

Willer,C.J., Speliotes,E.K., Loos,R.J., Li,S., Lindgren,C.M., Heid,I.M., Berndt,S.I., Elliott,A.L., Jackson,A.U., Lamina,C., Lettre,G., Lim,N., Lyon,H.N., McCarroll,S.A., Papadakis,K., Qi,L., Randall,J.C., Roccasecca,R.M., Sanna,S., Scheet,P., Weedon,M.N., Wheeler,E., Zhao,J.H., Jacobs,L.C., Prokopenko,I., Soranzo,N., Tanaka,T., Timpson,N.J., Almgren,P., Bennett,A., Bergman,R.N., Bingham,S.A., Bonnycastle,L.L., Brown,M., Burtt,N.P., Chines,P., Coin,L., Collins,F.S., Connell,J.M., Cooper,C., Smith,G.D., Dennison,E.M., Deodhar,P., Elliott,P., Erdos,M.R., Estrada,K., Evans,D.M., Gianniny,L., Gieger,C., Gillson,C.J., Guiducci,C., Hackett,R., Hadley,D., Hall,A.S., Havulinna,A.S., Hebebrand,J., Hofman,A., Isomaa,B., Jacobs,K.B., Johnson,T., Jousilahti,P., Jovanovic,Z., Khaw,K.T., Kraft,P., Kuokkanen,M., Kuusisto,J., Laitinen,J., Lakatta,E.G., Luan,J., Luben,R.N., Mangino,M., McArdle,W.L., Meitinger,T., Mulas,A., Munroe,P.B., Narisu,N., Ness,A.R., Northstone,K., O'Rahilly,S., Purmann,C., Rees,M.G.,

Ridderstrale,M., Ring,S.M., Rivadeneira,F., Ruokonen,A., Sandhu,M.S., Saramies,J., Scott,L.J., Scuteri,A., Silander,K., Sims,M.A., Song,K., Stephens,J., Stevens,S., Stringham,H.M., Tung,Y.C., Valle,T.T., Van Duijn,C.M., Vimaleswaran,K.S., Vollenweider,P., Waeber,G., Wallace,C., Watanabe,R.M., Waterworth,D.M., Watkins,N., Witteman,J.C., Zeggini,E., Zhai,G., Zillikens,M.C., Altshuler,D., Caulfield,M.J., Chanock,S.J., Farooqi,I.S., Ferrucci,L., Guralnik,J.M., Hattersley,A.T., Hu,F.B., Jarvelin,M.R., Laakso,M., Mooser,V., Ong,K.K., Ouwehand,W.H., Salomaa,V., Samani,N.J., Spector,T.D., Tuomi,T., Tuomilehto,J., Uda,M., Uitterlinden,A.G., Wareham,N.J., Deloukas,P., Frayling,T.M., Groop,L.C., Hayes,R.B., Hunter,D.J., Mohlke,K.L., Peltonen,L., Schlessinger,D., Strachan,D.P., Wichmann,H.E., McCarthy,M.I., Boehnke,M., Barroso,I., Abecasis,G.R., and Hirschhorn,J.N. (2009). Six new loci associated with body mass index highlight a neuronal influence on body weight regulation. Nat. Genet. *41*, 25-34.

Winslow,A.R. and Rubinsztein,D.C. (2008). Autophagy in neurodegeneration and development. Biochim. Biophys. Acta *1782*, 723-729.

Wong,W. and Minchin,R.F. (1996). Binding and internalization of the melanocyte stimulating hormone receptor ligand [Nle4, D-Phe7] alpha-MSH in B16 melanoma cells. Int. J. Biochem. Cell Biol. *28*, 1223-1232.

Wright,J.M., Zeitlin,P.L., Cebotaru,L., Guggino,S.E., and Guggino,W.B. (2004). Gene expression profile analysis of 4-phenylbutyrate treatment of IB3-1 bronchial epithelial cell line demonstrates a major influence on heat-shock proteins. Physiol Genomics *16*, 204-211.

Wu,W.C., Kao,Y.H., Hu,P.S., and Chen,J.H. (2007). Geldanamycin, a HSP90 inhibitor, attenuates the hypoxia-induced vascular endothelial growth factor expression in retinal pigment epithelium cells in vitro. Exp. Eye Res. *85*, 721-731.

Xiang,Z., Litherland,S.A., Sorensen,N.B., Proneth,B., Wood,M.S., Shaw,A.M., Millard,W.J., and Haskell-Luevano,C. (2006). Pharmacological characterization of 40 human melanocortin-4 receptor polymorphisms with the endogenous proopiomelanocortin-derived agonists and the agouti-related protein (AGRP) antagonist. Biochemistry *45*, 7277-7288.

Xiang,Z., Pogozheva,I.D., Sorenson,N.B., Wilczynski,A.M., Holder,J.R., Litherland,S.A., Millard,W.J., Mosberg,H.I., and Haskell-Luevano,C. (2007). Peptide and small molecules rescue the functional activity and agonist potency of dysfunctional human melanocortin-4 receptor polymorphisms. Biochemistry *46*, 8273-8287.

Yam,G.H., Roth,J., and Zuber,C. (2007). 4-Phenylbutyrate rescues trafficking incompetent mutant alpha-galactosidase A without restoring its functionality. Biochem. Biophys. Res. Commun. *360*, 375-380.

Yang,D.S., Yip,C.M., Huang,T.H., Chakrabartty,A., and Fraser,P.E. (1999). Manipulating the amyloid-beta aggregation pathway with chemical chaperones. J. Biol. Chem. *274*, 32970-32974.

Yeo,G.S., Farooqi,I.S., Aminian,S., Halsall,D.J., Stanhope,R.G., and O'Rahilly,S. (1998). A frameshift mutation in MC4R associated with dominantly inherited human obesity. Nat. Genet. *20*, 111-112.

Yeo,G.S., Lank,E.J., Farooqi,I.S., Keogh,J., Challis,B.G., and O'Rahilly,S. (2003). Mutations in the human melanocortin-4 receptor gene associated with severe familial obesity disrupts receptor function through multiple molecular mechanisms. Hum. Mol. Genet. *12*, 561-574.

Young,J.C., Barral,J.M., and Ulrich,H.F. (2003). More than folding: localized functions of cytosolic chaperones. Trends Biochem. Sci. *28*, 541-547.

Younger,J.M., Chen,L., Ren,H.Y., Rosser,M.F., Turnbull,E.L., Fan,C.Y., Patterson,C., and Cyr,D.M. (2006). Sequential quality-control checkpoints triage misfolded cystic fibrosis transmembrane conductance regulator. Cell *126*, 571-582.

Yurugi-Kobayashi,T., Asada,H., Shiroishi,M., Shimamura,T., Funamoto,S., Katsuta,N., Ito,K., Sugawara,T., Tokuda,N., Tsujimoto,H., Murata,T., Nomura,N., Haga,K., Haga,T., Iwata,S., and Kobayashi,T. (2009). Comparison of functional non-glycosylated GPCRs expression in Pichia pastoris. Biochem. Biophys. Res. Commun. *380*, 271-276.

Zhang,Y., Proenca,R., Maffei,M., Barone,M., Leopold,L., and Friedman,J.M. (1994). Positional cloning of the mouse obese gene and its human homologue. Nature *372*, 425-432.

Zobel,D.P., Andreasen,C.H., Grarup,N., Eiberg,H., Sorensen,T.I., Sandbaek,A., Lauritzen,T., Borch-Johnsen,K., Jorgensen,T., Pedersen,O., and Hansen,T. (2009). Variants near MC4R are associated with obesity and influence obesity-related quantitative traits in a population of middle-aged people: studies of 14,940 Danes. Diabetes *58*, 757-764.

Zoghbi,H.Y. and Orr,H.T. (2000). Glutamine repeats and neurodegeneration. Annu. Rev. Neurosci. *23*, 217-247.

Appendix

1. Laboratory Equipment

General

Water purification system

Purite Select Analyst HP50 (Purite Ltd, UK)

Water baths

Grant JB1 and SE10 (Grant instruments Ltd, UK)

Ice machine

Scotsman AF 10 ASB 2700 (Scotsman Ice Systems, Italy)

Centrifuges

Sorvall Cooling centrifuge legend RT (Thermal scientific, USA)
Eppendorf Cooling centrifuge 5804R (Eppendorf, UK)
Micro Centaur microcentrifuge (MSE, UK)

Balances

B30015 balance (Mettler Toledo, UK)

Micro balance AB54 (Mettler Toledo, UK)

Ultra micro balance UMX2 (Mettler Toledo, UK)

pH meter

Mettler Delta 320 (Mettler Toledo Ltd, UK)

DNA/RNA

PCR machines

GeneAmp PCR system 2400 (PE Biosystems, UK)
GeneAmp PCR system 9700 (PE Biosystems, UK)

Electrophoresis tanks

Mini-Sub Cell GT (Bio-Rad Laboratories Ltd, UK)

Wide Mini-Sub Cell GT (Bio-Rad Laboratories Ltd, UK)

Electrophoresis power supply units

Atto AE3105 (Genetic Research Instruments, UK)
GIBCO BRL 400L (Life Technologies Ltd, UK)
LKM Bromma 2197 (LKB Instruments Ltd, UK)

Spectrophotometer

GeneQuant RNA/DNA Calculator (Pharmacia Biotech, UK)
NanoDrop ND1000 spectrophotometer (NanoDrop Technologies, USA)

Ultraviolet transilluminator
UVP20 (UVP, CA, USA)
UVIdoc (UVItec Ltd, UK)

Proteins and tissues

Homogeniser

Precellys 24 tissue homogeniser (Bertin Technologies, France)

Microtome

Rotary microtome RM2145 (Leica Microsystems Ltd, UK)

Western blotting equipment
Mini PROTEAN 3 electrophoresis apparatus (Bio-Rad Laboratories Ltd, UK)
Mini Trans-Blot® Electrophoretic Transfer Cell (Bio-Rad Laboratories Ltd, UK)
Semi-dry blotter: Trans-Blot SD semidry transfer cell (Bio-Rad Laboratories Ltd, UK)

Protein imaging/quantification
Compact X4 automatic film processor (Xonograph Imaging Systems, UK)

Odyssey Infrared Imaging System with Li-COR Odyssey Software 2.1 (Li-COR BioSciences Ltd, UK)

UVmax kinetic microplate reader (Molecular devices, USA)

Cell work

Laminar flow cabinet

Envair MSCII (Envair Ltd, UK)

Microscopes

Nikon Eclipse TS100 with Nikon C-SHG fluorescene observation device (Nikon Instruments, Netherlands)

Leic DMIL with DC 200 digital camera system (Leic Microsystems, UK)

LSM 510 confocal laser scanning microscope (Carl Zeiss Ltd, UK)

Liquid nitrogen storage

Cryolab25 (Statebourne Cryogenics, UK)

Cell culture incubator

CO_2 research incubator (LEEC Ltd, UK)

Assays

Liquid Scintillation counter

Wallac 1409 DSA (Perkin Elmer, UK)

Fluorescence Polarization microplate reader

POLARstar Omega (BMG Labtech, Germany)

2. Commercial Peptides

NDP-MSH (H-1100, Bachem, Switzerland)

Ac-Ser-Tyr-Ser-Nle-Glu-His-D-Phe-Arg-Trp-Gly-Lys-Pro-Val-NH_2

ACTH[1-39] (human) (H-1160, Bachem, Switzerland)

H-Ser-Tyr-Ser-Met-Glu-His-Phe-Arg-Trp-Gly-Lys-Pro-Val-Gly-Lys-Lys-Arg-Arg-Pro-Val-Lys-Val-Tyr-Pro-Asn-Gly-Ala-Glu-Asp-Glu-Ser-Ala-Glu-Ala-Phe-Pro-Leu-Glu-Phe-OH

3. Vector Maps

pcDNA3.1(+) Vector Map (Invitrogen Ltd, UK)

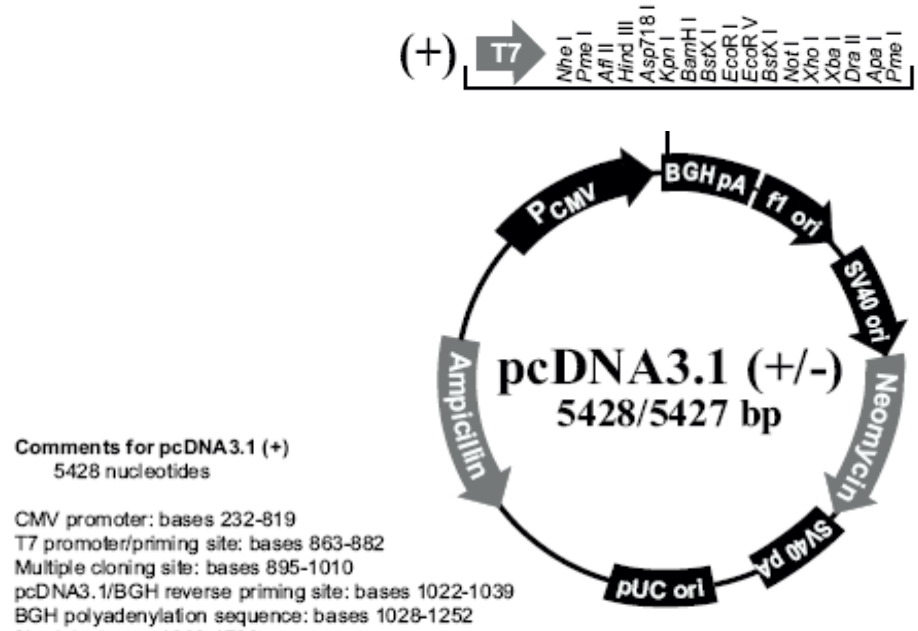

Comments for pcDNA3.1 (+)
5428 nucleotides

CMV promoter: bases 232-819
T7 promoter/priming site: bases 863-882
Multiple cloning site: bases 895-1010
pcDNA3.1/BGH reverse priming site: bases 1022-1039
BGH polyadenylation sequence: bases 1028-1252
f1 origin: bases 1298-1726
SV40 early promoter and origin: bases 1731-2074
Neomycin resistance gene (ORF): bases 2136-2930
SV40 early polyadenylation signal: bases 3104-3234
pUC origin: bases 3617-4287 (complementary strand)
Ampicillin resistance gene (*bla*): bases 4432-5428 (complementary strand)
ORF: bases 4432-5292 (complementary strand)
Ribosome binding site: bases 5300-5304 (complementary strand)
bla promoter (P3): bases 5327-5333 (complementary strand)

pGEM®-T Easy Vector Map (Promega)

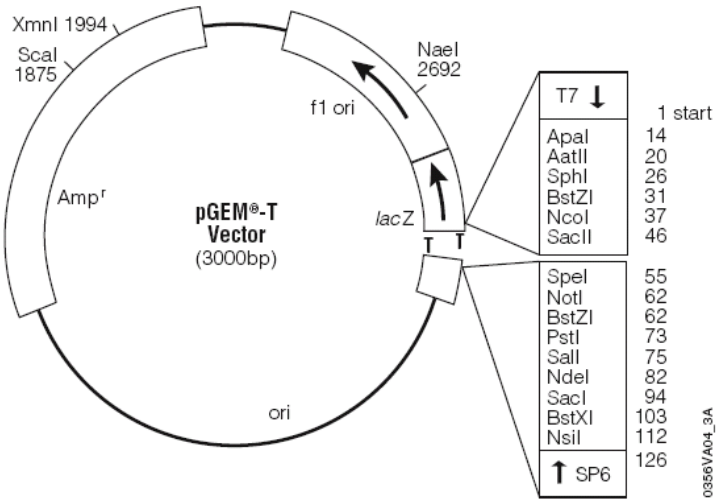

pEGFP-N1 vector map (Clonetech)

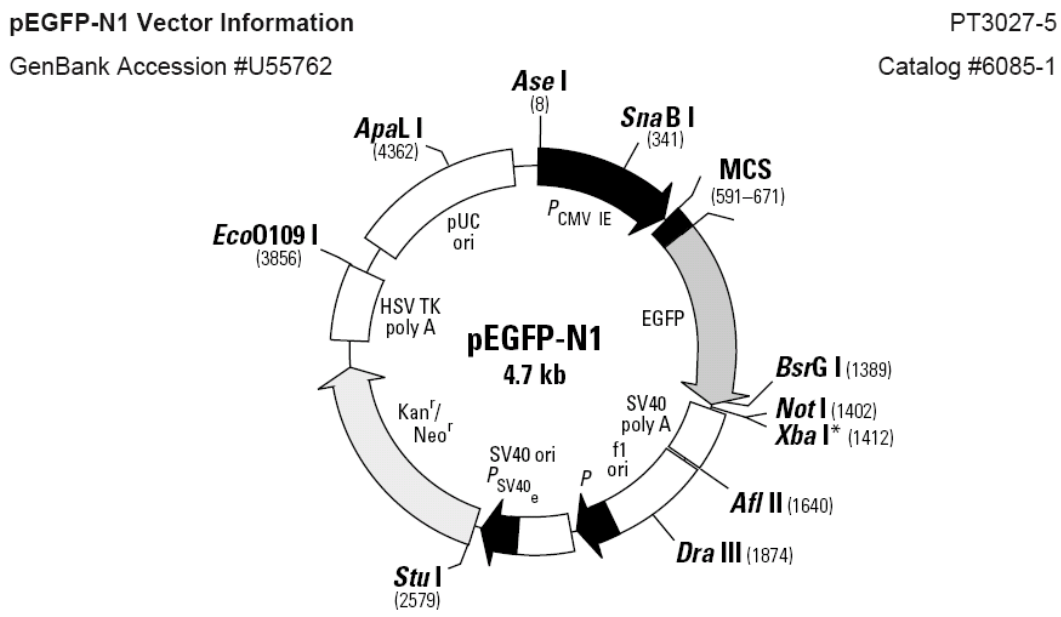

p3XFLAG-CMV™-14 Vector map (Sigma)

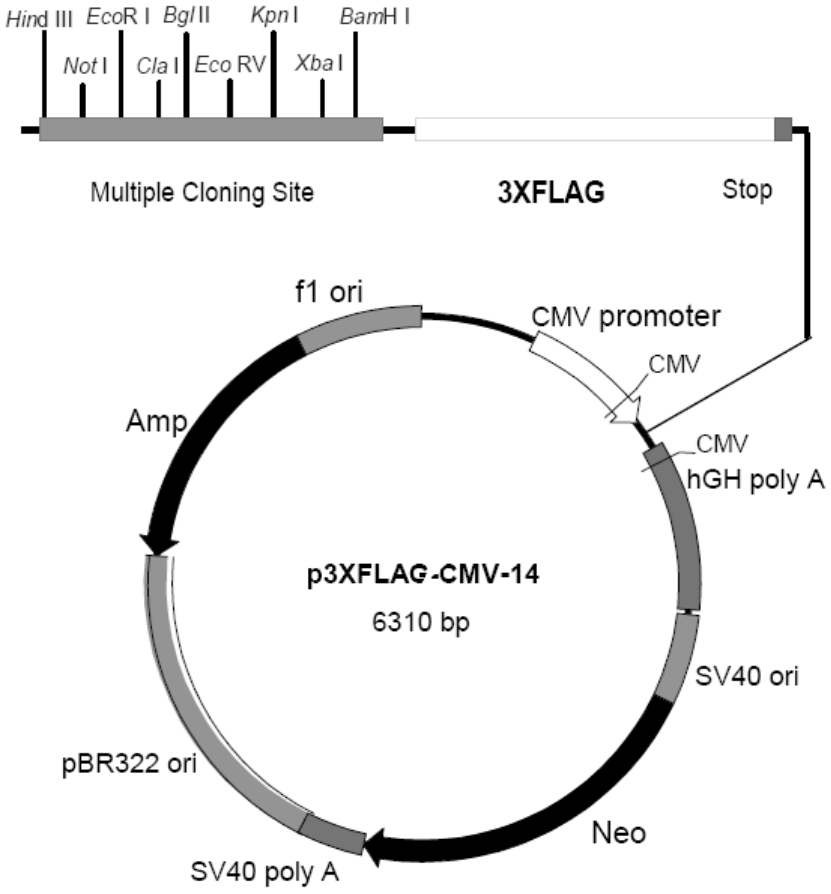

F1007 mammalian expression vector map (Institute of cancer research, London, UK)

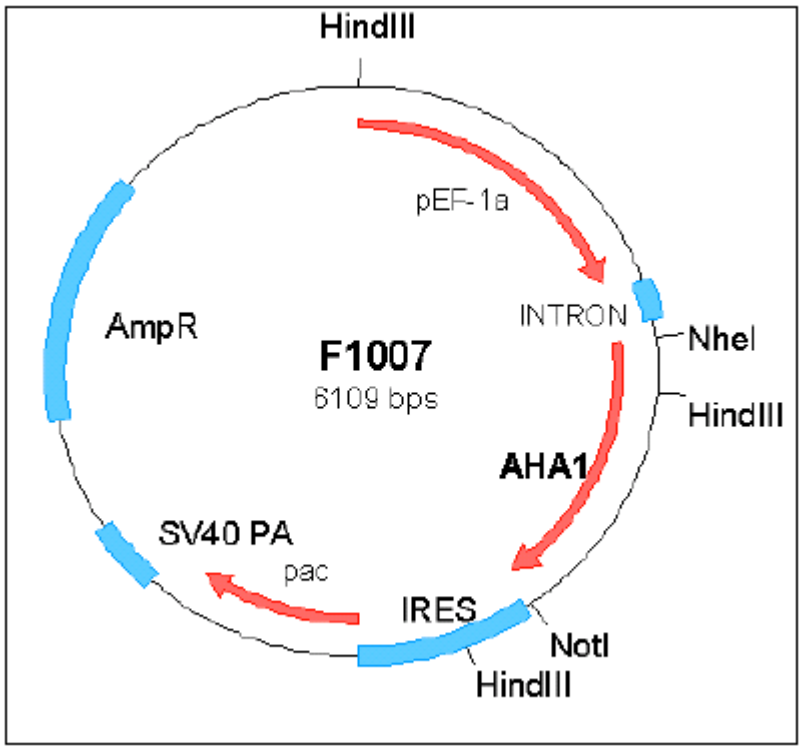

pCDNA3.1 5/FRT/TO Vector map (Invitrogen, UK)

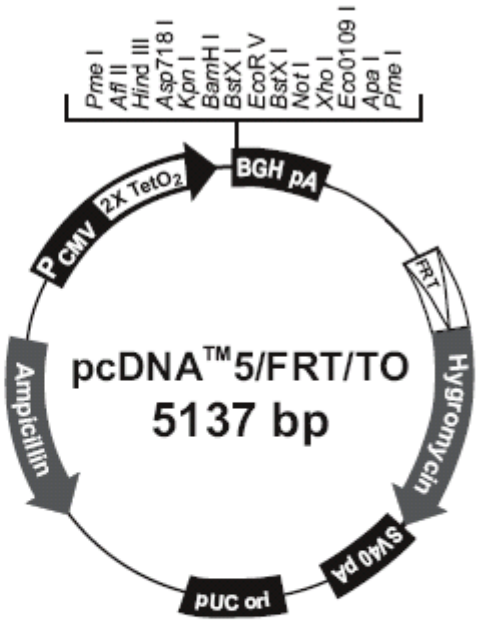

Comments for pcDNA™5/FRT/TO
5137 nucleotides

CMV promoter: bases 232-958
TATA box: bases 804-810
Tetracycline operator (2X $TetO_2$) sequences: bases 820-859
CMV forward priming site: bases 769-789
Multiple cloning site: bases 968-1077
BGH reverse priming site: bases 1089-1106
BGH polyadenylation signal: bases 1095-1319
FRT site: bases 1603-1650
Hygromycin resistance gene (no ATG): bases 1658-2678
SV40 early polyadenylation signal: bases 2810-2940
pUC origin: bases 3323-3996 (complementary strand)
bla promoter: bases 5002-5100 (complementary strand)
Ampicillin (*bla*) resistance gene: bases 4141-5001 (complementary strand)

4. Presentations and Publications

Manuscript in preparation for submission to the Journal of Biological Chemistry
Gooljar,S.B., Meimaridou,E., and Chapple,J.P. (with Gooljar,S.B and Meimaridou,E as joint first authors). Hsp70 and Hsp90 chaperone systems can modulate the cellular processing of the obesity linked melanocortin-4 receptor.

Meimaridou,E., Gooljar,S.B., and Chapple,J.P. (2009). From hatching to dispatching: the multiple cellular roles of the Hsp70 molecular chaperone machinery. J. Mol. Endocrinol. *42*, 1-9. Review article.

Poster: Modifying cell surface expression of the obesity linked G-protein coupled receptor MC4R by targeting protein folding
Annual meeting ENDO 2009
June 10th-13th, 2009. Washington DC, USA.

Poster: Monitoring cellular trafficking of the obesity linked G-protein coupled receptor MC4R
Society for Endocrinology BES 2009
March 16th-19th, 2009. Harrogate, UK.

Poster: Monitoring trafficking of MC4R to the plasma membrane
Spring meeting for the British Society for Cell Biology
March 31st – April 3rd, 2008. Warwick, UK.